

ABSTRACT

Title of Document: DEVELOPMENT OF A PROTEOMIC STRATEGY FOR
ANALYSIS OF PLASMA MEMBRANE PROTEINS

Waeowalee Choksawangkar, Doctor of Philosophy, 2013

Directed By : Professor Catherine Fenselau,
Department of Chemistry and Biochemistry

Plasma membrane (PM) proteins play crucial roles in cell signaling and communications, and they are the targets of more than two thirds of drugs currently under development. Studies on changes in protein content, quantity and modifications of the PM proteins indicate metabolic alteration of disease related cells; therefore, mass spectrometry-based proteomic studies may lead to improved understanding of the pathology, the characterization of novel biomarkers, and discovery of future drug targets. The main objectives of my research are to develop an effective enrichment strategy and to optimize the proteomic workflow for analysis of PM proteins from cells in suspension. Strategies were optimized with human multiple myeloma cells cultured in suspension, and optimized strategies were applied

to study the PM proteome of myeloid-derived suppressor cells (MDSC) collected from an animal model.

We focus on optimization of the cationic nanoparticle pellicle method for enrichment of PM proteins. The principle of this method is to attach cationic nanoparticles to the cell surface by electrostatic interaction between the positively charged nanoparticles and the negatively charged cell surface. Thus, the heavier coated-plasma membrane sheets can be separated more easily from cellular organelles by centrifugation after cell lysis. The isolated PM proteins were identified by LC-MS/MS analysis. We have also optimized the workflow for proteolysis to enhance identification of hydrophobic PM proteins. Our studies reveal that higher density nanoparticle pellicles provide higher enrichment efficiency of the PM proteins and that a procedure using digestion in the gel matrix enhances the analysis of highly hydrophobic proteins.

The most effective enrichment technique and optimized proteomic procedures were applied to characterize the PM proteins from MDSC obtained from BALB/c mice carrying 4T1 mammary carcinomas. These cells are known to accumulate in individuals with cancer and suppress anti-tumor immunity. Their accumulation and activity are increased with heightened-levels of inflammation. Comparative studies of the PM proteins expressed in the cells derived from basal- and heightened- levels of inflammation were performed using the spectral counting method. This work reveals a set of protein candidates that have a high potential to be involved in the inflammation-driven immunosuppressive activity of the MDSC.

DEVELOPMENT OF A PROTEOMIC STRATEGY FOR
ANALYSIS OF PLASMA MEMBRANE PROTEINS

By

Waeowalee Choksawangkar

Dissertation submitted to the Faculty of the Graduate School of the
University of Maryland, College Park, in partial fulfillment
of the requirements for the degree of
PhD
2013

Advisory Committee:
Professor Catherine Fenselau, Chair
Professor Robert Peters, Dean's Representative
Professor Douglas Julin
Professor Nicole LaRonde-LeBlanc
Professor Kwaku Dayie

© Copyright by

Waeowalee Choksawangarn

2013

Dedication

This thesis is dedicated to my parents,
Mr. Prasert Choksawangkarn and Mrs. Wanna Choksawangkarn,
who have always encouraged and inspired me.

Acknowledgements

Completion of the work in this dissertation would not have been possible without the support and assistance of many people. Above all, I would like to express my deepest gratitude to my advisor, Prof. Catherine Fenselau, for her continued guidance, invaluable support, and exceptional mentorship throughout my graduate career. She has not only mentored my research project with her knowledge and expertise, but also helped shape my scientific and academic philosophy. I appreciate this great opportunity to work with her. In the years to come, she will always be my inspiring role model. Besides my advisor, I would like to thank my committee members, Prof. Douglas Julin, Prof. Nicole LaRonde-LeBlanc, Prof. Kwaku Dayie, and Prof. Robert Peters for their time and intellectual contributions throughout my graduate studies.

I would like to acknowledge several collaborators and colleagues who have strongly contributed to this interdisciplinary project. I am especially grateful to Prof. Nathan Edwards for his invaluable advice and insightful assistance with bioinformatics. I would like to show my greatest appreciation to Dr. Yan Wang, the director of the Proteomics Core Facility, for her enormous help and fruitful discussion of method development and instrumentation. I acknowledge Prof. Peter Gutierrez who always provides me constructive comments and warm encouragement. I would like to acknowledge Prof. Sang Bok Lee, Dr. Sung-Kyoung Kim, and Lauren Graham, for hands on and intellectual contributions to the nanoparticle work and helpful comments about experimental design. I would also like to thank Prof. Suzanne Ostrand-Rosenberg for providing myeloid-derived suppressor cells and for

her generous assistance with interpreting experimental data. I acknowledge the support of Laboratory for Biological Ultrastructure, and the Maryland NanoCenter and its NispLab for providing a facility for scanning and transmission electron microscopy. Special thanks go to Tim Maugel for assisting with the SEM and TEM processing.

My graduate study would not have been successful without academic and social interactions from all former and current Fenselau Lab members: Meghan Burke, Rebecca Rose, Sara Moran, Dr. Karen Lohnes, Dr. Colin Wynne, Dr. Jinxi Li, Maria Oei, Amanda Lee, and Sitara Chauhan. I acknowledge all of them for many scientific discussions and friendship. I would like to offer my special appreciation to Dr. Joe Cannon, who has always supported me with his invaluable guidance, intellectual knowledge, and optimism, which has helped me pass through the most difficult times. I would like to address another special thanks to Avantika Dhabaria, for her scientific support, friendship, and encouragement throughout my graduate studies.

The work presented in this dissertation was funded by grant from National Institutes of Health (GM 021248). Also, I acknowledge the financial support from the Royal Thai government fellowship.

I also thank many friends and colleagues for encouraging me with their best wishes. I deeply appreciate generous supports from Dr. Salil Chanroj and Dr. Nuttinee Teerakulkittipong, who have always cheered me up and been there for me. Finally, I would like to thank and dedicate this thesis to my parents and family members for their unconditional love and support.

Table of Contents

Dedication	ii
Acknowledgements	iii
Table of Contents	v
List of Tables	viii
List of Figures	x
List of Abbreviations.....	xv
List of Appendix Tables.....	xviii
List of Appendix Figure.....	xix
Chapter 1: Introduction	1
<u>Research Significance and Objectives</u>	1
<u>Plasma Membrane Protein Enrichment</u>	3
<u>Mass Spectrometry-based Proteomics</u>	6
<u>Bottom-up Proteomics</u>	7
<u>Electrospray Ionization (ESI)</u>	9
<u>Tandem Mass Spectrometry</u>	11
<u>LTQ-Orbitrap</u>	12
<u>Bioinformatics</u>	14
<u>Myeloid-Derived Suppressor Cells</u>	16
Chapter 2: Enrichment of Plasma Membrane Proteins using Silica	
Nanoparticle Pellicles.....	18
<u>Introduction</u>	18

<u>Materials and Methods</u>	21
<u>Results and Discussion</u>	28
<u>Summary</u>	36
Chapter 3: Optimization of Proteomic Workflow for Analysis of	
Plasma Membrane Proteins.....	39
(A) Comparative Study of Workflows Optimized for In-gel, In-solution,	
and On-filter Proteolysis in the Analysis of Plasma Membrane Proteins.....	39
<u>Introduction</u>	39
<u>Materials and Methods</u>	41
<u>Results and Discussion</u>	46
<u>Summary</u>	50
(B) Evaluation of Enzymatic Digestion Methods using a Model	
Transmembrane Protein and a Complex Mixture of Plasma Membrane	
Proteins.....	51
<u>Introduction</u>	51
<u>Materials and Methods</u>	53
<u>Results and Discussion</u>	59
<u>Summary</u>	64
Chapter 4: Enrichment of Plasma Membrane Proteins Using Nanoparticle	
Pellicles: Comparison between Silica and Higher Density Nanoparticles.....	65
<u>Introduction</u>	65
<u>Materials and Methods</u>	68

<u>Results and Discussion</u>	75
<u>Summary</u>	85
Chapter 5: Use of Iron Oxide Nanoparticle Pellicles for Enrichment of Plasma Membrane Proteins from MDSC.....	86
<u>Introduction</u>	86
<u>Materials and Methods</u>	88
<u>Results and Discussion</u>	95
<u>Summary</u>	108
Chapter 6: Conclusions and Prospectus.....	110
Appendices.....	114
Bibliography	181

List of Tables

Table 1. Density of cellular organelles.....	20
Table 2. Proteomic analysis of the PM protein enrichment by the pellicle technique integrated with three different centrifugation methods.....	31
Table 3. Number of proteins identified in each step of sequential extraction.....	36
Table 4. Number of PM proteins and PM peptides identified using three different methods.....	46
Table 5. Sequence coverage of bacteriorhodopsin from LC-MS/MS analysis of tryptic and chymotryptic peptides.....	61
Table 6. Properties of the nanoparticles studied.....	76
Table 7. Proteomic analysis of plasma membrane (PM) and transmembrane (TM) protein enrichment by three pellicles; average % (standard deviation) of six technical replicates.....	80
Table 8. Proteomic analysis of PM and TM proteins enriched by three nanoparticle pellicles and whole cell lysate; average % (standard deviation) of three biological replicates.....	81
Table 9. Number of proteins identified with in-gel digestion of conventional and inflammatory MDSC samples, their % assigned as plasma membrane by GO annotation, and % assigned as transmembrane by TMHMM 2.0.....	97
Table 10. Number of proteins identified with digestion in solution from conventional and inflammatory MDSC collected from three pairs of animals.....	99

Table 11. Proteins quantified with significantly higher abundances ($R_{sc} > 1$, Bonferroni corrected p -value < 0.05). $R_{sc} = \log_2$ [ratio of abundance between inflammatory vs. conventional MDSC].....	101
Table 12. Proteins quantified with significantly lower abundances ($R_{sc} < -1$, Bonferroni corrected p -value < 0.05). $R_{sc} = \log_2$ [ratio of abundance between inflammatory vs. conventional MDSC].....	103
Table 13. List of proteins associated in the KEGG pathways.....	106

List of Figures

Figure 1. A schematic diagram of the plasma membrane with different types of the PM proteins.....	4
Figure 2. Typical workflow for bottom-up proteomics: (1) proteins are isolated from cells/tissues/animals and pre-fractionated, (2) enzymatic or chemical cleavages are performed, (3) peptides products are fractionated by HPLC and ionized by ESI, (4) precursor ion spectrum is acquired by the first stage MS, and (5) the selected precursor ion is subjected to CID, and the MS/MS spectra are recorded.....	8
Figure 3. Schematic diagram of electrospray ionization.....	10
Figure 4. Fragmentation pattern of peptide backbone. Series of b- and y-ions are generated by CID fragmentation technique.....	12
Figure 5. Schematic diagram of the plasma membrane nanoparticle pellicle technique.....	21
Figure 6. SEM micrographs of (A) human multiple myeloma cells, (B) silica nanoparticles coated cells, (C) poly(acrylic) acid coated cells, and (D) a lysed plasma membrane sheet.....	28
Figure 7. (A) Chromatogram of tryptic peptides from in-gel digestion, and (B) precursor scan at retention time 23.19, and (C) MS2 spectra of the peptide LTLSALLDGKNVNAGGHK from the precursor 904.51 ($z=2$), with E-value 3.3×10^{-5} . This peptide is from the voltage-dependent anion selective channel protein.....	29

Figure 8. Comparison of two lysis buffers by (A) Western blotting of a plasma membrane protein marker, Na⁺-K⁺ ATPase, and (B) numbers of proteins identified from LC-MS/MS experiment and the percent of identified proteins that were located in the plasma membrane (%PM).....31

Figure 9. Silver-stained SDS-PAGE gels showing (i) the presence of soluble proteins after removal from the pellicles by washes in lysis buffer, high pH (1 M Na₂CO₃), and high salt (1 M KCl) buffers, (ii) the presence of proteins after releasing from the pellicles into extraction buffer, and (iii) the absence of proteins after three extractions in Laemmli buffer.....33

Figure 10. Comparison of extraction buffer efficiency: Buffer A; 2% SDS, 62.5 mM Tris-HCl, 5% β- mercaptoethanol, Buffer B; 6 M Urea, 9 mM EDTA, 9% SDS, 0.5 M Tris-HCl, 3.6% β- mercaptoethanol, Buffer C; 6 M urea, 2 M thiourea, 100 mM Tris-HCl, 10 mM DTT, and Buffer D; 8 M urea in 50 mM NH₄HCO₃. (A) percentage of plasma membrane and membrane proteins and (B) total number of proteins identified from MASCOT with E-values <0.05.....34

Figure 11. (A) Bar chart showing protein concentration in Laemmli buffer after reiterative extractions. (B) Bar chart showing the concentration of proteins released from the silica pellicle in Laemmli buffer and 0.1% RapiGest™ SF.....35

Figure 12. Western blotting of Na⁺-K⁺ ATPase of aluminosilicate enriched samples vs. whole cell lysate control37

Figure 13. Cellular components of proteins identified from (A) whole cell

lysate control and (B) PM pellicle-enriched sample.....	38
Figure 14. Venn diagram showing overlap in proteins identified using in-gel, in-solution, and on-filter digestion.....	47
Figure 15. Correlation between fractions of plasma membrane proteins identified and the number of transmembrane helices	48
Figure 16. Correlation between the number of plasma membrane proteins identified and their hydrophobicity.....	49
Figure 17. (A) Different types of integral membrane proteins. The gray areas show parts of the protein sequence that are available for enzymatic digestion, (B) structure of bacteriorhodopsin.....	53
Figure 18. Distribution of predicted peptide length after <i>in silico</i> digestion by trypsin and chymotrypsin with complete cleavages.....	60
Figure 19. Example of (A) precursor ion spectrum, and (B) MS/MS spectrum of the peptide from transmembrane domain. The peptide VGALTKVY were identified from the chymotryptic digestion in 0.1% RapiGest™ SF. The sequences highlighted in green represent the transmembrane amino acid residues.....	62
Figure 20. Comparison of proteolysis protocol by LC-MS/MS analysis of PM proteins after enrichment by silica nanoparticle pellicle techniques.....	63
Figure 21. Micrographs of (Columns 1 to 4) multiple myeloma cells, the cells coated with nanoparticles, poly(acrylic acid) cross-linked coated cells, and fragments of the pellicle-coated PM. The nanoparticles are (Rows A-F) Fe ₃ O ₄ /Al ₂ O ₃ , aluminosilicate, SiO ₂ /Al ₂ O ₃ , Fe ₃ O ₄ /NH ₂ , 29 nm Au/NH ₂ ,	

and 77 nm Au/NH₂. The scale bars indicate 5 μm. Micrographs (*) were taken with a Hitachi SU-70 field emission scanning electron microscope. Micrographs (**) were taken with an Amray 1820 scanning electron microscope.....77

Figure 22. Analysis of abundances of PM protein markers by (A) Western blotting of Na⁺-K⁺ ATPase and (B) spectral counts for Na⁺-K⁺ ATPase and other PM protein markers.....79

Figure 23. Spectral counts from three biological replicates of (A) plasma membrane proteins as a percent of total spectral counts and (B) transmembrane proteins as a percent of total spectral counts. Error bars indicate range of observed values.....82

Figure 24. Spectral counts from six technical replicates of (A) plasma membrane proteins as a percent of total spectral counts; and (B) transmembrane proteins as a percent of total spectral counts. Error bars indicate range of observed values.....83

Figure 25. Number of common, shared, and unique protein identifications for Al₂O₃-coated Fe₃O₄, aluminosilicate, and Al₂O₃- coated SiO₂ nanoparticles.....84

Figure 26. Morphology of the cells (A) conventional MDSC (B) Fe₃O₄ nanoparticle-coated conventional MDSC, (C) inflammatory MDSC, and (D) Fe₃O₄ nanoparticle-coated inflammatory MDSC. White scale bars indicate 1 μm.....96

Figure 27. Venn diagram of showing overlapping between proteins identified from conventional and inflammatory MDSC using in-gel digestion.....97

Figure 28. (A) Subcellular location and (B) functional distribution of proteins identified from conventional and inflammatory MDSC using in-gel digestion.....98

Figure 29. A distribution of the combined \log_2 ratios of abundances between inflammatory vs. conventional MDSC (R_{sc}) and their statistical significance. R_{sc} values >1 or <-1 indicate 2-fold or greater changes.....100

Figure 30. Networks of the proteins quantified with higher abundances in inflammatory MDSC ($R_{sc} > 1$, FDR corrected p -value < 0.05), evaluated by STRING. The network cluster is shown in a confident view. Thicker line represents stronger interaction between proteins. The gene names and their associated KEGG pathways are specified.....108

List of Abbreviations

ATP	Adenosine triphosphate
CID	Collision-induced dissociation
DAVID	Database for Annotation, Visualization and Integrated Discovery
DC	Direct current
DTT	Dithiothreitol
ECM	Extracellular matrix
EDTA	Ethylenediaminetetraacetic acid
EGTA	Ethyleneglycoltetraacetic acid
ER	Endoplasmic reticulum
ESI	Electrospray ionization
ETD	Electron transfer dissociation
E-value	Expect value
FDR	False discovery rate
GM-CSF	Granulocyte-macrophage colony-stimulating factor
GO	Gene Ontology
GOA	Gene Ontology Annotation
GRAVY	Grand average of hydropathy
HCl	Hydrochloric acid
HPLC	High performance liquid chromatography
IL1- β	Interleukin1- β
iNOS	Inducible nitric oxide synthase

iTRAQ	Isobaric tags for relative and absolute quantitation
kDa	Kilodalton
LC-MS/MS	Liquid chromatography/Tandem mass spectrometry
LTQ	Linear trap quadrupole
MALDI	Matrix-assisted laser desorption/ionization
MES	2-(N-morpholino)ethanesulfonic acid
MDSC	Myeloid-derived suppressor cells
MS	Mass spectrometry
MS2	Tandem mass spectrometry
MS/MS	Tandem mass spectrometry
MW	Molecular weight
PCR	Polymerase chain reaction
PGE ₂	Bioactive lipid prostaglandin E2
pI	Isoelectric point
PIPES	Piperazine-N,N-bis(2-ethanesulfonic acid)
PM	Plasma membrane
PMCBA	Plasma membrane coating buffer A
psi	Pounds per square inch
RF	Radio frequency
ROS	Reactive oxygen species
SAGE	Serial analysis of gene expression
SDS	Sodium dodecyl sulfate
SDS-PAGE	Sodium dodecyl sulfate polyacrylamide gel electrophoresis

SILAC	Stable isotope labeling by amino acids in cell culture
TM	Transmembrane
TMD	Transmembrane domain
VEGF	Vascular endothelial growth factor

List of Appendix Tables

Appendix Table 1. Proteins identified from at least two peptides with FDR<10% as summarized in Figure 14.....	115
Appendix Table 2. Summary of proteins identified from the three pellicle samples and the cell lysate control.....	128
Appendix Table 3. List of proteins identified from conventional (CON) and inflammatory (INF) MDSC and their spectral counts. $R_{sc} = \log_2$ ratio of abundance between inflammatory vs. conventional MDSC proteins.....	167

List of Appendix Figure

Appendix Figure 1. (A) different domains (helix: blue, strand: green, turn: yellow)
of bacteriorhodopsin molecule; (B) and (C) the regions of identified
peptides from bacteriorhodopsin using trypsin and chymotrypsin
proteolysis, respectively, in five different conditions.....126

Chapter 1: Introduction

Research Significance and Objectives

Plasma membrane (PM) serves as a semipermeable barrier between cellular components and extracellular environment. It plays important roles in many biological pathways, including cell-cell communication, environmental responses, cellular signaling, and molecular transport.^{1, 2} Because of these crucial functions, proteins embedded in or bound to the PM are potential targets for drug development and biomarker discovery.³ It has been reported that more than 60% of drugs under development are targeted to the PM proteins⁴, and that more than 30% of cancer biomarker candidates are classified as membrane proteins.⁵

We have employed mass spectrometry-based proteomic strategies to study the PM proteome using both qualitative and quantitative approaches. Interrogation of the PM proteome reveals a better understanding of disease mechanisms, which leads to novel diagnostics and therapeutics. Mass spectrometry (MS) has become a powerful technology for large-scale proteomic analysis for a number of reasons, including capabilities to identify proteins in a short time scale, localize post-translational

modifications, and quantify protein abundances from different samples. Due to advanced development of robust and highly sensitive instrumentation, complex protein mixtures with wide dynamic range can be rapidly analyzed by the mass spectrometer coupled with high performance liquid chromatography (HPLC).

Membrane proteins have been predicted to account for about 30% of the human genome⁶; however, unlike soluble proteins, only small fractions have been investigated. The plasma membrane proteins are known to be undersampled in the proteomic study due to their low abundance, low solubility, high hydrophobicity, various post-translational modifications, and dynamic populations. Successful interrogation of the PM proteome by mass spectrometry can be obtained by optimizing the strategies for (1) protein enrichment, (2) protein solubilization, (3) detergent removal and delipidation, (4) proteolysis, (5) protein or peptide fractionation and MS analysis, and (6) assignment of the PM proteins by database searching.

We aim to cope with the underrepresentation by developing effective PM enrichment techniques for suspended cells prior to the proteomic analysis, as well as optimizing the downstream workflows to enhance identification of highly hydrophobic proteins.^{7, 8} First, we have improved the silica nanoparticle pellicle enrichment technique by maximizing PM protein extraction and simplifying the procedures. Second, we have optimized the strategies for delipidation, detergent removal, proteolysis, and LC-MS/MS analysis of poorly soluble proteins. Third, we have developed, for the first time, the use of higher density cationic nanoparticle pellicles and nanowires to enrich the PM proteins. Following optimization of

conditions evaluated with cultured human multiple myeloma cells in suspension, we aim to apply these procedures to investigate the PM proteome of myeloid-derived suppressor cells (MDSC) collected from tumor-bearing mice. Comparative quantitative measurement of enriched PM proteins from MDSC derived from heightened- and basal- inflammatory conditions have been performed to examine changes in protein abundances upon increased inflammation. Our study will lead to a greater understanding of the mechanisms of MDSC accumulation and their immune suppressive activity, as well as the signaling between inflammation and cancer.

Plasma Membrane Protein Enrichment

Plasma membrane is composed of phospholipid bilayers, membrane proteins, cholesterol, and carbohydrate moieties modified on either lipids or proteins. It occupies only about 2% of the total cell volume.⁹ The PM proteins contribute to more than a half of the PM mass.¹⁰ There are various types of PM proteins as shown in **Figure 1**, including integral membrane proteins spanning through the phospholipid bilayers, integral membrane proteins forming pore complexes, proteins embedding on the inner or outer sites of the phospholipids, and peripheral membrane proteins interacting with the proteins or lipids on either sides of the PM.¹¹ Studies of membrane proteomics, in general, remain problematic owing to their intrinsic properties. Despite the low abundance, a majority of the PM proteins are poorly soluble, particularly those that contain transmembrane domains.

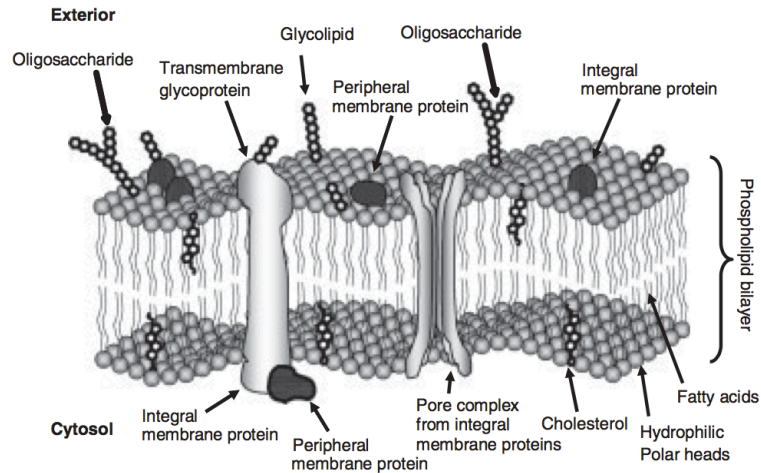


Figure 1. A schematic diagram of the plasma membrane with different types of the PM proteins.¹¹

To overcome the problem of underrepresentation of the PM proteome from tissue, cell lysates, or plasma samples, a number of techniques have been developed for improving enrichment efficiency. Traditionally, a density gradient centrifugation, such as sucrose or Nycodenz gradients, has been employed to fractionate intracellular organelles based on their density differences.^{12, 13} Similarities in the density of organelle membranes cause difficulties with this technique because the membranes from different organelles tend to be enriched in the same density fractions. Moreover, there are various sizes and forms of PM after cell lysis, including vesicles and open sheets; therefore, they could be present in several centrifugal fractions.¹⁴ A number of studies focus on enriching the cell surface proteins using chemical labeling of primary amine or sulfhydryl groups exposed on the extracellular side of the surface, followed by an affinity enrichment of the tagged-proteins.^{15, 16} Commonly, biotin-linked reagents are used for protein derivatization, prior to affinity purification

by avidin/streptavidin molecules, which is based on stable non-covalent interaction between the biotin and avidin/streptavidin.¹⁶ Likewise, several studies employ a similar technique to capture cell surface glycoproteins.¹⁷⁻¹⁹ Since glycosylation is frequently found on the PM proteins, carbohydrate moieties serve as favorable targets for biotinylation. Aldehyde groups formed by periodate-oxidation of sugars are reactive with biotin-labeled reagents, which are suitable for the downstream affinity enrichment. Another membrane purification technique, two-phase aqueous/polymer or detergent/polymer partitioning, takes advantage of higher hydrophobicity of the membrane bilayers to separate them from other compositions.^{20, 21} The PM bilayers can be further purified by adding PM-specific affinity ligands to one of the polymer layers.²²

We focus on another distinct enrichment technique, which utilizes cationic silica nanoparticle pellicles to isolate the PM proteins. The pellicles are formed by electrostatic interaction between positively charged nanoparticles and negatively charged cell surfaces; and the high-density pellicles can be separated from cellular organelles by sedimentation. It has been reported that the PM nanoparticle pellicle method produces large open membrane sheets, without formation of vesicles or small sheets²³; therefore, these PM fragments can be isolated in the same centrifugal gradient fraction. This method was first developed by Chaney and Jacobson in 1983²⁴ and integrated with proteomic analysis by Rahbar and Fenselau in 2004.²⁵

Mass Spectrometry-based Proteomics

As proteins are functional products of the genes, they possess high heterogeneity, owing to the gene polymorphism, alternative splicing, and also post-translational modifications. It has been predicted that there are approximately 20,000 human genes; however, a range of 20,000 to millions proteins have been estimated.²⁶ The term “proteome” was initiated by Marc Wilkins in 1996; it was defined as the entire set of proteins expressed in the system, e.g., cells, tissues, biological fluids, at a specific condition and a given time.²⁷ Systematic study of the expressed proteins, so-called proteomics, has been focused on rapid identification of the proteins, as well as quantification, sequencing, localization of post-translational modifications, protein interaction, subcellular distribution, activity measurement and structural characterization.²⁸ In the long term, proteomics is advantageous for understanding mechanisms of diseases and may lead to development of novel biomarkers and drug targets. The major challenges in proteomic study result from a high degree of complexity and high dynamic range of protein abundances. Unlike genomic study, in which the genes can be amplified by the polymerase chain reaction (PCR), the amounts of protein samples are limited to those isolated directly from the cells without amplification. A number of methodologies have been employed to advance proteomic research, including two-dimensional gel electrophoresis, protein microarray, protein enrichment techniques and mass spectrometry.

As instrumentation has been rapidly developed over years, MS has increasingly become a remarkable and indispensable tool for proteomic research.²⁹

One of the critical advantages of using the MS is the ability to identify proteins in a complex mixture in high-throughput fashion by interfacing with a front-end chromatographic separation. Also, several types of commercially available mass spectrometers provide (i) high sensitivity, with capability to analyze the protein ranges from femtomol to attomol, (ii) high accuracy, with the mass accuracy between <2 ppm and 100 ppm, and (iii) high resolving power, with resolution ranges from 2,000 to 500,000.³⁰ The basic principle of mass spectrometer is to measure mass to charge ratios (m/z) of ionized analytes. Generally, mass spectrometers are composed of three main parts: an ion source to generate gas-phase ions, a mass analyzer to separate the ions according to their m/z , and a detection system to record the abundances of the ions. Since proteins and peptides are composed of 20 common amino acids with 19 different residue masses, they can be readily characterized based on their unique m/z , by the MS-based techniques.

Bottom-up Proteomics

There are three main approaches in MS-based proteomics; these include analysis of intact proteins (top-down approach), analysis of large digested peptides with a mass range between 3-20 kDa (middle-out approach)³¹ and analysis of small digested peptide products (bottom-up approaches). While the top-down and middle-out strategies provide higher sequence coverage of the protein identified, in most of the large-scale proteome profiling, the bottom-up strategy is the method of choice due to the feasibility of handling highly complexed mixtures. A common platform

(shown in **Figure 2**) involves an extraction or an enrichment of proteins from biological samples, proteolysis, peptide pre-fractionation, peptide separation using HPLC, ionization via electrospray, and analysis by tandem mass spectrometry (MS/MS), followed by data interpretation. Because protein digestion results in a large increase in complexity, separation techniques must be implemented, at either the protein or peptide level.

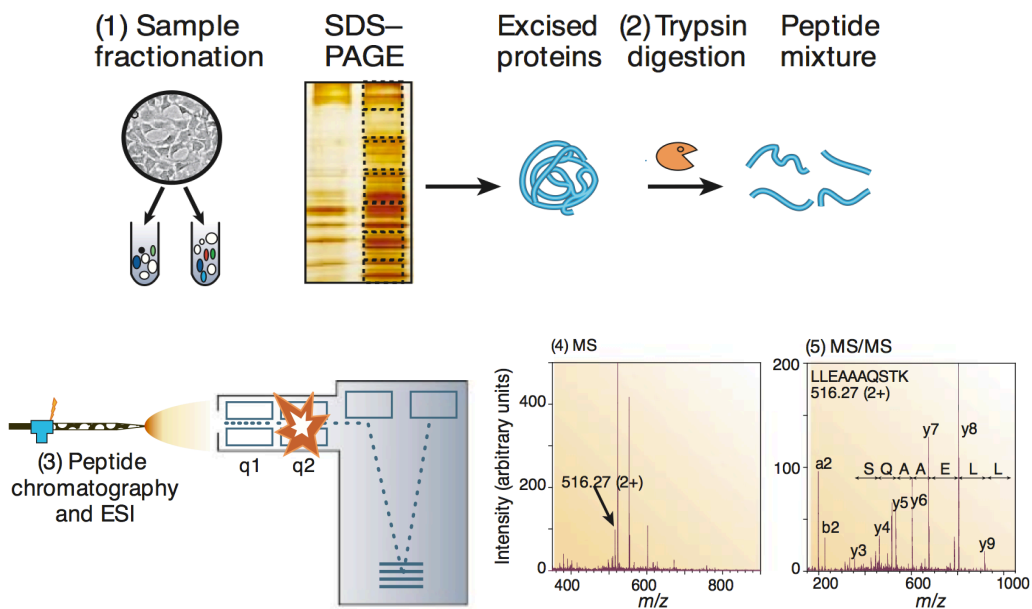


Figure 2. Typical workflow for bottom-up proteomics³²: (1) proteins are isolated from cells/tissues/animals and pre-fractionated, (2) enzymatic or chemical cleavages are performed, (3) peptides products are fractionated by HPLC and ionized by ESI, (4) precursor ion spectrum is acquired by the first stage MS, and (5) the selected precursor ion is subjected to CID, and the MS/MS spectra are recorded.

Typically, protein identification is inferred by the presence of peptides, which are produced by enzymatic or chemical cleavages. The most common enzyme used in this strategy is trypsin, which cleaves after the C-terminus of lysine and arginine residues. Using MS/MS analysis, the peptides are subjected to precursor mass measurement, followed by fragmentation in the mass spectrometer. After acquiring tandem mass spectra, the peptide identification can be accomplished by a database search, which compares the experimental MS/MS spectra with the predicted fragmentation spectra of peptides from proteins in available databases. Identification of digested peptides implies the existence of proteins in samples.

Electrospray Ionization (ESI)

Since the invention of the first mass spectrometer by Thompson in 1912, MS has become one of the most useful tools for analytical research. Prior to development of desorption techniques, the MS was mainly used to analyze small organic molecules. At that time, the analysis of biological macromolecules was troublesome due to the inability to preserve intact molecular ions during the vaporization process. Thus, advancement of desorption techniques has been beneficial for the MS-based proteomics, since proteins or peptides can be vaporized and ionized without pyrolysis and internal fragmentation. The importance of these ionization methods was recognized by the Nobel Prize in Chemistry in 2002, of which one half of the award was shared between Fenn and Tanaka for their development of the two soft ionization techniques, electrospray ionization (ESI)³³ and laser desorption ionization

(MALDI)³⁴, respectively. ESI can be interfaced on-line with HPLC and MS; therefore, it is suitable for analyzing complex mixtures. The molecules are transferred from liquid-phase to gas-phase by the high voltage in the range of 2-6 kV, which is applied between the spray needle and a counter-electrode connected to the mass spectrometer as shown in **Figure 3**. The ionization process involves dispersion of an electrical spray, formation of charged liquid droplets, and solvent evaporation to produce ions in the gas-phase prior to analysis by the mass analyzer. Generally, droplet reduction and ion formation are assisted by a flow of nitrogen gas and a heated capillary tube at the inlet of the mass spectrometer. These ionized molecules possess either single or multiple charges with low internal energy; thus, the internal fragmentation is minimized.³⁵

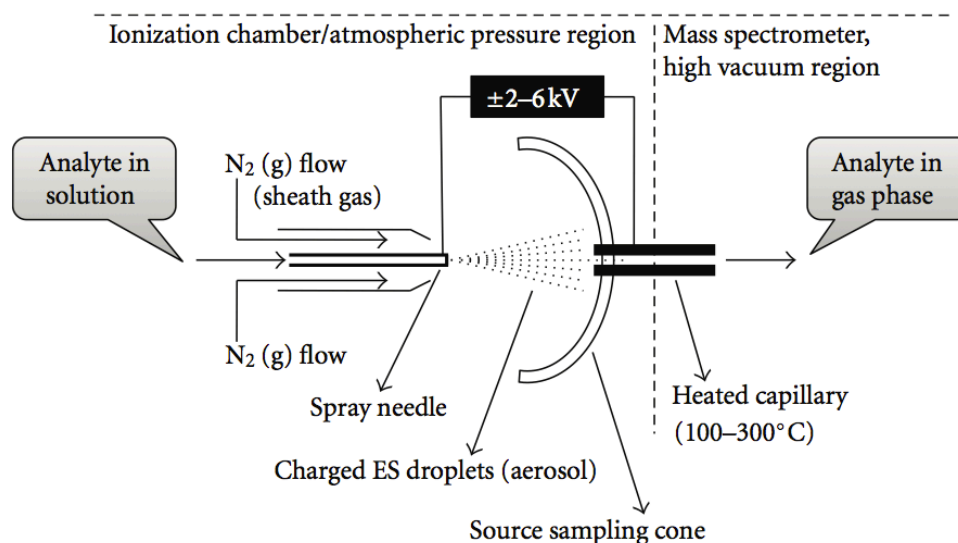


Figure 3. Schematic diagram of electrospray ionization.³⁵

Tandem Mass Spectrometry

A key technology for high-throughput protein identification and post-translational modification characterization by MS-based proteomics is tandem mass spectrometry (MS/MS or MS2), which involves two stages of mass analysis: (i) the precursor scan records the total molecular mass of peptides or proteins and (ii) the MS2 scan records the masses of product ions after fragmentation. Following acquisition of each precursor ion spectrum, a range of m/z values of interest are isolated and sent to the fragmentation chamber. Subsequently, the m/z of the product ions are recorded in the second stage of mass analysis. The complementary information from both MS1 and MS2 spectra leads to peptide sequencing, identification of proteins, and analysis of post-translational modifications.

There are several types of fragmentation techniques that provide different cleavage patterns along the peptide backbone. The most common method widely used in proteomics is called collision-induced dissociation (CID).³⁶ Protein or peptide ions in the gas phase are collided with an inert gas multiple times, producing a characteristic series of fragment ions as a result of collisional energy. Preferentially, the fragmentation takes place at the weakest bonds, which can be either peptide bonds in the polypeptide backbone or post-translational modifications in the polypeptide side chains. A series of b- and y-ions, containing amino and carboxy termini, are produced from cleavages of the peptide bonds as shown in **Figure 4**. Because CID is a slow heating process, labile post-translational modifications are normally undetectable, and fragmentation of large peptides is likely

to be incomplete.³⁷ Alternative fragmentation techniques can provide complementary information of the protein fragments, for example, electron transfer dissociation (ETD), which fragments at the covalent bond between N and C α . The ETD process is initiated by a transfer of electrons from anionic radicals to positively charged amino groups; it is not involved in energy transfer, so the post-translational modifications can be retained.³⁸

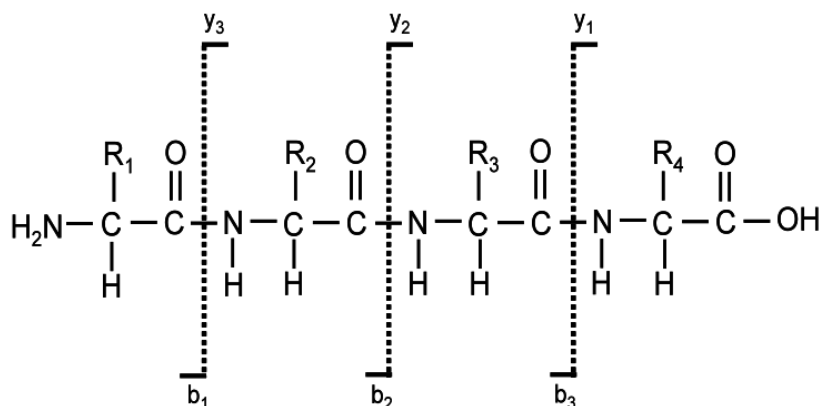


Figure 4. Fragmentation pattern of peptide backbone. A series of b- and y-ions is generated by CID fragmentation technique.

LTQ-Orbitrap

Each type of mass spectrometer provides distinct advantages and limitations. The LTQ-orbitrap mass spectrometer is a hybrid instrument that combines the advantages of fast scan rate, high sensitivity, robustness, and MS/MS performance of the linear ion trap and the superiorities of high resolution and high mass accuracy of

the Orbitrap mass analyzer. Thus, this hybrid mass spectrometer is beneficial for a high-throughput proteomic analysis.²⁹

In the LTQ, the ions in a mass range of interest are trapped in a presence of oscillating direct current (DC) and radio frequency (RF) voltages. Changing the amplitude of RF voltage causes the ions of a particular m/z range to be unstable in the trapped region; thus, they can be ejected from the mass analyzer, as described by the mass selective instability principle.³⁹ The precursor ions in a given m/z range are isolated and fragmented in the ion trap and are then detected by an electron multiplier. Using CID, the peptide precursor ions are collided with helium gas to produce fragmented ions with a specific pattern.

The orbitrap mass analyzer was invented by Makarov and coworkers in 1999.⁴⁰ It consists of a central spindle-like electrode and a pair of outer electrodes. The ions are confined and oscillated around the central electrode, forming orbital trapping in an electrostatic field. The characteristic frequency of a harmonic oscillation (ω) depends on the mass (m), and charge (q) of the ions, and a potential constant between the electrodes (k), as shown in equation (1).^{40,41} The mass spectrum can be acquired by detecting an image current in the outer electrode followed by Fourier transform from the time-domain image current transients into the frequency-domain.

$$\omega = \left(\frac{kq}{m} \right)^{1/2}$$

[equation 1]

The two mass analyzers can be operated in parallel; the full scans are achieved in the orbitrap while fragmentation happens in the ion trap. For shotgun proteomics, data-dependent acquisition is commonly used for automated MS/MS analyses, in which the fragmentation selection can be triggered based on abundances of the precursor ions. The combination of the LTQ and the orbitrap mass analyzers has become fruitful for proteomic research because it provides high resolution, high mass accuracy, high sensitivity, MS/MS capability, large dynamic range, and speed scan which allows acquisition in the chromatographic time scale.

Bioinformatics

Tandem mass spectrometry provides information about peptide sequences based on m/z differences between adjacent product ions, which correspond to the mass of each amino acid residue. Interpretation of the mass spectra is time-consuming. Automated database searching has become one of the most important strategies for high-throughput proteomic research. The identification is based on prior knowledge of proteins in the database. Theoretical masses of peptides and their possible fragments can be predicted from *in silico* digestion of each protein by enzymatic or chemical cleavage. Following data acquisition, tandem mass spectra are compared with product ion spectra theoretically generated by various algorithms, which are specific features of each search engine.⁴² Many computational algorithms have been developed and integrated in the search engines, such as MASCOT⁴³, SEQUEST⁴⁴, X!Tandem⁴⁵, OMSSA⁴⁶, and InsPecT⁴⁷, and PepArML.⁴⁸

Following the spectra comparison, a score and statistical values are calculated, based on the number of matched MS/MS spectra as well as the number of random matches. These values refer to the significance of the peptide identification, as well as the inferred protein candidates. Two common statistical values are Expect value (E-value) and false discovery rate (FDR). The E-value is defined as the expected number of peptides identified with scores higher than or equal to those observed from a peptide-spectrum matched by random chance. The FDR reflects the proportion of false peptide identifications from the database search. Practically, it is calculated by searching the observed spectra against a target-decoy database, which refers to reverse or shuffled versions of peptides from the correct database.⁴⁹

Protein databases provide a repository of primary protein sequences, as well as other information about such proteins, including their biological functions, post-translational modifications, structures, subcellular localizations, and protein interactions. The sequence databases used in proteomics can be classified into three major groups: translated databases, curated databases, and a combination of the two. The translated databases are derived from translation of gene sequences in the genomic databases, such as, TrEMBL. On the other hand, information present in curated databases is manually collected from existing reports with experimental evidence, such as, SwissProt. The translated databases provide a larger number of protein sequences with high redundancy; while the curated databases contain fewer redundant sequence entries and reveal biologically relevant functions of proteins. In this report, the combination of the translated and the curated databases, i.e., UniProt

KnowledgeBase, was chosen for database searching in order to maximize the number of sequence entries and minimize the redundant identifications.

Myeloid-Derived Suppressor Cells

Myeloid-derived suppressor cells (MDSC) refer to a heterogeneous population of immature myeloid cells. They are characterized by their immature state, myeloid-origin, and potent activity to suppress innate and adaptive immune responses. Accumulation of MDSC has been observed in several pathological conditions, e.g., cancer, chronic infection, trauma, and sepsis.⁵⁰ It has been reported that failure of immunotherapies for cancer treatment is related to the inflammation-driven accumulation of MDSC in the tumor microenvironment, and that depletion of MDSC enhances functions of the immune system in individuals with cancer.^{51, 52}

An accumulation and increased suppressive activity of MDSC have been found to result from a set of chronic inflammation-associated mediators, such as Interleukin-1 β , Interleukin-6, S100A8/A9 proteins, complement component C5a, vascular endothelial growth factor (VEGF), granulocyte macrophage colony-stimulating factor (GM-CSF), and the bioactive lipid prostaglandin E2 (PGE₂), which are generated by malignant cells or adjacent cells within tumor microenvironment. These factors promote an expansion of MDSC in tumor-sites, bone marrow, lymph nodes, and blood where they stimulate the tumor progression.⁵¹

There are several proposed mechanisms by which MDSC suppress the immune function of T-cells. One of the well-established mechanisms is depletion of

L-arginine from the tumor microenvironment, which was observed via high levels of arginase and inducible nitric oxide synthase (iNOS) in intracellular MDSC.⁵³ L-arginine is a substrate for both arginase and iNOS, and it is known to be essential for T-cell proliferation.⁵⁴ Other mechanisms include the production of reactive oxygen species (ROS) and peroxynitrite to catalyze nitration of the T-cell receptor⁵⁵, deprivation of cysteine which is also necessary for the T-cell activation⁵⁶, and depletion of L-selectin, which is essential for T-cell migration.⁵⁷

Numerous studies have demonstrated that MDSC serve as a key connection between cancer and chronic inflammation in the tumor microenvironment. Therefore, a better understanding of the effects of inflammation on MDSC expansion and heightened immunosuppressive activity will lead to development of more effective cancer immunotherapy for clinical application.

Chapter 2: Enrichment of Plasma Membrane Proteins using Silica Nanoparticle Pellicles

Introduction

Analysis of the plasma membrane (PM) proteome is beneficial for a global understanding of the role of the PM proteins in response to extracellular stimuli and signaling. Integral membrane proteins have been reported to be the largest class of drug targets, especially G-protein coupled receptors, transporters, and ion channel.⁵⁸ Major challenges in the analysis of the PM proteome result from characteristics of the PM proteins, including hydrophobicity and low copy numbers, which cause the PM proteins to be underrepresented in the proteomic study.¹¹ It has been reported that the PM occupies only about 2% of the total cell volume in epithelial cells, while other parts of the cells contribute to larger fractions; for example, the cytoplasm accounts for 55%, the ER contributes to 15%, and the nucleus is considered to be 10% of the total volume.⁹ Therefore, subcellular fractionation prior to the LC-MS/MS analysis is needed to improve the identification of the PM proteins, by reducing sample complexity, and depleting highly abundant proteins from the cytosol and nucleus.

As mentioned in Chapter 1, a number of strategies have been developed for enrichment of the PM proteins, such as density gradient centrifugation¹³, affinity purification of chemically labeled proteins or glycans on the cell surfaces¹⁸, two-phase partitioning²⁰, and cationic nanoparticle pellicle methods.^{24,25} In this study, we aim to optimize the cationic nanoparticle pellicle strategy for the PM protein enrichment prior to proteomic analysis of PM proteins isolated from suspension cell cultures.

The cationic silica nanoparticle pellicle method was developed by Jacobson and coworkers in 1983 to enrich PM proteins.²⁴ The concept was built around multiple electrostatic interactions between positively charged silica nanoparticles and negatively charged cell surfaces. The excess unbound surface charge of the silica is neutralized by crosslinking with anionic polymer, such as poly(acrylic) acid. The cross-linking process is beneficial for reducing contamination from the binding of other organelle membranes to the cationic silica and for preventing internalization of the silica nanoparticles. The interactions between the cell membranes, the nanoparticles, and the anionic polymers are strong enough to be retained as large open PM-pellicle sheets after cell disruption by a high-pressure nitrogen cavitation. The pellicle sheets are denser than other cellular organelles, so they can be isolated by centrifugation. Without the pellicle formation, the PM sheets possess similar density to the other organelles as listed in **Table 1**; therefore, they are likely to be present in the same fraction when subjected to density gradient centrifugation.

This pellicle technique could be applied to the analysis of the PM proteins from many types of samples, including adherent cell culture monolayers^{25, 59},

suspended cells in culture²⁵, tissue-derived cells in suspension⁶⁰, and rat lung microvascular endothelial cells *in vivo* and *in vitro*⁶¹; however, a majority of the published reports focus on the analysis of polarized adherent cells. Our work emphasizes the optimization of the procedures for enrichment of the PM from suspended cells. For method development purposes, the human multiple myeloma cell line RPMI 8226 was used as a model.

Table 1. Density of cellular organelles.⁶²

Organelle	Density in sucrose media (g/ml)
Nuclei	>1.3
Mitochondria	1.17 – 1.21
Lysosomes	1.19 – 1.21
Peroxisomes	1.18 – 1.23
Golgi membranes	1.05 - 1.12
Plasma membranes	1.14 – 1.19

The nanoparticle pellicle enrichment technique was first integrated with high-throughput proteomic analysis by Rahbar and Fenselau in 2004.²⁵ A schematic diagram of the workflow is shown in **Figure 5**. In this study, further optimization is established by focusing on the cell lysis procedure, centrifugation technique, removal of non-PM proteins, and release of PM proteins from the pellicles.

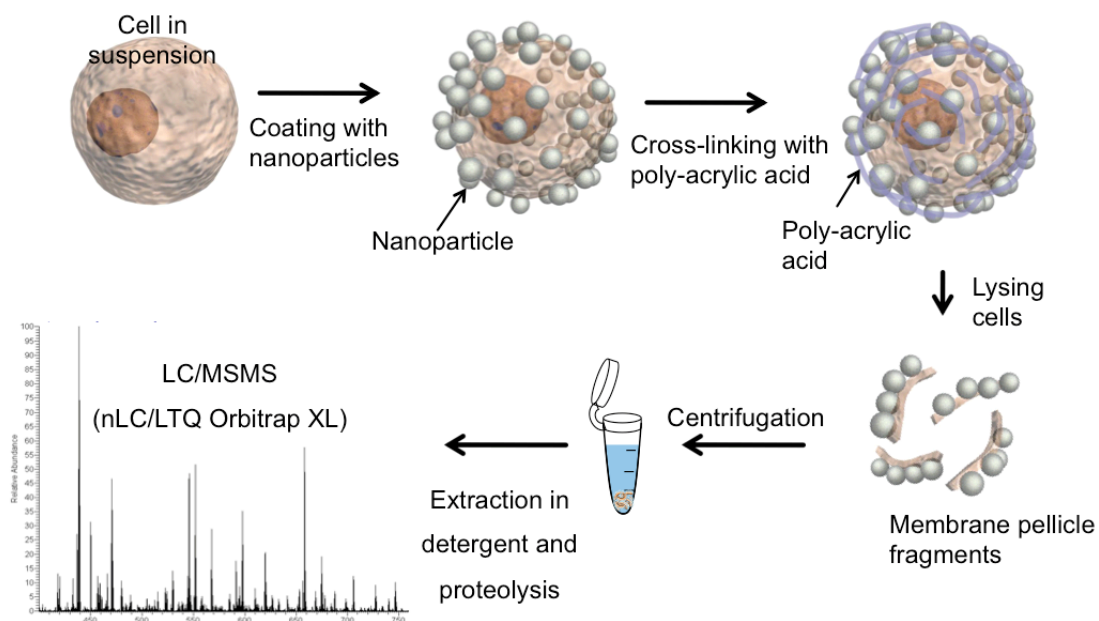


Figure 5. Schematic diagram of the plasma membrane nanoparticle pellicle technique (adapted from Kim et al., *Nanomedicine*, 2013).

Materials and Methods

Materials

The human multiple myeloma cell line RPMI 8226 and RPMI 1640 culture medium were purchased from American Type Culture Collection (Manassas, VA). Fetal bovine serum was purchased from Atlanta Biologicals (Lawrenceville, GA). Ludox CL colloidal silica, mouse monoclonal anti-human Na⁺-K⁺ ATPase primary antibody (α -subunit), alkaline phosphatase-conjugated goat anti-mouse IgG secondary antibody, BCIP/NBT solution, Nycodenz, protease inhibitor cocktail, and other chemicals were purchased from Sigma-Aldrich (St. Louis, MO) unless otherwise specified. Acetonitrile, LC/MS grade H₂O, and Pierce C18 spin columns were

purchased from Fisher Scientific (Pittsburgh, PA). Criterion Tris-HCl polyacrylamide gels, molecular weight markers, Tris-glycine-SDS buffer and RC DC™ protein assay kit were purchased from Bio-Rad (Hercules, CA). Mass-spectrometry grade trypsin and Endoproteinase Lys-C were obtained from Promega (Madison, WI). PVDF membrane was purchased from Millipore (Billerica, MA).

Cell Culture and Nanoparticle Coating

Human multiple myeloma cells were grown in RPMI 1640 medium supplemented with 5% fetal bovine serum and antibiotics. The cells were maintained at 37°C in the presence of 5% CO₂. The nanoparticle coating was performed according to a published protocol²⁵ with modifications. At confluence, 1x10⁸ cells were centrifuged at 900 xg for 5 min and washed three times with the plasma membrane coating buffer A (PMCBA, 800 mM sorbitol, 20 mM MES, 150 mM NaCl, pH 5.3). The cells were resuspended in 2 mL PMCBA and added to 10% (w/v) cationic colloidal silica in the coating buffer in a dropwise fashion, using a syringe. The cell coating was performed at 4°C for 15 min, with gentle rocking. Excess silica was removed with three washes of PMCBA, and the coated cells were collected at 900 xg for 5 min and resuspended in 2 mL PMCBA. The cells were placed dropwise into a cross-linking solution, 10 mg/mL poly(acrylic acid) in PMCBA buffer, pH 6.0 - 6.5, to neutralize the excess surface charges. The cross-linked cells were then collected and washed three times to remove the excess poly(acrylic acid). The intact cells were placed in lysis buffer in the presence of a protease inhibitor cocktail to swell the cells at 4°C for 30 min. The two lysis buffers evaluated were; (i) 2.5 mM

imidazole, pH 7.0, and (ii) relaxation buffer (50 mM KCl, 1.5 mM NaCl, 5mM PIPES, 1.75mM MgCl₂, 1mM ATP, 0.62mM EGTA, pH 7.25). Using 2.5 mM imidazole, the lysis was performed by nitrogen cavitation at 1500 psi for 30 min. For the cells in the relaxation buffer, the nitrogen cavitation was carried out at 500 psi for 10 min.

The plasma membrane nanoparticle pellicles were collected by centrifugation. Three methods of centrifugation were examined; (i) Nycodenz gradient ultracentrifugation (50% and 70% Nycodenz) at 60,000 xg for 23 min in an SW60Ti rotor, (ii) 2 M sucrose cushion centrifugation at 900 xg for 5 min, and (iii) low speed centrifugation at 100 xg for 7 min. Associated proteins were removed by washing three times each in 1 M Na₂CO₃, pH 11.4, and 1 M KCl.

Scanning electron microscopy

The cells or the PM pellicles were washed with Millonig's phosphate buffer⁶³, pH 7.3. Primary fixation was performed in 2% glutaraldehyde, and secondary fixation was performed in 1% OsO₄. The samples were dehydrated using a series of ethanol washes, followed by drying with CO₂ in a DCP-1 critical point dryer (Denton Vacuum, LLC, Moorestown, NJ). The samples were then coated with Au/Pd in a DV-503 vacuum evaporator (Denton Vacuum, LLC, Moorestown, NJ). Scanning electron micrographs were taken on an Amray 1820 scanning electron microscope (Amray Inc., Bedford, MA).

Protein extraction

An extraction of proteins from the pellicles was performed by incubation in the following buffers: 2% SDS, 62.5 mM Tris-HCl, pH 6.8, and 5% β -mercaptoethanol (buffer A), 6 M urea, 9 mM EDTA, 9% SDS, 0.5 M Tris-HCl, pH 6.8, 3.6% β -mercaptoethanol (buffer B), 6 M urea, 2 M thiourea, 100 mM Tris-HCl, pH 6.8, 10 mM DTT, pH 8.0 (buffer C), and 8 M urea in 50 mM NH_4HCO_3 , pH 7.8 (buffer D), or 0.1% RapiGestTM SF in 50 mM NH_4HCO_3 , pH 7.8, at 100°C for 5 min in a microwave (CEM Corporation, Matthews, NC). The concentration of proteins released from the pellicles was estimated by using an RC DCTM protein assay kit (Bio-Rad, Hercules, CA). For buffer A, sequential extraction was performed up to five times.

SDS-PAGE

The samples were loaded onto an 8-16% linear gradient polyacrylamide gel (Bio-Rad Criterion precast gel) and run at 200 V for 90 min. Following fixation, the gel was stained with Coomassie blue and destained. The gel image was taken on a GS-800 Densitometer (Bio-Rad, Hercules, CA) with the Bio Rad PDQuest software.

Western Blot Analysis

Proteins (25 μg) were subjected to SDS-PAGE using a 7.5% polyacrylamide gel. Following electrophoresis, the proteins were transferred to a PVDF membrane using a Bio-Rad Mini trans-blot system, at 4°C, 100 V, for 1 h. The Western blotting was performed according to a protocol from Sigma-Aldrich.⁶⁴ Mouse antibody against $\text{Na}^+\text{-K}^+$ ATPase (α -subunit) was used as a primary antibody, and an alkaline

phosphatase-conjugated goat anti-mouse IgG was used as a secondary antibody. The colorimetric detection was carried out using a BCIP/NBT substrate.⁶⁴ Imaging was performed on a ChemiDoc XRS+ system with an Image Lab Software (Bio-Rad, Hercules, CA).

Protein digestion

Comparison of lysis conditions

Extracted proteins from the pellicles were subjected to a chloroform/methanol precipitation with the sample : chloroform : methanol : water ratio of 1:1:4:3.⁶⁵ The precipitate was redissolved in 50 mM NH₄HCO₃. The proteins were reduced with 20 mM DTT at 56°C for 30 min, and alkylated with 40 mM iodoacetamide in the dark for 30 min. Digestion by Lys-C enzyme was achieved in 8 M urea/50 mM NH₄HCO₃ for 3 h (enzyme to protein ratio of 1:50 w/w), followed by trypsin proteolysis in 1.6 M urea/50 mM NH₄HCO₃ for 16 h at 37°C (enzyme to protein ratio of 1:25 w/w). Tryptic peptides were desalted by a Thermo C18 spin column using a manufacturer's instruction.

Comparison of extraction buffers

Precipitation of the proteins from each extraction buffer was achieved by incubation with four volumes of acetone at 20°C for 2 h. The proteins were re-solubilized by Laemmli buffer and subjected to 1D-gel electrophoresis. Subsequently, proteins were digested in the gel and extracted for analysis by LC-MS/MS, following a standard procedure.⁶⁶ Briefly, the proteins in gel matrices were

reduced with 10 mM DTT at 56°C for 30 min, and alkylated with 55 mM iodoacetamide in the dark for 20 min. The gel bands were destained with 50% acetonitrile in 50 mM NH₄HCO₃ and dehydrated with pure acetonitrile. Then the gels were rehydrated in a digestion buffer containing 13 ng/ μ L trypsin in 10 mM NH₄HCO₃ containing 10% (v/v) acetonitrile for 120 min. Trypsin digestion was carried out overnight at 37°C in an incubator with thermostat control. After proteolysis, peptide products were extracted from the gels by adding an extraction buffer (1:2 (v/v) 5% formic acid/acetonitrile) to the digest, so that the ratio of extraction buffer/digest is approximately 2:1. Protein extraction was performed at 37°C in a shaker for 15 min. Then the digest was lyophilized and resuspended in 0.1% formic acid.

LC-MS/MS analysis

Digested peptides were separated and analyzed by a Shimadzu Prominent nanoHPLC (Shimadzu Scientific Instruments, Columbia, MD) interfaced to an LTQ-orbitrap XL (Thermo Fisher Scientific, San Jose, CA). The digests were injected to an Acclaim PepMap 300 C18 trapping column (Dionex, Sunnyval, CA) via an autosampler, and desalted with solvent A (97.5% H₂O, 2.5% acetonitrile, 0.1% formic acid) for 10 min. The fractionation was performed on a reverse phase, 0.075mm x 150mm, Zorbax 300SB-C18 nanobore column (Agilent Technologies, Palo Alto, CA). The peptides were eluted at a flow rate of 300 nL/min by a linear gradient increasing from 10% to 60% solvent B (97.5% acetonitrile, 2.5% H₂O, 0.1% formic acid) in 90 min and 60% to 85% solvent B in the next 20 min. The column

was connected to a 15 μm fused-silica PicoTip® (New Objective, Inc., Woburn, MA) and a nano-electrospray ionization source (Thermo Fisher Scientific, San Jose CA), interfaced with the LTQ-orbitrap XL mass spectrometer. The precursor ions were recorded in the orbitrap at a resolving power of 30,000 at m/z 400, while the product ions were acquired in the LTQ. In each activation cycle, the nine most abundant precursor ions were subjected to collision-induced dissociation (CID), with a normalized collision energy of 35, precursor ion isolation window of 3 Da and activation time of 30 ms. Dynamic exclusion was enabled to exclude the precursor ions that were previously scanned within 180 s. MS spectra were acquired using Xcalibur 2.0 software (Thermo Fisher Scientific, San Jose, CA).

Bioinformatics

Mass spectra in .RAW format were converted to .mgf format using Proteome Discover 1.2 (Thermo Fisher Scientific, San Jose, CA), and searched against a human UniProt/SwissProt database on MASCOT⁶⁷ server. The significance threshold of peptide identification was set at E-value lower than 0.05. Scaffold 2.6 (Proteome Software Inc, Portland, OR) was used to remove redundant peptide identifications, as well as to designate a cellular location based on a Gene Ontology Annotation (GOA).⁶⁸ Alternatively, mass spectra were submitted to a PepArML batch uploader and searched against a human UniProt database using PepArML meta-search engine.⁴⁸ The data was processed by an in-house software with a parsimony function to remove redundant peptide identifications. The proteins were identified based on the spectrum level false discovery rate (FDR) lower than 10%. The cellular

localization was assigned by GO Slim annotation using the Protein Information Resource server (<http://pir.georgetown.edu/>).

Results and Discussion

Using the workflow shown schematically in **Figure 5**, the morphology of the cells from each coating step was observed by a scanning electron microscope as shown in **Figure 6**. Prior to coating with the nanoparticles, the micrographs revealed the characteristic microprojections of multiple myeloma cell surfaces. After applying the cationic silica nanoparticles and cross-linking with poly(acrylic) acid, a uniform and complete coating was observed. Large open PM pellicle sheets were obtained following a cell disruption by N₂ decompression.

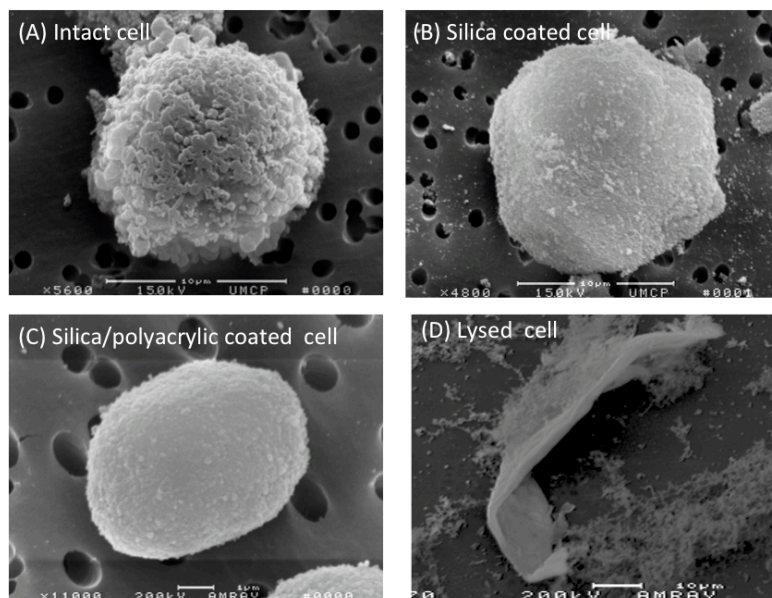


Figure 6. SEM micrographs of (A) human multiple myeloma cell, (B) silica nanoparticles coated cell, (C) poly(acrylic) acid coated cell, and (D) a lysed plasma membrane sheet.

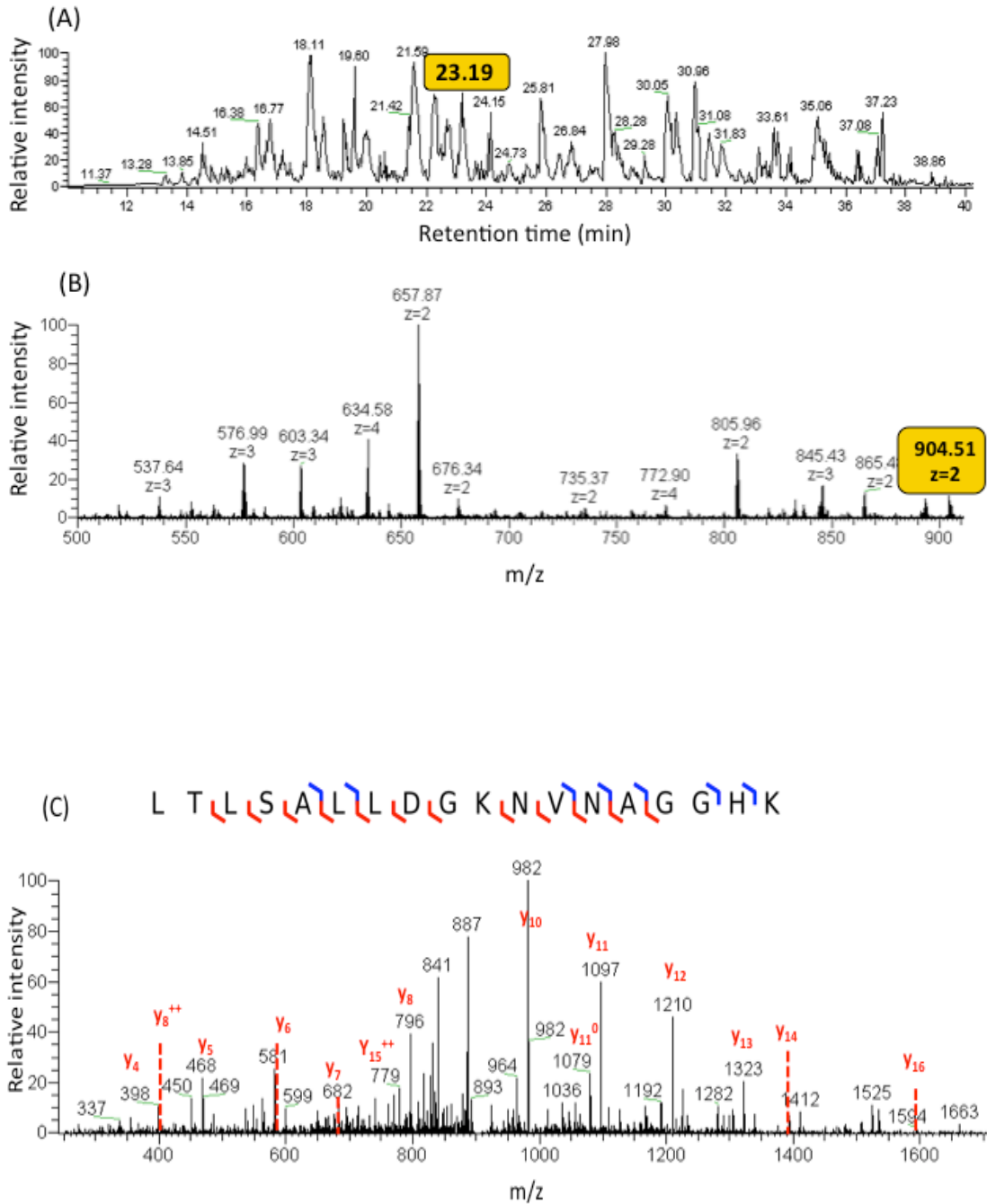


Figure 7. (A) Chromatogram of tryptic peptides from in-gel digestion, and (B) precursor scan at retention time 23.19, and (C) MS2 spectra of the peptide L T L S A L L D G K N V N A G G H K from the precursor 904.51 ($z=2$), with E-value $3.3E-5$. This peptide is from the **voltage-dependent anion selective channel protein**.

The pellicles were collected by centrifugation, and associated proteins were removed by washing with salt solutions prior to protein extraction in a detergent solution, proteolysis, and LC-MS/MS analysis. **Figure 7** represents an example of chromatograms from the analysis, as well as a precursor ion spectrum, and a product ion spectrum of a peptide from the PM protein, voltage-dependent anion selective channel. Several factors were considered to enhance the efficiency of the PM protein enrichment prior to protein digestion, including (i) lysis conditions, (ii) centrifugation procedures, (iii) non-PM proteins removal, and (iv) PM protein extraction.

Two types of cell lysis buffer have been shown to be compatible with N₂ cavitation, a hypotonic buffer (2.5 mM imidazole) and a relaxation buffer.^{25, 69} In this study, the PM protein enrichment was investigated by Western blotting of a PM protein marker, Na⁺-K⁺ ATPase and a large-scale proteomic analysis. The Western blot in **Figure 8(A)** reveals that the lysis in the hypotonic buffer provides higher intensity of the Na⁺-K⁺ ATPase, in comparison to the lysis in the relaxation buffer. For LC-MS/MS analysis, subcellular locations of the identified proteins were assigned according to GOA.⁶⁸ Considering the percentage of PM proteins identified, the hypotonic buffer also provides a larger proportion of the PM proteins (**Figure 8(B)**). This observation suggests that the hypotonic buffer may provide more successful lysis of the nanoparticle-coated cells; thus, the level of contamination from other organelle proteins is lower.

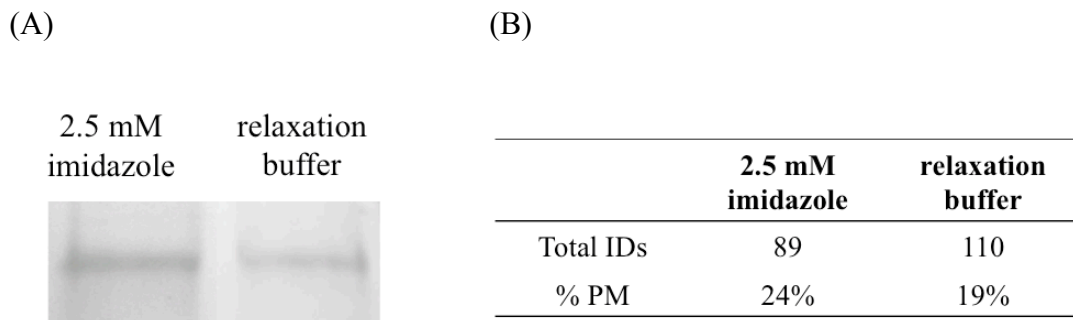


Figure 8. Comparison of two lysis buffers by (A) Western blotting of a plasma membrane protein marker, Na⁺-K⁺ ATPase, and (B) numbers of proteins identified from LC-MS/MS experiment and the percent of identified proteins that were located in the plasma membrane (%PM).

Table 2. Proteomic analysis of the PM protein enrichment by the pellicle technique integrated with three different centrifugation methods.

	Nycodenz gradient	sucrose cushion	low speed centrifugation
% PM	8% - 22%	18-20%	16%-25%

After the PM-nanoparticle pellicles were generated, they were isolated by centrifugation. Previous studies have demonstrated the use of density gradient centrifugation for subcellular fractionation such as sucrose and Nycodenze gradients.¹³ Since the formation of the PM pellicle increases the density of the PM, we evaluated the low-speed centrifugation in parallel with the gradient centrifugation. The proportion of the PM proteins listed in **Table 2** indicates that the simple centrifugation of the PM-nanoparticle pellicles provides a slightly higher percentage of the PM proteins, in comparison to the two gradient centrifugation techniques. This result suggests that the pellicle isolation procedure could be simplified by using the low-speed centrifugation, which illustrates an advantage of increasing density of the PM sheets.

Following the sedimentation, procedures for removal of soluble proteins associated with the pellicles and for releasing of the PM proteins from the pellicles were optimized. For the contaminants removal, the PM pellicles were subjected to a non-PM protein removal by high-pH and high-ionic strength buffers.⁷⁰ The patterns of proteins removed by a series of washing with the lysis buffer (2.5 mM imidazole), 1 M Na₂CO₃, pH 11.4, and 1 M KCl were visualized by a gel electrophoresis, followed by silver staining as shown in **Figure 9**. The gel indicates that high amount of proteins, possibly soluble proteins, were removed from the pellicle, as shown by the decrease in intensity of protein bands prior to the extraction.

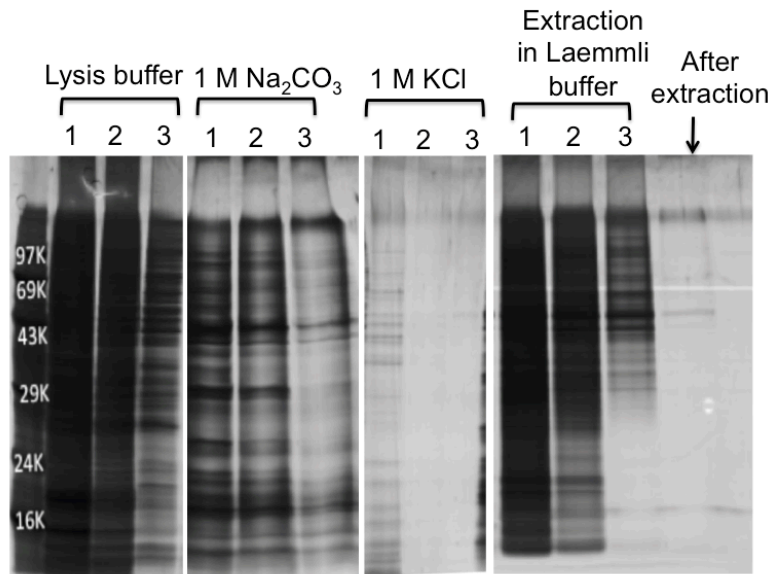


Figure 9. Silver-stained SDS-PAGE gels showing (i) the presence of soluble proteins after removal from the pellicles by washes in lysis buffer, high pH (1 M Na_2CO_3), and high salt (1 M KCl) buffers, (ii) the presence of proteins after releasing from the pellicles into extraction buffer, and (iii) the absence of proteins after three extractions in Laemmli buffer.

Next, the method for releasing of the PM proteins from the PM pellicle sheets was evaluated. It is a critical step due to the strong interaction between proteins, especially transmembrane proteins, and phospholipids, as well as the interaction between the PM sheets, silica particles, and poly(acrylic) acid. The solubilization abilities of detergents and chaotropes were evaluated using the number and the percentage of plasma membrane proteins identified in each analysis. Four buffers subjected to this examination are listed in **Figure 10**. Protein extraction for each was performed at 100°C , for 5 min, with microwave irradiation at 50 W. The spectra from LC-MS/MS analysis were searched against a human SwissProt database on a

MASCOT server. **Figure 10** reveals that buffer A provided the highest number of proteins, of which 19% have been located in the PM. The same percentage of the PM proteins was found in the extraction from buffer D, with a lower number of the total proteins. Even though buffer B and buffer C provided a higher percentage of the PM proteins, the total numbers of proteins were relatively low. Thus, buffer A was chosen for further experiments.

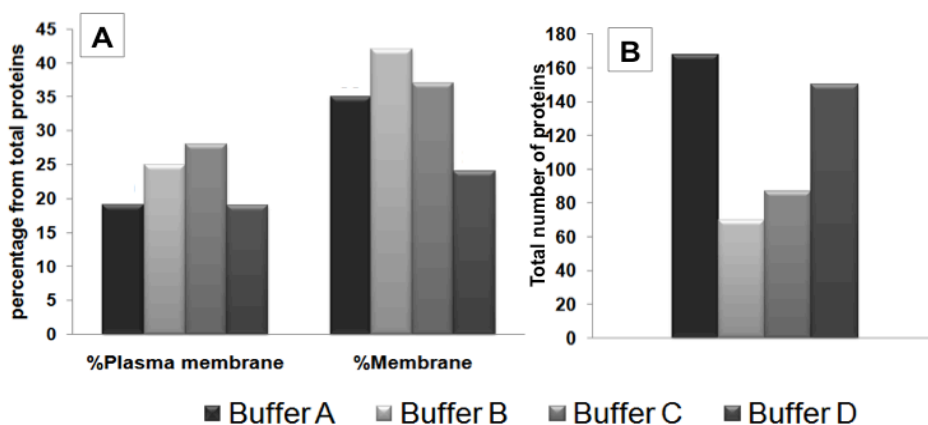


Figure 10. Comparison of extraction buffer efficiency: **Buffer A**; 2% SDS, 62.5 mM Tris-HCl, 5% β - mercaptoethanol, **Buffer B**; 6 M Urea, 9 mM EDTA, 9% SDS, 0.5 M Tris-HCl, 3.6% β - mercaptoethanol, **Buffer C**; 6 M urea, 2 M thiourea, 100 mM Tris-HCl, 10 mM DTT, and **Buffer D**; 8 M urea in 50 mM NH_4HCO_3 . (A) percentage of plasma membrane and membrane proteins and (B) total number of proteins identified from MASCOT with E-values <0.05.

Since the embedded PM proteins are difficult to solubilize, sequential extraction was performed in buffer A (Laemmli buffer) to ensure a complete

recovery. As shown in **Figure 9**, a significant amount of proteins were detected by silver staining up to the third extraction. A concentration of recovered proteins was determined by RC DCTM protein assay (Bio-Rad, Hercules, CA). The protein concentration shown in **Figure 11 (A)** suggests that three repetitions of the protein extraction from the pellicles are sufficient, which is in good agreement with the intensity on the silver-stained gel. In addition, an MS-compatible surfactant, 0.1% RapiGestTM SF (Waters, Milford, MA) in 50 mM NH₄HCO₃, was also examined as an extraction buffer. **Figure 11 (B)** reveals that Laemmli buffer provided higher protein concentration than 0.1% RapiGestTM SF. However, both types of buffers were used in additional experiments; since the RapiGestTM SF is compatible with enzymatic digestion and the downstream LC-MS/MS analysis, while Laemmli buffer requires additional sample processing to remove the detergent.

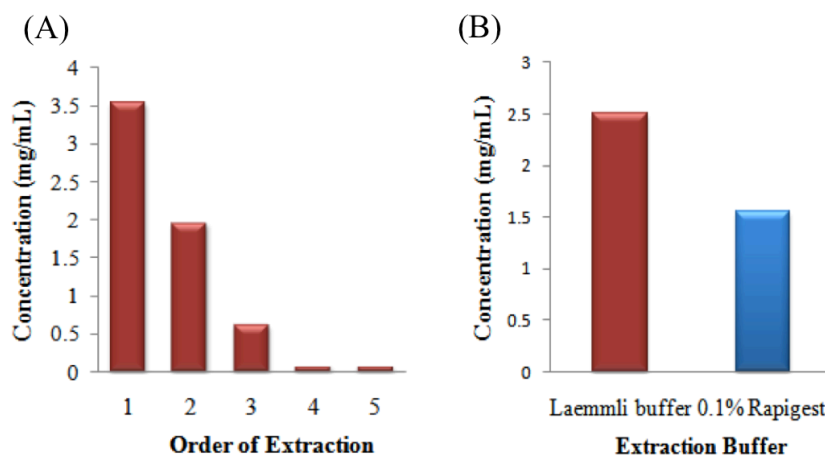


Figure 11. (A) Bar chart showing protein concentration in Laemmli buffer after reiterative extractions. (B) Bar chart showing the concentration of proteins released from the silica pellicle in Laemmli buffer and 0.1% RapiGestTM SF.

The results from LC-MS/MS analysis, followed by MASCOT searching against a human UniProt database, are summarized in **Table 3**. The percentage of the PM proteins identified from the triplicate extraction is only slightly different; therefore, the three fractions could be combined for the downstream protein characterization.

Table 3. Number of proteins identified in each step of sequential extraction.

	Order of extraction		
	1	2	3
Number of proteins identified	320	337	314
% PM	19%	17%	21%

Summary

The procedure for the PM protein enrichment by silica nanoparticles has been optimized and simplified. With cell lysis in 2.5 mM imidazole, low-speed centrifugation, high-pH and high-ionic strength salt stripping, and sequential extraction in Laemmli buffer, a high level of enrichment of the PM protein was observed. Based on Western blotting (**Figure 12**), a significantly higher signal intensity of the PM protein marker Na⁺-K⁺ ATPase was observed in the pellicle-enriched sample than the cell lysate control. Cellular locations of the proteins

identified from LC-MS/MS analysis of the silica nanoparticle-enriched PM sample and the cell lysate control are shown in **Figure 13**. In the enriched samples, 18% of identified proteins were located in the PM; while 12% PM was observed in the cell lysate control. In addition, it is notable that the fractions of PM and membrane proteins are higher in the enriched sample than in the control, while the nucleoprotein fraction is depleted. These optimized procedures could be integrated to further analyses and characterization of the PM proteins.

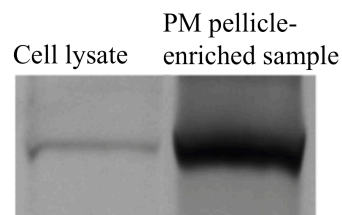


Figure 12. Western blotting of $\text{Na}^+\text{-K}^+$ ATPase of aluminosilicate enriched samples vs. whole cell lysate control (adapted from Reference 8).

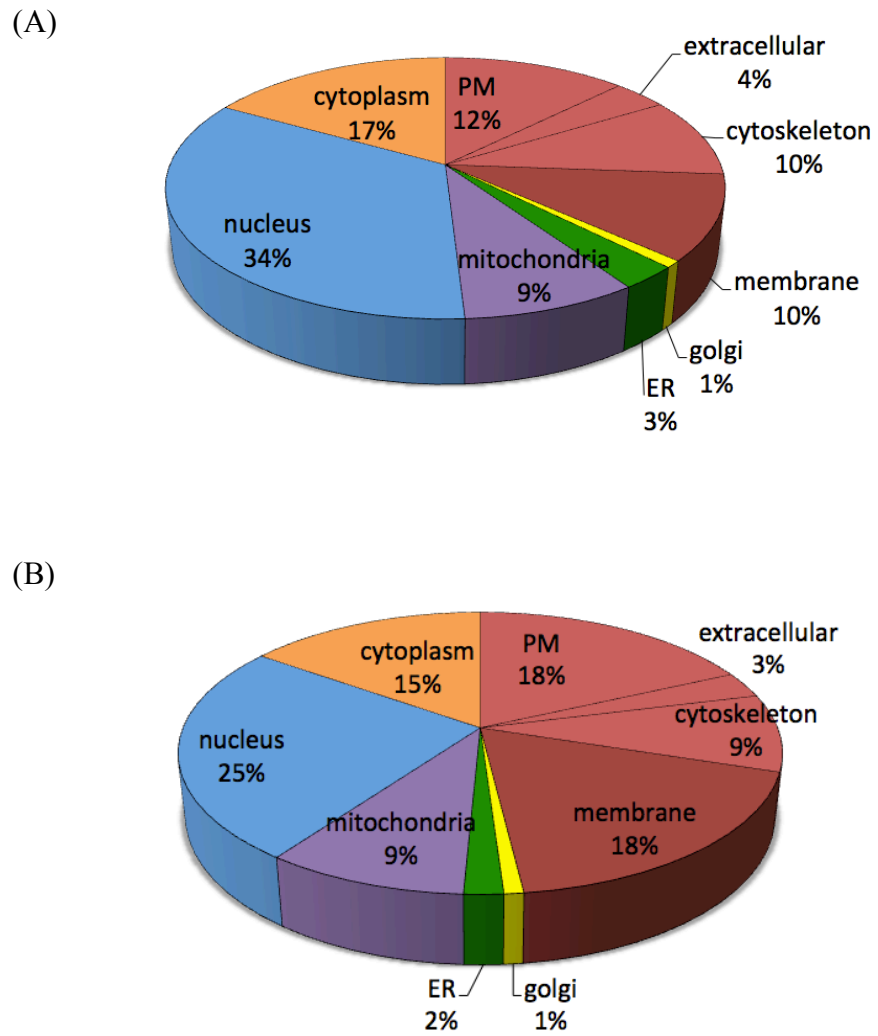


Figure 13. Cellular components of proteins identified from (A) whole cell lysate control and (B) PM pellicle - enriched sample.

Chapter 3: Optimization of Proteomic Workflow for Analysis of Plasma Membrane Proteins

(A) Comparative Study of Workflows Optimized for In-gel, In-solution, and On-filter Proteolysis in the Analysis of Plasma Membrane Proteins

(Adapted from Reference 7: Choksawangarn, W.; Edwards, N.; Wang, Y.; Gutierrez, P.; Fenselau, C., Comparative Study of Workflows Optimized for In-gel, In-solution, and On-filter Proteolysis in the Analysis of Plasma Membrane Proteins. *J Proteome Res* **2012**, 11, 3030-4)

Introduction

The comparison of three strategies to study proteins recovered from the eukaryotic plasma membrane (PM) is evaluated. These strategies have been widely used and optimized by the proteomics community and are designed to solubilize hydrophobic proteins, provide tryptic digestion, and remove SDS. They are: (1) protein digestion in polyacrylamide gel matrix⁶⁶ (in-gel digestion of proteins); (2)

protein precipitation in chloroform/methanol followed by resolubilization and digestion in urea⁶⁵ (in-solution digestion); and (3) filter-aided sample preparation (on-filter digestion), in which the SDS–urea exchange and enzymatic cleavage take place in a molecular weight cut off filter.^{71, 72} Each one of these strategies has its advantages and disadvantages. Briefly, the first technique, in-gel digestion, is robust, reproducible and effective; however, it is laborious and time-consuming. The second method, precipitation/in-solution digestion, requires less time for preparation, but it introduces sample losses due to a low resolubilization of aggregated proteins.⁷³ The third method, on-filter digestion, has been described as universal and enhancing membrane protein identification^{71, 72}, but other reports dispute the universality of the method and report limited reproducibility and the loss of protein on the filter.^{74, 75}

Although instrumental technologies for handling complex protein mixtures are continually being improved (e.g., aspects of tandem mass spectrometry and high performance liquid chromatography), effective strategies for preparation of hydrophobic samples are still imperfect. Ideally, bottom-up analysis of plasma membrane proteins would include enrichment of the plasma membrane followed by solubilization of the hydrophobic proteins to accommodate proteolysis. Organic solvents have been successfully demonstrated for solubilization of membrane proteins, proteolysis, and compatibility with mass spectrometry.⁷⁶⁻⁷⁹ Urea and SDS solutions have classically been used to solubilize hydrophobic proteins, and these have been shown to accommodate tryptic proteolysis at dilute concentrations.^{75, 76, 80,}

⁸¹ Even at low concentrations, these detergents must be removed after digestion to

maintain optimal ionization conditions. Mass spectrometry-compatible surfactants have also been proposed to support enzymatic cleavage of membrane proteins.^{77, 78}

In this study, plasma membrane proteins were enriched by cationic silica nanoparticle coating, following the method developed by Jacobson.^{24, 25} In our hands, repeated incubation with 2% SDS is required to recover plasma membrane proteins from the pellicle, and this is the solution with which we have compared the three workflows. This study explores the effectiveness of each strategy in identifying plasma membrane peptides and proteins and investigates the properties of the peptides and proteins identified, including hydrophobicity and transmembrane characteristics.

Materials and Methods

Materials

Ludox CL colloidal silica 30 wt% was purchased from Sigma-Aldrich (St. Louis, MO). Other chemicals were also obtained from Sigma-Aldrich unless specified otherwise. Endoproteinase Lys-C and trypsin were obtained from Promega (Madison, WI). Criterion Tris-HCl (8-16%) precast gels, Tris-glycine-SDS buffer, molecular weight standards, and protein assay kit reducing agent and detergent compatible (RC DCTM) were purchased from Bio-Rad (Hercules, CA). Amicon 3 kDa centrifugal filters were purchased from Millipore (Billerica, MA). RPMI 1640 tissue culture medium was obtained from American Type Culture Collection (Manassas, VA), and fetal bovine serum was purchased from Atlanta Biologicals (Lawrenceville, GA).

Isolation of plasma membrane proteins using silica nanoparticle pellicles

Human multiple myeloma RPMI 8226 cells were grown in RPMI 1640 minimum essential medium as previously described in Chapter 2. Plasma membrane proteins were obtained from 1×10^8 RPMI 8226 cells following published methods that employ cationic silica nanoparticles²⁵ with slight modifications. Briefly, the cells were washed and resuspended in plasma membrane coating buffer A (PMCBA = 800 mM sorbitol, 20 mM MES, 150 mM NaCl, pH 5.3). The suspension was added in a dropwise fashion to a suspension of silica nanoparticles in PMCBA (10% weight by volume) and gently rocked at 4°C for 15 min. Silica surfaces were neutralized by placing the coated cells dropwise into a solution of 10 mg/mL of poly(acrylic acid) in PMCBA buffer, pH 6.0–6.5, and gently rocking at 4°C for 15 min. The intact coated cells were incubated in 2.5 mM imidazole buffer with protease inhibitor cocktail (Sigma) at 4°C for 30 min. Lysis by N₂ cavitation followed at 1250 psi. The plasma membrane/nanoparticle pellicles were sedimented at 100 xg for 7 min and subjected to a sucrose (2 M) cushion centrifugation. Associated cytosolic proteins were removed by washing three times each with 1 M KCl and 1 M Na₂CO₃, pH 11.4. Protein was solubilized from the pellicles by triplicate incubations in 2% SDS, 62.5 mM Tris-HCl, and 5% β- mercaptoethanol at 100°C for 5 min in a microwave oven (CEM Corporation, Matthews, NC). Protein concentration was determined using an RC DCTM protein assay kit (Bio-Rad).

Protein Digests

In-gel digestion was performed by standard procedures.⁶⁶ Proteins (80 µg) were loaded onto an 8-16% Bio-Rad Criterion precast gel and run at 200 V for 90 min. The gel was then stained with Coomassie blue, and 17 bands were excised. Each was reduced with 10 mM DTT at 56°C for 30 min and alkylated with 55 mM iodoacetamide for 20 min. The gel bands were destained with 50% acetonitrile in 50 mM NH₄HCO₃ and dehydrated with 100% acetonitrile. Trypsin digestion (13 ng/µL) was performed overnight prior to peptide extraction in 1:2 (v/ v) 5% formic acid/acetonitrile.

Precipitation and in-solution digestion were carried out using standard methods⁶⁵. Proteins (80 µg) were precipitated by the addition of chloroform and methanol (sample/chloroform/ methanol/water 1:1:4:3 by volume) and redissolved in 8 M urea. Reduction and alkylation were performed by incubation with 20 mM DTT at 56°C for 30 min and 40mM iodoacetamide in the dark for 30 min, respectively. Lys-C digestion (16 ng/µL) was performed in 8 M urea for 3 h, followed by trypsin cleavage (32 ng/µL) in 1.6 M urea for 16 h at room temperature.

Lastly, on-filter digestion was performed on a 3 kDa molecular weight cut off filter using the procedure described by Wisniewski et al.⁷¹ Briefly, 80 µg of protein was applied to the filter in Laemmli buffer containing 100 mM DTT. The solution was exchanged with 8 M urea in 0.1 M Tris HCl, pH 8.5, and the retentate was incubated for 5 min with 50 mM iodoacetamide. The retentate was again exchanged three times with 8 M urea in 0.1 M Tris HCl, pH 8.0. Lys-C digestion (16 ng/µL) was achieved on the filter in a wet chamber at room temperature overnight. This

incubation was terminated by adding 300 μL of 50 mM NH_4HCO_3 to dilute the urea to 2 M and make the solution suitable for trypsin digestion. Trypsin digestion followed (32 ng/ μL) at room temperature for 4 h. Tryptic peptides prepared from the last two methods were desalted with a Thermo C18 spin column prior to HPLC separation.

HPLC-MS/MS analysis

Analyses were carried out on a Shimadzu Prominent nanoHPLC (Shimadzu, Columbia MD) interfaced to an LTQ-orbitrap XL (Thermo Fisher Scientific, San Jose CA). Peptide mixtures obtained from the in-solution and on-filter digestions were each injected via an autosampler in six aliquots in order to optimize precursor selection⁸². Extracts from the 17 gel slices were injected separately under the same experimental conditions. Peptides were injected into an Acclaim PepMap 300 C18 precolumn (Dionex, Sunnyvale CA) and desalted by solvent A (97.5% H_2O , 2.5% acetonitrile, 0.1% formic acid) for 10 min. The separation was performed in a Zorbax 300SB-C18 (Agilent Technologies, Palo Alto CA) nanobore column (0.075 \times 150 mm) with a linear gradient increasing from 10 to 60% solvent B (97.5% acetonitrile, 2.5% H_2O , 0.1% formic acid) in 90 min, followed by another increase from 60% B to 85% B through 20 min. The flow rate was 10 $\mu\text{L}/\text{min}$ for peptide trapping and 300 nL/min for separation. Precursor ions were scanned in the orbitrap with a resolution of 30000 at m/z 400. In each activation cycle, the nine most abundant ions were fragmented by collisional induced dissociation (CID) prior to product ion scans in the

LTQ. Dynamic exclusion was enabled with 1 repeat count for 180 s. Data were acquired using Xcalibur 2.0 software (Thermo Fisher Scientific, San Jose, CA).

Bioinformatics

Following spectral acquisition, .RAW data files from Xcalibur were submitted to the PepArML batch uploader and searched with the PepArML meta-search engine (<https://edwardslab.bmcb.georgetown.edu/PepArML/>)⁴⁸ against the human IPI database. PepArML combines search results from Mascot and six open source search engines. Results were processed by an in-house tool to remove redundant peptide identifications. The spectrum level false discovery rate (FDR) filter was set lower than 10%, and two or more peptides were required for protein identification. Protein localization was assigned by GO Slim annotation using the Protein Information Resource server (<http://pir.georgetown.edu/>). The number of transmembrane helices in proteins was predicted by TMHMM 2.0⁸³. Protein GRAVY (grand average of hydrophathy) scores were determined using the GRAVY Calculator (<http://www.gravy-calculator.de/>). A reference set of 3965 plasma membrane proteins was assembled by combining the human plasma membrane and cell surface categories in the UniProt database (<http://UniProt.org>) to provide theoretical values for comparison of transmembrane helices and hydrophobicity.

Results and Discussion

The efficiency of the three different procedures for detergent removal and digestion of PM proteins was evaluated on the basis of the number of PM proteins identified, PM protein hydrophobicity determined by GRAVY scores, and the number of PM proteins containing transmembrane helices predicted by the TMHMM algorithm. As shown in **Tables 4** and **Appendix Table 1**, the highest number of PM proteins identified was obtained using in-gel digestion, followed by on-filter digestion and in-solution digestion, respectively. To further test this observation, the number of peptides required for protein identification was varied, and the relative performance of the methods was unchanged. In-gel digestion provided a significantly higher number of PM protein identifications.

Table 4. Number of PM proteins and PM peptides identified using three different methods.

	in-gel	in-solution	on-filter
PM protein IDs (on the basis of 2 peptides)	272	106	118
PM proteins containing TMDs (on the basis of 2 peptides)	106	33	37
total PM peptide IDs	2580	967	1009

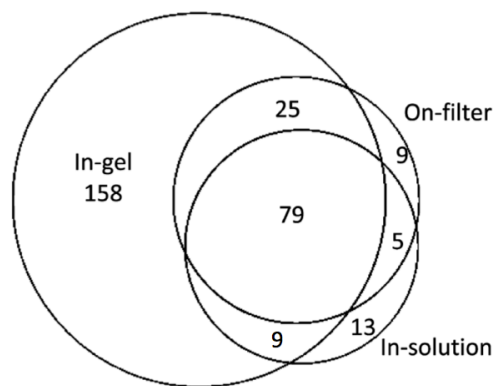


Figure 14. Venn diagram showing overlap in proteins identified using in-gel, in-solution, and on-filter digestion.

While it is not unexpected that the protein-level fractionation afforded by the in-gel method might identify more low abundance proteins than the other techniques, a comparison of spectral counts suggests that additional factors contribute to the identification of fewer plasma membrane proteins by the in-solution and on-filter methods. The Venn diagram in **Figure 14** shows that 79 proteins were identified by all three strategies (see also **Appendix Table 1**). An estimate of the relative abundances of these proteins in each of the digestion matrices was provided by spectral counting⁸², with spectral counts for each of the six replicate injections of the in-solution and on-filter digestion products summed. For each of the 79 in-common proteins, the method (in-gel, in-solution, on-filter) with the largest spectral count was identified. Of 78 proteins, 59 from the in-gel method had the largest spectral-count (p -value $< 2.3 \times 10^{-15}$, χ^2 -test). One protein was discarded because the spectral counts from the in-gel method and on-filter digestion were equivalent. This indicates that peptides from the in-common proteins provide more recorded spectra⁸² when the in-gel method is used. Since all three digestions were initiated with equivalent amounts of total protein, one interpretation is that protein has been lost during

precipitation/resolubilization in the solution workflow, and that on the filter incomplete resolubilization and incomplete enzyme access contribute to the reduced levels of peptide spectra recorded.

The distribution of transmembrane domains (TMD) in the PM proteins identified using the three procedures were compared to each other, and also to the distribution of transmembrane domains in a reference set of proteins listed as plasma membrane or cell surface in the UniProt database (**Figure 15**). The natural abundance of 7 TM receptors in the plasma membrane is reflected in the distribution of the reference set, though not in the experimental samples. In-gel digestion provided 106 proteins containing one or more transmembrane helices, whereas on-filter digestion and in-solution digestion provided 37 and 33 transmembrane proteins, respectively (**Table 4**).

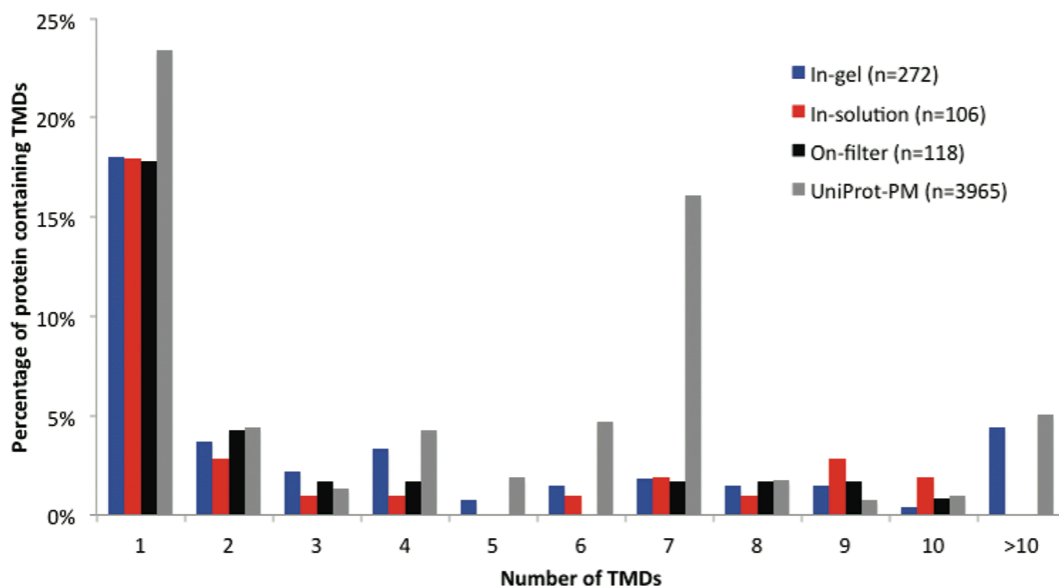


Figure 15. Correlation between fractions of plasma membrane proteins identified and the number of transmembrane helices.

The hydrophobicity⁸⁴ of the plasma membrane proteins identified in our three experiments is summarized in **Figure 16**, along with the reference set. Higher GRAVY scores indicate higher hydrophobicity. All sample sets are maximally represented around -0.2; however, the reference set exhibits a second maximum, between 0.4 and 1.0. The in-gel values provide the best match for this second maximum. On the basis of the distributions and averages, PM proteins identified by in-gel digestion are more hydrophobic compared to those identified using on-filter and in-solution digestion.

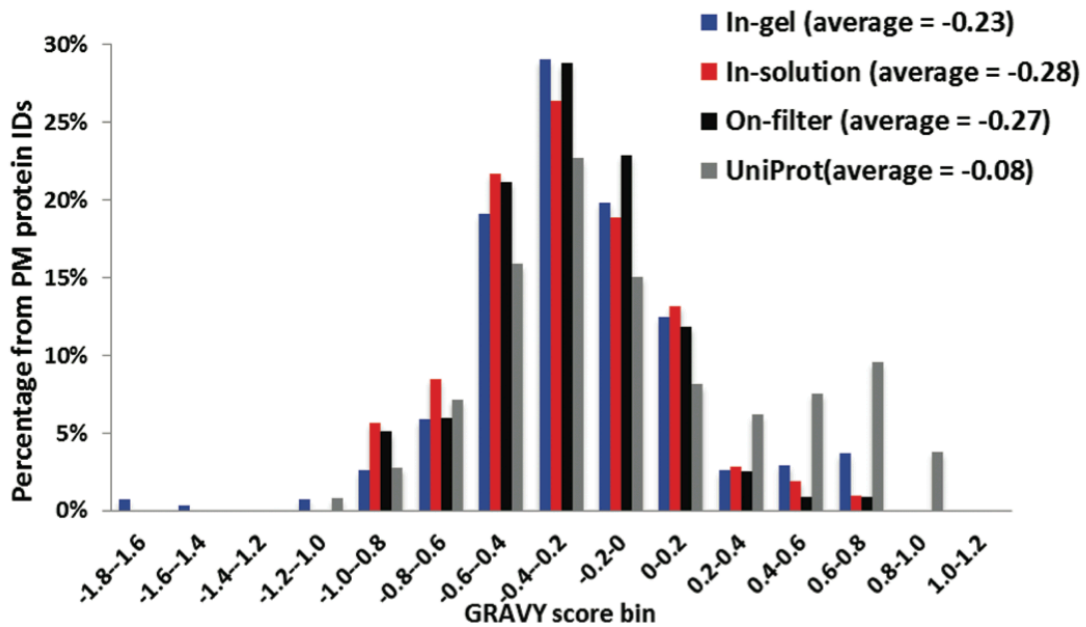


Figure 16. Correlation between the number of plasma membrane proteins identified and their hydrophobicity.

Summary

This comparison of three workflows to provide tryptic digestion of plasma membrane proteins and removal of 2% SDS indicates that in-gel digestion provides advantages over workflows optimized for on-filter and in-solution digestions, on the basis of the number of plasma membrane proteins identified, and the numbers of transmembrane proteins and hydrophobic proteins characterized, which are commonly underrepresented in proteomic analysis of the plasma membrane. Consequently, and acknowledging the additional experimental manipulation required, one-dimensional gel fractionation and in-gel digestion are found to provide superior analysis of plasma membrane proteins.

(B) Evaluation of Enzymatic Digestion Methods using a Model Transmembrane Protein and a Complex Mixture of Plasma Membrane Proteins

Introduction

In bottom-up proteomics, a high percentage of sequence coverage is required for reliable protein identification. The highly structured and hydrophobic properties of membrane proteins make enzymatic cleavages difficult, resulting in limited sequence coverage. The membrane proteins identified in proteomic analyses are commonly underrepresented owing to their intrinsic characteristics. The main subgroup of integral membrane proteins that causes difficulties in proteomic research is α -helical proteins, which displays higher hydrophobicity than the β -barrel proteins.⁷⁰

Integral membrane proteins are classified into several types including Type 1 and Type 2 single-pass and multi-pass membrane proteins as shown in **Figure 17(A)**.⁸⁵ During enzymatic digestion, the proteins containing long hydrophilic chains, globular domains, or loops can be easily observed in LC-MS/MS analysis; however, those containing membrane-spanning segments (25-30 residues) with short hydrophilic loops are difficult to detect. Technical challenges involve: (1) protein precipitation during isolation and pre-fractionation, (2) limited enzyme accessible sites, and (3) less frequent lysine and arginine residues, which results in relatively long tryptic peptides with a few charges, and provide poor MS/MS signals.

The most common enzyme used in proteomic study is trypsin, which cleaves the proteins at the C-terminus of lysine and arginine residues, except when they are followed by proline. The conventional tryptic digestion method has been optimized to facilitate more enzyme-accessible sites, resulting in higher percent sequence coverage, using an appropriate amount of detergents or organic solvent, such as 0.1% SDS,⁷⁵ 60% MeOH,⁷⁹ 80% acetonitrile,⁸⁶ MS-compatible surfactants.⁷⁸ Also, the use of other enzymes has been reported to accommodate the lack of K and R residues in the transmembrane regions, as well as to maintain enzymatic activity in harsh conditions to solubilize the membrane proteins. Thingholm et al. employed proteolysis by endoproteinase Lys-C in 8 M urea prior to trypsin digestion in 1.6 M urea solution⁸⁷; and Washburn et al. published methods for cleaving methionine residues in membrane proteins by CNBr in 90% formic acid prior to sequential digestion of Lys-C and trypsin⁸⁸, since methionine has been predicted to be frequently presented in transmembrane region.⁸⁹ Fischer and Poetsch revealed that the combination chymotrypsin and staphylococcal peptidase I provide better % sequence coverage of the membrane proteins than trypsin digestion.⁹⁰

In this work, we aimed to optimize digestion strategies for analysis of plasma membrane proteins, especially ones containing transmembrane helices. We evaluated the use of the enzymes trypsin and chymotrypsin in the presence of organic solvents or MS-compatible surfactants. Two types of samples were investigated: a model transmembrane protein, bacteriorhodopsin, and a complex mixture of plasma membrane proteins enriched by the cationic silica nanoparticle technique. Bacteriorhodopsin serves as a good representative for highly hydrophobic

transmembrane proteins, since it has a high GRAVY score of 0.72, and contains seven transmembrane helices (**Figure 17(B)**).

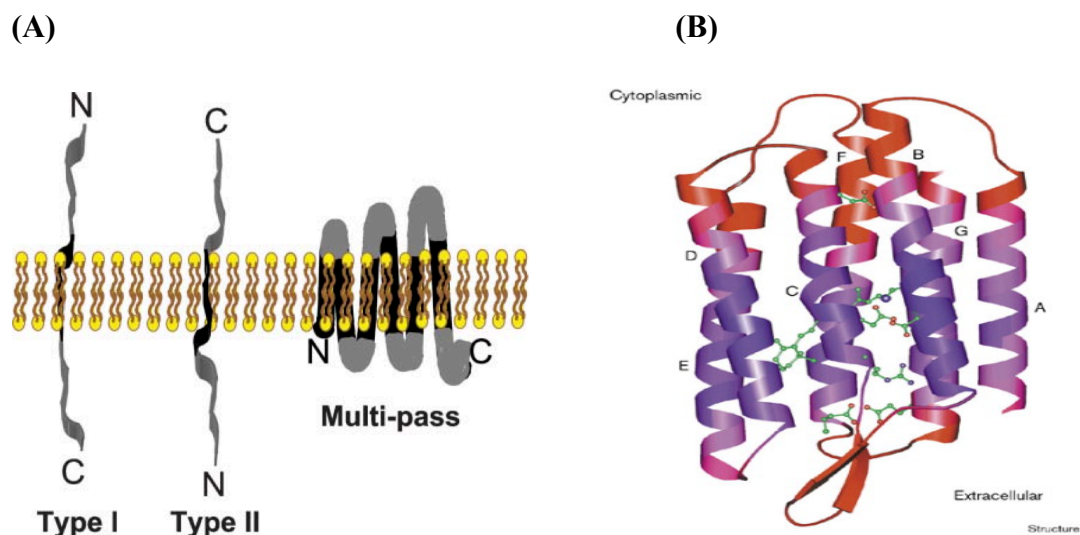


Figure 17. (A) Different types of integral membrane proteins.⁸⁵ The gray areas show parts of the protein sequence that are available for enzymatic digestion, (B) structure of bacteriorhodopsin.⁹¹

Materials and Methods

Materials

Bacteriorhodopsin from *Halobacterium salinarum*, Ludox CL colloidal silica, and other chemicals were purchased from Sigma Aldrich (St.Louis, MO) unless otherwise noted. RapiGestTM SF surfactant was purchased from Waters Corporation (Milford, MA). Mass-spectrometry grade trypsin, sequencing grade chymotrypsin, and ProteaseMaxTM Surfactant were obtained from Promega (Madison, WI). Immobilized chymotrypsin was purchased from ProteoChem, Inc. (Cheyenne, WY).

Acetonitrile and methanol were supplied from Fisher Scientific (Pittsburgh, PA). Multiple myeloma cell line RPMI 8226 and cell culture media RPMI 1640 were purchased from American Type Culture Collection (Manassas, VA). Fetal bovine serum was supplied from Atlanta Biologicals (Lawrenceville, GA). PPSTM Silent surfactant was purchased from Protein Discovery Inc. (Knoxville, TN).

Digestion of bacteriorhodopsin

For trypsin digestion, 20 µg of bacteriorhodopsin were resuspended in 100 µL of various digestion buffers; (i) a control condition (50 mM NH₄HCO₃), (ii) 60% MeOH in 50 mM NH₄HCO₃, (iii) 0.1% RapiGestTM SF in 50 mM NH₄HCO₃, (iv) 0.1% RapiGestTM SF in 60% MeOH in 50 mM NH₄HCO₃, and (v) 80% acetonitrile, 20% 50 mM Tris-HCl and 10 mM CaCl₂. The protein was dissolved in each of the buffers by sonication and intermittent vortexing for 15 min. For condition (iii), the sample was further incubated at 95°C for 5 min. Trypsin was added to each sample to an enzyme to protein ratio of 1:20 (w/w). The digestion was carried out at 37°C overnight. The reaction was terminated by adding 0.1% trifluoroacetic acid, followed by incubation with shaking at room temperature for 10 min. The samples were then desalted using Thermo Scientific Pierce C18 spin columns following the manufacture protocol. The digests were lyophilized and resuspended in 100 µL 0.1% formic acid.

The digestion by chymotrypsin was performed with similar protocol as described above for tryptic digestion, with the exception of two changes in the control buffer and the digestion temperature. The control reaction buffer was 100 mM Tris-HCl, 10 mM CaCl₂ and the digestion was taken place at room temperature.

LC-MS/MS analysis of bacteriorhodopsin peptides

The digests were subjected to an LC-MS/MS analysis using a Thermo LTQ-orbitrap coupled with a Shimadzu nano HPLC. The peptides were loaded using solvent A to an Acclaim PepMap 300 C8 trapping column (Dionex, Sunnyval, CA), for 10 min, via a Shimadzu autosampler. Reverse phase chromatography was performed in a Zorbax C18 nanobore column with the diameter of 0.075 mm and the length of 150 mm (Agilent Technologies, Palo Alto, CA). A linear solvent gradient was increased from 10% to 90% solvent B within 40 min. The column was interfaced with a Thermo nano-ESI source and the LTQ-orbitrap XL via a 15 μ m fused-silica PicoTip® (New Objective, Inc., Woburn, MA). Data acquisition was recorded by Xcalibur 2.0 software, and the data dependent acquisition was enabled. The precursor ion scans were performed in the orbitrap at a resolution of 30,000 at m/z 400; and the six most abundant ions were subjected to a CID fragmentation prior to the product ion scans in the LTQ. Analyses were carried out under the following tuning parameters: tube lens voltage 100 V, capillary voltage 35 V, capillary temperature 275°C, and spray voltage 1.6 kV. Dynamic exclusion was enabled with 1 repeat count and exclusion time 180 s.

Following the data acquisition, the spectra were search against SwissProt database of Archaeobacteria, using a MASCOT search engine with the following parameters: precursor mass tolerance of 10 ppm, MS/MS mass tolerance of 0.6 Da, enzyme specified as either trypsin (K and R) or chymotrypsin (FYWL), maximum

missed cleavages of 4, and variable modification specified as oxidation of methionine.

Analysis of plasma membrane proteins from multiple myeloma cells

The human multiple myeloma cells were grown in suspension, and the PM proteins were enriched by using cationic silica nanoparticle pellicle method, as described in the previous section. Protein extraction in Laemmli buffer was followed by chloroform/methanol precipitation. Then, the protein pellets were subjected to four different digestion conditions. Another pellicle sample was extracted directly in 0.1% RapigestTM SF by using the microwave at 100°C, 50 W, for 5 min. The PM pellicles were removed by centrifugation at 15,000 xg for 10 min, and the proteins dissolved in 0.1% RapigestTM SF were recovered for further analysis.

The digestion conditions are as follow:

(Amount of starting materials ranged from 50 µg to 300 µg)

(i) Trypsin digestion in 1.6 M urea in 50 mM NH₄HCO₃

One hundred microliters of 1.6 M urea in 50 mM NH₄HCO₃ was added to the pellet. Protein reduction and alkylation were performed in the presence of 5 mM DTT at 56°C for 20 min, and 15 mM iodoacetamide in the dark for 15 min, respectively. Trypsin digestion was carried out at 37°C for 16 h, using 1:25 (w/w) enzyme: protein ratio.

(ii) Lys-C digestion in 8 M urea followed by trypsin digestion in 1.6 M urea

The protein pellet was dissolved in 100 μ L 8 M urea in 50 mM NH_4HCO_3 . Protein reduction was performed in 5 mM DTT at 56°C for 20 min, and alkylation was carried out by incubation with 15 mM iodoacetamide in the dark for 15 min. Lys-C was added to the sample with an enzyme/substrate ratio of 1:50 (w/w). The digestion was performed at 37°C for 3h. The digest was diluted five times with 50 mM NH_4HCO_3 prior to trypsin digestion for 16 h, using an enzyme/substrate ratio of 1:25 (w/w).

(iii) Trypsin digestion in 1.6 M urea/0.1% ProteaseMaxTM surfactant

Proteins were solubilized in 1.6 M urea/0.1% ProteaseMaxTM surfactant in 50 mM NH_4HCO_3 . Protein reduction and alkylation were performed in 5 mM DTT at 56°C for 20 min, and 15 mM iodoacetamide in the dark for 15 min, respectively. Tryptic proteolysis was carried out at 37°C for 3 h with the enzyme/substrate ratio of 1:25 (w/w).

(iv) Trypsin digestion in 60% MeOH/0.1%PPSTM Silent surfactant

Protein pellet was dispersed in 5 mM DTT in 50 mM NH_4HCO_3 and incubated at 56°C for 20 min for reduction of disulfide bonds. Subsequently, alkylation was performed by incubation with 15 mM iodoacetamide in the dark for 15 min. The proteins were re-pelleted by centrifugation at max speed for 10 min, followed by solubilization 100 μ L in 60% MeOH/0.1% PPSTM surfactant in 50 mM NH_4HCO_3 , with 10 cycles of brief sonication and vortexing. The proteins were

denatured by incubation at 90°C for 1 min. The trypsin digestion was performed at 37°C for 20 h with an enzyme to protein ratio of 1:20.

(iv) Chymotrypsin digestion in 0.1% RapiGest™ SF

One hundred microliters of 0.1% RapiGest™ SF in 100 mM NH₄HCO₃ was added to protein pellet. The proteins were reduced by 5 mM DTT at 56°C for 20 min, and then alkylated by 15 mM iodoacetamide in the dark for 15 min. Immobilized chymotrypsin was prepared by centrifugation at 2,000 rpm for 1 min, followed by three washes in 100 mM NH₄HCO₃. The enzyme was added to the sample tube using approximately 1:25 (w/w) enzyme to protein ratio. The mixture was incubated in a shaker at 37°C for 16 h.

(v) Chymotrypsin digestion in 0.1% RapiGest™ SF (proteins extracted in 0.1% RapiGest™ SF)

Proteins extracted in 0.1% RapiGest™ SF were reduced by 5 mM DTT at 56°C for 20 min, and then alkylated by 15 mM iodoacetamide in the dark for 15 min. The digestion was carried out by incubation with immobilized chymotrypsin in a shaker at 37°C for 16 h. The enzyme to proteins ratio was 1:25 (w/w).

The digestion reactions were terminated by addition of 0.1% TFA. Subsequently, the digests were desalted using C18 spin column prior to injection to the nano HPLC interfaced with the LTQ-Orbitrap. Peptides were identified using LC-MS/MS experiments as described in the previous section. Data was searched

against Swissprot/Uniprot database on the MASCOT server. Subcellular localization of identified proteins was predicted by Gene Ontology Annotation on Scaffold 3.0 program.

Results and Discussion

In order to achieve high sequence coverage of highly hydrophobic proteins, different digestion conditions were evaluated using a model transmembrane protein, as well as the pellicle-enriched PM protein mixture. For the model protein, digestion efficiency of enzyme trypsin and chymotrypsin was investigated, based on % sequence coverage of the proteins and the transmembrane helices. In the case of the complex mixture, the proteolysis efficiency was evaluated based on the number of plasma membrane proteins identified and their percent of total protein identifications.

Approximately 52% of amino acid residues from bacteriorhodopsin resided in the seven transmembrane helices, which makes it difficult for enzymatic cleavage. Trypsin cleaves proteins after K or R residues, which are rare in the transmembrane helices; while chymotrypsin preferentially cleaves at the C-terminus of amino acid with aromatic side chains (FYW), which are frequently found in the α -helical domain. In addition, the chymotrypsin also cleaves after leucine residue at a slower rate.⁶⁷ The length of predicted tryptic and chymotryptic peptides from bacteriorhodopsin is shown in **Figure 18**. Although a majority of theoretical chymotryptic peptides were too small to be detected in the mass spectrometer, larger

peptides were experimentally observed due to the missed cleavages of well-structure regions.

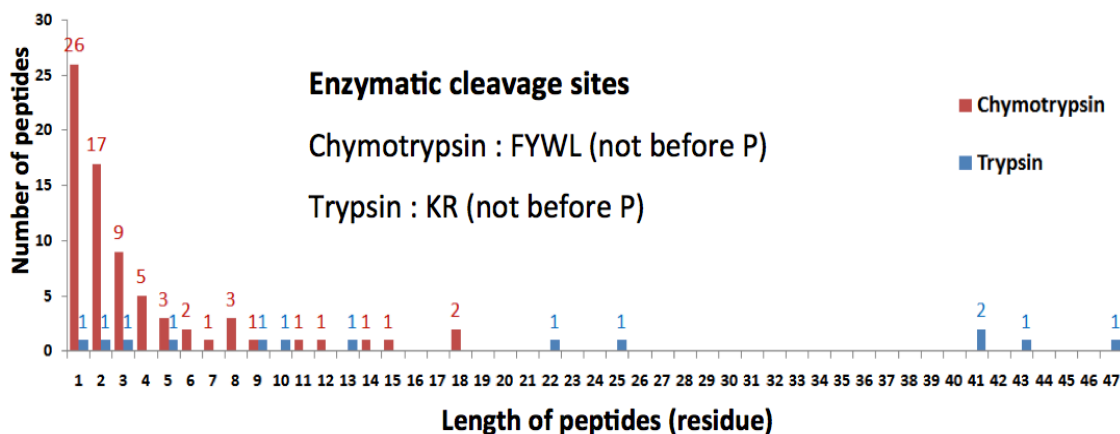


Figure 18. Distribution of predicted peptide length after *in silico* digestion by trypsin and chymotrypsin with complete cleavages.

Protein digestion was carried out in various buffers containing 50 mM NH_4HCO_3 , 60% MeOH, 0.1% RapiGestTM SF, 0.1% RapigestTM SF in 60% MeOH, and 80% acetonitrile. The protein sequence coverage is shown in **Table 5**. In all buffer conditions, chymotrypsin provided higher sequence coverage (20-72%) as compared to trypsin (8-10%), and the highest sequence coverage (72%) was found when 0.1% RapiGestTM SF was used as a digestion buffer. The diagram of transmembrane peptides identified from tryptic and chymotryptic digestion is shown in an **Appendix Figure 1**. It is not unexpected that the transmembrane regions can be observed with chymotrypsin cleavage since they possess highly hydrophobic amino

acid content. An example of MS/MS spectrum of a peptide residing in the transmembrane region is shown in **Figure 19**.

Table 5. Sequence coverage of bacteriorhodopsin from LC-MS/MS analysis of tryptic and chymotryptic peptides.

Digestion buffer	Sequence coverage	
	Trypsin	Chymotrypsin
50 mM NH ₄ HCO ₃	9%	60%
60% MeOH	9%	45%
0.1% RapiGest TM SF	8%	72%
0.1% RapiGest TM SF, 60% MeOH	8%	36%
80% acetonitrile	10%	20%

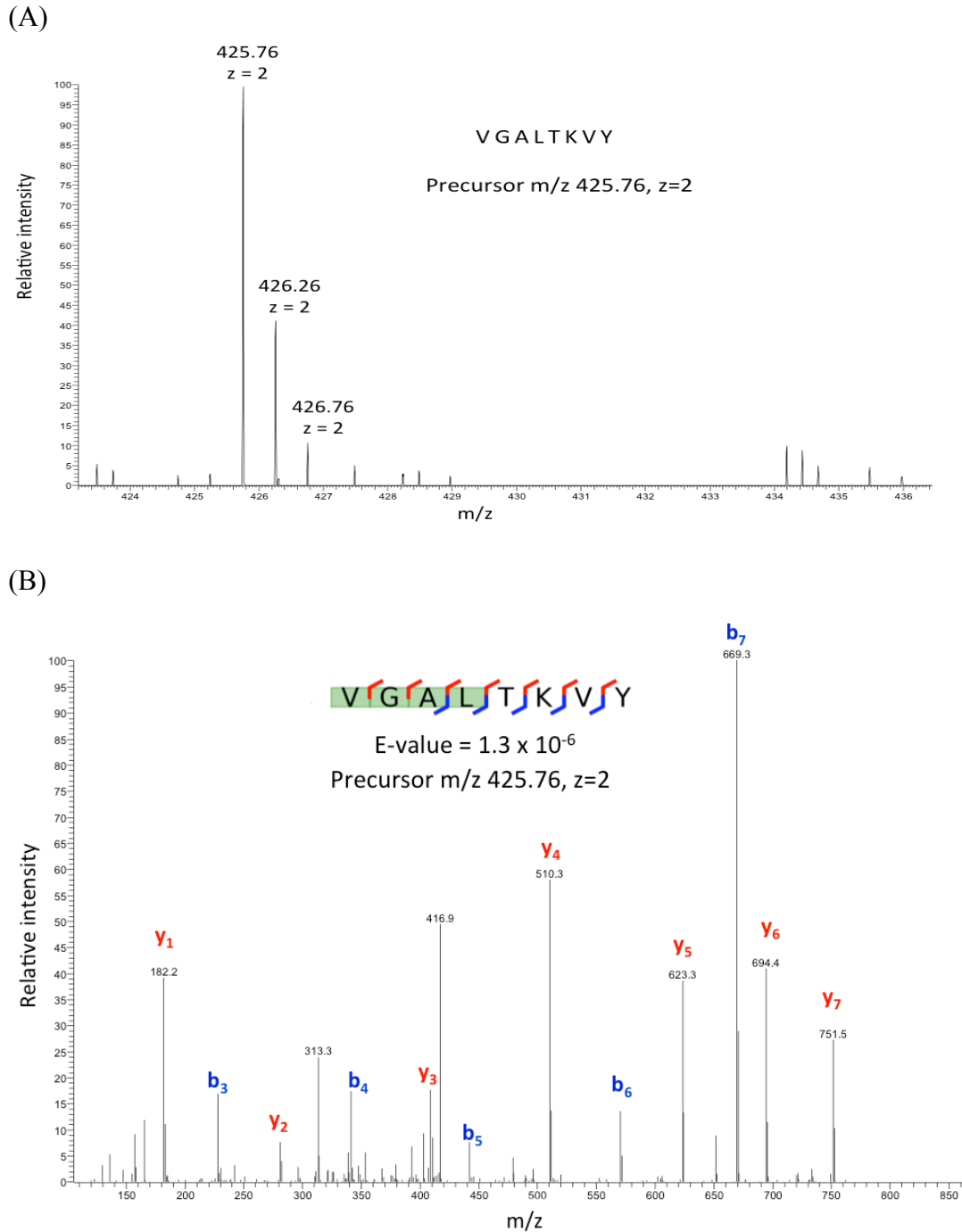


Figure 19. Example of (A) precursor ion spectrum, and (B) MS/MS spectrum of the peptide from transmembrane domain. The peptide VGALTKVY was identified from the chymotryptic digestion in 0.1% RapiGestTM SF. The sequences highlighted in green represent the transmembrane amino acid residues.

For analysis of the PM protein complex mixture enriched by silica nanoparticle pellicle technique, three types of enzymes with different specificity were examined; trypsin, Lys-C, and chymotrypsin. Digestion was performed in the presence of a chaotropic agent, organic solvents, or MS-compatible surfactants following the procedures from previous literature.^{78, 79, 92, 93} In **Figure 20**, the numbers of total proteins and PM proteins identified from LC-MS/MS analyses are summarized, and the digestion conditions are denoted. Considering the percent PM proteins as a fraction of the total proteins identified, chymotrypsin provided higher %PM compared to trypsin, especially when the digestion was performed without prior precipitation; however, significantly lower numbers of identifications were observed. It could be a result of a high false discovery rate from the database search, owing to less specificity of the enzyme chymotrypsin.

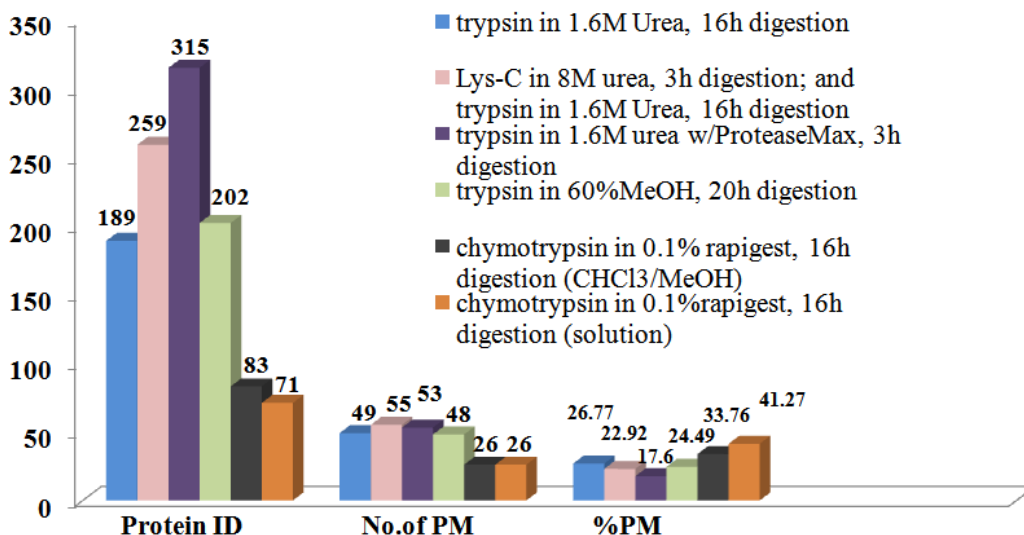


Figure 20. Comparison of proteolysis protocol by LC-MS/MS analysis of PM proteins after enrichment by silica nanoparticle pellicle techniques.

Among trypsin digestion procedures, the digestion in 1.6 M urea with ProteaseMaxTM surfactant provided the highest number of proteins identified; however, the %PM proteins were lower than other techniques. The digestion with Lys-C in 8 M urea coupled with trypsin in 1.6 M urea revealed the second highest number of total proteins, and the highest number of PM proteins identified. Therefore, this proteolysis procedure was employed for later analyses that required in-solution digestion.

Summary

Since each enzyme provided distinct advantages, both chymotrypsin and trypsin could be used in complementary to obtain more complete PM proteome coverage. Chymotrypsin enabled higher %sequence coverage, while trypsin provided feasibility of protein identification from the complex mixture.

Chapter 4: Enrichment of Plasma Membrane Proteins Using Nanoparticle Pellicles: Comparison between Silica and Higher Density Nanoparticles

(Adapted from Reference 8: Choksawangkarn, W.; Kim, S. K.; Cannon, J. R.; Edwards, N. J.; Lee, S. B.; Fenselau, C., Enrichment of Plasma Membrane Proteins Using Nanoparticle Pellicles: Comparison between Silica and Higher Density Nanoparticles. *J Proteome Res* **2013**, 12, 1134-41.)

Introduction

Thirty percent of the human genome is predicted to express plasma membrane (PM) proteins⁶, which play critical roles in communications and interactions between cells and their environment. Reflecting these functions, proteins in the PM and cell surface are reported to account for more than 60% of the drug targets currently under development.^{4,94} However, they are present in the cell in low abundance, on average, and are characterized by their hydrophobicity and glycosylation. Consequently, they are usually underrepresented in untargeted biochemical and proteomic studies. Several strategies have been proposed to enrich PM proteins that take advantage of

accessibility to the exterior cell surface. These include affinity capture using immobilized antibodies or lectins⁷⁰ and the alkylation of reactive amino acid residues or oxidized carbohydrate moieties with reagents linked to biotin^{18, 95, 96} to isolate cell surface proteins and glycoproteins. We have undertaken to enrich the entire PM to analyze integral proteins and proteins from both the inner and outer surfaces, using pellicles formed with cationic nanoparticles. We are also optimizing a proteomic workflow to provide proteolysis of highly hydrophobic proteins.⁷

The use of cationic colloidal silica was first introduced by Jacobson and co-workers^{24, 97} to increase the density of the PM and enhance its separation by centrifugation from the rest of the lysed cell. Jacobson and many subsequent researchers have synthesized alumina-coated silica nanoparticles to achieve a cationic surface at physiological pH, which is attracted electrostatically to the anionic cell surface (Alumina functional groups have isoelectric points (pI) around pH 8.) A nanostructure is defined as having at least one dimension between 1 and 100 nm. The reported average diameter of Jacobson's nanoparticles is reported to be around 50 nm.⁹⁷⁻⁹⁹ A related, commercial product has also been used, an aluminosilicate colloid sold as Ludox, with a diameter close to 20 nm.^{25, 59, 60, 99-102}

Two distinct applications of pellicles have been reported through the last thirty years: enrichment of the PM and associated proteins from cells grown in suspension or isolated in suspension from blood or tissue⁶⁰, and use of the heavy silica nanoparticles to fracture the apical from the basolateral PM domains in luminal cells in microvasculature²³ or adherent cells in culture.⁵⁹ The present study addresses the enrichment of PM proteins from a multiple myeloma cell line cultured and coated

in suspension and supports our ongoing studies of PM proteins in myeloid derived suppressor cells isolated from mouse blood. Prior reports of work with suspended mammalian cells have assessed the enrichment of PM proteins by Western blotting of marker proteins, most frequently Na⁺-K⁺ ATPase. Enrichments of Na⁺-K⁺ ATPase from cells coated in suspension have been reported between 15-fold and 20-fold.^{25, 60,}

103

Recently, the Fenselau group^{25, 59} and other laboratories (for example, references 60, 61, 94, 99, 101, 103-107) have integrated the use of nanoparticle pellicles into high throughput proteomic workflows. This advanced technology allows broad evaluation of enrichment, based on the identification of large numbers of proteins and their classification as plasma membrane, transmembrane, cell surface, cytoskeletal, etc., using Gene Ontology (GO) cellular component annotations. In these experiments, enrichment can be evaluated by reporting cohorts such as the PM proteins as a percent of total proteins identified. PM proteins characterized in this manner from suspended mammalian cells are previously reported to comprise between 18 and 42% of total proteins identified.^{25, 60, 103, 104} These estimates are uncertain for several reasons. First, experimentally based assignments of cellular locations are incomplete, and computationally based annotations are prone to false positives and false negatives. Different data-resources, notably, UniProt and the GO, provide similar, but distinct, cellular location namespaces and annotations, which may or may not apply the same evidence to determine cellular location; in some cases, these data-resources even cite each other. In addition, many cellular proteins move dynamically through the plasma membrane but are annotated as belonging to

other parts of the cell.^{94, 108} Often these proteomic studies do not provide an analysis of the whole cell lysate or other control sample, thus obscuring the actual effect of the pellicle treatment. Lastly, counting identified proteins with a particular GO annotation does not reflect qualitative enrichment of different proteins in the PM fraction, and both spectral counting¹⁰⁵ and isotope labeling¹⁰⁴ have been employed to augment the protein counting approach.

Given the real need for effective enrichment of the PM, can more effective pellicle nanostructures be designed? In the present work, we test the hypothesis that enrichment of the PM of multiple myeloma cells can be enhanced by the use of nanoparticles with higher density.

Materials and Methods

Materials

Human multiple myeloma RPMI 8226 and RPMI 1640 medium were purchased from American Type Culture Collection (Manassas, VA). Fetal bovine serum was obtained from Atlanta Biologicals (Lawrenceville, GA). Poly(acrylic acid) (MW = 100,000), penicillin-streptomycin solution, mouse monoclonal anti-Na⁺-K⁺ ATPase (α -subunit) primary antibody, alkaline phosphatase-conjugated goat antimouse IgG, BCIP/NBT solution, Tween-20, D-sorbitol, 2-(N-morpholino)-ethanesulfonic acid (MES), NaCl, imidazole, protease inhibitor cocktail solution, Na₂CO₃, KCl, NH₄HCO₃, urea, dithiothreitol (DTT), iodoacetamide, glutaraldehyde, Tris-HCl, β -mercaptoethanol, and SDS were purchased from Sigma-Aldrich (St.

Louis, MO). Criterion Tris-HCl precast gels, Tris-glycine-SDS buffer, molecular weight standards, and RC DC™ protein assay kit were purchased from Bio-Rad (Hercules, CA). Endoproteinase Lys-C and trypsin were purchased from Promega (Madison, WI). PVDF membrane was purchased from Millipore (Billerica, MA). Optima LC/MS grade acetonitrile, formic acid, trifluoroacetic acid, Pierce C18 spin columns were purchased from Fisher Scientific (Pittsburgh, PA). Deionized water was obtained by a Milli-Q A10 system and was used for all the experiments.

SiO₂/Al₂O₃ nanoparticles were kindly provided by Professor Donna Beer Stolz, University of Pittsburgh.⁹⁷ LUDOX-CL cationic colloidal silica (aluminosilicate) was purchased from Sigma-Aldrich. Fe₃O₄ and Au nanoparticles coated with Al₂O₃ and aminopropyl groups were synthesized in Professor Sang Bok Lee's laboratory at the University of Maryland, College Park.⁸

Cell Culture and Pellicle Coating

Human multiple myeloma RPMI 8226 cells were cultured in RPMI 1640 medium supplemented with 10% fetal bovine serum and antibiotics at 37°C and 5% CO₂, and harvested at confluence. Although different harvests were used to evaluate the different pellicles, all preparations were made in the same manner, to the best of our ability. Approximately 6×10^7 cells in suspension were collected at 900 xg for 5 min, and washed with plasma membrane coating buffer A (PMCBA, 800 mM sorbitol, 20 mM MES, 150 mM NaCl, pH 5.3). The cells were coated with cationic nanoparticles, including SiO₂/Al₂O₃, LUDOX-CL SiO₂ (comprising aluminosilicate), Fe₃O₄/Al₂O₃, Fe₃O₄/NH₂, and Au/NH₂ nanoparticles, following our published

procedures with slight modifications.^{7, 25} In brief, the cells resuspended in PMCBA were placed dropwise into 10% (w/v) cationic nanoparticle solutions and rocked gently at 4°C for 15 min. The nanoparticle-coated cells were added dropwise to 10 mg/ mL poly(acrylic acid) in PMCBA, pH 6.0–6.5, and incubated at 4°C for 15 min with gently rocking. The poly(acrylic acid) cross-linked cells were sedimented and washed with PMCBA to remove unbound poly(acrylic acid). The cells were incubated in 2.5 mM imidazole with a protease inhibitor cocktail, at 4°C for 30 min, and disrupted using N₂ cavitation at 1500 psi for 30 min. Following lysis, pellicle-bound PM sheets were separated from other cellular components by low speed sedimentation at 100 xg for 7 min, and washed three times with the lysis buffer, three times with 1 M Na₂CO₃, pH 11.4, and three more times with 1 M KCl. The PM proteins were extracted in triplicate from the pellicles in 2% SDS, 62.5 mM Tris-HCl, and 5% β- mercaptoethanol at 100°C for 5 min in a microwave oven (CEM Corporation, Matthews, NC). Care was taken that all preparations were made in the same manner. Protein concentration was determined using an RC DC™ protein assay kit (Bio-Rad, Hercules, CA).

Although we have made multiple analyses with all three pellicles, each of the three experiments reported here began with about 60 million cells, which provided a 1/6 aliquot for SEM and TEM characterization, 5 or 6 Western blots, and 6 (technical) replicate LC-MS/MS analyses.

Western Blotting

Twenty-five micrograms of each pellicle enriched protein sample and 25 μg of protein from a whole cell lysate were subjected to gel electrophoresis together on a 7.5% Bio-Rad Criterion precast gel and transferred to a PVDF membrane using the Bio-Rad Mini trans-blot electrophoretic transfer cell. The PM marker, $\text{Na}^+\text{-K}^+$ ATPase (α -subunit), was detected using mouse anti- $\text{Na}^+\text{-K}^+$ ATPase (α -subunit) as the primary antibody and an alkaline phosphatase-conjugated goat antimouse IgG as the secondary antibody. Colorimetric detection was performed by incubating in BCIP/NBT solution (Sigma-Aldrich, St. Louis MO).⁶⁴ The protein bands were interrogated using ChemiDoc XRS+ System with Image Lab Software (Bio-Rad, Hercules CA).

Sample Preparation for Scanning Electron Microscopy

The cells or the PM sheets were washed with 0.12 M Millonig's phosphate buffer, pH 7.3⁶³, and fixed with 2% glutaraldehyde, followed by 1% OsO_4 . Then, the cells were dehydrated in a series of ethanol solutions and subjected to a critical point drying with CO_2 using a Denton DCP-1 critical- point dryer (Denton Vacuum, LLC, Moorestown, NJ). The samples were coated with Au:Pd in a DV-503 Denton Vacuum evaporator (Denton Vacuum, LLC, Moorestown, NJ). SEM and TEM microscopy were performed on a Hitachi SU-70 Field Emission scanning electron microscope (Hitachi, Gaithersburg MD), and an Amray 1820 scanning electron microscope (Amray Inc., Bedford, MA) was also used for SEM.

Proteomic Analysis

For each type of pellicle, 90 µg of proteins was precipitated with chloroform/methanol⁶⁵ to remove phospholipids and detergent. The protein pellets were resolubilized in 8 M urea in 50 mM NH₄HCO₃, reduced by 20 mM DTT at 56°C for 30 min, and alkylated by 40 mM iodoacetamide in the dark for 30 min. Lys-C digestion was performed in the presence of 8 M urea for 3 h at 37°C, using a 1:50 enzyme/protein ratio. Trypsin cleavage was performed in 1.6 M urea for 16 h at 37°C, using the enzyme/protein ratio of 1:25. Tryptic peptides were desalted using Pierce C18 spin columns and subjected to HPLC-MS/MS analysis.

The HPLC-MS/MS analyses were carried out using a Shimadzu Prominent nanoHPLC (Shimadzu Corporation, Columbia MD) interfaced to an LTQ-orbitrap XL (Thermo Fisher Scientific, San Jose, CA). For each pellicle, six (technical) replicate injections were performed in order to maximize peptide identification from the complex mixtures. Three biological replicate experiments, from different batches of cell culture, were carried out in order to evaluate reproducibility of the entire enrichment procedure. Fifteen micrograms of the peptides extracted using each pellicle were injected to an Acclaim PepMap 300 C18 precolumn (Dionex, Sunnyvale, CA) and desalted by 10% solvent A (97.5% H₂O, 2.5% acetonitrile, and 0.1% formic acid) for 10 min, using a flow rate of 10 µL/min. Following trapping, peptides were fractionated in a Zorbax 300SB-C18 (Agilent Technologies, Palo Alto CA) nanobore column (0.075 × 150 mm) with a linear gradient increasing from 10 to 60% solvent B (97.5% acetonitrile, 2.5% H₂O, and 0.1% formic acid) in 90 min, followed by another increase from 60% B to 85% B in 20 min. The fractionation flow rate was set at 300 nL/min. A 15 µm fused-silica PicoTip (New Objective, Inc.,

Woburn, MA) was used as an emitter, interfaced with a Thermo nanoelectrospray ionization (ESI) source (Thermo Fisher Scientific, San Jose CA). Electrospray parameters included a spray voltage of +2.0 kV, a capillary temperature of 275°C , and a tube lens voltage of 100 V. Precursor ions were measured in the orbitrap at a resolution of 30,000 at m/z 400. In each activation cycle, the nine most abundant precursor ions were fragmented by collision-induced dissociation (CID) with normalized collision energy of 35; and the product ions were scanned in the LTQ at unit resolution. The peptide precursor ions were isolated within a 3 Da window for activation through 30 ms. Ions with unassigned or +1 charge states were excluded from selection for MS/MS. Dynamic exclusion was enabled to exclude precursor ions that were previously scanned within 3 min. Spectra were recorded using Xcalibur 2.0 software (Thermo Fisher Scientific, San Jose, CA).

Bioinformatics

RAW spectral files were subject to centroiding and mzXML reformatting using msconvert from the ProteoWizard project¹⁰⁹ and submitted to the PepArML meta-search engine (March 2012)⁴⁸ using the PepArML batch uploader. Tandem mass spectra were searched against the human reference proteome from the UniprotKnowledgeBase (March 2012) with enumerated isoforms. Carbamidomethylation was specified as a fixed modification on Cys, and oxidation of Met was allowed as a variable modification.

Peptide identifications from PepArML were filtered at 10% (spectral) FDR and a global parsimony analysis used to eliminate redundantly identified proteins.

The global parsimony analysis ensures, in particular, that groups of equivalent proteins with identical peptide evidence are consistently represented by a specific protein from the group, even in different data sets. The (generalized) parsimony analysis applied here using an in-house tool requires that each retained protein be supported by at least two distinct peptides not shared with any other (retained) protein. This filtering criterion allows us to establish an upper-bound estimate of 1% on the protein false-discovery rate, presuming distinct peptide errors are independent.

Spectral counts for retained protein were determined from filtered peptide identifications, without adjustment for shared peptides or length of the protein sequence. As such, these spectral counts are only appropriate for comparison of protein abundance across samples (pellicles) and should not be used to compare the abundance of different proteins within a sample. Protein (or protein group) spectral counts expressed as percentages are with respect to the total number of peptide identifications for the pellicle samples. In-house software (SpectralCount v1.5) was used to compute spectral counts from PepArML peptide identifications.

Subcellular localization of identified proteins to PM was determined by an in-house application of the map2slim script from the go-perl software package available from the GO project, the Uniprot human GOA, and a specialized in-house defined GO Slim. Identified proteins were categorized as transmembrane based on the “Transmembrane” keyword annotations in UniProt or by the application of the web-based TMHMM 2.0 tool⁸³ for predicting transmembrane helices from protein sequence.

Results and Discussion

Since the rationale of the pellicle method is based on increasing the density of the PM prior to centrifugation, we have examined nanoparticles with higher density including Fe₃O₄, and Au nanoparticles, compared to the SiO₂. The six types of the nanoparticles were investigated: Al₂O₃ coated SiO₂, aluminosilicate, Al₂O₃ coated Fe₃O₄, aminopropyltriethoxysilane-modified Fe₃O₄, aminopropyl thiol-modified 30 nm Au, and aminopropyl thiol-modified 80 nm Au. Fe₃O₄ and Au nanoparticles were synthesized in Professor Sang Bok Lee's laboratory. The diameter of the dry nanoparticles and the aggregated nanoparticles in a buffered solution used to coat suspended cells were measured using SEM and TEM. The zeta potential of the aggregates was measured using a particle analyzer. Physical properties for these synthesized nanoparticles, commercial cationic nanoparticles comprising aluminosilicate, and a sample of Al₂O₃-coated SiO₂ nanoparticles (provided by Professor Donna Beer Stolz)⁹⁷ were determined by Dr. Sung-Kyoung Kim in Professor Lee's laboratory. These are summarized in **Table 6**.

Figure 21 shows the electron micrographs of multiple myeloma cells, cells coated with the six kinds of nanoparticles, coated cells cross-linked with poly acrylate, and a piece of the pellicle coated PM produced with each of the six pellicles. These micrographs indicate that the cell surfaces were completely coated with nanoparticles, and that PM pellicle sheets were obtained after lysis.

The ideal properties of nanoparticles used to construct the PM pellicles include (1) high density, (2) high surface charges that can form strong pellicles with

the PM, and (3) a high degree of dispersion and stability in the coating buffer. In this study, two types of cationic groups, Al₂O₃ and 3-aminopropyl were examined (**Table 6**). Based on the zeta potential measurement and experimental observation, the three Al₂O₃-modified nanoparticles provided higher surface charge and better stability, compared to the three amine-modified nanoparticles. Therefore, we focused on the Al₃O₄ modified nanoparticles, which included Fe₃O₄/Al₂O₃, aluminosilicate, and SiO₂/Al₂O₃ for studying the effect of nanoparticle density on enrichment efficiency of PM proteins.

Table 6. Properties of the nanoparticles studied.

nanoparticles	diameter (nm)	density (g/mL)	size in solution (nm)	cationic group	zeta potential (mV)
Fe ₃ O ₄ /Al ₂ O ₃	17 ± 6	5.17 ^a	99 ± 55	Al ₂ O ₃	64 ± 3
Aluminosilicate	18 ± 5	1.23 ^b	55 ± 2	Al ₂ O ₃	86 ± 2
SiO ₂ /Al ₂ O ₃	20-100	2.65 ^a	31 ± 6	Al ₂ O ₃	50 ± 6
Fe ₃ O ₄ /NH ₂	18 ± 5	5.17 ^a	156 ± 68	3-aminopropyl	55 ± 4
Au/NH ₂	29 ± 2	19.3 ^a	99 ± 33	3-aminopropyl	51 ± 4
Au/NH ₂	77 ± 5	19.3 ^a	101 ± 35	3-aminopropyl	54 ± 4

^a Bulk density of the core. ^b Density provided by Sigma-Aldrich.

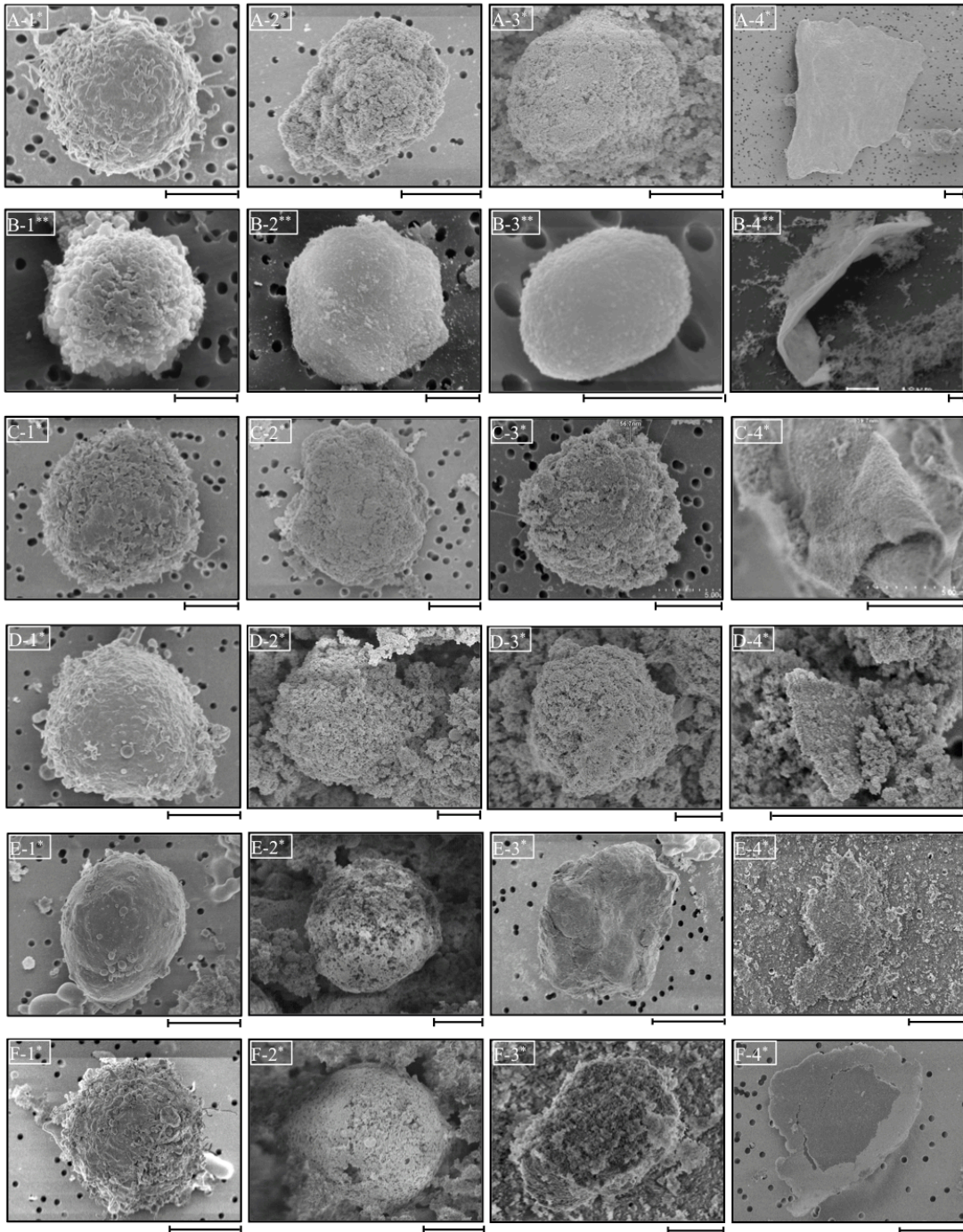


Figure 21. Micrographs of (Columns 1 to 4) multiple myeloma cells, the cells coated with nanoparticles, poly(acrylic acid) cross-linked coated cells, and fragments of the pellicle-coated PM. The nanoparticles are (Rows A-F) $\text{Fe}_3\text{O}_4/\text{Al}_2\text{O}_3$, aluminosilicate, $\text{SiO}_2/\text{Al}_2\text{O}_3$, $\text{Fe}_3\text{O}_4/\text{NH}_2$, 29 nm Au/NH_2 , and 77 nm Au/NH_2 .

Figure 21. (Continued) The scale bars indicate 5 μm . Micrographs (*) were taken with a Hitachi SU-70 field emission scanning electron microscope. Micrographs (**) were taken with an Amray 1820 scanning electron microscope.

The size of the synthetic Fe_3O_4 particles was controlled to match the uniform size of the commercial particles and the lower range of the Al_2O_3 coated SiO_2 particles. The Fe_3O_4 core provides significantly increased density, which was expected to enhance differential centrifugation of coated PM fragments. Zhang et al.⁹⁴ and Li et al.¹⁰³ have previously reported construction of pellicles using cationic amino group coated magnetite nanoparticles with diameters of 200 and 10 nm, respectively. They focused their studies on magnetic field-based separations of pellicles, while we compare the high density property of magnetite with densities of conventionally used silica nanoparticles.

These three different nanoparticles, $\text{Fe}_3\text{O}_4/\text{Al}_2\text{O}_3$, aluminosilicate, and $\text{SiO}_2/\text{Al}_2\text{O}_3$, were used to coat multiple myeloma cells in suspension and capped with polyacrylate. The coated cells were lysed by nitrogen cavitation, and fragments of the pellicle-covered PM were isolated by low speed centrifugation (**Figure 21 (A)-(C)**). Pellicle-coated membrane fragments were washed as described in the experimental section, and pellicle-bound proteins were solubilized. The concentration of $\text{Na}^+\text{-K}^+$ ATPase was assayed in each of the three isolates, relative to its presence in whole cell lysate, using Western blotting. These bands are shown in **Figure 22(A)**. Significant enrichment of $\text{Na}^+\text{-K}^+$ ATPase is revealed, measured

spectroscopically as 50-, 33-, and 7-fold for the Al₂O₃-coated Fe₃O₄ particles, aluminosilicate particles, and Al₂O₃-coated SiO₂ particles, respectively. The enrichment of this marker protein was also evaluated by spectral counting (**Figure 22 (B)**), which confirms the enrichment of Na⁺-K⁺ ATPase observed by Western blotting. Spectral counts of a small number of other PM marker proteins are also provided (**Figure 22(B)**).

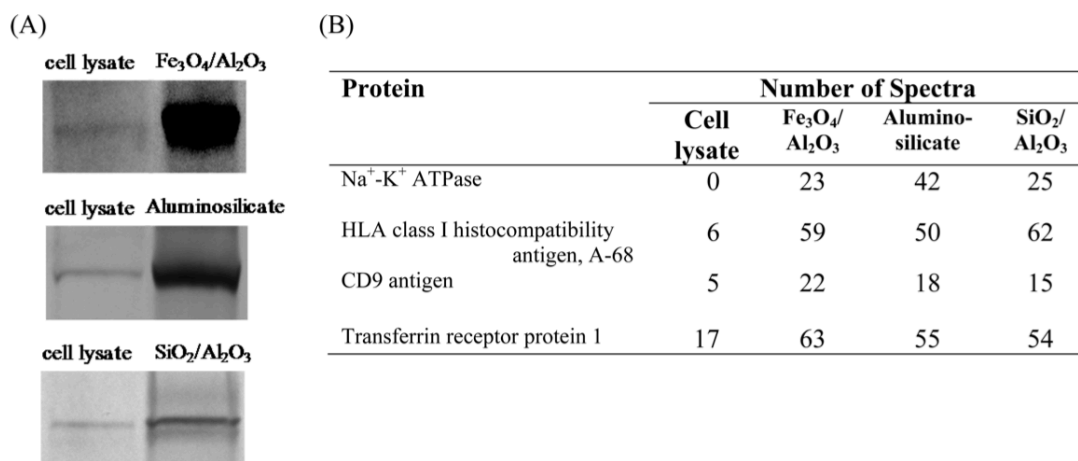


Figure 22. Analysis of abundances of PM protein markers by (A) Western blotting of Na⁺-K⁺ ATPase and (B) spectral counts for Na⁺-K⁺ ATPase and other PM protein markers.

The desired outcome of efforts to improve PM enrichment in this and other laboratories is to increase the number of peptide and protein identifications and quantifications made using high throughput LC-MS/MS technologies. In our case, we expect to apply an optimized workflow to the qualitative and quantitative proteomic analyses of cells isolated from mouse blood. Previous workers using the pellicle technique (e.g., references 25, 104, and 105) have reported enrichments of

individual markers, judged by Western blotting, that correlated poorly with overall proteomic identifications. In order to evaluate enrichment based on proteomic analysis in our experiments, the protein mixture recovered from each of the pellicles was digested with trypsin. Six replicate injections were made for LC-MS/MS analyses of each of the three tryptic peptide mixtures. We found peptide sampling to be saturated⁸² after six injections. In **Table 7**, identifications of PM proteins are summarized as a percent of total protein identifications and can be compared to an analogous analysis of whole cell lysate. In this analysis, the proportion of PM proteins in pellicle samples are enriched, with the pellicles providing 16% to 24% PM proteins compared to just 13% from the whole cell lysate. Lists of proteins identified in each of the pellicle samples and the whole cell lysate are provided in **Appendix Table 2**.

Table 7. Proteomic analysis of plasma membrane (PM) and transmembrane (TM) protein enrichment by three pellicles; average % (standard deviation) of six technical replicates.

nanoparticle	distinct proteins	...with GO annotation	average % annot. PM	average % annot. TM	average % pred. TM
Fe ₃ O ₄ /Al ₂ O ₃	341	311	23.6 (0.5)	13.9 (0.7)	12.4 (0.7)
aluminosilicate	381	337	18.5 (0.3)	13.0 (0.4)	12.3 (0.4)
SiO ₂ /Al ₂ O ₃	530	435	16.7 (1.0)	10.6 (0.5)	10.6 (0.4)
whole cell lysate	658	589	13.1 (0.6)	4.6 (0.2)	4.5 (0.5)

Although the cellular localization annotations cannot be considered entirely reliable, the assignments in the **Table 7** were made consistently for all experiments and thus can be compared. The most dense pellicle, Al₂O₃-coated Fe₃O₄, provides the best enrichment (as a percent of total identifications) relative to the whole cell lysate control analysis. A similar trend was observed from multiple batches of cell culture (three biological replicates) shown in **Table 8**, indicating good consistency and reproducibility of this technique.

Figure 23(A) shows the average spectral count assigned to PM proteins in each of three biological replicates as a percent of the total number of peptide identifications and again provides a comparison with the whole cell lysate control.

Table 8. Proteomic analysis of PM and TM proteins enriched by three nanoparticle pellicles and whole cell lysate; average % (standard deviation) of three biological replicates.

nanoparticles	average	average	average
	% annot. PM	% annot.TM	% pred. TM
Fe ₃ O ₄ /Al ₂ O ₃	24.0 (1.1)	14.1 (1.9)	11.3 (2.6)
aluminosilicate	20.2 (3.2)	13.7 (3.6)	14.7 (4.0)
SiO ₂ /Al ₂ O ₃	19.2 (2.0)	12.2 (1.6)	11.1 (2.4)
whole cell lysate	15.2 (2.0)	5.5 (1.2)	5.3 (0.6)

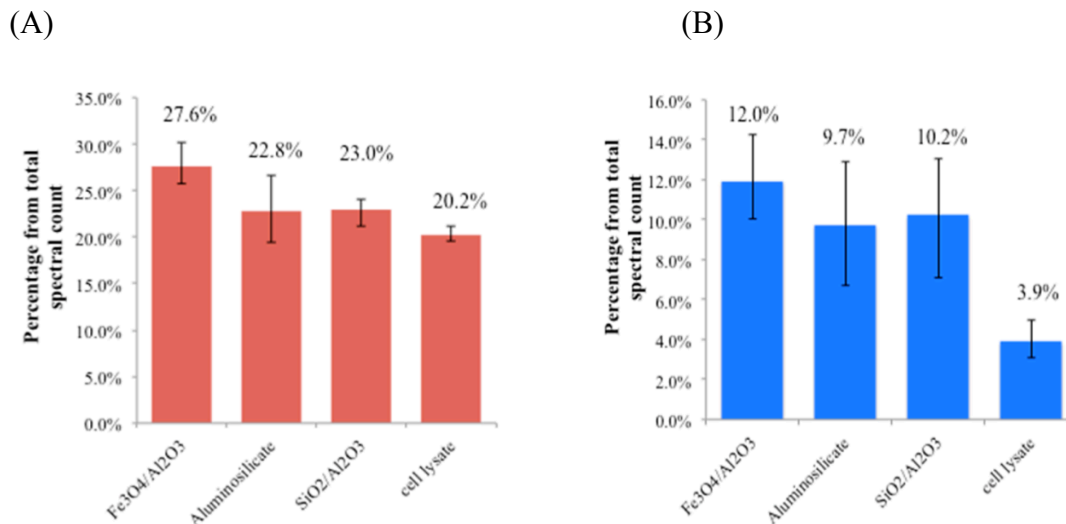


Figure 23. Spectral counts from three biological replicates of **(A)** plasma membrane proteins as a percent of total spectral counts and **(B)** transmembrane proteins as a percent of total spectral counts. Error bars indicate range of observed values.

The proportion of spectral counts for PM proteins ranges from 23 to 28%, compared to the control at 20%. Minimum and maximum values for the three (biological) replicates are shown as error bars in the figure. With this small sample size ($n = 3$), it is difficult to conclude that the enrichment due to the aluminosilicate and Al₂O₃/SiO₂ pellicles is statistically significant, but for the Fe₃O₄/Al₂O₃ pellicles, the enrichment is clear. The corresponding plot for the six technical replicates (**Figure 24(A)**) shows a clearer separation from the whole cell-lysate for all three pellicles.

All three pellicles show (**Table 7**, six technical replicates each) much stronger enrichment, compared to whole cell lysate, of proteins classified by UniProt annotation as transmembrane proteins, and also of transmembrane proteins as predicted by TMHMM 2.0. This is hardly surprising, as the annotated and predicted transmembrane proteins are largely concordant. Enrichment of transmembrane

proteins was further confirmed by spectral counting, as shown in **Figure 23(B)** (three biological replicates) and **Figure 24(B)** (six technical replicates). It can be seen that enrichment in the pellicle experiments is 3- to 4-fold relative to whole cell lysate.

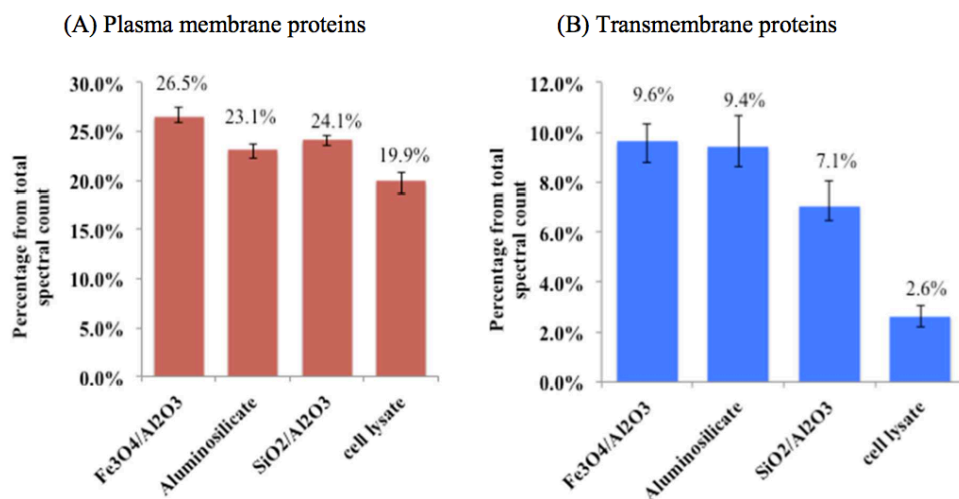


Figure 24. Spectral counts from six technical replicates of **(A)** plasma membrane proteins as a percent of total spectral counts; and **(B)** transmembrane proteins as a percent of total spectral counts. Error bars indicate range of observed values.

The possibility that different pellicles might preferentially enrich different sets of proteins was examined, given the rather striking difference in the enrichment of annotated PM proteins vs. TM proteins. A Venn diagram (**Figure 25**) illustrates the overlapping and unique PM proteins identified by the three types of pellicles. We stress that the global parsimony analysis used (see Materials and Methods) ensures that identified proteins can be reliably classified as overlapping or unique. The majority of proteins identified are common to all three experiments, and a smaller number of proteins were identified uniquely by each pellicle. A functional

enrichment analysis of the proteins uniquely identified with each pellicle was made using GO FAT cellular component categories in the functional annotation tool from the Database for Annotation, Visualization, and Integrated Discovery (DAVID). The background set comprised the three lists of pellicle-unique proteins. This analysis suggests that each set of pellicle-unique proteins has a distinct cellular origin in comparison to the other pellicles. The aluminosilicate particles appear to enrich basic proteins from the ribosome (Fisher's exact test p -value 5.8×10^{-4}) and cytosol (p -value 1.1×10^{-2}), while proteins uniquely associated with the Al_2O_3 -coated Fe_3O_4 pellicle originate primarily from the PM (p -value 9.8×10^{-3}). Unique proteins recovered by the Al_2O_3 -coated SiO_2 pellicles do not show a significant bias in cellular localization, compared to the background set. The possibility of differential enrichment by different pellicles is intriguing and deserves additional study.

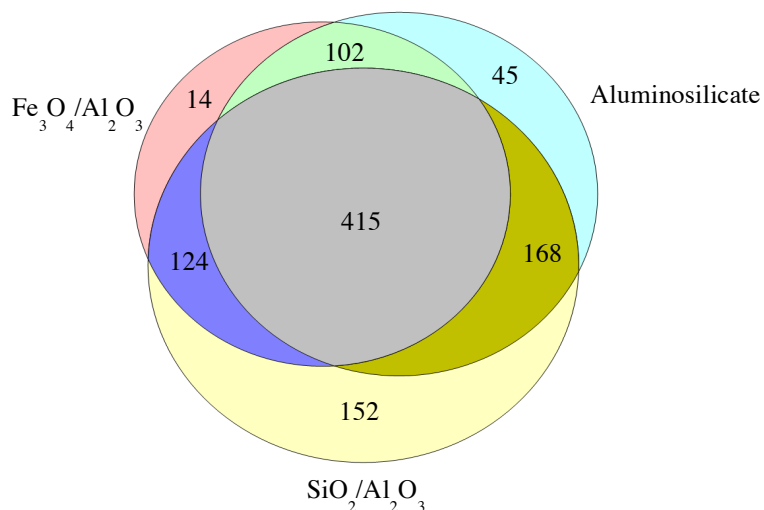


Figure 25. Number of common, shared, and unique protein identifications for Al_2O_3 -coated Fe_3O_4 , aluminosilicate, and Al_2O_3 -coated SiO_2 nanoparticles.

Summary

On the basis of both protein identifications and spectral counts, the capability of the nanoparticle pellicles studied to provide enriched samples of PM proteins from suspended cells is real, though limited. The enrichment provided by Al₂O₃-coated Fe₃O₄ particles trends higher than the other two studied, consistent with the hypothesis that higher density particles are more effective. PM protein identifications and spectral counts determined as percentages of total proteins in the three pellicle samples (18–26%) are within the range of observations published by others for suspended cells (18–42%).^{25, 60, 103, 104} The comparison provided here, with a control analysis of whole cell lysate, indicates that improvements in the proportion of PM protein identifications and spectral counts are provided by using the pellicles. Enrichment of the more limited category of transmembrane proteins is found to be about 3-fold greater than the control lysate, based on identifications and spectral counts, and the pellicle method seems well suited for this target group. Enrichments of individual protein markers (Western blotting and spectral counting) were found to correlate poorly with changes in the percentages of identifications and spectral counts of all PM proteins.

Chapter 5: Use of Iron Oxide Nanoparticle Pellicles for Enrichment of Plasma Membrane Proteins from MDSC

(Adapted from Choksawangkarn, W.; Graham, L.M.; Edwards, N.J.; Lee, S. B.; Ostrand-Rosenberg, S.; Fenselau, C., Inflammation induces myeloid-derived suppressor cells to express a diverse pattern of plasma membrane proteins., *manuscript under review*).

Introduction

Chronic inflammation in the tumor microenvironment is known to be associated with tumor promotion and progression.^{51, 110} Previous studies have demonstrated that a group of immune suppressive cells, referred to as myeloid-derived suppressor cells (MDSC), are induced by inflammation and facilitate tumor development. MDSC are a heterogeneous population of immature cells of myeloid origin which exhibit potent suppressive activities for both innate and adaptive immunity.¹¹¹ In normal physiological conditions, the immature myeloid cells are generated in the bone marrow and differentiate into functional mature cells, including

dendritic cells, granulocytes, and macrophages. However, the tumor microenvironment perturbs normal differentiation processes and causes an increase in MDSC.¹¹² It has been reported that inflammatory mediators secreted by malignant cells promote MDSC accumulation and heighten their potent activities.⁵¹ Multiple inflammation-associated factors have been reported to be involved in regulating MDSC expansion and suppressive functions, including the S100A8/A9 heterodimer¹¹³, interleukin-1 β ¹¹⁴, interleukin-6¹¹⁵, vascular endothelial growth factor (VEGF)¹¹⁶, granulocyte macrophage colony-stimulating factor (GM-CSF)¹¹⁷, bioactive lipid prostaglandin E2¹¹⁸, and complement component C5a¹¹⁹. Recently, inflammation has been hypothesized to induce MDSC accumulation by enhancing resistance to apoptosis via the Fas-mediated pathway.¹²⁰ Although the mechanism by which MDSC mediate suppression of the immune function is not yet fully understood, several observations support the involvement of reactive oxygen species, nitric oxide, and peroxynitrite, as well as the deprivation of L-arginine and cysteine, which are essential for activation of T-cells.^{53, 55, 56, 121}

It has been recognized that the inflammation-driven accumulation of MDSC plays an important role in the failure of cancer immunotherapy and that depletion of MDSC enhances the function of antitumor T-cell activities. A better understanding of molecular signaling between MDSC, tumor cells, T-cells, and inflammatory mediators is necessary to achieve more effective cancer immunotherapy. The plasma membrane (PM) proteins of MDSC are potential targets for signaling mechanisms that activate these cells, and in this study, we focus on how the MDSC plasma membrane proteome changes when the level of inflammation is increased. We have

employed mass spectrometry-based quantitative proteomic analysis to investigate the difference between the PM proteins of MDSC induced in less inflammatory and high inflammatory environments. The MDSC induced under lower levels of inflammation are designated as “conventional MDSC”; while those induced under heightened levels of inflammation are designated as “inflammatory MDSC”. Both MDSC populations are obtained from BALB/c mice carrying 4T1 mammary carcinoma tumors. Heightened inflammatory conditions were generated using 4T1 cells transfected with and expressing high levels of the pro-inflammatory cytokine IL-1 β .¹¹⁴

In general, PM proteins are of relatively low abundance and highly hydrophobic; so they remain problematic for mass-spectrometry detection and thus are underrepresented in most proteomic studies. We have applied our optimized nanoparticle pellicle technique^{8, 24, 25} to enrich the PM and its proteins from MDSC prior to label-free quantitative proteomic analysis. This enrichment technique increases the density of the PM sheets by electrostatic interaction between cationic nanoparticles and anionic cell surfaces; therefore they can be more readily separated from cellular organelles by centrifugation. In an earlier chapter of this thesis, higher density iron oxide nanoparticle pellicles were observed to provide the best enrichment, compared to two lighter silica-based nanoparticle pellicles.⁸

Materials and Methods

Materials

Al₂O₃ coated Fe₃O₄ nanoparticles were synthesized by Lauren Graham from Professor Sang Bok Lee's laboratory. BALB/c mice were obtained from the Jackson Laboratory (Bar Harbor, ME). The 4T1 cell line derived from a BALB/c spontaneous mammary carcinoma¹²² was kindly provided by Dr. Fred R. Miller from the Michigan Cancer Foundation. Poly(acrylic acid) (MW=100,000), protease inhibitor cocktail, and other chemicals were purchased from Sigma-Aldrich (St. Louis, MO), unless otherwise specified. Trypsin and endoproteinase Lys-C were supplied by Promega (Madison, WI). Criterion Tris-HCl 8-16% precast linear gradient gels, Tris/glycine/SDS buffer, molecular weight standards, and RC DCTM protein assay kit were purchased from Bio-Rad (Hercules, CA). Optima LC/MS grade acetonitrile, Optima LC/MS grade H₂O, formic acid, trifluoroacetic acid, and sodium acetate were purchased from Fisher Scientific (Pittsburgh PA). TopTip C18 micro-spin columns were purchased from Glygen Corporation (Columbia, MD). 1,2-Propanediol was purchased from Macron Chemicals (Phillipsburg, NJ). Deionized water was obtained using a Milli-Q A10 system from Millipore (Billerica, MA).

Mice and Cell Lines

Wild type BALB/c mice were bred and maintained according to the NIH guidelines for the humane treatment of laboratory animals in Prof. Ostrand-Rosenberg's laboratory, University of Maryland Baltimore County. All animal procedures were approved by the university's Institutional Animal Care and Use Committee. The 4T1 mammary carcinoma cell line and the transfected 4T1/IL1 β cell line were maintained as previously described.^{114, 123}

MDSC Harvesting

BALB/c mice were inoculated in the abdominal mammary gland with 4T1 or 4T1/IL-1 β tumor cells and MDSC were harvested in Professor Ostrand-Rosenberg's laboratory as described by Chornoguz, et al.¹²⁰ Briefly, mice with primary 4T1 or 4T1/IL1 β tumors of ~7-10 mm in diameter and established metastatic disease were bled from the submandibular vein, and red blood cells were removed by lysis. The remaining leukocytes were identified by immunofluorescence and flow cytometry as previously described¹²⁰. Samples with >90% Gr1⁺ CD11b⁺ cells were used in the experiments.

Constructing the Pellicle

The pellicle was constructed following the procedure introduced in chapter 4 of this thesis. Preparation of the PM pellicles on conventional and inflammatory MDSC was performed in parallel. Approximately 1×10^8 MDSC cells from each type were resuspended in 2 mL PMCBA (800 mM sorbitol, 20 mM MES, 150 mM NaCl, pH 5.3) and added dropwise to a 10%(w/v) Al₂O₃ coated Fe₃O₄ suspension. Coating was performed at 4°C by gently rocking the mixture for 15 min. Excess nanoparticles were removed by collecting the nanoparticle-coated cells at 900 xg for 5 min and washing three times. The coated cells were cross-linked by adding the suspension to 10 mg/ml poly(acrylic acid) in PMCBA, pH 6.0-6.5, in a dropwise fashion, and incubated at 4°C for 15 min with gentle rocking. The cross-linked cells were collected by centrifugation at 900 xg for 5 min and washed with PMCBA to remove excess poly(acrylic acid). The cell pellet was placed in 2.5 mM imidazole with

protease inhibitor cocktail and incubated at on ice for 30 min to swell the cells. Cell lysis was carried out by using N₂ cavitation at 1500 psi for 30 min. The cell lysate was spun at 100 xg for 7 min to isolate the PM nanoparticle pellicles from cellular organelles and lysates, and washed three times with the lysis buffer, three times with 1 M Na₂CO₃, pH 11.4, and another three times with 1 M KCl. Proteins were released from the pellicles by triplicate extractions in 2% SDS, 62.5 mM Tris-HCl, and 5% β-mercaptoethanol, at 100°C for 5 min in a lab microwave oven (CEM corporation, Matthews, NC). The protein concentration was measured using an RC DC™ protein assay kit, prior to 1D-gel electrophoresis or proteolysis in-solution.

Scanning Electron Microscopy

Intact MDSC or nanoparticle-coated MDSC were collected by sedimentation at 900 xg for 5 min. The cells were washed with PMCBA and fixed with 2% glutaraldehyde. Secondary fixation was performed in 1% OsO₄ for 60 min. The cells were then dehydrated using an ethanol solution followed by critical point drying with CO₂ in a Denton DCP-1 critical point dryer (Denton Vacuum, LLC, Moorestown, NJ). The samples were subjected to Au/Pd coating in a DV-503 vacuum evaporator (Denton Vacuum, LLC, Moorestown, NJ), prior to imaging by a Hitachi SU-70 Field Emission scanning electron microscope and a Hitachi S-4700 Field Emission scanning electron microscope (Hitachi, Gaithersburg, MD).

Proteomic Analysis by HPLC-MS/MS

Proteins were analyzed using in-gel digestion following the procedure from Shevchenko, et al.⁶⁶ with slight modification. For each of the MDSC samples, 80 μ g of protein was loaded onto an 8-16% linear gradient polyacrylamide gel with the CriterionTM electrophoresis system (Bio-Rad, Hercules, CA). The gel was developed with Coomassie blue, and excised in 21 bands. The proteins in each band were reduced with 10 mM DTT at 56°C for 30 min, and alkylated with 55 mM iodoacetamide in the dark, for 20 min. The gel pieces were incubated in 13 ng/ μ L trypsin in 10 mM NH_4HCO_3 containing 10% (v/v) acetonitrile, and tryptic digestion was carried out at 37°C for 16 h. Extraction of peptides were performed in 1:2 (v/v) 5% formic acid/acetonitrile, at 37°C for 15 min.

Quantitative measurements were performed using spectral counting to compare protein abundances in conventional and inflammatory conditions. To reduce variability across samples, proteins were digested in-solution. Thirty to one hundred micrograms of proteins was precipitated using a chloroform/methanol precipitation, followed by re-solubilization in 8 M urea in 50 mM NH_4HCO_3 . The proteins were reduced by DTT at 56°C for 30 min, and alkylated by iodoacetamide at room temperature, in the dark, for 30 min. Lys-C digestion was carried out in 8 M urea/50 mM NH_4HCO_3 solution at 37°C for 3 h, using an enzyme to protein ratio of 1: 50. After five fold dilution, tryptic digestion was performed at 37°C for 16 h, using an enzyme to protein ratio of 1: 25. The digests were desalted using a TopTip C18 spin column (Glygen Corporation, Columbia, MD).

LC-MS/MS analysis was performed using a Shimadzu Prominent nanoHPLC (Shimadzu, Columbia, MD) interfaced to an LTQ-orbitrap XL (ThermoFisher

Scientific, San Jose, CA). Peptides from 15 µg of proteins were loaded onto a Zorbax 300SB-C18 trap column (Agilent Technologies, Palo Alto, CA) via an autosampler (Shimadzu, Columbia, MD), using solvent A (97% H₂O, 2.5% acetonitrile, 0.1% formic acid) at the flow rate of 10 µL/min for 10 min. The peptide fractionation was carried out in a Vydac Everest C18 column (150 mm x 150 µm) with 300 Å pore size and 5 µm particle size (Grace Vydac, Deerfield, IL), using a flow rate of 500 nL/min. A linear gradient was programmed to increase from 0% to 60% solvent B (97% acetonitrile, 2.5% H₂O, 0.1% formic acid) in 90 min, and then increase from 60% to 85% solvent B for 20 min. The column was connected to a 15 µm fused-silica Pico Tip (New Objective, Inc., Woburn, MA) and interfaced with a Thermo nanoelectrospray ionization source. The samples were ionized using a spray voltage of +1.8 kV, a tube lens voltage of 100 kV, and a capillary temperature of 275°C. The mass spectrometer was operated in a data-dependent mode, and the data acquisition was performed using Xcalibur 2.0 software (Thermo Fisher Scientific, San Jose, CA). Precursor ions were scanned in the orbitrap at a resolution set at 30,000 at m/z 400. In each cycle, the nine most abundant ions above the threshold of 50,000 ions were isolated for collision-induced dissociation (CID), using a normalized collision energy of 35 and an activation time of 30 ms, followed by product ion scans in the LTQ. The precursor ions were isolated using an isolation window of 3 Da. Dynamic exclusion was enabled to allow detection of low abundance ions with a repeat count of 1 and exclusion duration of 180 s. Replicate injections (2-6 injections) were performed to maximize the identification of low abundance proteins. For label-free quantitation, three biological replications were carried out to evaluate the statistical significance.

Bioinformatics

Spectra acquired in .RAW format were subjected to centroiding and mzXML reformatting using msconvert from the ProteoWizard project.¹⁰⁹ All data sets were searched against the reference set of mouse proteins in UniProtKnowledgeBase, using the PepArML meta-search engine.⁴⁸ Carbamidomethylation of cysteine was chosen as a fixed modification, and oxidation of methionine and diglycine tagged lysine residues were specified as variable modifications. The search results were filtered with the criteria of at least two distinct peptides identified with FDR lower than 1%. A global parsimony analysis was applied to ensure that the peptides were not shared with other retained proteins. Subcellular localization of each protein was assigned by in-house software, which determines the location based on the information available from the UniProt mouse Gene Ontology Annotation (GOA).⁶⁸ Transmembrane proteins were predicted based on the protein sequence, using a hidden Markov model on a TMHMM 2.0 server.⁸³ Functional annotation clustering analysis was performed using a Database for Annotation, Visualization, and Integrated Discovery (DAVID) v. 6.7.¹²⁴ The interactions between proteins were visualized using a Search Tool for the Retrieval of Interacting Genes/Proteins (STRING)¹²⁵ v 9.05, and the protein networks were clustered by MCL clustering algorithm implemented in STRING.¹²⁶

To compare protein abundances between samples, the in-house software, SpectralCount v.1.5, was used to compute the number of acquired spectra for identified proteins. Fisher's Exact test was applied to assess the analysis. Multiple testing methods were also applied to adjust the *p*-values, using the Bonferroni correction and the FDR-based correction.¹³⁰ A fold change between two samples was

estimated using a serial analysis of gene expression (SAGE) approach¹²⁷, which was applied to spectral counting techniques as reported by Old et al¹²⁸. Differences in protein abundances were calculated based on the number of normalized spectral counts using an equation:

$$R_{sc} = \log_2 [(n_{inf} + f)/(n_{con} + f)] + \log_2 [(t_{con} - n_{con} + f)/(t_{inf} - n_{inf} + f)]$$

Where $R_{sc} = \log_2$ ratio of abundance between inflammatory vs conventional MDSC proteins, n = spectral counts of each protein in conventional (con) or inflammatory (inf) samples, t = total spectral counts in conventional (con) or inflammatory (inf) samples, $f = 1.25$ (correction factor as per Old et al¹²⁸).

Results and discussion

Plasma membrane proteins were enriched by the pellicle technique using Al₂O₃-coated Fe₃O₄ nanoparticles. Cell surface morphology of MDSC observed by SEM is shown in **Figure 26(A)** and **26(C)**. Both conventional and inflammatory MDSC exhibited heterogeneous cell surface morphology, including extrusions of various sizes and microvilli. Observations of multiple cells indicate that there is no substantial change in morphology between the two types of MDSC. Micrographs in **Figure 26(B)** and **26(D)** indicate successful coating of the nanoparticles on the MDSC surfaces.

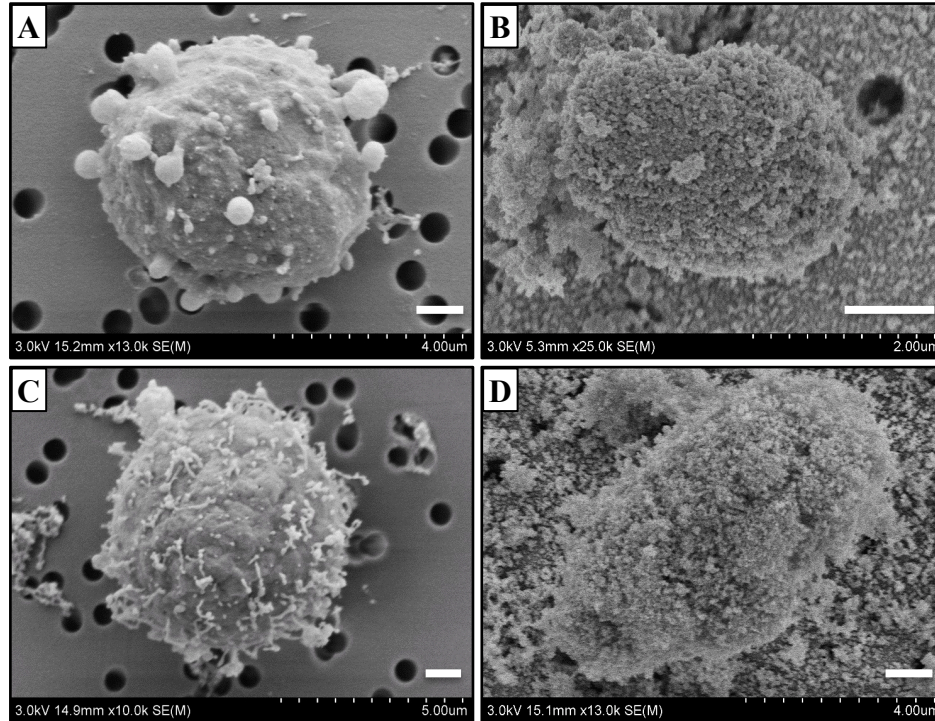


Figure 26. Morphology of the cells (A) conventional MDSC (B) Fe₃O₄ nanoparticle-coated conventional MDSC, (C) inflammatory MDSC, and (D) Fe₃O₄ nanoparticle-coated inflammatory MDSC. White scale bars indicate 1 μ m.

A single protein analysis identified 483 proteins from conventional MDSC and 421 proteins from inflammatory MDSC; of those, 386 proteins are shared by both samples (**Table 9, Figure 27**). Cellular localization and functional distribution of the proteins identified is demonstrated in **Figure 28**. There was no significant difference in the cellular locations or the functional distribution between the conventional and the inflammatory samples. Due to the highly dynamic behavior of these cellular proteins, a majority was annotated in multiple locations. **Table 9** and **Figure 28** suggest comparable enrichment of the PM proteins (38% vs. 36%), while more transmembrane proteins were identified from conventional MDSC.

Table 9. Number of proteins identified with in-gel digestion of conventional and inflammatory MDSC samples, their % assigned as plasma membrane by GO annotation, and % assigned as transmembrane by TMHMM 2.0.

	Distinct protein IDs	Proteins identified with GO annotation	% Annotated PM	% Assigned TM
Conventional	483	450	38%	30%
Inflammatory	421	396	36%	24%

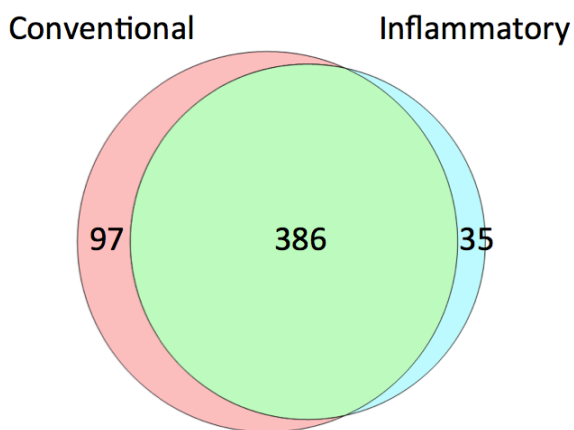
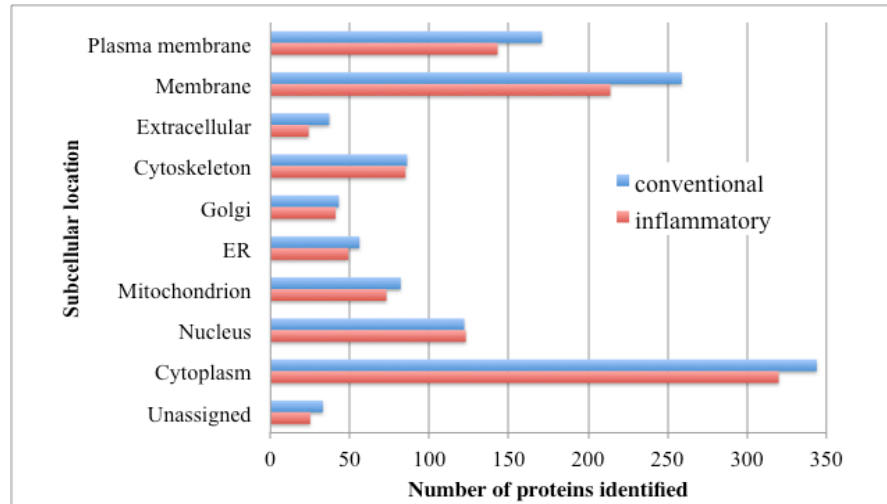


Figure 27. Venn diagram of showing overlapping between proteins identified from conventional and inflammatory MDSC using in-gel digestion.

(A)



(B)

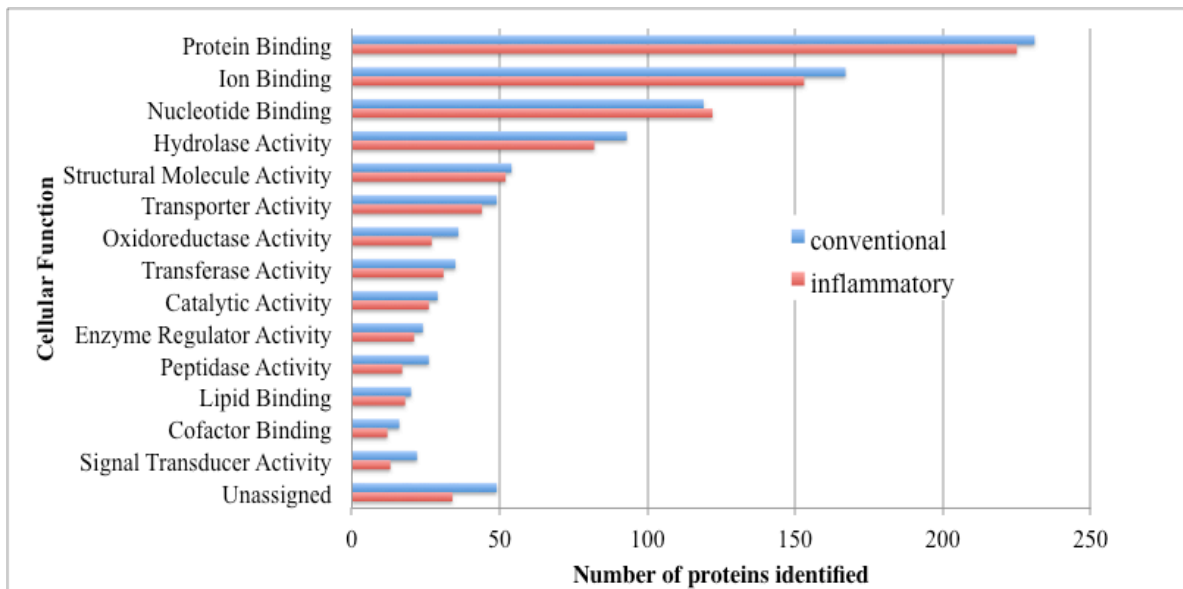


Figure 28. (A) Subcellular location and (B) functional distribution of proteins identified from conventional and inflammatory MDSC using in-gel digestion.

Table 10. Number of proteins identified with digestion in solution from conventional and inflammatory MDSC collected from three pairs of animals.

Samples	Total Number of proteins	% Plasma membrane proteins			
		Total	Experiment 1	Experiment 2	Experiment 3
Conventional	342	35%	41%	39%	39%
Inflammatory	380	36%	42%	37%	37%

Quantitative analysis was performed with three pairs of biological replicates, using spectral counting following LC-MS/MS analysis of peptides from in-solution digestion. A summary of the results and lists of proteins identified are provided in **Appendix Table 3**. **Table 10** indicates 342 and 380 total proteins identified from conventional and inflammatory MDSC, respectively. Averaging the three biological replicates, 40% and 39% of the total proteins identified are considered to be located on the PM from conventional MDSC and inflammatory MDSC, in good agreement with the identifications obtained from in-gel digestion. The consistently proportion of the proteins located on the PM from independent biological experiment is shown in **Table 10**.

The protein abundance changes were calculated and normalized using serial analysis of gene expression (SAGE)¹²⁷, which provides a correction factor for the fold change to avoid discontinuity of the data in case that a given protein is identified in

only one sample. Proteins with \log_2 ratio of abundance between inflammatory vs. conventional MDSC (R_{sc}) greater than 1 or less than -1 and Fisher's exact test p -values less than 0.05 (Bonferroni multiple-test correction) were considered to be significantly changed. From the total of 394 proteins identified from six biological experiments, 32 proteins were shown to have significantly higher abundances in the inflammatory MDSC (**Table 11**), and 13 proteins were quantified as significantly lower abundance (**Table 12**). A distribution of the R_{sc} (**Figure 29**) indicates that about 11% of the proteins identified show significant changes in their abundances. From the set of proteins with increased abundances (**Table 11**), 28 proteins have associated GO terms for cellular locations; and 20 of those are considered to be located on the PM or the extracellular matrices (ECM). A list of proteins with decreased abundances (**Table 12**) reveals 11 proteins with cellular localization GO annotations, of which 4 proteins are annotated as located on the PM or the ECM.

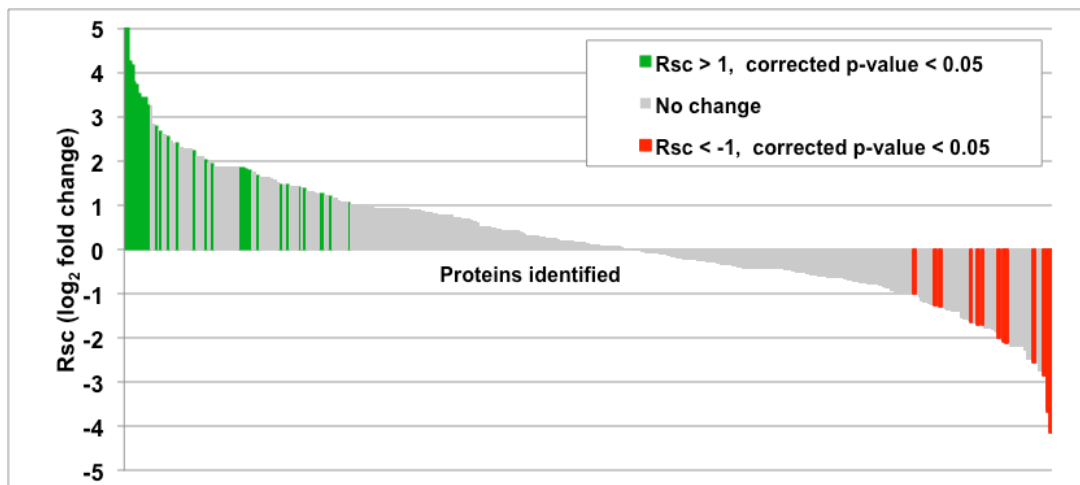


Figure 29. A distribution of the combined \log_2 ratios of abundances between inflammatory vs. conventional MDSC (R_{sc}) and their statistical significance.

R_{sc} values >1 or <-1 indicate 2-fold or greater changes.

Table 11. Proteins quantified with significantly higher abundances ($R_{sc} > 1$, Bonferroni corrected p -value < 0.05). $R_{sc} = \log_2$ [ratio of abundance between inflammatory vs. conventional MDSC].

Protein	Description	Corrected p -value	R_{sc}	Located on PM or ECM
P27005	Protein S100-A8	4.31E-36	1.85	✓
P31725	Protein S100-A9	8.19E-18	1.20	✓
P17182	Alpha-enolase	1.54E-12	1.26	✓
Q00612	Glucose-6-phosphate 1-dehydrogenase X	2.39E-12	2.02	-
Q61233	Plastin-2	3.10E-11	1.79	✓
P11276	Fibronectin	6.95E-11	5.01	✓
Q8K0E8	Fibrinogen beta chain	6.95E-11	5.01	✓
Q9D154	Leukocyte elastase inhibitor A	4.62E-10	2.22	✓
Q8VCM7	Fibrinogen gamma chain	1.64E-09	4.16	✓
P52480	Pyruvate kinase isozymes M1/M2	4.53E-08	1.26	✓
Q61096	Myeloblastin	6.11E-07	2.55	✓
P40124	Adenylyl cyclase-associated protein 1	6.79E-07	1.40	✓
Q8BWM3	MCG130173	1.38E-05	4.26	unassigned
P26041	Moesin	1.85E-05	1.78	✓
P17742	Peptidyl-prolyl cis-trans isomerase A	7.38E-05	2.67	✓
P20152	Vimentin	2.60E-04	2.77	✓
Q99JY9	Actin-related protein 3	3.04E-04	1.46	-

P04919	Band 3 anion transport protein	4.89E-04	1.82	✓
Q9QZU3	Platelet glycoprotein V (Fragment)	9.38E-04	3.27	unassigned
B2RV77	MCG130182, isoform CRA_a	2.02E-03	3.78	unassigned
D3Z3G6	Mitogen-activated protein kinase 3	3.51E-03	3.72	-
Q9DBJ1	Phosphoglycerate mutase 1	4.07E-03	1.86	-
P62962	Profilin-1	1.03E-02	1.07	✓
P99029	Peroxiredoxin-5, mitochondrial	1.31E-02	1.48	-
Q61210	Rho guanine nucleotide exchange factor 1	1.83E-02	2.40	-
Q9WVK4	EH domain-containing protein 1	1.85E-02	3.51	✓
O08808	Protein diaphanous homolog 1	2.23E-02	1.67	✓
Q8CIZ8	von Willebrand factor	3.22E-02	3.43	✓
P09411	Phosphoglycerate kinase 1	3.22E-02	3.43	-
Q497J0	MCG130175, isoform CRA_b	3.22E-02	3.43	unassigned
A6ZI44	Fructose-bisphosphate aldolase	3.39E-02	1.93	-
P26040	Ezrin	3.79E-02	1.37	✓

Table 12. Proteins quantified with significantly lower abundances ($R_{sc} < -1$, Bonferroni corrected p -value < 0.05). $R_{sc} = \log_2$ [ratio of abundance between inflammatory vs. conventional MDSC].

Protein	Description	Corrected p -value	R_{sc}	Located on PM or ECM
P49290	Eosinophil peroxidase	0	-1.70	-
P51881	ADP/ATP translocase 2	0	-1.99	-
Q61878	Bone marrow proteoglycan	0	-2.08	-
P28293	Cathepsin G	1.75E-10	-1.63	✓
Q8VDN2	Sodium/potassium-transporting ATPase subunit alpha-1	9.31E-09	-2.55	✓
Q9Z1R9	MCG124046	8.39E-08	-1.01	unassigned
Q9D1G1	Ras-related protein Rab-1B	1.71E-06	-2.84	-
Q5SZV3	40S ribosomal protein S8	1.81E-04	-3.68	-
Q8CFQ9	Fusion, derived from t(12;16) malignant liposarcoma (Human)	1.05E-03	-4.14	-
P51437	Cathelin-related antimicrobial peptide	1.18E-02	-1.29	✓
D3Z627	Integrin alpha-L	1.55E-02	-1.69	✓
P23116	Eukaryotic translation initiation factor 3 subunit A	1.82E-02	-1.26	-
Q9CPN9	Protein 2210010C04Rik	4.38E-02	-2.12	unassigned

Functional annotation enrichment of differentially abundant proteins with respect to KEGG pathways¹²⁹ was carried out using the DAVID bioinformatics resources¹²⁴, using the set of all proteins identified in both samples as background. For the pathway analysis, proteins quantified with R_{sc} greater than 1 or less than -1 and Fisher's exact test p -values less than 0.05 (FDR multiple-test correction¹³⁰) were considered to be significantly changed. With these criteria, there were 58 proteins with increased abundance and 34 proteins with decreased abundance under elevated inflammation. KEGG pathways with at least 4 differentially abundant proteins and Fisher's Exact test p -value less than 0.05 were retained. The proteins with increased abundances at a higher level of inflammation (58 proteins) reveal enrichment in (i) regulation of the actin cytoskeleton (p -value = 1.7×10^{-4}), (ii) the glycolysis/gluconeogenesis pathway (p -value = 5.8×10^{-4}), (iii) ECM-receptor interaction (p -value = 6.2×10^{-3}), and (iv) leukocyte transendothelial migration (p -value = 2.9×10^{-2}) (**Table 13**). Known and predicted interactions between the differentially abundant proteins were evaluated using STRING v.9.05 (**Figure 30**). Proteins with increased abundances show interactions between and within the four enriched pathways. STRING also linked S100A8 and S100A9 proteins to other increased abundance proteins. Previous studies have reported that S100A8 and S100A9 form a heterodimer that facilitates the accumulation of MDSC in the tumor microenvironment via an NF- κ B-dependent pathway¹¹³, or by inhibiting the normal differentiation process via a STAT3-dependent pathway.¹³¹ Our work is in good agreement with previous reports that the level of S100A8/A9 increases in the inflammatory environment.¹¹³ Based on the STRING database, both S100A8 and

S100A9 interact with the proteins in the leukocyte transendothelial migration pathway. This cell migration process is known to be involved with the other two enriched pathways: the actin cytoskeleton rearrangement pathway and the ECM-receptor interaction pathway.¹³² The significance of leukocyte transendothelial migration has been confirmed by previous functional studies⁵⁷ in which MDSC were shown to prevent T-cells from entering lymph nodes where they could become activated. However, the effect of inflammation on MDSC migration has not been fully elucidated. We propose that the pathways for transendothelial cell migration, cytoskeleton rearrangement, and ECM-receptor interaction that are elevated in inflammation may contribute to both the activation and function of MDSC. Furthermore, it is likely that the inflammation-driven up-regulation of the glycolysis pathway provides an acidic pH in the tumor microenvironment that promotes MDSC expansion and subsequent suppression of anti-tumor immunity.¹³³ Collectively, these effects inhibit an anti-tumor immune response and promote tumor growth. Considering the proteins with decreased abundances under elevated inflammation (34 proteins), no pathway was identified above the criteria. This study reveals protein candidates, especially the plasma membrane proteins, for further studies.

Table 13. List of proteins associated in the KEGG pathways.

Pathways	Fisher's Exact test <i>p</i>-value	Protein name
Regulation of actin cytoskeleton	1.7×10^{-4}	Rho guanine nucleotide exchange factor 1 Protein diaphanous homolog 1 Ezrin Fibronectin Moesin Profilin-1 Actin-related protein 2/3 complex subunit 1B Alpha-actinin-1 Vinculin Integrin alpha-IIb Actin-related protein 2/3 complex subunit 4
Glycolysis	5.8×10^{-4}	Fructose-bisphosphate aldolase Phosphoglycerate kinase 1 Phosphoglycerate mutase 1 Alpha-enolase Pyruvate kinase isozymes M1/M2 Hexokinase-3 Hexokinase-1

ECM-receptor interaction	6.2×10^{-3}	von Willebrand factor Fibronectin Platelet glycoprotein V (Fragment) Integrin alpha-IIb
Leukocyte transendothelial migration	2.9×10^{-2}	Mitogen-activated protein kinase 14 Neutrophil cytosol factor 4 Neutrophil cytosol factor 2 Alpha-actinin-1 Vinculin Ezrin Moesin

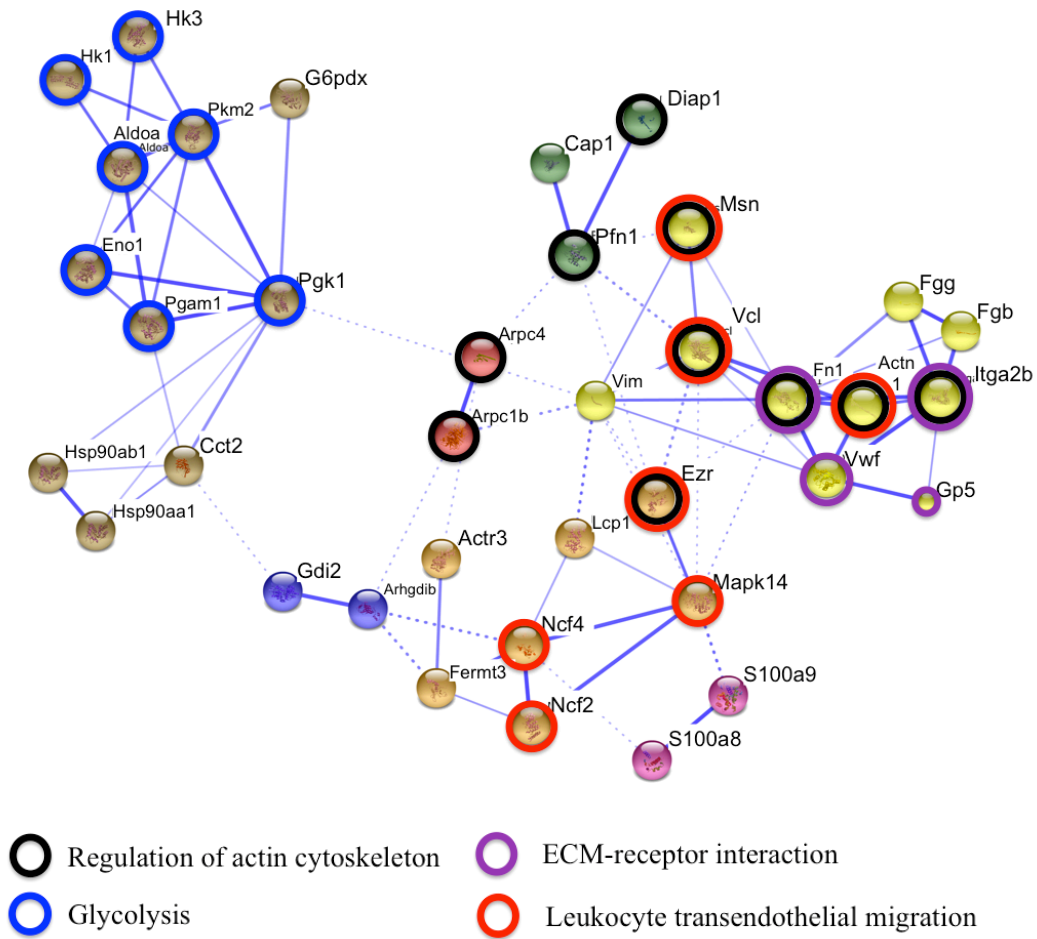


Figure 30. Networks of the proteins quantified with higher abundances in inflammatory MDSC ($R_{sc} > 1$, FDR corrected p -value < 0.05), evaluated by STRING. The network cluster is shown in a confident view. Thicker line represents stronger interaction between proteins. The gene names and their associated KEGG pathways are specified.

Summary

We have integrated the Fe₃O₄ nanoparticle pellicle enrichment technique with label-free quantitative proteomic analysis to assess PM proteins from MDSC and to compare their abundances under conventional and inflammatory conditions. In the enriched samples 36-42% of the proteins identified were located in the plasma membrane. By comparing the abundances of the enriched proteins from the cells derived from the heightened- and basal- levels of inflammation, we find that increases in the abundances of proteins involved in the pathways for cytoskeleton arrangement, glycolysis, ECM-receptor interaction, and leukocyte transendothelial migration are associated with inflammation and thus with the activities of MDSC enhanced by inflammation.

Chapter 6 : Conclusions and Prospectus

This dissertation outlines methods for enrichment and characterization of the PM proteins from suspended cells using the cationic nanoparticle pellicle technique integrated with mass-spectrometry-based proteomic analysis. This research project is achieved by a cross-disciplinary collaboration from different areas of research including proteomics, nanotechnology, bioinformatics, biochemistry, analytical chemistry, and immunology. This collaboration provides an opportunity for different perspectives and skills to solve the outlined problems, which are valuable for advancement in scientific research.

A large-scale identification and quantification of the PM proteome provides crucial information about alterations of the protein content and their abundances in the cells under normal conditions and various diseased states. Since the PM encloses intracellular components from extracellular environments, its proteins regulate a number of signaling processes, cell communications, and molecular transports; thus, they are involved in many pathological conditions. The main problems in PM proteomic research result from the hydrophobic property of the PM proteins and their low expression levels in the cells. This study reports a comprehensive evaluation of multiple steps to improve the analysis of the PM proteins, including the PM enrichment method, protein solubilization, proteolysis procedures, LC-MS/MS, and integrated bioinformatics resources.

Although the cationic silica nanoparticle pellicle method has been reported in the literature for decades, this work demonstrated, for the first time, that the higher density nanoparticles improves an enrichment efficiency of the plasma membrane proteins, as compared to the silica-based nanoparticles used in previously published reports. In this study, suspended eukaryotic cells grown in cultures and collected from animal model were investigated; it is plausible that this high density nanoparticle pellicle method could be apply to study other systems, such as polarized cells attached on the surface, cells derived from various tissues, and prokaryotic cells. However, the coating and lysis protocol should be further optimized for each types of sample.

In addition to the density, we observed that other properties, such as functional groups and the nanoparticle shape, also affect the enrichment process. Inorganic surface modification, i.e., Al_2O_3 , reveals a better dispersion and a higher stability in the plasma membrane coating buffer, compared to the molecules with hydrophobic tails, such as aminopropyl thiol and cetyltrimethylammonium bromide. The wire-shaped nanoparticles provide minimal internalization and multiple interactions between their surfaces and the cell membranes, which increase strength of pellicle interactions. Because of a formation of stronger pellicles, the coating and lysis procedures must be optimized in order to achieve a better enrichment of the cell membrane proteins.

After enriching the plasma membrane pellicles, careful attention must be given to ensure complete release and high recovery of those membrane proteins, as well as efficient digestion strategies. Strong detergents, such as SDS, are optimal for

the solubilization; however, they are commonly not compatible with the downstream proteolysis and LC-MS/MS. This conundrum remains to be solved. The sample preparation is a critical step prior to mass-spectrometry analysis. The combination of a good enrichment technique for depletion of high abundance proteins, optimal procedures for proteolysis, and pre-fractionation methods will improve a problem of underrepresentation of the membrane proteomics from highly complex mixtures.

For a quantitative analysis, in addition to the spectral counting method used in this study for comparison of protein abundances, other types of quantitative techniques could also be integrated with the high-density nanoparticle pellicle technique. There are numerous methods recently developed for quantitative proteomics, including isotope labeling approaches such as stable isotope labeling by amino acids in cell culture (SILAC)¹³⁴, isobaric tags for relative and absolute quantitation (iTRAQ)¹³⁵, and ¹⁸O-enzymatic labeling⁸⁰, as well as label-free approaches, such as spectral counting¹³⁶, and chromatographic peak area intensity measurement¹³⁷. Each method has its advantages and limitations. The labeled methodologies provide highly accurate and highly reproducible quantitation, while the label-free approaches are cost-effective, less-time consuming, and applicable to the comparison of multiple samples.

One of the most important steps in a high-throughput proteomic study is the data interpretation. Currently, there are many open-source software tools for advanced proteomics data analysis, including search engines, protein databases, functional annotation tools, gene ontology annotation, and algorithms for prediction of protein properties. Using a combination of multiple search engines, such as

PepArML⁴⁸, drastically increases the number of protein identifications, compared to a single search engine. This work utilizes strength of available software to interpret the data from acquired mass spectra to explain biological relevance, for example, GOA⁶⁸ for protein function and location annotation, DAVID¹²⁴ for a gene set enrichment and pathway analysis, STRING¹²⁵ for prediction protein interaction, and TMHMM⁸³ for prediction a number of transmembrane domains.

This dissertation demonstrates successful integration of the proteomic strategies and the high-density cationic nanoparticle pellicle method for the PM proteome characterization of two types of cells in suspension. It is notable that this method is also applicable to other types of suspended cells including clinical samples. In the long term, the study of changes in PM proteomes will lead to a better understanding of disease mechanisms and a better development of potential diagnostics and therapeutics.

Appendices

Appendix Table 1. Proteins identified from at least two peptides with FDR<10% as summarized in **Figure 14**.

Proteins Identified in all three experiments (79)			
UniProt Accession number	Protein Description	GRAVY SCORE	Number of transmembran domains
P05023	Sodium/potassium-transporting ATPase subunit alpha-1	0.011241447	10
Q15758	Neutral amino acid transporter B(0)	0.643807763	9
Q99805	Transmembrane 9 superfamily member 2	0.271794872	9
P16615	Sarcoplasmic/endoplasmic reticulum calcium ATPase 2	0.096641075	8
Q8TCT9	Minor histocompatibility antigen H13	0.363660477	7
P04839	Cytochrome b-245 heavy chain	0.049122807	4
P05141	ADP/ATP translocase 2	0.051677852	3
Q00325	Phosphate carrier protein, mitochondrial	0.023756906	2
Q9NQC3	Reticulon-4	-0.414261745	2
P35613	Basigin	-0.322857143	2
Q92542	Nicastrin	-0.139633286	1
P27105	Erythrocyte band 7 integral membrane protein	0.043402778	1
P08195	4F2 cell-surface antigen heavy chain	-0.146825397	1
O14672	Disintegrin and metalloproteinase domain-containing protein 10	-0.598930481	1
P02786	Transferrin receptor protein 1	-0.242631579	1
Q8IXI1	Mitochondrial Rho GTPase 2	-0.102588997	1
P26010	Integrin beta-7	-0.274561404	1
P05362	Intercellular adhesion molecule 1	-0.271428571	1
P54709	Sodium/potassium-transporting ATPase subunit beta-3	-0.144086022	1
P28907	ADP-ribosyl cyclase 1	-0.305666667	1
Q9HDC9	Adipocyte plasma membrane-associated protein	-0.186298077	1
Q9P0L0	Vesicle-associated membrane protein-	-0.467871486	1

	associated protein A		
P16188	HLA class I histocompatibility antigen, A-30 alpha chain	-0.500547945	1
P06733	Alpha-enolase	-0.221428571	0
P49368	T-complex protein 1 subunit gamma	-0.252477064	0
P25705	ATP synthase subunit alpha, mitochondrial	-0.066726944	0
P15924	Desmoplakin	-0.823371648	0
Q00839	Heterogeneous nuclear ribonucleoprotein U	-0.977575758	0
P08237	6-phosphofructokinase, muscle type	-0.171666667	0
P52272	Heterogeneous nuclear ribonucleoprotein M	-0.341643836	0
Q9UJS0	Calcium-binding mitochondrial carrier protein Aralar2	0.031703704	0
Q00610	Clathrin heavy chain 1	-0.242746269	0
Q15149	Plectin	-0.665029889	0
P63244	Guanine nucleotide-binding protein subunit beta-2-like 1	-0.251419558	0
P04792	Heat shock protein beta-1	-0.566829268	0
P14618	Pyruvate kinase isozymes M1/M2	-0.128060264	0
P08574	Cytochrome c1	-0.137538462	0
P49327	Fatty acid synthase	-0.069693349	0
P46940	Ras GTPase-activating-like protein	-0.494749547	0
P21796	Voltage-dependent anion-selective channel protein 1	-0.410954064	0
Q99714	3-hydroxyacyl-CoA dehydrogenase type-2	0.232950192	0
P35579	Myosin-9	-0.853520408	0
P17987	T-complex protein 1 subunit alpha	-0.037769784	0
P14868	Aspartyl-tRNA synthetase	-0.416367265	0
P14625	Endoplasmin	-0.712702366	0
P00505	Aspartate aminotransferase, mitochondrial	-0.205813953	0
P61006	Ras-related protein Rab-8A	-0.380676329	0
P31146	Coronin-1A	-0.319305857	0
P61026	Ras-related protein Rab-10	-0.33	0
P38646	Stress-70 protein, mitochondrial	-0.400294551	0
P08865	40S ribosomal protein SA	-0.309491525	0
Q15046	Lysyl-tRNA synthetase	-0.449748744	0

P0CG47	Polyubiquitin-B	-0.476419214	0
Q14676	Mediator of DNA damage checkpoint protein 1	-0.824461465	0
P07900	Heat shock protein HSP 90-alpha	-0.750273224	0
P15153	Ras-related C3 botulinum toxin substrate 2	-0.120833333	0
P63000	Ras-related C3 botulinum toxin substrate 1	-0.100520833	0
P06576	ATP synthase subunit beta, mitochondrial	0.018147448	0
Q9Y490	Talin-1	-0.240377804	0
P40926	Malate dehydrogenase, mitochondrial	0.143491124	0
P11142	Heat shock cognate 71 kDa protein	-0.456037152	0
P37802	Transgelin-2	-0.613567839	0
P35232	Prohibitin	0.024264706	0
Q8WXH0	Nesprin-2	-0.633957879	0
P14174	Macrophage migration inhibitory factor	-0.00173913	0
P51159	Ras-related protein Rab-27A	-0.356561086	0
P07954	Fumarate hydratase, mitochondrial	-0.07372549	0
P07237	Protein disulfide-isomerase	-0.430511811	0
P51148	Ras-related protein Rab-5C	-0.33287037	0
P48047	ATP synthase subunit O, mitochondrial	-0.01971831	0
P53618	Coatomer subunit beta	-0.091185729	0
P61106	Ras-related protein Rab-14	-0.399069767	0
Q14258	E3 ubiquitin/ISG15 ligase TRIM25	-0.436984127	0
O76094	Signal recognition particle 72 kDa protein	-0.642026826	0
O00116	Alkyldihydroxyacetonephosphate synthase, peroxisomal	-0.33449848	0
P04899	Guanine nucleotide-binding protein G(i) subunit alpha-2	-0.363661972	0
Q15084	Protein disulfide-isomerase A6	-0.275	0
P06744	Glucose-6-phosphate isomerase	-0.344444444	0
Q9H4M9	EH domain-containing protein 1	-0.360299625	0
Proteins Identified in the In-gel and In-solution Experiments (9)			
UniProt Accession number	Protein Description	GRAVY SCORE	Number of transmembrane domains
P43007	Neutral amino acid transporter A	0.52537594	9

Q03519	Antigen peptide transporter 2	0.13877551	6
Q99720	Sigma non-opioid intracellular	0.134080717	1
Q01082	Spectrin beta chain, brain 1	-0.766116751	0
P04264	Keratin, type II cytoskeletal 1	-0.625776398	0
Q15286	Ras-related protein Rab-35	-0.472636816	0
P00734	Prothrombin	-0.539228296	0
Q92974	Rho guanine nucleotide exchange factor 2	-0.602941176	0
P13987	CD59 glycoprotein	0.06640625	0
Proteins Identified in the In-gel & On-filter Experiments (25)			
UniProt Accession number	Protein Description	GRAVY SCORE	Number of transmembrane domains
P23634	Plasma membrane calcium-transporting ATPase 4	-0.11353747	8
Q03518	Antigen peptide transporter 1	0.14220297	7
P21926	CD9 antigen	0.487280702	4
P51572	B-cell receptor-associated protein 31	-0.157317073	3
Q8WTV0	Scavenger receptor class B member 1	0.124637681	2
Q9BV40	Vesicle-associated membrane protein 8	-0.049	1
P22897	Macrophage mannose receptor 1	-0.552472527	1
P13591	Neural cell adhesion molecule 1	-0.410606061	1
P43121	Cell surface glycoprotein MUC18	-0.41625387	1
Q9BX59	Tapasin-related protein	0.010470085	1
P01893	Putative HLA class I histocompatibility antigen, alpha chain H	-0.575966851	1
Q7L576	Cytoplasmic FMR1-interacting protein 1	-0.263926576	0
P09382	Galectin-1	-0.151111111	0
Q92930	Ras-related protein Rab-8B	-0.360386473	0
Q02978	Mitochondrial 2-oxoglutarate/malate carrier protein	0.11656051	0
Q15907	Ras-related protein Rab-11B	-0.435321101	0
P63010	AP-2 complex subunit beta	-0.094877268	0
P61224	Ras-related protein Rap-1b	-0.389673913	0

P11413	Glucose-6-phosphate 1-dehydrogenase	-0.370097087	0
O00299	Chloride intracellular channel protein 1	-0.283817427	0
P50570	Dynamin-2	-0.433218391	0
P62873	Guanine nucleotide-binding protein G(I)/G(S)/G(T) subunit beta-1	-0.231176471	0
P62879	Guanine nucleotide-binding protein G(I)/G(S)/G(T) subunit beta-2	-0.177058824	0
P38606	V-type proton ATPase catalytic subunit A	-0.186061588	0
P50395	Rab GDP dissociation inhibitor beta	-0.332134831	0
Proteins Identified in the In-solution & On-filter Experiments (5)			
UniProt Accession number	Protein Description	GRAVY SCORE	Number of transmembrane domains
P04222	HLA class I histocompatibility antigen, Cw-3 alpha chain	-0.494262295	1
O75955	Flotillin-1	-0.338407494	0
O96019	Actin-like protein 6A	-0.268065268	0
Q14254	Flotillin-2	-0.148130841	0
P61158	Actin-related protein 3	-0.266267943	0
Proteins Identified in the In-gel Experiment (158)			
UniProt Accession number	Protein Description	GRAVY SCORE	Number of transmembrane domains
P30825	High affinity cationic amino acid transporter 1	0.592368839	14
Q92536	Y+L amino acid transporter 2	0.57184466	12
O15427	Monocarboxylate transporter 4	0.66172043	12
P11166	Solute carrier family 2, facilitated glucose transporter member 1	0.534146341	12
Q8WUX1	Sodium-coupled neutral amino acid transporter 5	0.748516949	11
Q01650	Large neutral amino acids transporter small subunit 1	0.739053254	11
Q9H2H9	Sodium-coupled neutral amino acid transporter 1	0.550308008	11

O15439	Multidrug resistance-associated protein 4	0.078716981	11
Q99808	Equilibrative nucleoside transporter 1	0.687280702	11
O00400	Acetyl-coenzyme A transporter 1	0.302367942	11
Q9Y666	Solute carrier family 12 member 7	0.122253001	11
P53985	Monocarboxylate transporter 1	0.348	11
Q13488	V-type proton ATPase 116 kDa subunit a isoform 3	0.175783133	8
Q16602	Calcitonin gene-related peptide type 1 receptor	0.198047722	8
Q93050	V-type proton ATPase 116 kDa subunit a isoform 1	0.008602151	7
P32246	C-C chemokine receptor type 1	0.488169014	7
P48960	CD97 antigen	-0.032335329	7
Q08722	Leukocyte surface antigen CD47	0.599380805	6
P55061	Bax inhibitor 1	0.655696203	6
Q9UNQ0	ATP-binding cassette sub-family G member 2	0.194503817	6
O96005	Cleft lip and palate transmembrane protein 1	-0.18490284	5
O43808	Peroxisomal membrane protein PMP34	0.274918567	5
O43760	Synaptogyrin-2	0.168303571	4
Q5BJF2	Transmembrane protein 97	0.216477273	4
O14735	CDP-diacylglycerol--inositol 3-phosphatidyltransferase	0.612676056	4
Q04941	Proteolipid protein 2	0.765131579	4
P08962	CD63 antigen	0.767226891	4
O95864	Fatty acid desaturase 2	-0.182207207	4
O15551	Claudin-3	0.605	4
P12235	ADP/ATP translocase 1	0.059395973	3
P42261	Glutamate receptor 1	-0.199227373	3
Q9NRZ7	1-acyl-sn-glycerol-3-phosphate acyltransferase gamma	0.142287234	3
P13498	Cytochrome b-245 light chain	0.030769231	3
P11279	Lysosome-associated membrane glycoprotein 1	-0.019664269	2
Q14108	Lysosome membrane protein 2	-0.038912134	2
P08842	teryl-sulfatase	-0.091595197	2

P08575	Receptor-type tyrosine-protein phosphatase C	-0.595015337	2
Q8N4V1	Membrane magnesium transporter 1	-0.183969466	2
P82279	Crumbs homolog 1	-0.206401138	2
Q8TAV4	Stomatin-like protein 3	0.143986254	1
O75578	Integrin alpha-10	-0.118766067	1
Q14517	Protocadherin Fat 1	-0.296185702	1
P21964	Catechol	0.159778598	1
O75787	Renin receptor	0.104285714	1
P04233	HLA class II histocompatibility antigen gamma chain	-0.6	1
P51809	Vesicle-associated membrane protein 7	0.055	1
P32942	Intercellular adhesion molecule 3	-0.057586837	1
P11717	Cation-independent mannose-6-phosphate receptor	-0.370172621	1
Q9UIQ6	Leucyl-cystinyl aminopeptidase	-0.193658537	1
Q8IXI2	Mitochondrial Rho GTPase 1	-0.266504854	1
P18084	Integrin beta-5	-0.235043805	1
P06756	Integrin alpha-V	-0.220515267	1
P13473	Lysosome-associated membrane glycoprotein 2	-0.043902439	1
P30464	HLA class I histocompatibility antigen, B-15 alpha chain	-0.539779006	1
Q07837	Neutral and basic amino acid transport protein rBAT	-0.437664234	1
Q86UE4	Protein LYRIC	-1.071134021	1
P30511	HLA class I histocompatibility antigen, alpha chain F	-0.534971098	1
P09601	Heme oxygenase 1	-0.426736111	1
P08473	eprilysin	-0.446666667	1
Q9NR96	Toll-like receptor 9	0.014825581	1
Q13444	Disintegrin and metalloproteinase domain-containing protein 15	-0.263847045	1
P10966	T-cell surface glycoprotein CD8 beta chain	-0.006190476	1
Q6ZRP7	Sulfhydryl oxidase 2	-0.229799427	1
P34910	Protein EVI2B	-0.522321429	1
P23276	Kell blood group glycoprotein	-0.259562842	1

Q9Y5Y6	Suppressor of tumorigenicity 14 protein	-0.364327485	1
P63027	Vesicle-associated membrane protein 2	-0.01637931	1
P18827	Syndecan-1	-0.548709677	1
O14980	Exportin-1	-0.091690009	0
P05109	Protein S100-A8	-0.396774194	0
Q8N6H7	ADP-ribosylation factor GTPase-activating protein 2	-0.616122841	0
P06239	tyrosine-protein kinase Lck	-0.469548134	0
Q9UHG3	Prenylcysteine oxidase 1	-0.060792079	0
O00422	Histone deacetylase complex subunit SAP18	-0.769281046	0
Q96F07	Cytoplasmic FMR1-interacting protein 2	-0.259467919	0
Q8TCS8	Polyribonucleotide nucleotidyltransferase 1, mitochondrial	-0.174968072	0
Q12860	Contactin-1	-0.307170923	0
P21333	Filamin-A	-0.316698149	0
Q02750	Dual specificity mitogen-activated protein kinase kinase 1	-0.304580153	0
Q8IY63	Angiomotin-like protein 1	-0.856380753	0
P53680	AP-2 complex subunit sigma	-0.052112676	0
Q4VCS5	Angiomotin	-0.711900369	0
Q12974	Protein tyrosine phosphatase type IVA 2	-0.349700599	0
Q93096	Protein tyrosine phosphatase type IVA 1	-0.300578035	0
Q14145	Kelch-like ECH-associated protein 1	-0.228205128	0
O15498	Synaptobrevin homolog YKT6	-0.28989899	0
Q15382	GTP-binding protein Rheb	-0.094021739	0
P62491	Ras-related protein Rab-11A	-0.420833333	0
P61586	Transforming protein RhoA	-0.367875648	0
P01111	GTPase NRas	-0.316931217	0
P62834	Ras-related protein Rap-1A	-0.375	0
O95970	Leucine-rich glioma-inactivated protein 1	-0.218671454	0
A6NMY6	Putative annexin A2-like protein	-0.54660767	0
O95716	Ras-related protein Rab-3D	-0.345205479	0
P20336	Ras-related protein Rab-3A	-0.479545455	0
P24666	Low molecular weight phosphotyrosine	-0.491772152	0

	protein phosphatase		
P17152	Transmembrane protein 11, mitochondrial	-0.011458333	0
P13796	Plastin-2	-0.311642743	0
Q16698	2,4-dienoyl-CoA reductase, mitochondrial	-0.019701493	0
P27797	Calreticulin	-1.104316547	0
O94973	AP-2 complex subunit alpha-2	-0.08658147	0
O95782	AP-2 complex subunit alpha-1	-0.089969294	0
P51151	Ras-related protein Rab-9A	-0.434328358	0
P61421	V-type proton ATPase subunit d 1	-0.094301994	0
Q13402	Myosin-VIIa	-0.426591422	0
O75323	Protein NipSnap homolog 2	-0.61048951	0
P56937	3-keto-steroid reductase	-0.011143695	0
P59190	Ras-related protein Rab-15	-0.558962264	0
Q5JWF2	Guanine nucleotide-binding protein G(s) subunit alpha isoforms XLas	-0.599903568	0
P20339	Ras-related protein Rab-5A	-0.427906977	0
P61020	Ras-related protein Rab-5B	-0.377209302	0
Q9NP72	Ras-related protein Rab-18	-0.315048544	0
P84085	ADP-ribosylation factor 5	-0.204444444	0
P14923	Junction plakoglobin	-0.157449664	0
P62330	ADP-ribosylation factor 6	-0.364571429	0
P15311	Ezrin	-0.97116041	0
P84095	Rho-related GTP-binding protein RhoG	-0.213089005	0
Q14232	Translation initiation factor eIF-2B subunit alpha	0.074098361	0
P09104	Gamma-enolase	-0.188248848	0
Q8WUD1	Ras-related protein Rab-2B	-0.367592593	0
P36404	ADP-ribosylation factor-like protein 2	-0.229347826	0
P61769	Beta-2-microglobulin	-0.376470588	0
Q9UPN3	Microtubule-actin cross-linking factor 1, isoforms 1/2/3/5	-0.588061722	0
Q92556	Engulfment and cell motility protein 1	-0.383356259	0
P63241	Eukaryotic translation initiation factor 5A-1	-0.264935065	0
O15144	Actin-related protein 2/3 complex	-0.439333333	0

	subunit 2		
P12259	oagulation factor V	-0.598741007	0
Q9UQP3	Tenascin-N	-0.580754426	0
Q92797	Symplekin	-0.19733124	0
O75369	Filamin-B	-0.292621061	0
P55160	Nck-associated protein 1-like	-0.041348713	0
P61077	Ubiquitin-conjugating enzyme E2 D3	-0.349659864	0
Q9H307	Pinin	-1.413807531	0
P63167	Dynein light chain 1, cytoplasmic	-0.448314607	0
Q5KSL6	Diacylglycerol kinase kappa	-0.440991345	0
P60953	Cell division control protein 42 homolog	-0.157068063	0
Q15771	Ras-related protein Rab-30	-0.235960591	0
Q86YS6	Ras-related protein Rab-43	-0.275	0
O43521	Bcl-2-like protein 11	-0.713131313	0
O95232	Luc7-like protein 3	-1.698611111	0
Q9UL26	Ras-related protein Rab-22A	-0.272164948	0
P54105	Methylosome subunit pICln	-0.656118143	0
Q6IAA8	Ragulator complex protein LAMT	-0.471428571	0
P51617	Interleukin-1 receptor-associated kinase 1	-0.28005618	0
P08754	Guanine nucleotide-binding protein G(k) subunit alpha	-0.361864407	0
P40763	Signal transducer and activator of transcription 3	-0.403376623	0
Q01518	Adenylyl cyclase-associated protein 1	-0.352210526	0
P06702	Protein S100-A9	-0.870175439	0
Q14160	Protein scribble homolog	-0.447300613	0
O00159	Myosin-Ic	-0.386735654	0
P41240	Tyrosine-protein kinase CSK	-0.268444444	0
P09429	High mobility group protein B1	-1.610232558	0
O95295	SNARE-associated protein Snapin	-0.364705882	0
Q9UQB8	Brain-specific angiogenesis inhibitor 1-associated protein 2	-0.667391304	0
Q99439	Calponin-2	-0.577993528	0
Q9UHD2	Serine/threonine-protein kinase TBK1	-0.347187929	0

P07858	Cathepsin B	-0.39439528	0
P52630	Signal transducer and activator of transcription 2	-0.420094007	0
Proteins identified in the In-solution Experiment (13)			
UniProt Accession number	Protein Description	GRAVY SCORE	Number of transmembrane domains
Q9NSA0	Solute carrier family 22 member 11	0.463454545	10
P35670	Copper-transporting ATPase 2	0.111399317	7
P18463	HLA class I histocompatibility antigen, B-37 alpha chain	-0.543093923	1
P30519	Heme oxygenase 2	-0.571518987	1
Q9NYQ8	Protocadherin Fat 2	-0.249643596	1
Q9Y4D7	Plexin-D1	-0.159012987	1
O15357	Phosphatidylinositol-3,4,5-trisphosphate 5-phosphatase 2	-0.481160572	0
P35580	Myosin-10	-0.863157895	0
P43403	Tyrosine-protein kinase ZAP-70	-0.426494346	0
P63092	Guanine nucleotide-binding protein G(s) subunit alpha isoforms short	-0.597208122	0
Q53GL0	Pleckstrin homology domain-containing family	-0.970171149	0
P23396	40S ribosomal protein S3	-0.152674897	0
P98171	Rho GTPase-activating protein 4	-0.542494715	0
Proteins identified in the On-filter Experiment (9)			
UniProt Accession number	Protein Description	GRAVY SCORE	Number of transmembrane domains
O94905	Erlin-2	-0.162536873	0
P30460	HLA class I histocompatibility antigen, B-8 alpha chain	-0.527071823	1
P51153	Ras-related protein Rab-13	-0.481280788	0
Q96CX2	BTB/POZ domain-containing protein KCTD12	-0.537538462	0
Q9NZI8	Insulin-like growth factor 2 mRNA-	-0.470710572	0

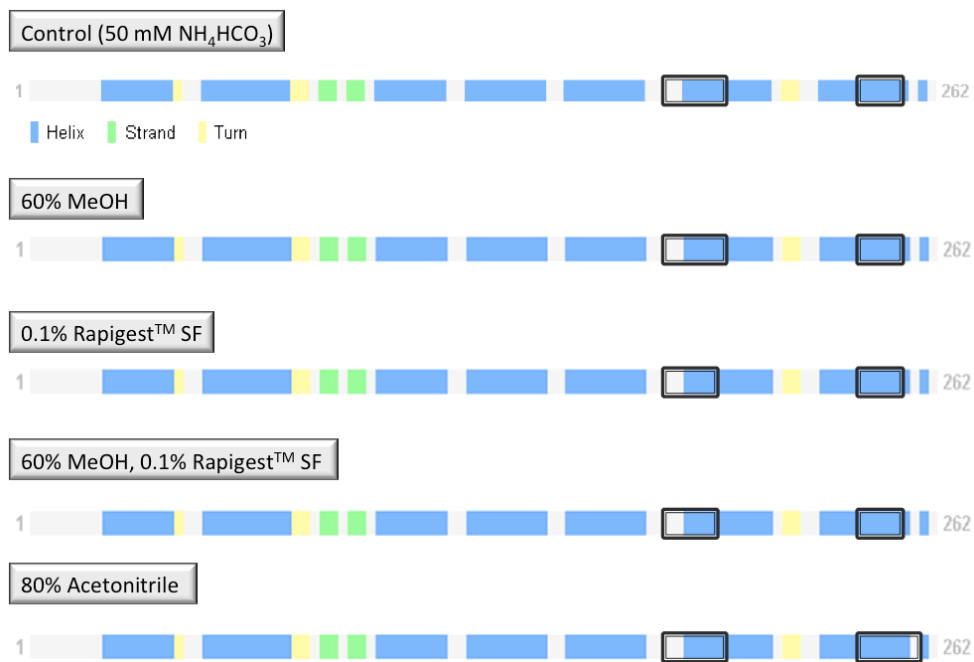
	binding protein 1		
A4UGR9	Xin actin-binding repeat-containing protein 2	-0.838381743	0
P13533	Myosin-6	-0.8057246	0
Q9UJF2	Ras GTPase-activating protein nGAP	-0.607813872	0
P49755	Transmembrane emp24 domain-containing protein 10	-0.170776256	2

Appendix Figure 1. (A) different domains (helix: blue, strand: green, turn: yellow) of bacteriorhodopsin molecule; (B) and (C) the regions of identified peptides from bacteriorhodopsin using trypsin and chymotrypsin proteolysis, respectively, in five different conditions.

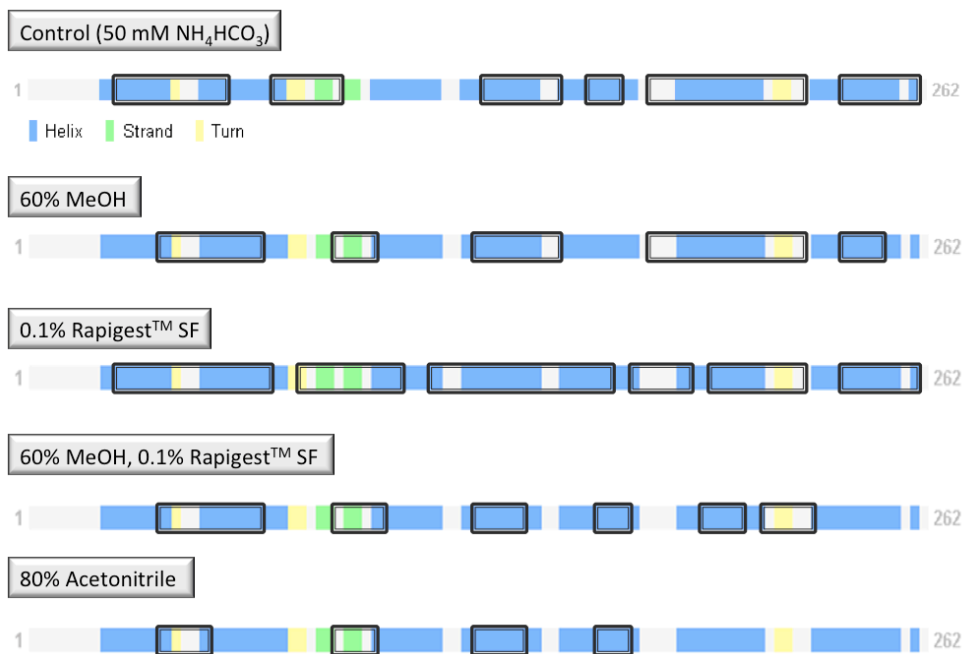
(A) Bacteriorhodopsin



(B) Trypsin digestion



(C) Chymotrypsin digestion



Appendix Table 2. Summary of proteins identified from the three pellicle samples and the cell lysate control.

SC : Spectral Count

FDR : Estimated False Discovery Rate

Protein	Description	Alumino silicate		Fe ₃ O ₄ -Al ₂ O ₃		SiO ₂ -Al ₂ O ₃		Cell Lysate	
		SC	FDR	SC	FDR	SC	FDR	SC	FDR
A0M8Q6	Ig lambda-7 chain C region	18	0.00	8	1.0E+00	3	1.0E+00	19	1.8E-03
A1A586	AHNAK nucleoprotein	3	1.00	0	1.0E+00	12	1.0E+00	7	1.1E-03
A1L0T0	Acetolactate synthase-like protein	1	0.00	1	1.9E-03	0	1.0E+00	0	1.0E+00
A3KMH1	Uncharacterized protein KIAA0564	1	0.02	0	1.0E+00	1	3.9E-03	0	1.0E+00
A4UGR9	Xin actin-binding repeat-containing protein 2	1	0.02	0	1.0E+00	1	9.8E-02	0	1.0E+00
A5A3E0	POTE ankyrin domain family member F	74	0.01	43	1.0E+00	108	9.8E-02	40	1.0E+00
A6NFA8	Histone H2A	0	1.00	2	1.0E+00	0	1.0E+00	25	9.0E-05
A6NGN4	Putative PRAME family member 25	0	1.00	0	1.0E+00	2	1.4E-03	0	1.0E+00
A6NGR9	Putative uncharacterized protein C8orf73	0	1.00	0	1.0E+00	2	4.9E-03	0	1.0E+00
A6NHL2	Tubulin alpha chain-like 3	12	1.00	7	4.2E-02	17	8.9E-02	5	1.0E+00
A6NHQ2	rRNA/tRNA 2'-O-methyltransferase fibrillar-like protein 1	7	1.00	3	1.0E+00	46	1.8E-12	14	1.2E-14
A6NHR9	Structural maintenance of chromosomes flexible hinge domain-containing protein 1	2	0.00	0	1.0E+00	15	3.9E-03	0	1.0E+00
A6NHU9	SH3 and multiple ankyrin repeat domains 2	0	1.00	0	1.0E+00	1	4.3E-02	1	8.7E-02
A6NJA2	Ubiquitin carboxyl-terminal hydrolase	0	1.00	0	1.0E+00	1	4.1E-02	1	2.3E-02
A6NKZ8	Putative tubulin beta chain-like protein ENSP00000290377	68	1.00	80	1.9E-04	57	9.4E-02	27	1.0E+00
A6NN01	Histone H2A	0	1.00	10	1.0E+00	11	3.9E-03	64	7.2E-10
A6XGN0	BORIS transcription factor transcript variant A6	1	0.08	0	1.0E+00	1	2.3E-02	0	1.0E+00
A8K8P3	Protein SFI1 homolog	0	1.00	0	1.0E+00	2	2.3E-03	0	1.0E+00
A8MPT4	Glutathione S-transferase theta-4	0	1.00	0	1.0E+00	2	5.1E-03	0	1.0E+00
A8MTM1	Carbonyl reductase 1	2	1.00	29	1.6E-02	0	1.0E+00	9	8.2E-04
A8MUW5	Family with sequence similarity 98, member B	18	0.00	0	1.0E+00	0	1.0E+00	55	8.2E-38
A8MW68	Uncharacterized protein	0	1.00	0	1.0E+00	0	1.0E+00	8	5.6E-08
A8MWI8	Chaperonin containing TCP1, subunit 7 (eta)	24	0.02	33	1.0E+00	54	1.5E-02	20	1.0E+00
A8MXH5	Collagen, type IV, alpha 6	0	1.00	1	6.5E-02	2	1.5E-03	0	1.0E+00
A9Z1Z3	Fer-1-like protein 4	1	0.04	0	1.0E+00	2	9.0E-03	0	1.0E+00
B0QZK4	Heterochromatin protein 1, binding protein 3 (Fragment)	0	1.00	0	1.0E+00	15	3.9E-03	14	4.0E-12
B0V043	Valyl-tRNA synthetase	84	0.00	90	8.8E-63	178	1.0E-30	71	9.6E-50

B0YIW6	Archain 1	0	1.00	0	1.0E+00	2	2.1E-02	8	4.8E-15
B1AHD1	NHP2 non-histone chromosome protein 2-like 1 (<i>S. cerevisiae</i>)	1	0.00	0	1.0E+00	27	6.4E-08	11	1.2E-07
B1ALA7	Phosphoribosyl pyrophosphate synthetase 1	0	1.00	0	1.0E+00	7	7.9E-05	1	2.8E-02
B1APE2	General transcription factor IIB (Fragment)	1	0.07	0	1.0E+00	1	9.8E-02	0	1.0E+00
B2RPK0	Putative high mobility group protein B1-like 1	12	0.00	0	1.0E+00	0	1.0E+00	6	1.0E+00
B3KNR9	Uncharacterized protein	0	1.00	0	1.0E+00	0	1.0E+00	3	7.1E-05
B3KRI2	NADH dehydrogenase (ubiquinone) Fe-S protein 7, 20kDa (NADH-coenzyme Q reductase)	0	1.00	0	1.0E+00	7	2.1E-11	0	1.0E+00
B3KSH1	HCG1784554, isoform CRA_a	17	0.00	19	1.0E-07	24	3.9E-03	19	4.7E-14
B3KT17	Uncharacterized protein	0	1.00	2	2.5E-02	0	1.0E+00	1	2.6E-02
B4DGR0	Uncharacterized protein	0	1.00	0	1.0E+00	6	2.0E-04	0	1.0E+00
B4DJV2	Citrate synthase	3	0.00	5	1.9E-03	63	3.8E-16	27	4.5E-23
B4DLN1	Solute carrier family 25 (mitochondrial carrier; dicarboxylate transporter), member 10	1	0.03	10	1.9E-03	1	8.1E-02	18	3.6E-17
B4DMY4	Cathepsin B	0	1.00	0	1.0E+00	0	1.0E+00	7	2.2E-10
B4DP27	Transmembrane emp24 domain trafficking protein 2	20	0.00	7	1.9E-03	0	1.0E+00	10	1.5E-06
B4DP52	DEAD (Asp-Glu-Ala-Asp) box polypeptide 39B	34	0.02	37	1.0E+00	90	1.0E+00	27	2.6E-02
B4DP75	Uncharacterized protein	50	0.00	44	1.9E-03	115	2.6E-04	47	1.8E-03
B4DPN6	DEAD (Asp-Glu-Ala-Asp) box polypeptide 1	12	0.00	6	1.9E-03	29	1.6E-05	5	1.8E-03
B4DTG2	Eukaryotic translation elongation factor 1 gamma	41	0.00	42	9.8E-17	106	4.8E-27	84	1.7E-41
B4DV35	Uncharacterized protein	0	1.00	0	1.0E+00	0	1.0E+00	2	7.0E-04
B4DV79	Eukaryotic translation initiation factor 3, subunit B	0	1.00	1	1.9E-03	1	3.9E-03	16	5.9E-15
B4DW05	Uncharacterized protein	43	1.00	38	1.9E-02	97	1.0E+00	39	2.0E-02
B4DW52	Actin, beta	250	0.00	215	7.2E-09	238	3.9E-03	251	3.1E-06
B4DW74	RAP1B, member of RAS oncogene family	5	0.00	7	1.9E-03	2	3.9E-03	9	1.8E-03
B4DWB7	Peptidyl-prolyl cis-trans isomerase	11	1.00	5	2.2E-02	0	1.0E+00	8	1.1E-02
B4DYH1	Heat shock 105kDa/110kDa protein 1	9	1.00	41	1.8E-06	43	1.0E+00	25	4.0E-12
B4E335	Actin, beta	202	0.03	178	1.4E-02	201	1.0E+00	203	1.0E+00
B5MCQ5	Protein disulfide isomerase family A, member 6	46	0.00	0	1.0E+00	17	3.9E-03	63	9.4E-30
B5MCY1	Uncharacterized protein (Fragment)	0	1.00	0	1.0E+00	0	1.0E+00	4	1.6E-03
B5MD66	Uncharacterized protein	0	1.00	0	1.0E+00	8	3.9E-03	11	2.8E-14
B5ME49	Mucin 16, cell surface-associated	0	1.00	2	8.2E-04	1	2.4E-02	0	1.0E+00
B7TY16	Actinin alpha 1 isoform 3	0	1.00	0	1.0E+00	0	1.0E+00	4	3.5E-06
B7Z4Q3	Uncharacterized protein	1	0.08	0	1.0E+00	0	1.0E+00	12	2.1E-03
B7Z7P8	Uncharacterized protein	1	0.05	0	1.0E+00	0	1.0E+00	1	3.0E-03
B7Z840	Uncharacterized protein	3	1.00	18	1.6E-02	0	1.0E+00	4	5.1E-02

B7Z8M7	RAB1A, member RAS oncogene family	4	0.02	9	1.6E-04	0	1.0E+00	0	1.0E+00
B8ZZL3	Eukaryotic translation initiation factor 4E family member 2	0	1.00	0	1.0E+00	12	1.7E-07	0	1.0E+00
B9A062	Methylenetetrahydrofolate dehydrogenase (NADP+-dependent) 2, methenyltetrahydrofolate cyclohydrolase	0	1.00	0	1.0E+00	34	6.4E-17	1	1.8E-03
B9A064	Immunoglobulin lambda-like polypeptide 5	29	0.00	17	3.8E-05	50	1.3E-05	44	3.9E-09
C4AM82	Uncharacterized protein	0	1.00	0	1.0E+00	2	4.8E-03	1	4.0E-02
C9IZN3	ARP3 actin-related protein 3 homolog C (yeast) (Fragment)	6	1.00	7	1.0E+00	32	6.7E-05	14	1.5E-06
C9J1T2	Ras homolog gene family, member A (Fragment)	0	1.00	4	1.9E-03	2	3.9E-03	0	1.0E+00
C9J5W8	Zinc finger protein 717	0	1.00	2	1.1E-04	0	1.0E+00	0	1.0E+00
C9JAB2	Serine/arginine-rich-splicing factor 7	0	1.00	0	1.0E+00	0	1.0E+00	28	2.9E-08
C9JR72	Kelch repeat and BTB domain-containing protein 13	1	0.07	0	1.0E+00	1	6.4E-02	0	1.0E+00
C9JWM7	Actin-related protein 2/3 complex, subunit 4, 20kDa	0	1.00	0	1.0E+00	13	3.9E-03	12	5.3E-09
C9JXB8	Ribosomal protein L24	7	0.00	1	1.9E-03	5	3.9E-03	11	1.5E-13
D3DU83	Ribosomal protein S2	17	1.00	13	1.0E+00	61	8.3E-04	25	1.0E+00
D6R962	Thioredoxin domain-containing 15	1	0.08	0	1.0E+00	1	8.1E-02	0	1.0E+00
D6R9R1	Methylcrotonoyl-Coenzyme A carboxylase 2 (Beta), isoform CRA_a	0	1.00	0	1.0E+00	0	1.0E+00	5	1.3E-03
D6RAQ3	Lamin A/C	3	1.00	0	1.0E+00	0	1.0E+00	35	7.1E-15
D6RAX2	C-terminal-binding protein 1 (Fragment)	0	1.00	14	3.7E-10	4	3.9E-03	0	1.0E+00
E5RI07	Transportin 1	16	0.02	5	1.0E+00	34	1.8E-03	8	7.1E-04
E5RIZ5	Peptidylprolyl isomerase A (cyclophilin A)	14	1.00	16	1.0E+00	34	3.2E-02	39	3.7E-02
E5RJT0	Eukaryotic translation initiation factor 3, subunit H (Fragment)	0	1.00	0	1.0E+00	3	7.6E-03	14	5.8E-18
E5RKB4	Uncharacterized protein	0	1.00	0	1.0E+00	0	1.0E+00	12	1.3E-03
E7EMA7	Pyruvate dehydrogenase phosphatase regulatory subunit	0	1.00	1	6.6E-02	6	3.9E-03	0	1.0E+00
E7EMY2	Phosphoribosyl pyrophosphate synthetase-associated protein 2	0	1.00	0	1.0E+00	0	1.0E+00	5	7.2E-10
E7ENH9	ATP citrate lyase	39	0.00	53	7.5E-25	11	3.7E-10	32	6.5E-25
E7ENK9	Uncharacterized protein	29	1.00	7	1.0E+00	143	4.6E-02	33	3.3E-02
E7ENU7	Ribosomal protein L15 (Fragment)	1	0.05	0	1.0E+00	0	1.0E+00	12	5.0E-09
E7EQC1	Ferredoxin reductase	0	1.00	5	4.6E-09	17	3.9E-03	0	1.0E+00
E7ERF4	Adenylosuccinate lyase	0	1.00	0	1.0E+00	17	2.7E-11	2	2.5E-03
E7ERJ4	Heterogeneous nuclear ribonucleoprotein A3	5	1.00	0	1.0E+00	9	1.0E+00	39	1.7E-07
E7ESM6	Staphylococcal nuclease and tudor domain-containing 1	96	1.00	65	1.0E+00	208	2.5E-03	137	3.2E-02
E7ESZ7	NADH dehydrogenase (ubiquinone) 1 alpha subcomplex, 10, 42kDa	2	0.00	0	1.0E+00	22	1.7E-09	0	1.0E+00

E7ETK5	IMP (inosine 5'-monophosphate) dehydrogenase 2 (Fragment)	11	0.03	7	1.0E+00	7	3.4E-02	14	2.0E-04
E7EU96	Casein kinase 2, alpha 1 polypeptide	0	1.00	0	1.0E+00	8	6.2E-05	11	1.6E-09
E7EUG1	Heat shock 105kDa/110kDa protein 1	9	1.00	37	1.0E+00	44	5.0E-02	19	2.6E-02
E7EUH1	Adaptor-related protein complex 1, gamma 1 subunit	0	1.00	0	1.0E+00	20	2.0E-23	0	1.0E+00
E7EVW0	DNA polymerase	0	1.00	2	8.1E-05	20	5.3E-07	0	1.0E+00
E7EWF1	Ribosomal protein L4	52	0.00	15	8.5E-11	23	8.7E-13	47	8.1E-26
E7EWI9	Heterogeneous nuclear ribonucleoprotein A3	5	1.00	0	1.0E+00	9	1.0E+00	37	1.6E-04
E7EWR4	Cleavage stimulation factor, 3' pre-RNA, subunit 2, 64kDa	0	1.00	0	1.0E+00	2	4.6E-03	21	2.7E-16
E7EWT1	Dolichyl-diphosphooligosaccharide--protein glycosyltransferase	103	0.00	79	6.3E-33	154	9.1E-26	19	9.0E-22
E7EWT5	Uncharacterized protein	0	1.00	7	8.8E-10	0	1.0E+00	29	1.7E-10
E7EX81	Nucleolin	3	0.00	2	1.9E-03	0	1.0E+00	134	3.9E-47
E9PAT9	Uncharacterized protein	4	0.00	6	1.9E-03	1	8.1E-02	36	2.1E-36
E9PAV3	Nascent polypeptide-associated complex alpha subunit	0	1.00	0	1.0E+00	0	1.0E+00	40	4.3E-23
E9PC52	Retinoblastoma-binding protein 7	0	1.00	0	1.0E+00	4	4.8E-02	4	3.2E-02
E9PCL6	Isocitrate dehydrogenase 3 (NAD+) gamma	0	1.00	1	8.3E-02	11	1.2E-11	1	5.5E-02
E9PF18	Uncharacterized protein	19	1.00	7	1.0E+00	46	3.8E-02	28	1.0E-06
E9PFF0	Uncharacterized protein	14	0.00	0	1.0E+00	16	3.8E-02	39	1.9E-12
E9PGK3	Tubulin, alpha 1c	212	0.00	214	3.7E-06	195	3.9E-03	133	3.1E-07
E9PH94	Uncharacterized protein	0	1.00	1	9.9E-02	1	8.5E-02	0	1.0E+00
E9PHN8	Hephaestin	1	0.00	0	1.0E+00	1	5.1E-02	0	1.0E+00
E9PI21	Hydroxysteroid (17-beta) dehydrogenase 12 (Fragment)	0	1.00	0	1.0E+00	19	2.8E-08	1	2.1E-02
E9PK25	Cofilin 1 (non-muscle)	66	0.00	27	2.5E-15	123	4.4E-15	92	1.1E-26
E9PKU4	Ribosomal protein L8 (Fragment)	5	0.00	0	1.0E+00	3	3.9E-03	15	2.1E-17
E9PRQ6	Acetyl-CoA acetyltransferase 1	27	1.00	43	1.5E-02	28	3.8E-04	30	1.0E+00
F5GWF6	Chaperonin-containing TCP1, subunit 2 (beta)	43	0.02	62	1.0E+00	36	3.3E-03	60	1.0E+00
F5GXI3	Uncharacterized protein	33	1.00	32	1.9E-03	13	4.9E-02	41	4.2E-02
F5GYB2	UDP-N-acetyl-alpha-D-galactosamine:polypeptide N-acetylgalactosaminyltransferase 2 (GalNAc-T2)	0	1.00	0	1.0E+00	10	1.0E-05	0	1.0E+00
F5GYR8	USO1 vesicle-docking protein homolog (yeast)	2	0.01	0	1.0E+00	2	4.6E-03	0	1.0E+00
F5GZ32	Inner membrane protein, mitochondrial	7	0.00	0	1.0E+00	0	1.0E+00	17	3.0E-24
F5GZW4	Catechol-O-methyltransferase domain-containing 1	0	1.00	0	1.0E+00	10	7.7E-08	0	1.0E+00
F5H018	RAN, member RAS oncogene family (Fragment)	41	0.04	16	2.0E-02	111	7.5E-04	30	2.8E-02
F5H0N0	Actin, gamma 1	200	1.00	178	6.8E-04	200	5.2E-02	204	2.9E-02
F5H0U9	Myosin IIIA	1	0.04	0	1.0E+00	1	7.5E-02	0	1.0E+00
F5H0Y3	Myeloid leukemia factor 2 (Fragment)	0	1.00	0	1.0E+00	1	2.6E-02	1	3.0E-02

F5H1E9	Minichromosome maintenance complex component 2	34	0.00	33	2.4E-26	8	3.3E-08	16	5.4E-09
F5H2A9	Acyl-CoA dehydrogenase, very long chain	21	0.00	3	1.9E-03	12	1.2E-06	7	1.8E-07
F5H2F4	Methylenetetrahydrofolate dehydrogenase (NADP+-dependent) 1, methenyltetrahydrofolate cyclohydrolase, formyltetrahydrofolate synthetase	21	0.00	45	4.6E-15	37	3.9E-09	18	1.5E-06
F5H3A6	ADP-ribosylation factor 1	12	1.00	34	1.9E-03	19	1.6E-03	13	2.2E-02
F5H3L8	Heat shock 70kDa protein 9 (mortalin)	35	0.03	68	1.6E-02	62	4.1E-06	59	1.0E+00
F5H423	ADP-ribosylation factor 3	20	0.00	30	1.4E-02	55	7.0E-07	20	9.5E-08
F5H4R2	Superoxide dismutase 2, mitochondrial (Fragment)	0	1.00	0	1.0E+00	1	4.0E-03	3	6.1E-02
F5H4Z5	Hypoxia up-regulated 1	107	0.00	69	1.3E-23	63	6.2E-12	82	7.0E-29
F5H776	Minichromosome maintenance complex component 7	95	0.03	55	1.7E-02	150	1.0E+00	51	2.9E-02
F6U211	Ribosomal protein S10	10	0.00	14	3.7E-06	33	5.0E-08	31	2.7E-08
F8VQY0	ATP synthase, H+-transporting, mitochondrial F1 complex, beta polypeptide (Fragment)	57	0.03	62	1.0E+00	81	3.2E-02	70	1.0E+00
F8VRG9	Poly(rC)-binding protein 2	26	0.00	57	1.0E+00	36	1.4E-05	38	1.8E-03
F8VS64	Keratin 4	0	1.00	0	1.0E+00	2	1.8E-03	0	1.0E+00
F8VU90	Peptidyl-prolyl cis-trans isomerase	13	0.00	5	1.0E+00	0	1.0E+00	4	1.0E+00
F8VUJ7	Tubulin, beta class I	414	0.00	493	1.6E-18	392	6.3E-08	207	1.5E-18
F8VWT9	Chromosome 12 open reading frame 51	0	1.00	0	1.0E+00	1	1.3E-02	1	1.1E-02
F8VYL7	Poly(rC)-binding protein 2	30	0.00	78	3.7E-06	65	1.1E-10	52	4.0E-08
F8W031	Uncharacterized protein (Fragment)	0	1.00	0	1.0E+00	1	4.2E-02	2	1.8E-03
F8W079	ATP synthase, H+-transporting, mitochondrial F1 complex, beta polypeptide (Fragment)	72	1.00	74	1.0E+00	109	7.6E-02	99	3.5E-02
F8W0P7	ATP synthase, H+-transporting, mitochondrial F1 complex, beta polypeptide (Fragment)	72	0.00	73	1.0E+00	113	1.0E+00	80	1.0E+00
F8W6I0	Elongation factor 1-alpha	909	0.00	500	3.8E-05	1185	2.6E-02	364	3.2E-02
F8W720	Guanine monophosphate synthetase	21	0.01	22	2.2E-05	21	1.0E+00	14	2.9E-02
F8W7I9	Ran GTPase-activating protein 1	5	1.00	13	1.0E+00	38	3.3E-03	1	1.0E+00
F8W8T1	Myxovirus (influenza virus) resistance 1, interferon-inducible protein p78 (mouse)	54	0.00	20	4.4E-13	27	1.5E-07	0	1.0E+00
F8W9U3	Abhydrolase domain-containing 14B	0	1.00	0	1.0E+00	19	2.7E-03	4	1.0E+00
F8WAI1	Immunoglobulin-like and fibronectin type III domain-containing 1	0	1.00	1	8.4E-02	1	5.7E-02	0	1.0E+00
F8WCL5	Nebulin	0	1.00	0	1.0E+00	5	1.5E-02	1	6.1E-02
F8WE95	NFAT-activating protein with ITAM motif 1	0	1.00	0	1.0E+00	35	4.5E-08	0	1.0E+00
G3V3L6	Methylenetetrahydrofolate dehydrogenase (NADP+-	16	1.00	20	1.5E-02	28	3.1E-02	14	1.0E+00

	dependent) 1, methenyltetrahydrofolate cyclohydrolase, formyltetrahydrofolate synthetase								
G3XAB4	Acetyl-CoA acetyltransferase 1	29	0.01	42	1.0E+00	26	2.6E-02	33	1.9E-03
G8JLB6	Heterogeneous nuclear ribonucleoprotein H1 (H)	34	0.00	64	2.7E-11	70	7.4E-11	54	6.1E-18
H0Y2S9	Myosin phosphatase Rho- interacting protein (Fragment)	1	0.02	0	1.0E+00	3	9.8E-03	0	1.0E+00
H0Y3J2	Proteasome subunit beta type	0	1.00	0	1.0E+00	0	1.0E+00	12	5.8E-08
H0Y4R1	IMP (inosine 5'-monophosphate) dehydrogenase 2 (Fragment)	25	0.03	8	1.0E+00	24	2.8E-02	20	1.0E+00
H0Y5F5	Poly(A)-binding protein, cytoplasmic 4 (inducible form) (Fragment)	4	1.00	3	1.0E+00	17	1.0E+00	34	1.1E-16
H0Y8X4	Chromosome 6 open reading frame 108 (Fragment)	0	1.00	4	1.9E-03	1	7.1E-02	14	1.1E-07
H0Y9N6	Hexokinase 3 (white cell) (Fragment)	0	1.00	1	7.3E-02	1	8.9E-02	0	1.0E+00
H0YBG6	Heat shock 70kDa protein 9 (mortalin) (Fragment)	7	1.00	13	1.5E-02	28	2.0E-02	21	3.4E-02
H0YCY7	Ribosomal protein S3 (Fragment)	35	0.00	23	3.7E-06	115	6.2E-08	34	3.4E-09
H0YCY6	Dihydroxyacetone kinase 2 homolog (<i>S. cerevisiae</i>) (Fragment)	0	1.00	8	4.0E-15	0	1.0E+00	0	1.0E+00
H0YEU2	Ribosomal protein S3 (Fragment)	34	0.00	33	7.1E-09	58	1.4E-07	50	4.3E-12
H0YF33	Nuclear autoantigenic sperm protein (histone-binding) (Fragment)	0	1.00	0	1.0E+00	0	1.0E+00	16	1.1E-03
H0YFE4	PTPRF-interacting protein,- binding protein 1 (liprin beta 1) (Fragment)	0	1.00	1	6.5E-02	2	1.6E-02	0	1.0E+00
H0YG33	Heat shock 70kDa protein 1B	11	0.00	75	8.2E-23	15	1.1E-10	39	1.4E-19
H0YKF0	Electron-transfer-flavoprotein, alpha polypeptide (Fragment)	16	1.00	24	2.2E-04	6	1.0E+00	3	1.0E+00
H0YLF6	SIX homeobox 5 (Fragment)	0	1.00	0	1.0E+00	0	1.0E+00	8	1.9E-07
H0YLU7	Electron-transfer-flavoprotein, alpha polypeptide (Fragment)	33	1.00	35	1.0E+00	55	2.1E-03	18	8.2E-02
H0YNF5	Isocitrate dehydrogenase 3 (NAD+) alpha	16	0.02	0	1.0E+00	51	4.9E-02	9	1.0E+00
O00116	Alkyldihydroxyacetonephosphate synthase, peroxisomal	0	1.00	0	1.0E+00	92	1.8E-22	0	1.0E+00
O00148	ATP-dependent RNA helicase DDX39A	39	0.00	40	1.4E-05	97	2.4E-09	43	5.7E-16
O00154	Cytosolic acyl coenzyme A thioester hydrolase	0	1.00	37	5.9E-16	0	1.0E+00	12	1.8E-03
O00217	NADH dehydrogenase [ubiquinone] iron-sulfur protein 8, mitochondrial	0	1.00	0	1.0E+00	4	4.0E-07	0	1.0E+00
O00231	26S proteasome non-ATPase regulatory subunit 11	8	0.00	19	1.4E-11	0	1.0E+00	3	1.9E-03
O00232	26S proteasome non-ATPase regulatory subunit 12	5	0.00	0	1.0E+00	1	3.9E-03	0	1.0E+00
O00299	Chloride intracellular channel	1	0.00	0	1.0E+00	0	1.0E+00	16	5.4E-09

	protein 1								
O00410	Importin-5	3	0.00	41	5.1E-17	51	1.4E-06	23	2.7E-27
O00429	Dynamin-1-like protein	0	1.00	9	2.9E-07	1	6.6E-02	0	1.0E+00
O00487	26S proteasome non-ATPase regulatory subunit 14	11	0.00	5	1.9E-03	2	2.4E-02	12	4.1E-12
O00567	Nucleolar protein 56	25	0.00	8	1.9E-03	28	1.0E-19	30	2.0E-30
O00571	ATP-dependent RNA helicase DDX3X	36	0.00	73	2.0E-13	44	3.9E-03	48	2.6E-08
O00629	Importin subunit alpha-4	7	0.00	11	1.9E-03	26	1.6E-05	9	1.8E-03
O00750	Phosphatidylinositol-4-phosphate 3-kinase C2 domain-containing subunit beta	0	1.00	0	1.0E+00	1	2.3E-02	1	7.9E-02
O00764	Pyridoxal kinase	0	1.00	1	2.0E-03	2	3.9E-03	1	5.5E-03
O14602	Eukaryotic translation initiation factor 1A, Y-chromosomal	0	1.00	0	1.0E+00	0	1.0E+00	8	1.2E-07
O14662	Syntaxin-16	0	1.00	10	2.5E-03	1	8.2E-02	0	1.0E+00
O14773	Tripeptidyl-peptidase 1	0	1.00	0	1.0E+00	2	3.9E-03	1	3.0E-03
O14976	Cyclin-G-associated kinase	0	1.00	0	1.0E+00	14	1.7E-04	0	1.0E+00
O14979	Heterogeneous nuclear ribonucleoprotein D-like	0	1.00	0	1.0E+00	1	1.0E+00	43	1.8E-20
O14980	Exportin-1	54	0.00	34	1.2E-21	32	1.6E-05	31	2.4E-26
O14981	TATA-binding protein-associated factor 172	0	1.00	1	6.7E-02	1	4.9E-02	0	1.0E+00
O15126	Secretory carrier-associated membrane protein 1	0	1.00	0	1.0E+00	1	4.8E-02	1	1.5E-02
O15143	Actin-related protein 2/3 complex subunit 1B	0	1.00	0	1.0E+00	13	3.9E-03	1	1.8E-03
O15144	Actin-related protein 2/3 complex subunit 2	0	1.00	0	1.0E+00	0	1.0E+00	4	5.5E-06
O15198	Mothers against decapentaplegic homolog 9	0	1.00	0	1.0E+00	6	9.5E-04	0	1.0E+00
O15296	Arachidonate 15-lipoxygenase B	0	1.00	0	1.0E+00	1	3.7E-02	3	3.1E-03
O15305	Phosphomannomutase 2	0	1.00	0	1.0E+00	0	1.0E+00	3	3.9E-05
O15371	Eukaryotic translation initiation factor 3 subunit D	1	0.05	1	3.5E-03	12	3.2E-05	8	5.4E-09
O15523	ATP-dependent RNA helicase DDX3Y	21	1.00	45	1.5E-08	18	1.0E+00	32	5.3E-07
O15533	Tapasin	8	0.00	9	1.8E-04	1	3.4E-02	0	1.0E+00
O43143	Putative pre-mRNA-splicing factor ATP-dependent RNA helicase DHX15	11	0.00	1	4.1E-02	55	6.6E-18	16	1.3E-13
O43156	TELO2-interacting protein 1 homolog	0	1.00	3	1.9E-03	1	3.0E-02	0	1.0E+00
O43169	Cytochrome b5 type B	0	1.00	0	1.0E+00	41	3.8E-08	1	2.2E-03
O43242	26S proteasome non-ATPase regulatory subunit 3	2	0.00	0	1.0E+00	1	6.9E-02	12	3.1E-12
O43324	Eukaryotic translation elongation factor 1 epsilon-1	0	1.00	0	1.0E+00	0	1.0E+00	6	5.9E-06
O43390	Heterogeneous nuclear ribonucleoprotein R	26	0.00	31	1.7E-16	23	1.4E-06	56	3.7E-33
O43423	Acidic leucine-rich nuclear phosphoprotein 32 family member C	0	1.00	0	1.0E+00	0	1.0E+00	11	6.7E-07
O43615	Mitochondrial import inner	0	1.00	0	1.0E+00	1	7.4E-03	3	1.8E-03

	membrane translocase subunit TIM44								
O43809	Cleavage and polyadenylation specificity factor subunit 5	0	1.00	3	1.9E-03	2	3.9E-03	13	6.4E-12
O43837	Isocitrate dehydrogenase [NAD] subunit beta, mitochondrial	0	1.00	0	1.0E+00	22	1.4E-09	2	1.9E-03
O43852	Calumenin	0	1.00	0	1.0E+00	0	1.0E+00	5	1.1E-08
O43933	Peroxisome biogenesis factor 1	1	0.04	1	6.2E-02	1	4.2E-02	1	8.2E-02
O60264	SWI/SNF-related matrix-associated actin-dependent regulator of chromatin subfamily A member 5	1	0.00	0	1.0E+00	33	1.8E-05	5	1.8E-03
O60281	Zinc finger protein 292	0	1.00	0	1.0E+00	1	2.7E-02	2	6.9E-03
O60287	Nucleolar pre-ribosomal-associated protein 1	0	1.00	0	1.0E+00	18	1.8E-04	0	1.0E+00
O60306	Intron-binding protein aquarius	0	1.00	0	1.0E+00	24	1.1E-08	1	3.8E-02
O60341	Lysine-specific histone demethylase 1A	0	1.00	0	1.0E+00	1	2.7E-02	2	8.9E-02
O60361	Putative nucleoside diphosphate kinase	1	1.00	12	1.7E-02	9	1.0E+00	27	3.2E-02
O60476	Mannosyl-oligosaccharide 1,2-alpha-mannosidase IB	1	0.07	0	1.0E+00	0	1.0E+00	1	2.9E-02
O60506	Heterogeneous nuclear ribonucleoprotein Q	36	0.00	18	5.0E-10	21	1.6E-04	43	6.1E-36
O60522	Tudor domain-containing protein 6	1	0.02	1	4.5E-03	0	1.0E+00	0	1.0E+00
O60610	Protein diaphanous homolog 1	0	1.00	17	1.4E-08	2	3.9E-03	1	6.1E-03
O60662	Kelch repeat and BTB domain-containing protein 10	2	0.01	0	1.0E+00	0	1.0E+00	0	1.0E+00
O60684	Importin subunit alpha-7	1	0.00	1	1.9E-03	49	2.2E-09	3	1.4E-02
O60762	Dolichol-phosphate mannosyltransferase	7	0.00	1	2.0E-03	13	3.6E-10	2	1.9E-03
O60814	Histone H2B type 1-K	19	0.00	37	4.8E-06	70	1.6E-05	289	2.9E-17
O60828	Polyglutamine-binding protein 1	1	0.10	0	1.0E+00	0	1.0E+00	1	1.8E-03
O60841	Eukaryotic translation initiation factor 5B	2	0.00	0	1.0E+00	2	4.0E-03	5	8.7E-10
O60884	DnaJ homolog subfamily A member 2	2	0.00	0	1.0E+00	0	1.0E+00	4	1.8E-03
O75027	ATP-binding cassette sub-family B member 7, mitochondrial	0	1.00	0	1.0E+00	18	1.9E-04	1	3.0E-03
O75037	Kinesin-like protein KIF21B	1	0.10	0	1.0E+00	1	2.9E-02	0	1.0E+00
O75083	WD repeat-containing protein 1	1	0.09	0	1.0E+00	1	7.4E-02	0	1.0E+00
O75131	Copine-3	14	0.00	24	5.1E-15	6	3.9E-04	24	2.2E-18
O75347	Tubulin-specific chaperone A	0	1.00	0	1.0E+00	0	1.0E+00	7	1.6E-08
O75351	Vacuolar protein sorting-associated protein 4B	0	1.00	1	2.7E-02	1	6.9E-03	1	2.8E-02
O75367	Core histone macro-H2A.1	0	1.00	1	6.6E-03	15	3.9E-03	28	5.3E-13
O75396	Vesicle-trafficking protein SEC22b	10	0.00	2	1.9E-03	12	3.9E-03	2	4.4E-05
O75439	Mitochondrial-processing peptidase subunit beta	7	0.00	0	1.0E+00	2	6.7E-03	1	8.3E-03
O75445	Usherin	1	0.01	0	1.0E+00	1	9.8E-02	0	1.0E+00
O75475	PC4 and SFRS1-interacting protein	0	1.00	0	1.0E+00	0	1.0E+00	3	1.6E-04
O75494	Serine/arginine-rich splicing factor 10	0	1.00	0	1.0E+00	0	1.0E+00	17	1.8E-15
O75531	Barrier-to-autointegration factor	0	1.00	0	1.0E+00	2	4.4E-02	21	6.0E-12

O75533	Splicing factor 3B subunit 1	18	0.00	2	3.8E-06	55	1.7E-14	35	1.3E-38
O75534	Cold shock domain-containing protein E1	3	0.00	9	1.7E-05	0	1.0E+00	1	6.1E-03
O75592	Probable E3 ubiquitin-protein ligase MYCBP2	0	1.00	1	4.4E-02	0	1.0E+00	1	4.7E-02
O75608	Acyl-protein thioesterase 1	1	0.07	1	1.9E-03	0	1.0E+00	0	1.0E+00
O75616	GTPase Era, mitochondrial	0	1.00	0	1.0E+00	16	2.9E-07	0	1.0E+00
O75643	U5 small nuclear ribonucleoprotein 200 kDa helicase	25	0.00	1	1.2E-02	61	3.2E-18	34	2.1E-47
O75678	Ret finger protein-like 2	0	1.00	0	1.0E+00	5	3.4E-08	0	1.0E+00
O75691	Small subunit processome component 20 homolog	0	1.00	0	1.0E+00	3	9.2E-07	1	4.7E-02
O75694	Nuclear pore complex protein Nup155	9	0.00	17	3.7E-06	68	2.6E-17	0	1.0E+00
O75746	Calcium-binding mitochondrial carrier protein Aralar1	8	1.00	6	1.0E+00	49	2.0E-16	4	1.0E+00
O75844	CAAX prenyl protease 1 homolog	12	0.00	5	1.9E-03	11	1.6E-05	4	1.4E-07
O75915	PRA1 family protein 3	13	0.00	12	9.7E-10	0	1.0E+00	1	1.9E-02
O75947	ATP synthase subunit d, mitochondrial	21	0.00	5	2.0E-03	1	4.0E-02	26	4.5E-13
O75955	Flotillin-1	0	1.00	3	1.9E-03	0	1.0E+00	1	1.8E-03
O75962	Triple functional domain protein	1	0.07	1	9.1E-02	0	1.0E+00	0	1.0E+00
O75964	ATP synthase subunit g, mitochondrial	0	1.00	0	1.0E+00	9	5.4E-08	1	5.0E-03
O76021	Ribosomal L1 domain-containing protein 1	4	0.00	9	1.9E-03	8	3.9E-03	30	1.6E-13
O94788	Retinal dehydrogenase 2	0	1.00	0	1.0E+00	1	9.8E-02	1	3.8E-02
O94826	Mitochondrial import receptor subunit TOM70	13	0.00	5	1.9E-03	4	3.9E-03	0	1.0E+00
O94901	SUN domain-containing protein 1	1	0.00	0	1.0E+00	0	1.0E+00	1	6.6E-02
O94925	Glutaminase kidney isoform, mitochondrial	0	1.00	1	2.0E-03	61	1.2E-20	1	1.8E-03
O94979	Protein transport protein Sec31A	0	1.00	4	4.2E-06	7	3.9E-03	0	1.0E+00
O95071	E3 ubiquitin-protein ligase UBR5	7	0.00	5	1.9E-03	0	1.0E+00	1	8.6E-02
O95347	Structural maintenance of chromosomes protein 2	7	0.00	0	1.0E+00	1	4.0E-03	1	5.7E-02
O95363	Phenylalanine--tRNA ligase, mitochondrial	0	1.00	0	1.0E+00	3	1.6E-05	0	1.0E+00
O95373	Importin-7	1	0.00	1	1.9E-03	0	1.0E+00	5	6.2E-05
O95393	Bone morphogenetic protein 10	1	0.10	1	8.5E-02	0	1.0E+00	0	1.0E+00
O95433	Activator of 90 kDa heat shock protein ATPase homolog 1	1	0.00	4	1.9E-03	1	4.5E-02	10	1.9E-13
O95455	dTDP-D-glucose 4,6-dehydratase	0	1.00	0	1.0E+00	0	1.0E+00	5	1.5E-07
O95466	Formin-like protein 1	0	1.00	1	4.4E-02	7	3.9E-03	0	1.0E+00
O95487	Protein transport protein Sec24B	0	1.00	0	1.0E+00	12	1.6E-05	0	1.0E+00
O95573	Long-chain-fatty-acid--CoA ligase 3	1	0.01	0	1.0E+00	1	5.4E-02	0	1.0E+00
O95714	E3 ubiquitin-protein ligase HERC2	0	1.00	1	5.7E-02	1	5.8E-02	1	4.7E-02
O95861	3'(2'),5'-bisphosphate nucleotidase 1	0	1.00	0	1.0E+00	1	3.6E-02	4	1.8E-03
O95876	WD repeat-containing and planar cell polarity effector protein fritz homolog	0	1.00	0	1.0E+00	0	1.0E+00	2	4.0E-03

O95996	Adenomatous polyposis coli protein 2	0	1.00	0	1.0E+00	2	2.5E-03	0	1.0E+00
O96005	Cleft lip and palate transmembrane protein 1	0	1.00	1	3.0E-02	19	3.9E-03	2	1.8E-03
O96008	Mitochondrial import receptor subunit TOM40 homolog	9	0.00	16	1.2E-14	36	8.9E-15	4	1.8E-03
P00338	L-lactate dehydrogenase A chain	6	0.00	51	2.4E-23	26	7.0E-11	77	3.1E-36
P00387	NADH-cytochrome b5 reductase 3	16	0.00	6	1.9E-03	11	3.9E-03	0	1.0E+00
P00403	Cytochrome c oxidase subunit 2	0	1.00	7	1.9E-03	24	1.6E-05	2	1.8E-03
P00505	Aspartate aminotransferase, mitochondrial	0	1.00	0	1.0E+00	0	1.0E+00	38	2.9E-27
P00558	Phosphoglycerate kinase 1	17	0.00	141	5.5E-38	88	4.8E-16	112	2.1E-33
P00734	Prothrombin	17	0.00	3	1.9E-03	1	2.3E-02	0	1.0E+00
P00966	Argininosuccinate synthase	0	1.00	0	1.0E+00	13	1.6E-05	10	3.4E-13
P01266	Thyroglobulin	0	1.00	0	1.0E+00	2	4.5E-03	0	1.0E+00
P01891	HLA class I histocompatibility antigen, A-68 alpha chain	50	0.00	59	4.9E-05	62	1.4E-02	6	1.0E+00
P01893	Putative HLA class I histocompatibility antigen, alpha chain H	24	0.00	34	3.7E-06	37	3.9E-03	1	1.8E-03
P02538	Keratin, type II cytoskeletal 6A	1	0.04	0	1.0E+00	2	5.9E-02	4	1.0E+00
P02549	Spectrin alpha chain, erythrocyte	0	1.00	2	5.2E-04	0	1.0E+00	0	1.0E+00
P02647	Apolipoprotein A-I	1	0.00	1	5.3E-02	0	1.0E+00	0	1.0E+00
P02786	Transferrin receptor protein 1	55	0.00	63	5.2E-34	54	1.1E-22	17	1.6E-20
P03891	NADH-ubiquinone oxidoreductase chain 2	0	1.00	0	1.0E+00	7	9.8E-07	0	1.0E+00
P04053	DNA nucleotidylexotransferase	1	0.00	0	1.0E+00	1	8.6E-02	0	1.0E+00
P04075	Fructose-bisphosphate aldolase A	0	1.00	146	2.0E-28	31	1.5E-14	116	3.3E-40
P04179	Superoxide dismutase [Mn], mitochondrial	0	1.00	0	1.0E+00	0	1.0E+00	7	4.8E-05
P04183	Thymidine kinase, cytosolic	8	0.00	14	3.3E-13	21	4.9E-11	0	1.0E+00
P04264	Keratin, type II cytoskeletal 1	72	0.00	31	2.1E-24	9	2.1E-04	48	6.0E-36
P04350	Tubulin beta-4A chain	304	0.00	431	1.2E-05	371	1.9E-06	189	1.8E-03
P04406	Glyceraldehyde-3-phosphate dehydrogenase	266	0.00	136	1.7E-35	263	5.2E-32	319	9.2E-53
P04424	Argininosuccinate lyase	1	0.08	0	1.0E+00	4	4.6E-03	0	1.0E+00
P04792	Heat shock protein beta-1	18	0.00	48	1.5E-18	0	1.0E+00	28	2.4E-17
P04843	Dolichyl-diphosphooligosaccharide--protein glycosyltransferase subunit 1	136	0.00	61	4.6E-35	168	3.0E-29	40	5.9E-32
P04899	Guanine nucleotide-binding protein G(i) subunit alpha-2	11	0.00	2	1.9E-03	16	3.9E-03	2	1.8E-03
P05023	Sodium/potassium-transporting ATPase subunit alpha-1	15	0.00	90	3.9E-45	13	3.9E-03	1	1.8E-03
P05141	ADP/ATP translocase 2	68	0.00	62	7.1E-09	114	9.8E-11	30	7.7E-08
P05161	Ubiquitin-like protein ISG15	10	0.00	8	1.9E-03	0	1.0E+00	0	1.0E+00
P05362	Intercellular adhesion molecule 1	1	0.00	17	7.1E-09	4	2.9E-04	0	1.0E+00
P05386	60S acidic ribosomal protein P1	0	1.00	0	1.0E+00	0	1.0E+00	11	1.1E-07
P05387	60S acidic ribosomal protein P2	11	0.00	0	1.0E+00	0	1.0E+00	81	2.0E-20
P05388	60S acidic ribosomal protein P0	13	0.00	21	3.0E-14	36	1.1E-13	29	5.9E-18
P05455	Lupus La protein	0	1.00	0	1.0E+00	0	1.0E+00	32	5.5E-19
P05534	HLA class I histocompatibility antigen, A-24 alpha chain	46	0.00	49	5.3E-05	52	1.0E+00	6	1.0E+00

P06493	Cyclin-dependent kinase 1	3	0.00	0	1.0E+00	17	6.1E-12	1	1.1E-02
P06576	ATP synthase subunit beta, mitochondrial	222	0.00	173	3.3E-11	287	1.6E-05	210	2.0E-13
P06733	Alpha-enolase	81	0.00	331	2.0E-44	436	4.5E-24	311	2.3E-54
P06744	Glucose-6-phosphate isomerase	0	1.00	32	4.4E-20	30	3.9E-03	56	4.2E-34
P06748	Nucleophosmin	77	0.00	15	1.9E-03	3	3.9E-03	94	1.5E-24
P06753	Tropomyosin alpha-3 chain	0	1.00	0	1.0E+00	0	1.0E+00	33	3.2E-17
P07099	Epoxide hydrolase 1	23	0.00	16	1.6E-10	16	3.9E-03	5	5.9E-06
P07195	L-lactate dehydrogenase B chain	0	1.00	34	2.0E-15	0	1.0E+00	72	1.1E-31
P07205	Phosphoglycerate kinase 2	1	1.00	39	1.1E-06	22	1.0E+00	24	8.1E-07
P07237	Protein disulfide-isomerase	68	0.00	6	1.9E-03	17	2.6E-10	84	4.6E-35
P07355	Annexin A2	0	1.00	0	1.0E+00	3	3.9E-03	19	5.4E-09
P07737	Profilin-1	17	0.00	21	7.1E-09	2	5.3E-02	37	5.1E-14
P07741	Adenine phosphoribosyltransferase	5	0.02	19	1.1E-10	32	1.8E-08	5	1.3E-08
P07814	Bifunctional glutamate/proline--tRNA ligase	11	0.00	17	1.4E-11	33	5.9E-12	49	1.7E-37
P07900	Heat shock protein HSP 90-alpha	111	0.00	104	1.0E-09	97	4.0E-11	130	1.5E-38
P07910	Heterogeneous nuclear ribonucleoproteins C1/C2	50	0.00	32	7.1E-09	70	6.2E-08	35	4.0E-16
P07954	Fumarate hydratase, mitochondrial	5	0.00	12	1.9E-03	28	3.5E-17	53	3.5E-21
P08195	4F2 cell-surface antigen heavy chain	13	0.00	45	9.3E-19	46	3.9E-03	13	1.6E-18
P08237	6-phosphofructokinase, muscle type	2	1.00	3	3.4E-02	16	1.0E+00	5	6.4E-09
P08238	Heat shock protein HSP 90-beta	201	0.00	170	5.1E-26	153	4.3E-15	213	2.3E-32
P08559	Pyruvate dehydrogenase E1 component subunit alpha, somatic form, mitochondrial	0	1.00	0	1.0E+00	7	3.9E-03	1	2.2E-02
P08574	Cytochrome c1, heme protein, mitochondrial	12	0.00	17	7.2E-09	14	3.9E-03	7	6.0E-12
P08708	40S ribosomal protein S17	10	0.00	31	2.3E-12	1	7.8E-02	38	1.1E-15
P08842	Steryl-sulfatase	0	1.00	0	1.0E+00	11	2.4E-05	0	1.0E+00
P08865	40S ribosomal protein SA	16	0.00	2	3.0E-05	49	2.8E-12	37	5.2E-24
P09382	Galectin-1	0	1.00	0	1.0E+00	0	1.0E+00	6	3.1E-05
P09543	2',3'-cyclic-nucleotide 3'-phosphodiesterase	0	1.00	1	1.9E-03	4	3.9E-03	0	1.0E+00
P09622	Dihydrolipoyl dehydrogenase, mitochondrial	0	1.00	0	1.0E+00	7	1.7E-04	30	8.2E-19
P09651	Heterogeneous nuclear ribonucleoprotein A1	30	1.00	38	1.9E-03	13	3.9E-03	128	5.0E-17
P09661	U2 small nuclear ribonucleoprotein A'	0	1.00	0	1.0E+00	0	1.0E+00	9	5.8E-15
P09874	Poly [ADP-ribose] polymerase 1	28	0.00	57	6.3E-25	60	4.3E-23	79	4.8E-59
P09972	Fructose-bisphosphate aldolase C	0	1.00	46	2.3E-10	0	1.0E+00	35	9.4E-08
P0CV98	Testis-specific Y-encoded protein 3	0	1.00	0	1.0E+00	19	1.8E-05	0	1.0E+00
P10155	60 kDa SS-A/Ro ribonucleoprotein	0	1.00	0	1.0E+00	2	3.9E-03	4	1.8E-03
P10515	Dihydrolipoyllysine-residue acetyltransferase component of pyruvate dehydrogenase complex, mitochondrial	5	0.00	36	2.5E-27	33	2.1E-20	6	1.8E-03
P10599	Thioredoxin	0	1.00	0	1.0E+00	0	1.0E+00	5	4.4E-06
P10809	60 kDa heat shock protein,	272	0.00	114	1.2E-34	968	1.5E-58	444	9.6E-93

	mitochondrial								
P11021	78 kDa glucose-regulated protein	116	0.00	48	1.2E-24	21	1.0E+00	143	7.8E-65
P11142	Heat shock cognate 71 kDa protein	108	0.00	128	4.1E-37	81	5.9E-19	199	1.8E-59
P11171	Protein 4.1	3	0.00	8	1.9E-03	1	4.0E-03	3	4.4E-04
P11177	Pyruvate dehydrogenase E1 component subunit beta, mitochondrial	0	1.00	1	8.4E-02	1	2.1E-02	12	4.1E-13
P11310	Medium-chain specific acyl-CoA dehydrogenase, mitochondrial	1	0.00	0	1.0E+00	42	9.4E-18	2	1.8E-03
P11388	DNA topoisomerase 2-alpha	8	0.00	2	1.9E-03	5	3.9E-03	7	1.0E-08
P11413	Glucose-6-phosphate 1-dehydrogenase	0	1.00	16	2.2E-11	6	3.9E-03	0	1.0E+00
P11532	Dystrophin	4	0.00	0	1.0E+00	2	4.1E-03	0	1.0E+00
P11717	Cation-independent mannose-6-phosphate receptor	2	0.00	0	1.0E+00	3	3.9E-03	0	1.0E+00
P11908	Ribose-phosphate pyrophosphokinase 2	0	1.00	1	1.9E-03	27	7.3E-09	19	1.6E-16
P11940	Polyadenylate-binding protein 1	5	1.00	10	1.9E-03	30	3.9E-03	41	4.1E-11
P12004	Proliferating cell nuclear antigen	2	0.00	1	3.5E-03	4	3.9E-03	29	2.8E-13
P12111	Collagen alpha-3(VI) chain	0	1.00	1	9.6E-02	0	1.0E+00	1	6.3E-02
P12235	ADP/ATP translocase 1	52	1.00	50	1.4E-02	89	3.2E-03	33	1.0E+00
P12236	ADP/ATP translocase 3	59	0.00	60	1.9E-03	57	3.2E-09	30	2.2E-09
P12268	Inosine-5'-monophosphate dehydrogenase 2	36	0.00	8	1.0E+00	42	1.6E-05	30	3.1E-06
P12270	Nucleoprotein TPR	0	1.00	0	1.0E+00	0	1.0E+00	2	4.3E-05
P12956	X-ray repair cross-complementing protein 6	30	0.00	10	3.7E-06	80	2.1E-22	63	2.7E-34
P13010	X-ray repair cross-complementing protein 5	23	0.00	0	1.0E+00	61	1.1E-22	69	2.5E-31
P13569	Cystic fibrosis transmembrane conductance regulator	0	1.00	2	1.7E-03	2	3.5E-04	0	1.0E+00
P13639	Elongation factor 2	220	0.00	215	1.2E-56	472	3.5E-53	231	4.2E-86
P13645	Keratin, type I cytoskeletal 10	34	0.00	9	3.7E-06	27	3.2E-05	18	5.5E-19
P13667	Protein disulfide-isomerase A4	0	1.00	0	1.0E+00	0	1.0E+00	31	6.1E-26
P13693	Translationally-controlled tumor protein	0	1.00	0	1.0E+00	0	1.0E+00	14	1.8E-14
P13796	Plastin-2	0	1.00	1	1.9E-03	1	8.3E-03	90	2.6E-59
P13804	Electron transfer flavoprotein subunit alpha, mitochondrial	33	1.00	38	1.9E-03	55	8.2E-04	21	4.8E-05
P13929	Beta-enolase	4	1.00	48	3.8E-06	134	3.9E-03	92	1.5E-19
P14174	Macrophage migration inhibitory factor	0	1.00	0	1.0E+00	36	6.3E-08	20	5.9E-09
P14314	Glucosidase 2 subunit beta	0	1.00	0	1.0E+00	0	1.0E+00	20	7.8E-20
P14543	Nidogen-1	0	1.00	1	6.8E-02	0	1.0E+00	1	7.9E-02
P14550	Alcohol dehydrogenase [NADP(+)]	1	0.00	0	1.0E+00	0	1.0E+00	4	9.2E-08
P14618	Pyruvate kinase isozymes M1/M2	300	0.00	408	5.2E-71	472	9.3E-42	328	6.0E-97
P14625	Endoplasmic reticulum chaperone protein BiP	53	0.00	44	9.2E-16	45	2.0E-05	101	2.8E-55
P14678	Small nuclear ribonucleoprotein-associated proteins B and B'	0	1.00	0	1.0E+00	58	6.2E-08	15	1.9E-18
P14866	Heterogeneous nuclear ribonucleoprotein L	12	0.00	0	1.0E+00	40	3.2E-17	71	1.2E-31
P14868	Aspartate--tRNA ligase,	12	0.00	28	2.6E-22	20	2.5E-07	16	2.0E-20

	cytoplasmic								
P14923	Junction plakoglobin	0	1.00	0	1.0E+00	4	5.0E-05	0	1.0E+00
P15121	Aldose reductase	0	1.00	0	1.0E+00	25	3.9E-03	2	1.8E-03
P15170	Eukaryotic peptide chain release factor GTP-binding subunit ERF3A	12	0.00	18	1.1E-07	2	1.0E+00	16	1.6E-10
P15259	Phosphoglycerate mutase 2	0	1.00	0	1.0E+00	0	1.0E+00	13	3.5E-04
P15311	Ezrin	0	1.00	5	1.9E-03	0	1.0E+00	11	4.5E-11
P15880	40S ribosomal protein S2	30	0.00	23	3.4E-10	60	3.9E-03	44	3.3E-10
P15924	Desmoplakin	13	0.00	26	1.4E-11	66	9.6E-13	21	7.7E-23
P16050	Arachidonate 15-lipoxygenase	0	1.00	0	1.0E+00	1	6.6E-02	1	9.5E-02
P16152	Carbonyl reductase [NADPH] 1	2	1.00	34	1.9E-03	0	1.0E+00	10	3.5E-05
P16189	HLA class I histocompatibility antigen, A-31 alpha chain	43	1.00	45	4.4E-08	59	1.0E+00	6	1.0E+00
P16402	Histone H1.3	0	1.00	0	1.0E+00	0	1.0E+00	35	5.2E-23
P16435	NADPH--cytochrome P450 reductase	7	0.00	0	1.0E+00	17	3.9E-03	0	1.0E+00
P16615	Sarcoplasmic/endoplasmic reticulum calcium ATPase 2	8	0.00	45	7.5E-26	0	1.0E+00	1	9.6E-02
P16989	DNA-binding protein A	0	1.00	0	1.0E+00	0	1.0E+00	15	1.9E-11
P17812	CTP synthase 1	20	0.00	10	8.5E-05	19	1.9E-12	1	1.6E-02
P17844	Probable ATP-dependent RNA helicase DDX5	41	0.00	43	6.7E-19	62	3.9E-03	39	1.9E-16
P17987	T-complex protein 1 subunit alpha	40	0.00	46	3.9E-26	94	6.1E-26	68	1.2E-41
P18085	ADP-ribosylation factor 4	14	0.00	17	6.3E-03	13	1.0E+00	15	8.7E-07
P18124	60S ribosomal protein L7	21	0.00	6	1.9E-03	78	1.0E-06	34	2.6E-20
P18505	Gamma-aminobutyric acid receptor subunit beta-1	0	1.00	0	1.0E+00	2	3.8E-03	0	1.0E+00
P18621	60S ribosomal protein L17	4	0.00	24	2.2E-12	0	1.0E+00	16	7.5E-12
P18669	Phosphoglycerate mutase 1	0	1.00	1	2.8E-02	0	1.0E+00	35	1.2E-13
P18858	DNA ligase 1	0	1.00	8	1.9E-03	0	1.0E+00	1	2.9E-03
P19012	Keratin, type I cytoskeletal 15	0	1.00	1	2.7E-02	0	1.0E+00	1	4.4E-03
P19105	Myosin regulatory light chain 12A	0	1.00	0	1.0E+00	0	1.0E+00	11	1.9E-09
P19623	Spermidine synthase	15	0.00	7	1.9E-03	70	7.5E-12	6	1.8E-03
P19784	Casein kinase II subunit alpha'	0	1.00	0	1.0E+00	0	1.0E+00	9	6.2E-07
P19971	Thymidine phosphorylase	0	1.00	0	1.0E+00	5	3.9E-03	1	1.1E-02
P20290	Transcription factor BTF3	1	0.00	7	1.9E-03	0	1.0E+00	29	1.1E-13
P20340	Ras-related protein Rab-6A	1	0.01	3	3.3E-03	9	1.6E-11	0	1.0E+00
P20592	Interferon-induced GTP-binding protein Mx2	34	0.00	14	8.4E-08	0	1.0E+00	0	1.0E+00
P20674	Cytochrome c oxidase subunit 5A, mitochondrial	0	1.00	0	1.0E+00	26	3.9E-03	15	8.2E-08
P20700	Lamin-B1	10	0.00	7	1.9E-03	0	1.0E+00	17	2.9E-13
P20839	Inosine-5'-monophosphate dehydrogenase 1	11	0.00	1	1.9E-03	3	1.2E-04	8	7.1E-12
P21108	Ribose-phosphate pyrophosphokinase 3	0	1.00	0	1.0E+00	23	3.1E-02	8	3.2E-02
P21291	Cysteine and glycine-rich protein 1	0	1.00	0	1.0E+00	0	1.0E+00	4	6.8E-07
P21333	Filamin-A	1	0.06	4	6.3E-05	0	1.0E+00	0	1.0E+00
P21796	Voltage-dependent anion-selective channel protein 1	86	0.00	107	6.4E-33	149	3.5E-29	39	5.0E-20
P21926	CD9 antigen	18	0.00	22	1.5E-10	15	3.9E-03	5	1.8E-03
P22087	rRNA 2'-O-methyltransferase	28	0.00	25	1.2E-12	80	3.1E-13	29	7.6E-20

	fibrillarlin								
P22102	Trifunctional purine biosynthetic protein adenosine-3	30	0.00	73	3.7E-44	110	6.4E-26	42	2.3E-41
P22234	Multifunctional protein ADE2	0	1.00	46	9.6E-20	19	3.8E-08	28	8.7E-23
P22314	Ubiquitin-like modifier-activating enzyme 1	39	0.00	126	8.1E-37	27	5.3E-25	80	2.8E-41
P22626	Heterogeneous nuclear ribonucleoproteins A2/B1	2	0.09	8	1.9E-03	59	7.1E-20	135	3.7E-59
P22695	Cytochrome b-c1 complex subunit 2, mitochondrial	15	0.00	3	1.9E-03	29	1.5E-12	3	3.4E-06
P23246	Splicing factor, proline- and glutamine-rich	30	0.00	47	2.1E-28	0	1.0E+00	76	1.6E-50
P23258	Tubulin gamma-1 chain	0	1.00	0	1.0E+00	19	3.9E-03	1	2.2E-03
P23284	Peptidyl-prolyl cis-trans isomerase B	1	0.03	0	1.0E+00	0	1.0E+00	70	1.3E-35
P23368	NAD-dependent malic enzyme, mitochondrial	0	1.00	1	9.7E-02	1	6.4E-02	9	2.9E-11
P23526	Adenosylhomocysteinase	14	0.00	26	1.4E-11	1	5.8E-02	6	1.8E-03
P23588	Eukaryotic translation initiation factor 4B	0	1.00	0	1.0E+00	0	1.0E+00	21	1.7E-16
P24534	Elongation factor 1-beta	0	1.00	0	1.0E+00	0	1.0E+00	22	1.9E-14
P24539	ATP synthase subunit b, mitochondrial	37	0.00	20	1.0E-09	67	2.5E-12	24	4.3E-13
P24752	Acetyl-CoA acetyltransferase, mitochondrial	55	0.00	91	1.7E-18	132	1.7E-08	62	1.9E-16
P25205	DNA replication licensing factor MCM3	24	0.00	37	2.2E-22	9	3.9E-03	42	9.3E-37
P25398	40S ribosomal protein S12	9	0.00	0	1.0E+00	36	3.9E-03	24	1.4E-07
P25705	ATP synthase subunit alpha, mitochondrial	277	0.00	260	3.5E-54	541	7.9E-40	144	6.4E-57
P25786	Proteasome subunit alpha type-1	0	1.00	0	1.0E+00	0	1.0E+00	5	6.6E-09
P26010	Integrin beta-7	10	0.00	14	5.6E-15	0	1.0E+00	5	3.1E-06
P26038	Moesin	0	1.00	0	1.0E+00	4	3.9E-03	6	1.8E-03
P26196	Probable ATP-dependent RNA helicase DDX6	13	0.00	7	1.9E-03	7	3.9E-03	13	7.3E-13
P26368	Splicing factor U2AF 65 kDa subunit	3	0.00	0	1.0E+00	1	4.8E-02	16	6.4E-13
P26373	60S ribosomal protein L13	15	0.00	14	7.9E-10	0	1.0E+00	9	1.3E-10
P26599	Polypyrimidine tract-binding protein 1	0	1.00	37	2.3E-18	14	2.5E-05	60	1.2E-31
P26639	Threonine--tRNA ligase, cytoplasmic	0	1.00	0	1.0E+00	0	1.0E+00	2	9.2E-04
P27105	Erythrocyte band 7 integral membrane protein	24	0.00	42	1.9E-20	15	3.9E-03	6	1.8E-09
P27348	14-3-3 protein theta	0	1.00	0	1.0E+00	10	1.2E-02	42	5.1E-19
P27635	60S ribosomal protein L10	17	0.00	28	1.1E-10	0	1.0E+00	32	4.3E-20
P27695	DNA-(apurinic or apyrimidinic site) lyase	0	1.00	2	1.9E-03	4	3.9E-03	11	2.9E-09
P27708	CAD protein	34	0.00	36	9.6E-20	113	8.4E-46	11	3.4E-14
P27797	Calreticulin	26	0.00	8	1.9E-03	2	3.9E-03	143	2.8E-38
P27816	Microtubule-associated protein 4	0	1.00	6	1.9E-03	0	1.0E+00	12	3.1E-06
P27824	Calnexin	60	0.00	11	4.4E-08	59	9.9E-10	50	6.7E-26
P28838	Cytosol aminopeptidase	9	0.00	11	4.9E-05	2	8.1E-05	3	2.1E-04

P29144	Tripeptidyl-peptidase 2	0	1.00	0	1.0E+00	0	1.0E+00	6	7.9E-10
P29353	SHC-transforming protein 1	1	0.00	1	6.5E-02	17	3.9E-03	0	1.0E+00
P29401	Transketolase	27	0.00	91	7.6E-35	109	4.3E-28	67	3.3E-38
P29692	Elongation factor 1-delta	0	1.00	0	1.0E+00	0	1.0E+00	26	2.4E-16
P29728	2'-5'-oligoadenylate synthase 2	14	0.00	2	6.0E-02	1	2.4E-02	0	1.0E+00
P30040	Endoplasmic reticulum resident protein 29	4	0.00	0	1.0E+00	0	1.0E+00	32	5.1E-14
P30041	Peroxiredoxin-6	0	1.00	0	1.0E+00	16	6.5E-07	31	6.7E-25
P30042	ES1 protein homolog, mitochondrial	0	1.00	0	1.0E+00	0	1.0E+00	13	3.3E-15
P30043	Flavin reductase (NADPH)	9	0.00	25	4.0E-13	0	1.0E+00	4	3.6E-07
P30044	Peroxiredoxin-5, mitochondrial	25	0.00	7	1.9E-03	31	2.2E-05	25	1.9E-17
P30048	Thioredoxin-dependent peroxide reductase, mitochondrial	0	1.00	0	1.0E+00	0	1.0E+00	23	5.4E-09
P30049	ATP synthase subunit delta, mitochondrial	0	1.00	7	1.9E-03	7	2.2E-02	3	1.5E-04
P30050	60S ribosomal protein L12	11	0.00	2	1.9E-03	0	1.0E+00	27	1.3E-13
P30086	Phosphatidylethanolamine-binding protein 1	0	1.00	0	1.0E+00	10	2.5E-05	43	1.7E-16
P30101	Protein disulfide-isomerase A3	16	0.00	0	1.0E+00	2	1.4E-02	47	5.1E-24
P30153	Serine/threonine-protein phosphatase 2A 65 kDa regulatory subunit A alpha isoform	0	1.00	32	5.8E-18	34	5.3E-07	13	5.3E-06
P30154	Serine/threonine-protein phosphatase 2A 65 kDa regulatory subunit A beta isoform	0	1.00	22	2.7E-05	53	1.5E-18	4	1.0E+00
P30419	Glycylpeptide N-tetradecanoyltransferase 1	0	1.00	0	1.0E+00	3	3.9E-03	3	3.4E-06
P30443	HLA class I histocompatibility antigen, A-1 alpha chain	48	1.00	49	3.7E-06	52	1.0E+00	6	1.0E+00
P30464	HLA class I histocompatibility antigen, B-15 alpha chain	60	0.00	61	8.1E-09	101	3.9E-03	6	1.0E+00
P30501	HLA class I histocompatibility antigen, Cw-2 alpha chain	33	0.00	33	1.9E-03	32	4.0E-03	6	1.0E+00
P30520	Adenylosuccinate synthetase isozyme 2	0	1.00	0	1.0E+00	0	1.0E+00	2	1.3E-04
P30825	High affinity cationic amino acid transporter 1	0	1.00	0	1.0E+00	1	1.0E-01	5	8.9E-07
P31146	Coronin-1A	33	0.00	31	9.0E-19	65	2.8E-09	28	1.4E-10
P31150	Rab GDP dissociation inhibitor alpha	0	1.00	0	1.0E+00	5	1.0E+00	24	2.7E-08
P31152	Mitogen-activated protein kinase 4	0	1.00	0	1.0E+00	2	6.7E-03	0	1.0E+00
P31153	S-adenosylmethionine synthase isoform type-2	6	0.00	14	3.7E-06	0	1.0E+00	1	1.8E-03
P31327	Carbamoyl-phosphate synthase [ammonia], mitochondrial	8	0.00	0	1.0E+00	0	1.0E+00	0	1.0E+00
P31689	DnaJ homolog subfamily A member 1	23	0.00	0	1.0E+00	23	8.1E-12	2	1.8E-03
P31930	Cytochrome b-c1 complex subunit I, mitochondrial	12	0.00	5	3.7E-06	24	3.8E-12	8	1.0E-07
P31939	Bifunctional purine biosynthesis protein PURH	0	1.00	60	2.7E-36	1	2.5E-02	3	3.1E-06
P31942	Heterogeneous nuclear ribonucleoprotein H3	2	0.00	20	5.9E-19	0	1.0E+00	26	6.6E-28

P31946	14-3-3 protein beta/alpha	0	1.00	0	1.0E+00	10	7.6E-05	31	2.8E-10
P31948	Stress-induced-phosphoprotein 1	0	1.00	0	1.0E+00	0	1.0E+00	60	5.9E-30
P31949	Protein S100-A11	0	1.00	0	1.0E+00	8	3.4E-05	40	9.4E-12
P32119	Peroxiredoxin-2	0	1.00	0	1.0E+00	0	1.0E+00	18	1.3E-12
P32322	Pyrroline-5-carboxylate reductase 1, mitochondrial	3	0.00	7	1.9E-03	14	3.9E-03	1	1.8E-03
P32942	Intercellular adhesion molecule 3	0	1.00	7	7.1E-06	1	8.1E-03	0	1.0E+00
P32969	60S ribosomal protein L9	24	0.00	28	1.4E-11	56	2.8E-09	37	1.2E-15
P33241	Lymphocyte-specific protein 1	0	1.00	0	1.0E+00	0	1.0E+00	16	2.3E-07
P33316	Deoxyuridine 5'-triphosphate nucleotidohydrolase, mitochondrial	0	1.00	10	1.2E-11	0	1.0E+00	38	3.5E-17
P33991	DNA replication licensing factor MCM4	34	0.00	20	7.1E-24	94	1.4E-28	39	2.2E-30
P33992	DNA replication licensing factor MCM5	37	0.00	57	4.8E-30	30	1.3E-16	31	1.8E-34
P33993	DNA replication licensing factor MCM7	99	0.00	61	3.5E-05	151	3.8E-02	60	2.1E-06
P34897	Serine hydroxymethyltransferase, mitochondrial	48	0.00	14	1.4E-13	124	1.1E-27	43	4.7E-24
P34931	Heat shock 70 kDa protein 1-like	13	0.00	61	1.0E+00	24	9.9E-02	29	1.0E+00
P34932	Heat shock 70 kDa protein 4	0	1.00	10	6.5E-06	0	1.0E+00	19	6.2E-33
P35221	Catenin alpha-1	0	1.00	1	7.4E-02	2	1.8E-02	0	1.0E+00
P35232	Prohibitin	97	0.00	68	1.8E-31	376	8.1E-22	47	6.1E-24
P35268	60S ribosomal protein L22	12	0.00	0	1.0E+00	24	3.9E-03	16	5.4E-09
P35443	Thrombospondin-4	0	1.00	0	1.0E+00	2	4.5E-03	0	1.0E+00
P35527	Keratin, type I cytoskeletal 9	42	0.00	0	1.0E+00	0	1.0E+00	24	2.5E-27
P35579	Myosin-9	33	0.00	38	2.6E-14	23	7.1E-08	118	1.5E-83
P35606	Coatomer subunit beta'	10	0.00	0	1.0E+00	1	4.6E-02	5	6.7E-05
P35613	Basigin	0	1.00	0	1.0E+00	1	6.2E-02	1	5.6E-02
P35637	RNA-binding protein FUS	11	0.00	41	1.6E-23	0	1.0E+00	62	5.3E-28
P35659	Protein DEK	5	0.00	0	1.0E+00	1	3.4E-02	14	1.8E-03
P35749	Myosin-11	0	1.00	4	1.0E+00	0	1.0E+00	5	3.6E-03
P35908	Keratin, type II cytoskeletal 2 epidermal	13	0.00	1	1.9E-03	1	8.1E-02	5	1.8E-03
P36268	Gamma-glutamyltranspeptidase 2	0	1.00	7	1.9E-03	1	7.0E-02	0	1.0E+00
P36542	ATP synthase subunit gamma, mitochondrial	16	0.00	19	7.1E-09	47	1.0E-13	10	7.9E-11
P36776	Lon protease homolog, mitochondrial	27	0.00	7	3.7E-06	61	5.8E-25	14	4.9E-17
P37108	Signal recognition particle 14 kDa protein	1	0.08	2	1.9E-03	0	1.0E+00	0	1.0E+00
P37198	Nuclear pore glycoprotein p62	0	1.00	3	3.7E-06	0	1.0E+00	0	1.0E+00
P37268	Squalene synthase	0	1.00	2	1.9E-03	7	1.7E-02	0	1.0E+00
P37802	Transgelin-2	12	0.00	3	1.9E-03	17	4.3E-11	37	4.0E-19
P37837	Transaldolase	0	1.00	0	1.0E+00	0	1.0E+00	7	5.7E-12
P38117	Electron transfer flavoprotein subunit beta	4	0.00	0	1.0E+00	0	1.0E+00	3	1.9E-03
P38159	RNA-binding motif protein, X chromosome	0	1.00	0	1.0E+00	0	1.0E+00	16	4.9E-05
P38606	V-type proton ATPase catalytic subunit A	0	1.00	0	1.0E+00	15	1.2E-14	0	1.0E+00
P38646	Stress-70 protein, mitochondrial	43	0.00	89	8.1E-11	62	7.7E-06	83	4.9E-15
P38919	Eukaryotic initiation factor 4A-III	2	0.01	3	1.9E-03	41	9.6E-20	2	1.0E+00

P39023	60S ribosomal protein L3	48	0.00	10	2.7E-10	26	5.7E-14	59	2.5E-25
P39687	Acidic leucine-rich nuclear phosphoprotein 32 family member A	0	1.00	0	1.0E+00	0	1.0E+00	22	4.2E-15
P39748	Flap endonuclease 1	3	0.00	2	1.9E-03	0	1.0E+00	15	7.6E-16
P40227	T-complex protein 1 subunit zeta	35	0.00	52	3.2E-22	78	1.3E-15	57	2.3E-29
P40306	Proteasome subunit beta type-10	0	1.00	1	6.1E-02	0	1.0E+00	1	7.4E-02
P40429	60S ribosomal protein L13a	12	0.00	11	2.1E-07	38	3.9E-03	18	1.9E-15
P40616	ADP-ribosylation factor-like protein 1	1	0.00	0	1.0E+00	45	1.4E-10	1	1.8E-03
P40692	DNA mismatch repair protein Mlh1	5	0.00	1	9.5E-02	0	1.0E+00	1	1.6E-02
P40926	Malate dehydrogenase, mitochondrial	16	0.00	15	1.1E-07	72	2.4E-20	58	2.2E-24
P40937	Replication factor C subunit 5	2	0.00	4	1.9E-03	11	3.9E-09	4	9.3E-08
P40939	Trifunctional enzyme subunit alpha, mitochondrial	8	0.00	47	1.7E-27	14	6.2E-08	34	7.8E-31
P41091	Eukaryotic translation initiation factor 2 subunit 3	0	1.00	0	1.0E+00	2	5.1E-02	4	1.8E-03
P41240	Tyrosine-protein kinase CSK	0	1.00	0	1.0E+00	2	4.7E-02	2	1.8E-03
P41250	Glycine--tRNA ligase	5	0.00	10	1.9E-07	16	8.2E-07	6	5.4E-09
P41252	Isoleucine--tRNA ligase, cytoplasmic	2	0.00	5	2.2E-03	33	4.0E-08	0	1.0E+00
P41567	Eukaryotic translation initiation factor 1	0	1.00	0	1.0E+00	0	1.0E+00	6	3.1E-06
P42166	Lamina-associated polypeptide 2, isoform alpha	0	1.00	3	1.9E-03	0	1.0E+00	9	2.0E-05
P42224	Signal transducer and activator of transcription 1-alpha/beta	1	0.00	0	1.0E+00	7	2.8E-07	0	1.0E+00
P42285	Superkiller viralicidic activity 2-like 2	5	0.00	0	1.0E+00	5	3.9E-03	6	1.9E-08
P42330	Aldo-keto reductase family 1 member C3	8	0.03	1	1.0E+00	0	1.0E+00	4	2.6E-02
P42345	Serine/threonine-protein kinase mTOR	0	1.00	0	1.0E+00	2	6.2E-03	0	1.0E+00
P42694	Probable helicase with zinc finger domain	0	1.00	2	1.5E-02	1	4.4E-02	1	8.9E-02
P42704	Leucine-rich PPR motif-containing protein, mitochondrial	44	0.00	56	3.4E-38	264	3.3E-51	83	2.1E-63
P42765	3-ketoacyl-CoA thiolase, mitochondrial	0	1.00	19	6.0E-15	6	3.9E-03	8	2.2E-12
P43007	Neutral amino acid transporter A	0	1.00	21	3.6E-19	1	9.4E-02	0	1.0E+00
P43034	Platelet-activating factor acetylhydrolase IB subunit alpha	1	0.04	0	1.0E+00	0	1.0E+00	9	2.3E-15
P43243	Matrin-3	78	0.00	62	2.6E-14	41	8.8E-05	31	2.9E-17
P43246	DNA mismatch repair protein Msh2	0	1.00	3	1.9E-03	0	1.0E+00	2	1.8E-03
P43250	G protein-coupled receptor kinase 6	2	0.00	0	1.0E+00	0	1.0E+00	0	1.0E+00
P43304	Glycerol-3-phosphate dehydrogenase, mitochondrial	1	0.00	0	1.0E+00	2	3.9E-03	0	1.0E+00
P43307	Translocon-associated protein subunit alpha	17	0.00	8	1.9E-03	6	3.9E-03	8	1.8E-03
P43490	Nicotinamide	0	1.00	2	6.3E-03	0	1.0E+00	13	1.0E-18

	phosphoribosyltransferase								
P45880	Voltage-dependent anion-selective channel protein 2	36	0.00	28	1.0E-13	43	1.3E-12	23	5.3E-15
P45973	Chromobox protein homolog 5	0	1.00	0	1.0E+00	0	1.0E+00	9	7.5E-08
P45974	Ubiquitin carboxyl-terminal hydrolase 5	0	1.00	1	5.3E-02	32	6.2E-08	20	1.2E-17
P46013	Antigen KI-67	12	0.00	0	1.0E+00	2	3.6E-02	1	5.8E-02
P46060	Ran GTPase-activating protein 1	5	1.00	13	1.0E+00	39	2.7E-03	1	1.0E+00
P46087	Putative ribosomal RNA methyltransferase NOP2	1	0.06	3	9.7E-06	5	2.6E-05	5	3.3E-03
P46379	Large proline-rich protein BAG6	0	1.00	0	1.0E+00	27	1.2E-06	0	1.0E+00
P46459	Vesicle-fusing ATPase	2	0.00	1	1.9E-03	7	1.9E-04	0	1.0E+00
P46776	60S ribosomal protein L27a	0	1.00	0	1.0E+00	1	1.6E-02	9	3.5E-11
P46777	60S ribosomal protein L5	10	0.00	11	1.0E+00	4	2.1E-03	25	1.3E-03
P46778	60S ribosomal protein L21	20	0.00	6	1.9E-03	23	3.9E-03	33	5.4E-09
P46781	40S ribosomal protein S9	5	0.00	3	1.9E-03	0	1.0E+00	8	2.2E-09
P46782	40S ribosomal protein S5	15	0.00	36	2.3E-10	12	8.6E-08	39	1.4E-14
P46940	Ras GTPase-activating-like protein IQGAP1	7	0.00	28	4.4E-14	18	3.9E-03	11	5.2E-14
P47756	F-actin-capping protein subunit beta	1	0.07	9	1.9E-03	32	3.9E-03	13	3.0E-15
P47871	Glucagon receptor	1	0.03	0	1.0E+00	1	6.6E-02	0	1.0E+00
P47897	Glutamine--tRNA ligase	31	0.00	32	3.3E-15	41	6.2E-08	19	5.1E-21
P47985	Cytochrome b-c1 complex subunit Rieske, mitochondrial	0	1.00	2	9.4E-03	0	1.0E+00	1	1.8E-03
P48047	ATP synthase subunit O, mitochondrial	0	1.00	16	1.4E-08	14	5.9E-10	21	1.4E-13
P48147	Prolyl endopeptidase	0	1.00	0	1.0E+00	14	4.0E-03	1	3.7E-02
P48556	26S proteasome non-ATPase regulatory subunit 8	1	0.06	0	1.0E+00	19	3.9E-03	0	1.0E+00
P48643	T-complex protein 1 subunit epsilon	22	0.00	13	5.2E-12	37	1.5E-24	72	1.5E-30
P48735	Isocitrate dehydrogenase [NADP], mitochondrial	36	0.00	17	1.4E-15	27	6.3E-08	4	3.1E-06
P48960	CD97 antigen	1	0.07	0	1.0E+00	7	3.9E-03	0	1.0E+00
P49189	4-trimethylaminobutyraldehyde dehydrogenase	0	1.00	0	1.0E+00	16	8.7E-15	0	1.0E+00
P49257	Protein ERGIC-53	19	0.00	17	2.6E-10	2	1.5E-02	15	1.7E-10
P49321	Nuclear autoantigenic sperm protein	7	0.00	0	1.0E+00	9	3.9E-03	23	8.7E-08
P49327	Fatty acid synthase	154	0.00	206	6.5E-95	243	1.0E-67	129	1.1E-109
P49366	Deoxyhypusine synthase	0	1.00	1	8.3E-02	0	1.0E+00	1	6.2E-02
P49368	T-complex protein 1 subunit gamma	19	0.00	19	5.6E-17	70	5.6E-24	46	4.3E-34
P49411	Elongation factor Tu, mitochondrial	98	0.00	81	2.8E-31	196	2.9E-31	51	2.7E-30
P49588	Alanine--tRNA ligase, cytoplasmic	9	0.00	29	2.0E-09	37	2.7E-07	14	3.3E-28
P49721	Proteasome subunit beta type-2	0	1.00	0	1.0E+00	0	1.0E+00	3	2.1E-06
P49756	RNA-binding protein 25	1	0.06	0	1.0E+00	14	3.9E-03	0	1.0E+00
P49773	Histidine triad nucleotide-binding protein 1	19	0.00	2	1.5E-02	0	1.0E+00	15	4.0E-13
P49792	E3 SUMO-protein ligase RanBP2	1	0.00	0	1.0E+00	11	3.0E-04	7	8.1E-06

P49915	GMP synthase [glutamine-hydrolyzing]	22	0.00	27	1.9E-03	34	2.2E-04	15	1.8E-03
P50213	Isocitrate dehydrogenase [NAD] subunit alpha, mitochondrial	16	0.00	0	1.0E+00	117	1.1E-14	9	1.0E+00
P50395	Rab GDP dissociation inhibitor beta	0	1.00	0	1.0E+00	5	1.0E+00	42	1.7E-15
P50416	Carnitine O-palmitoyltransferase 1, liver isoform	18	0.00	1	1.9E-03	76	2.8E-25	8	1.8E-03
P50454	Serpin H1	0	1.00	7	1.9E-03	2	5.6E-03	0	1.0E+00
P50502	Hsc70-interacting protein	0	1.00	0	1.0E+00	0	1.0E+00	10	5.4E-12
P50570	Dynammin-2	0	1.00	1	3.8E-03	25	3.9E-03	0	1.0E+00
P50914	60S ribosomal protein L14	13	0.00	5	1.9E-03	14	3.9E-03	2	1.8E-03
P50990	T-complex protein 1 subunit theta	18	0.00	24	7.1E-09	38	1.4E-18	41	1.2E-33
P50991	T-complex protein 1 subunit delta	3	0.00	35	5.0E-17	9	3.9E-03	52	1.2E-34
P50995	Annexin A11	0	1.00	3	1.9E-03	3	4.6E-03	3	1.8E-03
P51148	Ras-related protein Rab-5C	4	0.00	1	1.9E-03	1	3.8E-02	1	1.8E-03
P51149	Ras-related protein Rab-7a	15	0.00	8	6.6E-13	28	1.4E-10	6	5.4E-09
P51531	Probable global transcription activator SNF2L2	0	1.00	0	1.0E+00	3	2.6E-04	0	1.0E+00
P51571	Translocon-associated protein subunit delta	50	0.00	47	4.2E-13	100	4.8E-13	27	2.2E-14
P51572	B-cell receptor-associated protein 31	4	0.00	2	3.5E-03	0	1.0E+00	3	1.8E-03
P51610	Host cell factor 1	0	1.00	0	1.0E+00	1	1.3E-02	4	3.1E-06
P51659	Peroxisomal multifunctional enzyme type 2	10	0.00	8	7.2E-09	34	1.0E-25	3	3.1E-06
P51665	26S proteasome non-ATPase regulatory subunit 7	1	0.00	0	1.0E+00	26	3.9E-03	14	1.7E-10
P51812	Ribosomal protein S6 kinase alpha-3	4	0.00	0	1.0E+00	3	3.3E-04	1	1.0E+00
P51991	Heterogeneous nuclear ribonucleoprotein A3	5	1.00	0	1.0E+00	9	1.0E+00	42	2.3E-11
P52209	6-phosphogluconate dehydrogenase, decarboxylating	0	1.00	48	8.8E-25	0	1.0E+00	31	2.1E-19
P52272	Heterogeneous nuclear ribonucleoprotein M	141	0.00	70	2.3E-10	147	1.9E-15	105	2.6E-15
P52292	Importin subunit alpha-2	18	0.00	24	2.1E-12	27	1.6E-05	19	5.5E-23
P52294	Importin subunit alpha-1	0	1.00	2	1.9E-03	1	4.6E-03	2	1.0E+00
P52566	Rho GDP-dissociation inhibitor 2	5	0.00	1	2.9E-02	0	1.0E+00	13	7.1E-11
P52597	Heterogeneous nuclear ribonucleoprotein F	15	0.00	49	1.7E-12	43	2.5E-14	28	6.4E-16
P52701	DNA mismatch repair protein Msh6	3	0.00	0	1.0E+00	11	2.9E-06	2	3.0E-03
P52907	F-actin-capping protein subunit alpha-1	1	0.02	0	1.0E+00	0	1.0E+00	3	1.8E-03
P52948	Nuclear pore complex protein Nup98-Nup96	0	1.00	0	1.0E+00	14	1.5E-06	1	1.9E-03
P53004	Biliverdin reductase A	32	0.00	8	9.8E-09	53	1.2E-16	8	3.1E-06
P53007	Tricarboxylate transport protein, mitochondrial	0	1.00	0	1.0E+00	14	4.1E-08	0	1.0E+00
P53618	Coatomer subunit beta	17	0.00	11	8.7E-09	26	1.1E-07	1	4.3E-02
P53621	Coatomer subunit alpha	6	0.00	4	1.9E-03	59	6.2E-08	7	5.4E-09
P53985	Monocarboxylate transporter 1	0	1.00	3	1.2E-03	0	1.0E+00	0	1.0E+00

P54105	Methylosome subunit pICln	0	1.00	0	1.0E+00	6	4.6E-03	20	1.7E-10
P54136	Arginine--tRNA ligase, cytoplasmic	11	0.00	34	2.2E-23	10	3.9E-03	4	5.4E-09
P54577	Tyrosine--tRNA ligase, cytoplasmic	3	0.00	0	1.0E+00	40	2.8E-21	12	1.7E-17
P54709	Sodium/potassium-transporting ATPase subunit beta-3	0	1.00	23	4.3E-13	25	2.8E-08	0	1.0E+00
P54760	Ephrin type-B receptor 4	0	1.00	0	1.0E+00	1	4.2E-02	1	9.8E-02
P54819	Adenylate kinase 2, mitochondrial	0	1.00	0	1.0E+00	10	3.9E-03	21	3.1E-06
P54840	Glycogen [starch] synthase, liver	0	1.00	1	4.8E-02	1	4.0E-02	0	1.0E+00
P54886	Delta-1-pyrroline-5-carboxylate synthase	25	0.00	4	1.9E-03	91	2.8E-10	14	1.4E-07
P55060	Exportin-2	39	0.00	13	3.7E-06	174	9.4E-07	39	4.7E-05
P55072	Transitional endoplasmic reticulum ATPase	25	0.00	29	7.5E-19	19	7.6E-05	56	7.5E-44
P55084	Trifunctional enzyme subunit beta, mitochondrial	7	0.00	9	3.7E-06	17	1.8E-15	8	1.1E-12
P55145	Mesencephalic astrocyte-derived neurotrophic factor	0	1.00	0	1.0E+00	0	1.0E+00	9	2.7E-11
P55160	Nck-associated protein 1-like	0	1.00	0	1.0E+00	4	2.1E-05	0	1.0E+00
P55209	Nucleosome assembly protein 1-like 1	0	1.00	0	1.0E+00	0	1.0E+00	34	8.0E-19
P55263	Adenosine kinase	1	0.00	0	1.0E+00	24	3.4E-06	0	1.0E+00
P55265	Double-stranded RNA-specific adenosine deaminase	0	1.00	0	1.0E+00	19	8.6E-08	3	1.6E-06
P55327	Tumor protein D52	0	1.00	0	1.0E+00	0	1.0E+00	13	1.1E-04
P55786	Puromycin-sensitive aminopeptidase	0	1.00	1	5.7E-02	0	1.0E+00	1	2.1E-02
P55795	Heterogeneous nuclear ribonucleoprotein H2	28	0.00	40	1.9E-03	31	1.0E+00	24	1.6E-12
P55809	Succinyl-CoA:3-ketoacid-coenzyme A transferase 1, mitochondrial	0	1.00	0	1.0E+00	1	9.3E-02	3	3.4E-05
P56134	ATP synthase subunit f, mitochondrial	8	0.00	10	1.9E-03	7	3.9E-03	3	2.9E-05
P56192	Methionine--tRNA ligase, cytoplasmic	15	0.00	37	1.0E-27	37	1.6E-05	12	2.4E-12
P56537	Eukaryotic translation initiation factor 6	0	1.00	0	1.0E+00	8	3.9E-03	4	3.0E-05
P56559	ADP-ribosylation factor-like protein 4C	0	1.00	1	8.9E-02	0	1.0E+00	1	8.9E-02
P57086	SCAN domain-containing protein 1	0	1.00	1	4.7E-02	0	1.0E+00	1	9.2E-02
P57737	Coronin-7	29	0.00	48	5.5E-30	12	1.6E-05	4	3.0E-07
P58546	Myotrophin	0	1.00	0	1.0E+00	4	2.1E-05	1	1.1E-02
P59046	NACHT, LRR and PYD domains-containing protein 12	0	1.00	1	6.2E-02	2	2.3E-03	1	3.4E-02
P59510	A disintegrin and metalloproteinase with thrombospondin motifs 20	0	1.00	1	9.4E-02	1	8.1E-02	0	1.0E+00
P60174	Triosephosphate isomerase	0	1.00	0	1.0E+00	0	1.0E+00	72	2.6E-24
P60228	Eukaryotic translation initiation factor 3 subunit E	2	0.00	0	1.0E+00	41	1.6E-05	9	3.2E-13
P60842	Eukaryotic initiation factor 4A-I	39	0.00	80	9.6E-20	127	2.3E-07	57	2.3E-25

P60866	40S ribosomal protein S20	0	1.00	0	1.0E+00	1	4.5E-02	3	1.8E-03
P60953	Cell division control protein 42 homolog	6	0.00	20	7.1E-08	13	1.1E-08	11	9.0E-08
P60981	Destrin	2	0.00	0	1.0E+00	9	3.9E-03	1	2.6E-02
P61011	Signal recognition particle 54 kDa protein	0	1.00	0	1.0E+00	4	4.6E-03	19	3.4E-19
P61026	Ras-related protein Rab-10	10	0.00	11	3.8E-08	26	3.9E-03	7	4.0E-09
P61077	Ubiquitin-conjugating enzyme E2 D3	0	1.00	2	1.2E-02	15	1.6E-05	1	2.0E-03
P61106	Ras-related protein Rab-14	10	0.00	10	1.1E-07	0	1.0E+00	11	3.4E-06
P61158	Actin-related protein 3	6	1.00	11	1.9E-03	39	1.2E-11	37	5.3E-20
P61160	Actin-related protein 2	0	1.00	0	1.0E+00	5	4.4E-05	2	2.6E-03
P61201	COP9 signalosome complex subunit 2	0	1.00	4	2.2E-03	5	3.9E-03	0	1.0E+00
P61221	ATP-binding cassette sub-family E member 1	5	0.00	10	3.7E-06	67	2.2E-19	4	3.5E-06
P61247	40S ribosomal protein S3a	7	0.00	6	1.9E-03	2	4.6E-03	26	3.0E-13
P61289	Proteasome activator complex subunit 3	0	1.00	0	1.0E+00	3	3.9E-03	5	1.0E-07
P61353	60S ribosomal protein L27	0	1.00	0	1.0E+00	0	1.0E+00	6	1.4E-10
P61604	10 kDa heat shock protein, mitochondrial	8	0.00	3	1.9E-03	0	1.0E+00	59	1.2E-19
P61619	Protein transport protein Sec61 subunit alpha isoform 1	25	0.00	3	1.9E-03	25	6.2E-15	4	1.8E-03
P61758	Prefoldin subunit 3	0	1.00	0	1.0E+00	0	1.0E+00	5	5.3E-09
P61981	14-3-3 protein gamma	5	0.00	1	1.9E-02	33	1.6E-05	45	2.2E-16
P62081	40S ribosomal protein S7	29	0.00	50	7.4E-15	9	3.8E-06	43	2.1E-17
P62136	Serine/threonine-protein phosphatase PP1-alpha catalytic subunit	17	0.00	4	1.9E-03	31	3.0E-09	14	1.2E-08
P62191	26S protease regulatory subunit 4	6	0.00	0	1.0E+00	1	3.7E-02	6	3.5E-06
P62195	26S protease regulatory subunit 8	7	0.00	7	1.9E-03	16	1.2E-04	1	7.5E-02
P62241	40S ribosomal protein S8	19	0.00	14	7.7E-08	27	1.0E-10	21	1.2E-15
P62244	40S ribosomal protein S15a	14	0.00	11	6.2E-08	28	4.2E-07	24	5.4E-09
P62249	40S ribosomal protein S16	2	0.00	8	5.8E-05	24	1.7E-04	10	3.9E-04
P62258	14-3-3 protein epsilon	0	1.00	0	1.0E+00	14	3.9E-03	46	3.3E-13
P62263	40S ribosomal protein S14	0	1.00	9	6.3E-08	19	3.9E-03	2	1.8E-03
P62269	40S ribosomal protein S18	12	0.00	7	1.5E-10	8	3.9E-03	5	3.3E-05
P62277	40S ribosomal protein S13	5	0.00	13	5.4E-06	0	1.0E+00	31	1.7E-10
P62280	40S ribosomal protein S11	16	0.00	15	1.9E-03	56	4.8E-07	24	1.4E-07
P62304	Small nuclear ribonucleoprotein E	1	0.02	0	1.0E+00	1	6.5E-03	11	2.4E-10
P62314	Small nuclear ribonucleoprotein Sm D1	25	0.00	4	1.9E-03	46	5.9E-09	40	5.8E-11
P62318	Small nuclear ribonucleoprotein Sm D3	3	0.00	6	1.9E-03	0	1.0E+00	13	1.0E-07
P62424	60S ribosomal protein L7a	1	0.00	17	1.4E-13	0	1.0E+00	44	1.1E-22
P62491	Ras-related protein Rab-11A	1	0.00	13	1.5E-11	0	1.0E+00	0	1.0E+00
P62701	40S ribosomal protein S4, X isoform	40	0.00	51	1.1E-13	83	5.6E-14	39	9.6E-19
P62753	40S ribosomal protein S6	5	0.00	20	7.5E-13	0	1.0E+00	9	1.8E-03
P62805	Histone H4	77	0.00	50	2.6E-14	135	3.1E-20	108	9.4E-37
P62826	GTP-binding nuclear protein Ran	40	0.01	15	1.0E+00	102	6.0E-02	28	1.0E+00
P62829	60S ribosomal protein L23	10	0.00	45	3.7E-06	22	2.0E-08	18	9.0E-10

P62841	40S ribosomal protein S15	0	1.00	8	1.9E-03	34	1.7E-11	33	5.4E-09
P62847	40S ribosomal protein S24	3	0.00	11	3.7E-06	13	3.9E-03	11	1.2E-07
P62851	40S ribosomal protein S25	7	0.00	0	1.0E+00	0	1.0E+00	3	1.8E-03
P62854	40S ribosomal protein S26	6	0.00	22	8.3E-11	0	1.0E+00	7	1.8E-03
P62873	Guanine nucleotide-binding protein G(I)/G(S)/G(T) subunit beta-1	0	1.00	4	1.9E-03	1	3.9E-03	1	2.8E-02
P62906	60S ribosomal protein L10a	10	0.00	6	2.0E-03	66	8.1E-05	28	7.7E-23
P62910	60S ribosomal protein L32	0	1.00	0	1.0E+00	24	3.9E-03	14	4.6E-12
P62913	60S ribosomal protein L11	17	0.00	17	8.0E-08	83	6.9E-09	14	5.4E-09
P62937	Peptidyl-prolyl cis-trans isomerase A	45	0.00	65	3.6E-14	187	8.5E-12	180	2.7E-24
P62979	Ubiquitin-40S ribosomal protein S27a	33	0.00	29	7.1E-09	56	1.6E-05	17	2.7E-10
P62995	Transformer-2 protein homolog beta	0	1.00	0	1.0E+00	2	4.1E-02	22	3.0E-13
P63104	14-3-3 protein zeta/delta	0	1.00	0	1.0E+00	10	3.9E-03	66	9.4E-12
P63173	60S ribosomal protein L38	4	0.00	0	1.0E+00	2	1.2E-02	11	1.8E-08
P63220	40S ribosomal protein S21	0	1.00	0	1.0E+00	0	1.0E+00	27	1.1E-10
P63241	Eukaryotic translation initiation factor 5A-1	28	0.00	0	1.0E+00	73	1.5E-09	56	1.1E-10
P63244	Guanine nucleotide-binding protein subunit beta-2-like 1	23	0.00	46	8.2E-18	48	1.2E-12	27	3.3E-17
P67809	Nuclease-sensitive element-binding protein 1	0	1.00	5	2.9E-02	0	1.0E+00	25	7.7E-11
P68032	Actin, alpha cardiac muscle 1	79	0.00	62	3.7E-06	144	1.6E-05	63	4.1E-09
P68366	Tubulin alpha-4A chain	559	0.00	360	7.1E-09	392	1.6E-05	152	1.8E-03
P68371	Tubulin beta-4B chain	379	1.00	494	2.3E-05	378	2.2E-02	222	4.2E-04
P68431	Histone H3.1	87	0.00	13	1.9E-03	317	3.9E-03	67	2.2E-08
P68871	Hemoglobin subunit beta	21	0.00	2	2.4E-03	10	3.9E-03	3	1.8E-03
P69905	Hemoglobin subunit alpha	48	0.00	26	1.9E-10	71	2.5E-17	14	5.3E-07
P78344	Eukaryotic translation initiation factor 4 gamma 2	0	1.00	1	5.5E-03	1	7.8E-02	2	1.9E-03
P78347	General transcription factor II-I	34	0.00	23	1.4E-11	12	6.2E-08	8	5.4E-09
P78363	Retinal-specific ATP-binding cassette transporter	1	0.02	0	1.0E+00	1	1.3E-02	0	1.0E+00
P78371	T-complex protein 1 subunit beta	43	0.02	73	2.1E-05	37	1.6E-03	65	5.3E-03
P78527	DNA-dependent protein kinase catalytic subunit	76	0.00	43	1.1E-27	152	4.9E-35	21	1.9E-26
P78539	Sushi repeat-containing protein SRPX	2	0.02	1	5.8E-02	0	1.0E+00	0	1.0E+00
P83916	Chromobox protein homolog 1	0	1.00	0	1.0E+00	0	1.0E+00	18	1.5E-06
P84085	ADP-ribosylation factor 5	11	1.00	23	1.0E+00	18	4.0E-02	20	7.3E-05
P84103	Serine/arginine-rich splicing factor 3	6	0.00	0	1.0E+00	0	1.0E+00	17	1.4E-07
P84243	Histone H3.3	36	0.00	7	1.9E-03	70	3.9E-03	47	1.4E-05
P98171	Rho GTPase-activating protein 4	13	0.00	19	1.4E-11	35	3.8E-11	0	1.0E+00
P98179	Putative RNA-binding protein 3	0	1.00	0	1.0E+00	0	1.0E+00	21	3.1E-06
P98194	Calcium-transporting ATPase type 2C member 1	1	0.08	2	6.2E-03	0	1.0E+00	0	1.0E+00
Q00325	Phosphate carrier protein, mitochondrial	46	0.00	18	2.0E-12	45	7.5E-10	30	5.3E-22
Q00341	Vigilin	11	0.00	7	7.3E-06	0	1.0E+00	1	1.8E-03

Q00610	Clathrin heavy chain 1	152	0.00	93	2.6E-45	400	1.5E-67	95	2.7E-88
Q00688	Peptidyl-prolyl cis-trans isomerase FKBP3	0	1.00	0	1.0E+00	0	1.0E+00	5	1.8E-07
Q00839	Heterogeneous nuclear ribonucleoprotein U	126	0.00	101	4.7E-47	169	2.1E-31	134	4.2E-56
Q01081	Splicing factor U2AF 35 kDa subunit	1	0.07	0	1.0E+00	1	8.5E-02	15	4.4E-14
Q01105	Protein SET	0	1.00	0	1.0E+00	0	1.0E+00	77	5.3E-31
Q01518	Adenylyl cyclase-associated protein 1	0	1.00	5	1.9E-03	2	7.8E-03	8	5.5E-10
Q02218	2-oxoglutarate dehydrogenase, mitochondrial	0	1.00	5	1.9E-03	42	2.9E-21	1	1.8E-03
Q02543	60S ribosomal protein L18a	13	0.00	10	8.6E-08	61	1.4E-15	22	4.3E-13
Q02790	Peptidyl-prolyl cis-trans isomerase FKBP4	1	0.00	0	1.0E+00	1	2.0E-02	29	4.6E-31
Q02878	60S ribosomal protein L6	22	0.00	11	1.9E-03	59	7.4E-07	34	1.6E-14
Q02978	Mitochondrial 2-oxoglutarate/malate carrier protein	0	1.00	0	1.0E+00	6	4.6E-08	0	1.0E+00
Q03001	Dystonin	0	1.00	0	1.0E+00	3	3.1E-04	1	7.9E-02
Q03252	Lamin-B2	2	0.03	0	1.0E+00	0	1.0E+00	2	7.2E-03
Q03519	Antigen peptide transporter 2	5	0.00	0	1.0E+00	2	3.9E-03	0	1.0E+00
Q03701	CCAAT/enhancer-binding protein zeta	2	0.00	0	1.0E+00	0	1.0E+00	1	6.0E-02
Q04323	UBX domain-containing protein 1	0	1.00	0	1.0E+00	0	1.0E+00	5	9.4E-07
Q04637	Eukaryotic translation initiation factor 4 gamma 1	5	0.00	18	9.3E-09	2	2.0E-04	5	1.8E-03
Q04828	Aldo-keto reductase family 1 member C1	8	0.02	1	1.0E+00	0	1.0E+00	7	7.5E-07
Q04837	Single-stranded DNA-binding protein, mitochondrial	0	1.00	0	1.0E+00	0	1.0E+00	14	1.0E-12
Q04917	14-3-3 protein eta	0	1.00	0	1.0E+00	0	1.0E+00	11	5.2E-06
Q04941	Proteolipid protein 2	0	1.00	3	3.8E-06	1	2.0E-02	0	1.0E+00
Q05639	Elongation factor 1-alpha 2	607	1.00	277	2.5E-04	1000	1.0E-03	230	2.7E-05
Q06323	Proteasome activator complex subunit 1	0	1.00	0	1.0E+00	0	1.0E+00	14	1.1E-11
Q06830	Peroxiredoxin-1	8	0.00	2	2.1E-03	74	2.9E-13	33	1.7E-19
Q07020	60S ribosomal protein L18	12	0.00	21	4.2E-08	8	6.9E-10	10	3.5E-09
Q07021	Complement component 1 Q subcomponent-binding protein, mitochondrial	0	1.00	0	1.0E+00	0	1.0E+00	64	1.1E-25
Q07666	KH domain-containing, RNA-binding, signal transduction-associated protein 1	5	0.00	12	1.9E-03	0	1.0E+00	39	1.4E-16
Q07912	Activated CDC42 kinase 1	1	0.02	0	1.0E+00	0	1.0E+00	1	4.9E-02
Q07955	Serine/arginine-rich splicing factor 1	0	1.00	0	1.0E+00	0	1.0E+00	12	7.9E-11
Q07960	Rho GTPase-activating protein 1	0	1.00	2	1.9E-03	0	1.0E+00	1	7.7E-02
Q08211	ATP-dependent RNA helicase A	122	0.00	66	4.6E-35	159	5.5E-42	84	1.6E-62
Q08945	FACT complex subunit SSRP1	0	1.00	0	1.0E+00	0	1.0E+00	17	8.2E-24
Q08AG7	Mitotic-spindle organizing protein 1	0	1.00	1	3.8E-03	1	4.1E-02	0	1.0E+00
Q09028	Histone-binding protein RBBP4	0	1.00	0	1.0E+00	0	1.0E+00	14	1.1E-18
Q09666	Neuroblast differentiation-associated protein AHNAK	3	1.00	20	7.2E-09	12	1.0E+00	149	4.5E-158

Q10567	AP-1 complex subunit beta-1	0	1.00	6	1.9E-03	22	3.9E-03	2	3.9E-06
Q10713	Mitochondrial-processing peptidase subunit alpha	10	0.00	1	4.1E-03	75	5.5E-20	14	3.1E-06
Q12769	Nuclear pore complex protein Nup160	0	1.00	0	1.0E+00	42	1.2E-08	0	1.0E+00
Q12788	Transducin beta-like protein 3	0	1.00	0	1.0E+00	8	1.4E-04	1	8.3E-03
Q12840	Kinesin heavy chain isoform 5A	0	1.00	0	1.0E+00	0	1.0E+00	2	3.7E-03
Q12904	Aminoacyl tRNA synthase complex-interacting multifunctional protein 1	2	0.00	0	1.0E+00	0	1.0E+00	6	7.0E-09
Q12905	Interleukin enhancer-binding factor 2	8	0.00	11	1.1E-04	2	8.2E-05	13	7.2E-17
Q12906	Interleukin enhancer-binding factor 3	7	0.00	8	1.9E-03	7	4.0E-03	10	3.1E-06
Q12907	Vesicular integral-membrane protein VIP36	29	0.00	14	1.6E-11	68	1.9E-12	7	5.0E-10
Q12923	Tyrosine-protein phosphatase non-receptor type 13	0	1.00	0	1.0E+00	2	4.3E-03	0	1.0E+00
Q12931	Heat shock protein 75 kDa, mitochondrial	43	0.00	19	1.2E-17	40	6.3E-08	28	1.5E-35
Q12955	Ankyrin-3	0	1.00	0	1.0E+00	0	1.0E+00	2	5.5E-03
Q13011	Delta(3,5)-Delta(2,4)-dienoyl-CoA isomerase, mitochondrial	0	1.00	0	1.0E+00	2	6.9E-03	9	3.5E-12
Q13148	TAR DNA-binding protein 43	6	0.00	4	3.8E-03	0	1.0E+00	7	1.8E-03
Q13151	Heterogeneous nuclear ribonucleoprotein A0	0	1.00	4	1.9E-03	14	3.9E-03	17	4.0E-11
Q13155	Aminoacyl tRNA synthase complex-interacting multifunctional protein 2	2	0.00	22	3.7E-06	6	3.9E-03	13	6.7E-17
Q13162	Peroxiredoxin-4	9	0.00	0	1.0E+00	0	1.0E+00	36	7.8E-20
Q13185	Chromobox protein homolog 3	2	0.00	0	1.0E+00	0	1.0E+00	26	8.1E-10
Q13200	26S proteasome non-ATPase regulatory subunit 2	2	0.00	7	1.9E-03	1	6.0E-02	25	1.7E-24
Q13243	Serine/arginine-rich splicing factor 5	0	1.00	0	1.0E+00	0	1.0E+00	6	4.2E-09
Q13263	Transcription intermediary factor 1-beta	19	0.00	9	1.9E-03	1	5.0E-02	9	2.8E-08
Q13283	Ras GTPase-activating protein-binding protein 1	0	1.00	11	1.9E-03	0	1.0E+00	14	1.6E-15
Q13332	Receptor-type tyrosine-protein phosphatase S	0	1.00	1	5.5E-02	0	1.0E+00	1	8.7E-02
Q13347	Eukaryotic translation initiation factor 3 subunit I	0	1.00	0	1.0E+00	0	1.0E+00	12	1.7E-16
Q13423	NAD(P) transhydrogenase, mitochondrial	1	0.00	9	1.9E-03	2	6.7E-03	1	5.8E-02
Q13435	Splicing factor 3B subunit 2	7	0.00	0	1.0E+00	0	1.0E+00	18	2.7E-23
Q13459	Unconventional myosin-IXb	1	0.09	0	1.0E+00	0	1.0E+00	1	5.2E-02
Q13509	Tubulin beta-3 chain	212	0.00	297	2.2E-12	273	1.0E+00	126	1.0E+00
Q13535	Serine/threonine-protein kinase ATR	7	0.00	0	1.0E+00	3	1.6E-03	2	7.1E-02
Q13547	Histone deacetylase 1	0	1.00	1	7.9E-02	0	1.0E+00	3	3.1E-06
Q13576	Ras GTPase-activating-like protein IQGAP2	10	0.00	1	1.9E-03	8	7.4E-07	11	3.1E-12
Q13616	Cullin-1	0	1.00	0	1.0E+00	40	1.6E-05	2	8.8E-06

Q13637	Ras-related protein Rab-32	3	0.04	0	1.0E+00	1	7.7E-02	0	1.0E+00
Q13698	Voltage-dependent L-type calcium channel subunit alpha-1S	0	1.00	0	1.0E+00	1	3.6E-02	1	5.7E-02
Q13724	Mannosyl-oligosaccharide glucosidase	6	0.00	0	1.0E+00	16	1.6E-05	0	1.0E+00
Q13813	Spectrin alpha chain, brain	2	0.01	0	1.0E+00	0	1.0E+00	3	3.3E-03
Q13838	Spliceosome RNA helicase DDX39B	47	1.00	44	1.0E+00	92	1.0E+00	40	8.1E-04
Q14008	Cytoskeleton-associated protein 5	7	0.00	12	1.9E-03	15	1.7E-09	1	3.6E-02
Q14103	Heterogeneous nuclear ribonucleoprotein D0	0	1.00	0	1.0E+00	1	1.0E+00	55	5.1E-23
Q14108	Lysosome membrane protein 2	1	0.07	0	1.0E+00	10	3.9E-03	0	1.0E+00
Q14137	Ribosome biogenesis protein BOP1	12	0.00	0	1.0E+00	49	1.1E-19	12	3.4E-06
Q14139	Ubiquitin conjugation factor E4 A	0	1.00	0	1.0E+00	4	1.1E-02	1	5.2E-02
Q14151	Scaffold attachment factor B2	0	1.00	0	1.0E+00	0	1.0E+00	20	2.0E-24
Q14152	Eukaryotic translation initiation factor 3 subunit A	3	0.00	21	2.7E-14	2	1.9E-02	14	1.6E-11
Q14157	Ubiquitin-associated protein 2-like	0	1.00	0	1.0E+00	0	1.0E+00	8	4.0E-08
Q14166	Tubulin--tyrosine ligase-like protein 12	0	1.00	5	1.9E-03	27	1.6E-05	2	6.9E-03
Q14204	Cytoplasmic dynein 1 heavy chain 1	26	0.00	67	8.7E-32	60	4.0E-21	12	1.9E-13
Q14240	Eukaryotic initiation factor 4A-II	21	0.03	36	4.7E-06	68	2.5E-03	28	7.9E-05
Q14254	Flotillin-2	2	0.00	0	1.0E+00	2	3.9E-03	0	1.0E+00
Q14258	E3 ubiquitin/ISG15 ligase TRIM25	0	1.00	0	1.0E+00	11	1.8E-05	0	1.0E+00
Q14444	Caprin-1	0	1.00	0	1.0E+00	0	1.0E+00	24	3.0E-24
Q14498	RNA-binding protein 39	2	0.00	1	9.6E-02	0	1.0E+00	2	1.8E-03
Q14517	Protocadherin Fat 1	1	0.07	0	1.0E+00	1	9.5E-02	0	1.0E+00
Q14566	DNA replication licensing factor MCM6	30	0.00	22	3.3E-08	59	1.4E-11	28	8.4E-30
Q14568	Putative heat shock protein HSP 90-alpha A2	50	1.00	40	2.0E-02	66	5.2E-03	45	3.6E-02
Q14573	Inositol 1,4,5-trisphosphate receptor type 3	1	0.10	0	1.0E+00	3	5.0E-04	0	1.0E+00
Q14643	Inositol 1,4,5-trisphosphate receptor type 1	2	0.00	0	1.0E+00	0	1.0E+00	0	1.0E+00
Q14676	DNA damage checkpoint protein 1	8	0.00	24	7.1E-09	21	6.8E-05	5	1.8E-03
Q14680	Maternal embryonic leucine zipper kinase	0	1.00	1	5.5E-02	1	9.7E-02	0	1.0E+00
Q14690	Protein RRP5 homolog	1	0.00	0	1.0E+00	2	6.0E-03	0	1.0E+00
Q14697	Neutral alpha-glucosidase AB	80	0.00	47	1.0E-30	223	1.2E-38	78	3.3E-54
Q14739	Lamin-B receptor	3	0.03	9	1.9E-03	21	5.3E-16	4	6.0E-06
Q14839	Chromodomain-helicase-DNA-binding protein 4	12	0.00	2	9.9E-05	16	2.7E-09	5	1.6E-07
Q14974	Importin subunit beta-1	56	0.00	33	2.6E-14	106	7.7E-24	45	8.4E-27
Q14980	Nuclear mitotic apparatus protein 1	7	0.00	1	7.2E-02	0	1.0E+00	3	1.8E-03
Q149N8	E3 ubiquitin-protein ligase SHPRH	0	1.00	1	7.3E-02	0	1.0E+00	1	9.2E-02
Q15020	Squamous cell carcinoma antigen recognized by T-cells 3	6	0.00	0	1.0E+00	2	3.9E-03	2	5.3E-05
Q15021	Condensin complex subunit 1	1	0.06	0	1.0E+00	21	1.6E-05	13	5.4E-09
Q15029	116 kDa U5 small nuclear ribonucleoprotein component	9	0.00	2	2.0E-03	25	9.4E-08	13	4.1E-22

Q15042	Rab3 GTPase-activating protein catalytic subunit	0	1.00	0	1.0E+00	1	7.9E-02	1	7.9E-02
Q15046	Lysine--tRNA ligase	0	1.00	0	1.0E+00	25	1.6E-05	20	8.2E-18
Q15061	WD repeat-containing protein 43	0	1.00	0	1.0E+00	6	2.6E-04	1	1.9E-02
Q15149	Plectin	7	0.00	16	7.1E-12	22	3.9E-03	6	8.5E-08
Q15155	Nodal modulator 1	1	0.00	4	1.9E-03	11	3.0E-05	0	1.0E+00
Q15181	Inorganic pyrophosphatase	4	0.00	0	1.0E+00	25	3.2E-12	22	9.8E-16
Q15185	Prostaglandin E synthase 3	0	1.00	0	1.0E+00	0	1.0E+00	8	7.2E-08
Q15233	Non-POU domain-containing octamer-binding protein	55	0.00	29	2.7E-20	77	3.9E-03	73	4.8E-34
Q15287	RNA-binding protein with serine-rich domain 1	0	1.00	0	1.0E+00	0	1.0E+00	11	1.3E-13
Q15349	Ribosomal protein S6 kinase alpha-2	1	0.08	1	5.6E-02	0	1.0E+00	1	1.0E+00
Q15365	Poly(rC)-binding protein 1	26	0.00	113	2.5E-22	62	1.2E-15	69	6.1E-28
Q15393	Splicing factor 3B subunit 3	0	1.00	0	1.0E+00	0	1.0E+00	13	4.0E-20
Q15397	Pumilio domain-containing protein KIAA0020	2	0.00	0	1.0E+00	16	3.9E-03	3	5.4E-04
Q15413	Ryanodine receptor 3	1	0.09	0	1.0E+00	3	1.2E-03	2	2.8E-03
Q15428	Splicing factor 3A subunit 2	0	1.00	0	1.0E+00	10	3.9E-03	4	2.4E-05
Q15437	Protein transport protein Sec23B	2	0.00	5	1.9E-03	17	8.1E-10	5	3.3E-05
Q15459	Splicing factor 3A subunit 1	0	1.00	7	3.7E-06	2	6.0E-03	3	1.8E-03
Q15477	Helicase SKI2W	0	1.00	10	1.9E-03	1	2.5E-02	0	1.0E+00
Q15637	Splicing factor 1	0	1.00	0	1.0E+00	0	1.0E+00	29	2.1E-13
Q15645	Pachytene checkpoint protein 2 homolog	0	1.00	6	4.2E-06	24	1.6E-05	8	8.2E-11
Q15652	Probable JmjC domain-containing histone demethylation protein 2C	1	0.06	0	1.0E+00	1	5.1E-02	0	1.0E+00
Q15717	ELAV-like protein 1	0	1.00	0	1.0E+00	0	1.0E+00	7	7.4E-07
Q15758	Neutral amino acid transporter B(0)	0	1.00	21	1.9E-18	0	1.0E+00	0	1.0E+00
Q15797	Mothers against decapentaplegic homolog 1	0	1.00	0	1.0E+00	9	5.2E-07	0	1.0E+00
Q15813	Tubulin-specific chaperone E	0	1.00	0	1.0E+00	6	1.4E-07	0	1.0E+00
Q15843	NEDD8	0	1.00	0	1.0E+00	0	1.0E+00	9	1.4E-06
Q16222	UDP-N-acetylhexosamine pyrophosphorylase	0	1.00	0	1.0E+00	11	1.6E-05	1	1.8E-03
Q16531	DNA damage-binding protein 1	0	1.00	0	1.0E+00	2	5.5E-02	6	3.1E-06
Q16666	Gamma-interferon-inducible protein 16	33	0.00	9	3.7E-06	15	3.9E-03	6	1.4E-10
Q16706	Alpha-mannosidase 2	1	0.08	0	1.0E+00	3	3.2E-03	0	1.0E+00
Q16760	Diacylglycerol kinase delta	0	1.00	0	1.0E+00	2	3.5E-03	0	1.0E+00
Q16774	Guanylate kinase	0	1.00	0	1.0E+00	19	1.6E-05	0	1.0E+00
Q16777	Histone H2A type 2-C	10	1.00	62	1.9E-03	18	1.0E+00	189	1.7E-14
Q16795	NADH dehydrogenase [ubiquinone] 1 alpha subcomplex subunit 9, mitochondrial	0	1.00	1	1.9E-03	2	1.5E-04	1	6.9E-02
Q16836	Hydroxyacyl-coenzyme A dehydrogenase, mitochondrial	22	0.00	7	1.0E+00	49	9.8E-06	26	1.2E-03
Q16880	2-hydroxyacylsphingosine 1-beta-galactosyltransferase	1	0.09	0	1.0E+00	1	6.5E-02	0	1.0E+00
Q1KMD3	Heterogeneous nuclear ribonucleoprotein U-like protein 2	3	0.00	0	1.0E+00	7	3.9E-03	3	1.9E-07

Q2LD37	Uncharacterized protein KIAA1109	1	0.03	0	1.0E+00	0	1.0E+00	1	6.4E-02
Q2WJ6	Kelch-like protein 38	1	0.00	1	3.0E-02	0	1.0E+00	0	1.0E+00
Q32P51	Heterogeneous nuclear ribonucleoprotein A1-like 2	30	1.00	33	1.0E+00	10	1.0E+00	74	6.3E-04
Q32Q12	Nucleoside diphosphate kinase	1	1.00	18	1.6E-06	9	1.0E+00	58	4.6E-15
Q3BDU5	Lamin A/C	5	0.00	0	1.0E+00	0	1.0E+00	23	1.2E-06
Q3SY69	Mitochondrial 10-formyltetrahydrofolate dehydrogenase	0	1.00	0	1.0E+00	2	1.2E-03	0	1.0E+00
Q3ZCM7	Tubulin beta-8 chain	87	0.00	112	4.6E-12	56	1.0E+00	38	5.8E-05
Q496M5	Inactive serine/threonine-protein kinase PLK5	0	1.00	3	1.9E-06	0	1.0E+00	0	1.0E+00
Q4LDE5	Sushi, von Willebrand factor type A, EGF and pentraxin domain-containing protein 1	0	1.00	1	9.6E-02	4	4.0E-03	0	1.0E+00
Q53H12	Acylglycerol kinase, mitochondrial	10	0.00	6	1.9E-03	3	3.9E-03	3	1.8E-03
Q562R1	Beta-actin-like protein 2	27	0.00	38	1.9E-03	32	3.9E-03	40	1.7E-19
Q58EX2	Protein sidekick-2	0	1.00	0	1.0E+00	1	4.3E-02	1	6.2E-02
Q58FF6	Putative heat shock protein HSP 90-beta 4	48	0.00	49	1.9E-03	1	1.0E+00	38	1.3E-10
Q58FF7	Putative heat shock protein HSP 90-beta-3	109	0.00	68	1.7E-02	64	1.0E+00	70	1.9E-08
Q58FF8	Putative heat shock protein HSP 90-beta 2	11	0.00	31	3.7E-05	8	1.0E-08	26	1.4E-06
Q58FG1	Putative heat shock protein HSP 90-alpha A4	43	1.00	20	1.0E+00	67	1.5E-07	55	3.0E-11
Q59ES8	Heterogeneous nuclear ribonucleoprotein M (Fragment)	118	0.00	62	1.0E+00	134	4.6E-03	81	3.1E-02
Q5CZC0	Fibrous sheath-interacting protein 2	0	1.00	1	6.1E-02	14	4.7E-03	1	5.6E-02
Q5EB52	Mesoderm-specific transcript homolog protein	0	1.00	0	1.0E+00	6	5.4E-09	0	1.0E+00
Q5GFL6	von Willebrand factor A domain-containing protein 2	0	1.00	1	1.8E-02	1	8.1E-02	0	1.0E+00
Q5HY75	Family with sequence similarity 3, member A	0	1.00	0	1.0E+00	1	8.2E-02	1	3.2E-02
Q5JP00	Retinoblastoma binding protein 7	0	1.00	0	1.0E+00	5	3.5E-02	8	5.1E-05
Q5JTH9	RRP12-like protein	2	0.00	8	7.1E-05	26	2.3E-05	3	1.8E-03
Q5JYR6	Ribophorin II	166	0.00	107	1.6E-44	175	4.6E-29	39	7.4E-33
Q5LJA5	Ubiquitin carboxyl-terminal hydrolase L5	0	1.00	0	1.0E+00	41	5.3E-03	0	1.0E+00
Q5LJA9	Ubiquitin carboxyl-terminal hydrolase L5 (Fragment)	0	1.00	0	1.0E+00	41	2.0E-03	0	1.0E+00
Q5S007	Leucine-rich repeat serine/threonine-protein kinase 2	1	0.05	0	1.0E+00	1	3.7E-02	0	1.0E+00
Q5SYB0	FERM and PDZ domain-containing protein 1	0	1.00	1	4.4E-02	0	1.0E+00	1	7.1E-02
Q5SZ07	Hepatoma-derived growth factor (High-mobility group protein 1-like)	0	1.00	0	1.0E+00	0	1.0E+00	19	1.3E-14
Q5T1A1	DC-STAMP domain-containing protein 2	0	1.00	0	1.0E+00	3	4.6E-04	0	1.0E+00
Q5T2N8	ATPase family AAA domain-	2	1.00	0	1.0E+00	59	1.2E-04	10	1.0E+00

	containing protein 3C								
Q5T4S7	E3 ubiquitin-protein ligase UBR4	0	1.00	4	1.9E-03	3	8.0E-05	1	7.0E-02
Q5T6W1	Heterogeneous nuclear ribonucleoprotein K	45	0.04	35	7.7E-03	100	1.0E+00	41	1.8E-03
Q5T6W5	Heterogeneous nuclear ribonucleoprotein K	44	1.00	64	7.1E-09	104	9.5E-05	86	7.2E-17
Q5T7N0	Ribosomal protein L5	7	1.00	11	1.0E+00	2	1.0E+00	25	1.9E-03
Q5T8U7	Surfeit 4	0	1.00	18	3.7E-06	20	2.8E-08	8	3.1E-12
Q5T9A4	ATPase family AAA domain-containing protein 3B	1	1.00	0	1.0E+00	9	1.1E-04	2	1.0E+00
Q5TCQ9	Membrane-associated guanylate kinase, WW and PDZ domain-containing protein 3	0	1.00	0	1.0E+00	3	6.1E-05	0	1.0E+00
Q5TEC6	Histone H3	9	0.00	0	1.0E+00	1	2.4E-02	27	1.7E-04
Q5VSR7	6-phosphofructokinase	2	1.00	14	3.7E-06	22	9.8E-08	2	1.9E-03
Q5VST9	Obscurin	0	1.00	1	2.6E-02	2	1.9E-02	1	7.5E-02
Q5VW36	Uncharacterized protein KIAA1797	0	1.00	1	1.9E-02	1	7.3E-02	0	1.0E+00
Q5VX84	Poly (ADP-ribose) polymerase 1	0	1.00	7	1.0E+00	2	2.4E-03	5	1.4E-03
Q5VZ89	DENN domain-containing protein 4C	0	1.00	0	1.0E+00	1	5.0E-02	1	6.4E-02
Q63HN8	E3 ubiquitin-protein ligase RNF213	1	0.08	1	7.0E-02	0	1.0E+00	0	1.0E+00
Q63ZY6	Putative methyltransferase NSUN5C	0	1.00	0	1.0E+00	5	2.4E-06	0	1.0E+00
Q66LE6	Serine/threonine-protein phosphatase 2A 55 kDa regulatory subunit B delta isoform	0	1.00	0	1.0E+00	2	3.3E-04	1	1.9E-03
Q68CZ2	Tensin-3	0	1.00	0	1.0E+00	2	3.5E-03	0	1.0E+00
Q68DK2	Zinc finger FYVE domain-containing protein 26	0	1.00	0	1.0E+00	1	4.0E-02	1	1.4E-02
Q6DD88	Atlastin-3	5	0.00	0	1.0E+00	14	1.0E-04	0	1.0E+00
Q6DKI1	60S ribosomal protein L7-like 1	0	1.00	0	1.0E+00	20	7.4E-11	0	1.0E+00
Q6DN03	Putative histone H2B type 2-C	0	1.00	0	1.0E+00	0	1.0E+00	16	6.2E-12
Q6IPX4	RPS16 protein	0	1.00	7	2.1E-02	10	3.1E-02	7	1.0E+00
Q6IQ15	EEF1A1 protein	1057	0.00	706	7.1E-09	1341	6.2E-08	526	4.6E-12
Q6KC79	Nipped-B-like protein	0	1.00	4	3.7E-03	2	7.4E-02	0	1.0E+00
Q6L8Q7	2',5'-phosphodiesterase 12	0	1.00	0	1.0E+00	16	1.6E-05	0	1.0E+00
Q6NVY1	3-hydroxyisobutyryl-CoA hydrolase, mitochondrial	0	1.00	0	1.0E+00	5	1.9E-07	1	1.8E-03
Q6NXE6	Armadillo repeat-containing protein 6	0	1.00	1	1.9E-03	1	3.9E-03	0	1.0E+00
Q6P1J9	Parafibromin	0	1.00	0	1.0E+00	0	1.0E+00	2	5.6E-03
Q6P2E9	Enhancer of mRNA-decapping protein 4	20	0.00	15	7.1E-09	5	5.1E-03	0	1.0E+00
Q6P2Q9	Pre-mRNA-processing-splicing factor 8	9	0.00	2	2.2E-03	79	1.4E-19	14	1.9E-17
Q6PI48	Aspartate--tRNA ligase, mitochondrial	1	0.01	0	1.0E+00	22	3.9E-03	0	1.0E+00
Q6PKG0	La-related protein 1	0	1.00	0	1.0E+00	2	2.8E-04	0	1.0E+00
Q6PKH6	Dehydrogenase/reductase SDR family member 4-like 2	0	1.00	0	1.0E+00	0	1.0E+00	2	7.1E-03
Q6Q0C1	Solute carrier family 25 member 47	1	0.08	0	1.0E+00	1	4.6E-02	0	1.0E+00

Q6SJ93	Protein FAM111B	0	1.00	5	1.9E-03	1	3.6E-02	0	1.0E+00
Q6UB35	Monofunctional C1-tetrahydrofolate synthase, mitochondrial	1	0.07	0	1.0E+00	4	6.4E-02	0	1.0E+00
Q6W4X9	Mucin-6	0	1.00	0	1.0E+00	1	8.6E-02	1	3.9E-03
Q6YHK3	CD109 antigen	0	1.00	9	1.9E-03	1	4.7E-02	0	1.0E+00
Q6YN16	Hydroxysteroid dehydrogenase-like protein 2	5	0.00	0	1.0E+00	0	1.0E+00	0	1.0E+00
Q6ZMT4	Lysine-specific demethylase 7	0	1.00	1	8.9E-02	1	4.8E-02	0	1.0E+00
Q6ZMW3	Echinoderm microtubule-associated protein-like 6	3	0.00	1	4.1E-02	3	2.6E-03	0	1.0E+00
Q6ZS81	WD repeat- and FYVE domain-containing protein 4	1	0.06	0	1.0E+00	1	6.8E-02	0	1.0E+00
Q709C8	Vacuolar protein sorting-associated protein 13C	0	1.00	0	1.0E+00	3	1.1E-03	0	1.0E+00
Q70J99	Protein unc-13 homolog D	0	1.00	0	1.0E+00	2	2.8E-04	0	1.0E+00
Q70UQ0	Inhibitor of nuclear factor kappa-B kinase-interacting protein	0	1.00	0	1.0E+00	0	1.0E+00	6	8.9E-10
Q71DI3	Histone H3.2	80	0.00	10	1.9E-03	347	3.9E-03	105	3.1E-06
Q71SY5	Mediator of RNA polymerase II transcription subunit 25	0	1.00	0	1.0E+00	0	1.0E+00	2	2.9E-03
Q71U36	Tubulin alpha-1A chain	446	0.00	301	1.9E-03	363	3.9E-03	195	1.8E-03
Q76N32	68 kDa	0	1.00	1	6.5E-02	0	1.0E+00	1	8.6E-02
Q7KZF4	Staphylococcal nuclease domain-containing protein 1	96	1.00	65	1.0E+00	211	9.2E-04	136	1.0E+00
Q7L014	Probable ATP-dependent RNA helicase DDX46	10	0.00	4	1.9E-03	12	3.9E-03	2	1.8E-03
Q7L2H7	Eukaryotic translation initiation factor 3 subunit M	0	1.00	0	1.0E+00	1	3.9E-03	15	6.2E-17
Q7L3H5	LIM domain kinase 2	1	0.07	0	1.0E+00	0	1.0E+00	9	2.7E-05
Q7L8L6	FAST kinase domain-containing protein 5	0	1.00	0	1.0E+00	0	1.0E+00	2	5.4E-03
Q7RTS1	Class A basic helix-loop-helix protein 15	0	1.00	0	1.0E+00	0	1.0E+00	3	2.1E-06
Q7Z2T5	TRMT1-like protein	0	1.00	0	1.0E+00	14	2.3E-13	0	1.0E+00
Q7Z2Y8	Interferon-induced very large GTPase 1	0	1.00	0	1.0E+00	3	7.8E-03	0	1.0E+00
Q7Z410	Transmembrane protease serine 9	1	0.07	2	3.9E-03	0	1.0E+00	0	1.0E+00
Q7Z4W1	L-xylulose reductase	3	0.00	6	1.9E-03	22	3.9E-03	6	3.1E-06
Q7Z589	Protein EMSY	0	1.00	0	1.0E+00	3	2.4E-03	0	1.0E+00
Q7Z5P9	Mucin-19	2	0.01	0	1.0E+00	0	1.0E+00	0	1.0E+00
Q7Z6L1	Tectonin beta-propeller repeat-containing protein 1	0	1.00	0	1.0E+00	1	4.3E-02	3	2.7E-02
Q7Z6Z7	E3 ubiquitin-protein ligase HUWE1	8	0.00	0	1.0E+00	25	1.8E-04	1	1.8E-03
Q7Z794	Keratin, type II cytoskeletal 1b	8	0.07	0	1.0E+00	2	4.4E-02	0	1.0E+00
Q7Z7G8	Vacuolar protein sorting-associated protein 13B	0	1.00	1	5.9E-02	1	2.4E-02	0	1.0E+00
Q7Z7H5	Transmembrane emp24 domain-containing protein 4	26	0.00	1	1.0E+00	0	1.0E+00	2	1.8E-03
Q7Z7H8	39S ribosomal protein L10, mitochondrial	0	1.00	6	1.9E-03	7	3.9E-03	0	1.0E+00
Q86SQ4	G-protein coupled receptor 126	0	1.00	0	1.0E+00	1	2.7E-02	1	6.3E-02
Q86TW2	Uncharacterized aarF domain-	10	0.00	0	1.0E+00	1	8.1E-02	0	1.0E+00

	containing protein kinase 1								
Q86U38	Pumilio domain-containing protein C14orf21	2	0.00	1	6.3E-02	19	1.1E-06	0	1.0E+00
Q86U86	Protein polybromo-1	0	1.00	0	1.0E+00	1	4.2E-02	1	9.5E-02
Q86UL8	Membrane-associated guanylate kinase, WW and PDZ domain-containing protein 2	0	1.00	1	6.2E-02	1	8.4E-02	0	1.0E+00
Q86UQ4	ATP-binding cassette sub-family A member 13	1	0.05	0	1.0E+00	2	6.5E-03	1	7.1E-02
Q86US8	Telomerase-binding protein EST1A	0	1.00	0	1.0E+00	2	3.1E-03	0	1.0E+00
Q86UY0	TXNDC5 protein	3	0.00	0	1.0E+00	0	1.0E+00	45	1.1E-27
Q86V81	THO complex subunit 4	0	1.00	0	1.0E+00	0	1.0E+00	34	5.9E-28
Q86VL8	Multidrug and toxin extrusion protein 2	1	0.06	0	1.0E+00	1	2.8E-02	0	1.0E+00
Q86VN1	Vacuolar protein-sorting-associated protein 36	1	0.08	0	1.0E+00	0	1.0E+00	1	9.2E-02
Q86VP6	Cullin-associated NEDD8-dissociated protein 1	6	0.00	29	5.0E-17	33	1.6E-05	14	3.4E-13
Q86VU5	Catechol O-methyltransferase domain-containing protein 1	0	1.00	0	1.0E+00	42	5.0E-07	0	1.0E+00
Q86VV8	Rotatin	1	0.07	0	1.0E+00	0	1.0E+00	1	4.7E-02
Q86WJ1	Chromodomain-helicase-DNA-binding protein 1-like	0	1.00	1	9.2E-02	1	6.4E-02	0	1.0E+00
Q86X76	Nitrilase homolog 1	0	1.00	7	6.2E-09	2	3.9E-03	0	1.0E+00
Q86XI2	Condensin-2 complex subunit G2	1	0.04	0	1.0E+00	4	3.9E-03	0	1.0E+00
Q86Y38	Xylosyltransferase 1	0	1.00	1	7.4E-02	0	1.0E+00	2	5.4E-04
Q8IVF4	Dynein heavy chain 10, axonemal	0	1.00	1	2.7E-02	0	1.0E+00	1	5.9E-02
Q8IW35	97 kDa	2	0.00	0	1.0E+00	0	1.0E+00	0	1.0E+00
Q8IWW7	E3 ubiquitin-protein ligase UBR1	0	1.00	0	1.0E+00	1	4.8E-02	1	8.4E-02
Q8IXI1	Mitochondrial Rho GTPase 2	0	1.00	0	1.0E+00	2	1.2E-03	0	1.0E+00
Q8IY67	Ribonucleoprotein PTB-binding 1	0	1.00	1	2.1E-03	13	3.9E-03	1	3.4E-03
Q8IY81	Putative rRNA methyltransferase 3	0	1.00	0	1.0E+00	16	3.9E-03	21	7.1E-23
Q8IYD1	Eukaryotic peptide chain release factor GTP-binding subunit ERF3B	8	1.00	13	1.0E+00	2	1.0E+00	12	2.2E-06
Q8IZ13	Transposon-derived Buster3 transposase-like protein	0	1.00	0	1.0E+00	0	1.0E+00	2	2.3E-03
Q8IZA0	Dyslexia-associated protein KIAA0319-like protein	2	0.01	0	1.0E+00	0	1.0E+00	0	1.0E+00
Q8IZC6	Collagen alpha-1(XXVII) chain	0	1.00	0	1.0E+00	1	6.4E-02	1	7.1E-02
Q8IZD4	mRNA-decapping enzyme 1B	0	1.00	1	6.2E-02	0	1.0E+00	1	8.7E-02
Q8IZD9	Dedicator of cytokinesis protein 3	0	1.00	0	1.0E+00	1	8.5E-02	1	9.6E-02
Q8IZT6	Abnormal spindle-like microcephaly-associated protein	2	0.01	0	1.0E+00	0	1.0E+00	0	1.0E+00
Q8N163	Protein KIAA1967	5	0.00	1	9.3E-02	1	3.9E-03	1	3.3E-03
Q8N1F7	Nuclear pore complex protein Nup93	0	1.00	4	1.9E-03	8	6.2E-08	2	1.8E-03
Q8N1G4	Leucine-rich repeat-containing protein 47	1	0.07	5	3.7E-06	6	6.6E-03	0	1.0E+00
Q8N1V2	WD repeat-containing protein 16	0	1.00	0	1.0E+00	1	1.9E-02	1	2.4E-02
Q8N2C3	DEP domain-containing protein 4	5	0.00	0	1.0E+00	0	1.0E+00	0	1.0E+00
Q8N2C7	Protein unc-80 homolog	1	0.08	0	1.0E+00	1	6.6E-02	0	1.0E+00

Q8N2K0	Monoacylglycerol lipase ABHD12	3	0.00	1	1.9E-03	25	2.0E-11	1	1.8E-03
Q8N3D4	EH domain-binding protein 1-like protein 1	2	0.00	2	1.9E-03	1	7.0E-02	1	7.8E-02
Q8N543	2-oxoglutarate and iron-dependent oxygenase domain-containing protein 1	0	1.00	0	1.0E+00	7	1.3E-08	1	1.7E-02
Q8N5H7	SH2 domain-containing protein 3C	0	1.00	1	3.0E-02	0	1.0E+00	1	8.9E-02
Q8N5Z0	Kynurenine/alpha-aminoadipate aminotransferase, mitochondrial	0	1.00	0	1.0E+00	0	1.0E+00	8	3.3E-12
Q8N766	Uncharacterized protein KIAA0090	3	0.00	2	1.3E-04	17	1.6E-05	0	1.0E+00
Q8N8A6	ATP-dependent RNA helicase DDX51	0	1.00	0	1.0E+00	20	1.6E-05	0	1.0E+00
Q8N944	APC membrane recruitment protein 3	0	1.00	1	4.4E-02	0	1.0E+00	1	3.3E-02
Q8NBF2	NHL repeat-containing protein 2	0	1.00	0	1.0E+00	0	1.0E+00	4	3.5E-06
Q8NBX0	Saccharopine dehydrogenase-like oxidoreductase	0	1.00	0	1.0E+00	32	5.3E-07	0	1.0E+00
Q8NC51	Plasminogen activator inhibitor 1 RNA-binding protein	0	1.00	7	1.9E-03	0	1.0E+00	21	1.8E-18
Q8NDW8	Tetratricopeptide repeat protein 21A	0	1.00	0	1.0E+00	0	1.0E+00	3	3.9E-03
Q8NE71	ATP-binding cassette sub-family F member 1	0	1.00	0	1.0E+00	1	2.2E-02	3	1.8E-03
Q8NEZ4	Histone-lysine N-methyltransferase MLL3	1	0.01	1	5.6E-02	1	3.6E-02	0	1.0E+00
Q8NF50	Dedicator of cytokinesis protein 8	0	1.00	0	1.0E+00	1	3.6E-02	1	1.8E-02
Q8NF91	Nesprin-1	0	1.00	0	1.0E+00	1	3.1E-02	2	3.4E-03
Q8NFF5	FAD synthase	1	0.07	15	3.3E-16	2	3.9E-03	0	1.0E+00
Q8NFP9	Neurobeachin	1	0.03	0	1.0E+00	1	4.5E-02	0	1.0E+00
Q8NFT2	Metalloreductase STEAP2	0	1.00	0	1.0E+00	9	6.3E-11	0	1.0E+00
Q8NFV4	Abhydrolase domain-containing protein 11	2	0.00	3	1.9E-03	31	2.7E-12	14	1.3E-13
Q8TAP6	76 kDa	1	0.07	0	1.0E+00	0	1.0E+00	1	7.5E-02
Q8TCJ2	Dolichyl-diphosphooligosaccharide--protein glycosyltransferase subunit STT3B	6	0.00	0	1.0E+00	21	6.9E-05	0	1.0E+00
Q8TCT9	Minor histocompatibility antigen H13	14	0.00	36	2.6E-14	15	2.8E-08	0	1.0E+00
Q8TD43	Transient receptor potential cation channel subfamily M member 4	1	0.04	1	4.6E-02	0	1.0E+00	0	1.0E+00
Q8TD47	40S ribosomal protein S4, Y isoform 2	0	1.00	1	1.0E+00	2	5.1E-02	4	9.3E-06
Q8TD57	Dynein heavy chain 3, axonemal	0	1.00	0	1.0E+00	2	1.9E-03	0	1.0E+00
Q8TDD1	ATP-dependent RNA helicase DDX54	0	1.00	1	2.2E-03	2	3.9E-03	0	1.0E+00
Q8TDW7	Protocadherin Fat 3	0	1.00	0	1.0E+00	1	9.1E-02	3	6.6E-05
Q8TE73	Dynein heavy chain 5, axonemal	0	1.00	0	1.0E+00	2	1.2E-03	0	1.0E+00
Q8TEM1	Nuclear pore membrane glycoprotein 210	34	0.00	27	3.0E-14	98	3.0E-33	3	2.7E-08
Q8TEQ6	Gem-associated protein 5	0	1.00	1	1.9E-03	7	3.9E-03	0	1.0E+00
Q8TEX9	Importin-4	6	0.00	16	1.4E-11	11	6.2E-08	9	2.8E-07
Q8WTT2	Nucleolar complex protein 3 homolog	0	1.00	1	1.6E-02	3	6.0E-03	0	1.0E+00

Q8WU39	Plasma cell-induced resident endoplasmic reticulum protein	0	1.00	0	1.0E+00	0	1.0E+00	84	3.1E-24
Q8WU90	Zinc finger CCCH domain-containing protein 15	0	1.00	0	1.0E+00	0	1.0E+00	4	1.5E-05
Q8WUM0	Nuclear pore complex protein Nup133	2	0.02	0	1.0E+00	0	1.0E+00	1	1.8E-03
Q8WUM4	Programmed cell death 6-interacting protein	1	0.04	22	8.4E-21	11	1.6E-05	6	3.1E-06
Q8WVM8	Sec1 family domain-containing protein 1	0	1.00	0	1.0E+00	36	2.5E-21	0	1.0E+00
Q8WWN8	Arf-GAP with Rho-GAP domain, ANK repeat and PH domain-containing protein 3	1	0.06	1	8.3E-02	0	1.0E+00	0	1.0E+00
Q8WZ42	Titin	2	0.00	2	2.3E-04	82	2.9E-04	4	6.5E-06
Q92508	Piezo-type mechanosensitive ion channel component 1	0	1.00	0	1.0E+00	3	1.3E-03	0	1.0E+00
Q92538	Golgi-specific brefeldin A-resistance guanine nucleotide exchange factor 1	0	1.00	0	1.0E+00	2	5.3E-03	0	1.0E+00
Q92545	Transmembrane protein 131	1	0.02	1	2.6E-02	0	1.0E+00	0	1.0E+00
Q92552	28S ribosomal protein S27, mitochondrial	0	1.00	0	1.0E+00	10	3.9E-03	1	1.4E-02
Q92608	Dedicator of cytokinesis protein 2	1	0.09	0	1.0E+00	10	3.0E-04	0	1.0E+00
Q92616	Translational activator GCN1	71	0.00	121	9.1E-39	183	4.1E-34	19	3.6E-14
Q92618	Zinc finger protein 516	1	0.06	0	1.0E+00	1	6.1E-02	1	5.7E-02
Q92620	Pre-mRNA-splicing factor ATP-dependent RNA helicase PRP16	1	0.07	3	7.3E-02	3	3.9E-03	0	1.0E+00
Q92621	Nuclear pore complex protein Nup205	12	0.00	0	1.0E+00	24	2.0E-11	1	4.0E-02
Q92630	Dual specificity tyrosine-phosphorylation-regulated kinase 2	0	1.00	0	1.0E+00	2	1.3E-03	0	1.0E+00
Q92797	Symplekin	3	0.00	0	1.0E+00	0	1.0E+00	0	1.0E+00
Q92820	Gamma-glutamyl hydrolase	0	1.00	1	1.1E-02	1	1.4E-02	5	1.2E-07
Q92839	Hyaluronan synthase 1	0	1.00	0	1.0E+00	9	3.8E-04	0	1.0E+00
Q92841	Probable ATP-dependent RNA helicase DDX17	44	0.00	37	2.5E-21	70	3.2E-05	31	7.2E-13
Q92896	Golgi apparatus protein 1	1	0.01	0	1.0E+00	27	4.0E-07	0	1.0E+00
Q92945	Far upstream element-binding protein 2	2	0.00	6	1.9E-03	3	3.9E-03	53	2.2E-28
Q92973	Transportin-1	32	0.00	5	1.0E+00	53	2.2E-12	11	1.0E-08
Q92974	Rho guanine nucleotide exchange factor 2	6	0.00	10	1.9E-03	15	1.3E-06	3	1.8E-03
Q92979	Ribosomal RNA small subunit methyltransferase NEP1	5	0.00	0	1.0E+00	4	1.6E-05	0	1.0E+00
Q93009	Ubiquitin carboxyl-terminal hydrolase 7	11	0.00	0	1.0E+00	14	1.6E-05	17	2.1E-20
Q93077	Histone H2A type 1-C	10	1.00	66	1.9E-03	20	3.9E-03	166	2.0E-09
Q969J3	Loss of heterozygosity 12 chromosomal region 1 protein	1	0.03	0	1.0E+00	0	1.0E+00	1	7.1E-02
Q969V3	Nicalin	0	1.00	0	1.0E+00	11	1.3E-04	0	1.0E+00
Q969X5	Endoplasmic reticulum-Golgi intermediate compartment protein 1	4	0.00	13	5.8E-08	14	3.9E-03	0	1.0E+00
Q969Z0	Protein TBRG4	2	0.00	0	1.0E+00	18	1.6E-05	0	1.0E+00

Q96A23	Copine-4	3	0.00	0	1.0E+00	1	5.8E-02	0	1.0E+00
Q96A33	Coiled-coil domain-containing protein 47	19	0.00	0	1.0E+00	2	3.9E-03	14	3.1E-06
Q96A72	Protein mago nashi homolog 2	0	1.00	0	1.0E+00	14	3.9E-03	10	3.5E-09
Q96AB3	Isochorismatase domain-containing protein 2, mitochondrial	6	0.00	3	2.0E-03	41	3.6E-08	2	1.8E-03
Q96AE4	Far upstream element-binding protein 1	0	1.00	0	1.0E+00	21	1.6E-05	20	8.6E-24
Q96AG4	Leucine-rich repeat-containing protein 59	15	0.00	14	3.5E-08	1	5.1E-02	20	3.1E-13
Q96E39	RNA binding motif protein, X-linked-like-1	0	1.00	0	1.0E+00	0	1.0E+00	12	3.8E-05
Q96EY1	DnaJ homolog subfamily A member 3, mitochondrial	3	0.00	0	1.0E+00	21	1.5E-15	2	7.0E-02
Q96FW1	Ubiquitin thioesterase OTUB1	0	1.00	0	1.0E+00	5	1.5E-04	2	1.8E-03
Q96GD4	Aurora kinase B	0	1.00	0	1.0E+00	8	4.4E-05	1	1.8E-03
Q96GQ5	UPF0420 protein C16orf58	3	0.00	0	1.0E+00	0	1.0E+00	0	1.0E+00
Q96GR2	Long-chain-fatty-acid--CoA ligase ACSBG1	1	0.08	0	1.0E+00	1	3.3E-02	0	1.0E+00
Q96HD9	Aspartoacylase-2	0	1.00	1	7.9E-02	0	1.0E+00	1	5.5E-02
Q96IU4	Abhydrolase domain-containing protein 14B	0	1.00	0	1.0E+00	19	1.8E-03	5	3.3E-02
Q96JF0	Beta-galactoside alpha-2,6-sialyltransferase 2	0	1.00	0	1.0E+00	1	3.9E-02	1	5.1E-02
Q96JH8	Ras-associating and dilute domain-containing protein	0	1.00	0	1.0E+00	1	8.6E-02	2	5.6E-04
Q96JQ0	Protocadherin-16	0	1.00	0	1.0E+00	2	6.3E-03	0	1.0E+00
Q96KA5	Cleft lip and palate transmembrane protein 1-like protein	9	0.00	0	1.0E+00	6	3.8E-07	1	3.1E-03
Q96KP4	Cytosolic non-specific dipeptidase	0	1.00	2	3.4E-03	0	1.0E+00	40	1.7E-28
Q96KS9	Protein FAM167A	1	0.08	0	1.0E+00	1	4.6E-02	0	1.0E+00
Q96M86	Dynein heavy chain domain-containing protein 1	1	0.03	0	1.0E+00	1	9.5E-02	0	1.0E+00
Q96MI6	Protein phosphatase 1M	0	1.00	0	1.0E+00	1	2.1E-02	1	8.9E-02
Q96NS5	Ankyrin repeat and SOCS box protein 16	2	0.00	0	1.0E+00	0	1.0E+00	0	1.0E+00
Q96NU0	Contactin-associated protein-like 3B	0	1.00	0	1.0E+00	1	7.7E-02	1	7.9E-02
Q96P11	Putative methyltransferase NSUN5	0	1.00	0	1.0E+00	8	1.8E-09	0	1.0E+00
Q96P31	Fc receptor-like protein 3	0	1.00	0	1.0E+00	2	3.6E-03	0	1.0E+00
Q96P70	Importin-9	3	0.00	16	3.7E-06	1	4.9E-02	0	1.0E+00
Q96PK6	RNA-binding protein 14	11	0.00	17	3.7E-06	0	1.0E+00	13	3.1E-06
Q96Q15	Serine/threonine-protein kinase SMG1	4	0.03	2	4.7E-02	1	2.6E-02	9	2.0E-04
Q96QK1	Vacuolar protein sorting-associated protein 35	0	1.00	0	1.0E+00	2	3.2E-05	0	1.0E+00
Q96QV6	Histone H2A type 1-A	10	1.00	79	4.2E-06	18	1.0E+00	157	1.1E-10
Q96RG2	PAS domain-containing serine/threonine-protein kinase	0	1.00	1	5.2E-02	1	4.5E-02	0	1.0E+00
Q96RP9	Elongation factor G, mitochondrial	1	0.04	19	3.7E-06	13	1.6E-05	0	1.0E+00
Q96RR1	Twinkle protein, mitochondrial	0	1.00	0	1.0E+00	1	3.1E-02	1	8.9E-02
Q96RT1	Protein LAP2	1	0.01	0	1.0E+00	1	5.8E-02	0	1.0E+00
Q96RW7	Hemicentin-1	1	0.09	0	1.0E+00	1	5.9E-02	0	1.0E+00

Q96RY7	Intraflagellar transport protein 140 homolog	0	1.00	0	1.0E+00	2	3.3E-03	0	1.0E+00
Q96S52	GPI transamidase component PIG-S	7	0.00	11	3.7E-06	23	2.4E-09	0	1.0E+00
Q96SQ9	Cytochrome P450 2S1	1	0.09	0	1.0E+00	1	7.0E-02	0	1.0E+00
Q96T76	MMS19 nucleotide excision repair protein homolog	0	1.00	0	1.0E+00	4	1.6E-05	1	5.7E-02
Q96TC7	Regulator of microtubule dynamics protein 3	3	0.00	0	1.0E+00	1	4.0E-02	0	1.0E+00
Q99460	26S proteasome non-ATPase regulatory subunit 1	0	1.00	1	6.4E-02	4	3.9E-03	3	2.6E-03
Q99497	Protein DJ-1	0	1.00	0	1.0E+00	0	1.0E+00	28	3.0E-13
Q99661	Kinesin-like protein KIF2C	1	0.00	3	1.9E-03	1	2.9E-02	0	1.0E+00
Q99714	3-hydroxyacyl-CoA dehydrogenase type-2	76	0.00	103	3.1E-26	97	7.8E-14	50	1.5E-24
Q99729	Heterogeneous nuclear ribonucleoprotein A/B	0	1.00	0	1.0E+00	0	1.0E+00	33	6.0E-20
Q99798	Aconitate hydratase, mitochondrial	0	1.00	8	3.7E-06	40	1.5E-11	2	1.8E-03
Q99829	Copine-1	7	0.00	11	2.4E-07	0	1.0E+00	0	1.0E+00
Q99832	T-complex protein 1 subunit eta	41	0.00	53	1.4E-11	76	5.5E-06	48	6.5E-12
Q99996	A-kinase anchor protein 9	2	0.07	0	1.0E+00	1	8.8E-02	1	6.4E-02
Q9BPX3	Condensin complex subunit 3	7	0.00	0	1.0E+00	20	1.6E-05	0	1.0E+00
Q9BQ52	Zinc phosphodiesterase ELAC protein 2	0	1.00	0	1.0E+00	17	7.4E-05	0	1.0E+00
Q9BQ69	MACRO domain-containing protein 1	0	1.00	1	9.5E-02	42	4.4E-12	2	1.9E-03
Q9BQG0	Myb-binding protein 1A	23	0.00	3	1.9E-03	89	4.7E-34	3	3.1E-06
Q9BS26	Endoplasmic reticulum resident protein 44	0	1.00	0	1.0E+00	0	1.0E+00	3	1.4E-06
Q9BSJ8	Extended synaptotagmin-1	5	0.00	9	1.0E-08	1	4.0E-03	0	1.0E+00
Q9BT22	Chitobiosyldiphosphodolichol beta-mannosyltransferase	4	0.00	1	1.9E-03	1	3.2E-02	0	1.0E+00
Q9BTE6	Alanyl-tRNA editing protein Aarsd1	0	1.00	0	1.0E+00	8	2.9E-04	0	1.0E+00
Q9BTT0	Acidic leucine-rich nuclear phosphoprotein 32 family member E	1	0.00	0	1.0E+00	0	1.0E+00	33	5.2E-16
Q9BTW9	Tubulin-specific chaperone D	3	0.00	1	1.7E-02	2	2.6E-03	0	1.0E+00
Q9BUF5	Tubulin beta-6 chain	94	0.00	146	1.4E-07	99	6.0E-07	42	9.5E-08
Q9BUJ2	Heterogeneous nuclear ribonucleoprotein U-like protein 1	5	0.00	0	1.0E+00	0	1.0E+00	2	5.1E-02
Q9BUN8	Derlin-1	0	1.00	5	2.0E-03	2	4.6E-03	0	1.0E+00
Q9BV38	WD repeat-containing protein 18	1	0.07	0	1.0E+00	23	1.3E-06	0	1.0E+00
Q9BVA1	Tubulin beta-2B chain	363	0.00	441	2.7E-14	316	3.9E-03	205	3.1E-06
Q9BVI4	Nucleolar complex protein 4 homolog	1	0.00	0	1.0E+00	1	3.4E-02	0	1.0E+00
Q9BVK6	Transmembrane emp24 domain-containing protein 9	21	0.00	5	2.6E-05	17	3.9E-03	4	1.8E-03
Q9BW19	Kinesin-like protein KIFC1	0	1.00	0	1.0E+00	1	6.8E-02	1	3.0E-03
Q9BW27	Nuclear pore complex protein Nup85	0	1.00	1	8.3E-02	9	3.5E-04	0	1.0E+00
Q9BWR0	Intercellular adhesion molecule 4 (Landsteiner-Wiener blood group)	0	1.00	1	5.4E-02	1	6.7E-02	0	1.0E+00
Q9BXL6	Caspase recruitment domain-	0	1.00	0	1.0E+00	1	7.5E-02	1	1.3E-02

	containing protein 14								
Q9BXS5	AP-1 complex subunit mu-1	0	1.00	0	1.0E+00	11	3.9E-03	1	6.0E-02
Q9BY44	Eukaryotic translation initiation factor 2A	0	1.00	0	1.0E+00	11	8.6E-11	0	1.0E+00
Q9BY77	Polymerase delta-interacting protein 3	0	1.00	0	1.0E+00	0	1.0E+00	7	4.2E-11
Q9BZA8	Protocadherin-11 Y-linked	1	0.06	1	2.8E-02	0	1.0E+00	0	1.0E+00
Q9BZB8	Cytoplasmic polyadenylation element-binding protein 1	0	1.00	1	1.6E-02	1	9.7E-02	0	1.0E+00
Q9BZE4	Nucleolar GTP-binding protein 1	9	0.00	0	1.0E+00	22	3.9E-03	15	2.7E-20
Q9BZJ0	Crooked neck-like protein 1	0	1.00	0	1.0E+00	1	3.1E-02	1	3.7E-02
Q9BZX2	Uridine-cytidine kinase 2	0	1.00	0	1.0E+00	23	6.5E-07	0	1.0E+00
Q9C0H5	Rho GTPase-activating protein 39	0	1.00	0	1.0E+00	1	3.7E-02	1	3.1E-02
Q9GZS3	WD repeat-containing protein 61	0	1.00	0	1.0E+00	28	3.9E-03	6	3.5E-09
Q9GZV4	Eukaryotic translation initiation factor 5A-2	4	1.00	0	1.0E+00	45	1.0E+00	16	1.6E-03
Q9H078	Caseinolytic peptidase B protein homolog	1	0.02	0	1.0E+00	1	8.4E-02	0	1.0E+00
Q9H0A0	N-acetyltransferase 10	7	0.00	5	1.5E-06	22	3.2E-16	4	4.2E-05
Q9H0L4	Cleavage stimulation factor subunit 2 tau variant	0	1.00	0	1.0E+00	0	1.0E+00	13	4.6E-11
Q9H0P0	Cytosolic 5'-nucleotidase 3	3	0.00	0	1.0E+00	0	1.0E+00	0	1.0E+00
Q9H0U4	Ras-related protein Rab-1B	16	0.00	10	3.0E-05	0	1.0E+00	2	1.8E-03
Q9H2A9	Carbohydrate sulfotransferase 8	1	0.08	0	1.0E+00	0	1.0E+00	1	1.1E-02
Q9H2U1	Probable ATP-dependent RNA helicase DHX36	0	1.00	0	1.0E+00	4	3.9E-03	2	3.5E-02
Q9H324	A disintegrin and metalloproteinase with thrombospondin motifs 10	0	1.00	0	1.0E+00	2	5.5E-02	1	7.1E-02
Q9H361	Polyadenylate-binding protein 3	5	1.00	2	1.0E+00	7	3.1E-02	14	6.1E-07
Q9H3K6	BolA-like protein 2	0	1.00	0	1.0E+00	15	3.9E-03	7	3.1E-06
Q9H3U1	Protein unc-45 homolog A	5	0.00	6	1.9E-03	8	1.6E-05	0	1.0E+00
Q9H400	Lck-interacting transmembrane adapter 1	1	0.04	0	1.0E+00	0	1.0E+00	1	8.2E-02
Q9H4A4	Aminopeptidase B	0	1.00	16	4.9E-10	0	1.0E+00	0	1.0E+00
Q9H4I3	TraB domain-containing protein	3	0.00	2	3.3E-02	14	3.5E-11	0	1.0E+00
Q9H4L7	SWI/SNF-related matrix-associated actin-dependent regulator of chromatin subfamily A containing DEAD/H box 1	1	0.06	0	1.0E+00	0	1.0E+00	2	5.1E-03
Q9H4M9	EH domain-containing protein 1	0	1.00	20	4.5E-11	2	3.9E-03	0	1.0E+00
Q9H4S2	GS homeobox 1	0	1.00	0	1.0E+00	9	1.3E-06	0	1.0E+00
Q9H568	Actin-like protein 8	0	1.00	0	1.0E+00	46	7.2E-07	9	1.3E-11
Q9H583	HEAT repeat-containing protein 1	10	0.00	0	1.0E+00	89	2.1E-14	8	1.8E-11
Q9H6R4	Nucleolar protein 6	0	1.00	0	1.0E+00	41	8.9E-17	0	1.0E+00
Q9H6S0	Probable ATP-dependent RNA helicase YTHDC2	2	0.00	0	1.0E+00	0	1.0E+00	1	8.6E-02
Q9H7H0	Methyltransferase-like protein 17, mitochondrial	0	1.00	3	1.7E-04	0	1.0E+00	0	1.0E+00
Q9H7M6	Zinc finger SWIM domain-containing protein 4	1	0.07	0	1.0E+00	1	5.3E-02	1	5.8E-02
Q9H7Z7	Prostaglandin E synthase 2	4	0.00	4	1.9E-03	13	2.4E-08	0	1.0E+00
Q9H845	Acyl-CoA dehydrogenase family	0	1.00	0	1.0E+00	1	3.1E-02	1	7.7E-03

	member 9, mitochondrial								
Q9H8H0	Nucleolar protein 11	1	0.00	0	1.0E+00	1	6.3E-02	0	1.0E+00
Q9H8H3	Methyltransferase-like protein 7A	18	0.00	9	1.9E-03	24	3.9E-03	7	3.1E-06
Q9H9A6	Leucine-rich repeat-containing protein 40	0	1.00	0	1.0E+00	2	8.7E-04	0	1.0E+00
Q9H9B4	Sideroflexin-1	6	0.00	6	1.9E-03	0	1.0E+00	0	1.0E+00
Q9H9P5	RING finger protein unkempt-like	2	0.00	0	1.0E+00	53	1.8E-16	22	6.8E-03
Q9HAV4	Exportin-5	5	0.00	0	1.0E+00	90	3.8E-30	15	3.1E-13
Q9HB71	Calcyclin-binding protein	10	0.00	0	1.0E+00	20	3.9E-03	7	7.5E-08
Q9HCC0	Methylcrotonoyl-CoA carboxylase beta chain, mitochondrial	0	1.00	0	1.0E+00	25	3.9E-03	9	5.4E-09
Q9HCL0	Protocadherin-18	1	0.10	0	1.0E+00	0	1.0E+00	1	1.6E-02
Q9HCS2	Cytochrome P450 4F12	0	1.00	3	3.8E-06	0	1.0E+00	0	1.0E+00
Q9HCU5	Prolactin regulatory element-binding protein	4	0.00	6	1.4E-09	0	1.0E+00	0	1.0E+00
Q9HD20	Probable cation-transporting ATPase 13A1	7	0.00	4	5.4E-05	7	2.9E-04	1	2.1E-02
Q9HDC9	Adipocyte plasma membrane-associated protein	15	0.00	15	9.3E-10	1	6.4E-03	0	1.0E+00
Q9NP73	UDP-N-acetylglucosamine transferase subunit ALG13 homolog	0	1.00	1	8.3E-02	1	5.9E-02	0	1.0E+00
Q9NP80	Calcium-independent phospholipase A2-gamma	0	1.00	0	1.0E+00	1	9.6E-02	1	5.0E-02
Q9NPY3	Complement component C1q receptor	0	1.00	1	5.0E-02	2	1.4E-02	0	1.0E+00
Q9NPZ5	Galactosylgalactosylxylosylprotein 3-beta-glucuronosyltransferase 2	0	1.00	0	1.0E+00	2	3.2E-03	0	1.0E+00
Q9NQ36	Signal peptide, CUB and EGF-like domain-containing protein 2	0	1.00	0	1.0E+00	0	1.0E+00	2	3.5E-03
Q9NQ39	Putative 40S ribosomal protein S10-like	0	1.00	7	3.7E-06	4	1.0E+00	8	6.7E-05
Q9NQC3	Reticulon-4	1	0.01	3	3.4E-03	0	1.0E+00	1	1.9E-03
Q9NQE9	Histidine triad nucleotide-binding protein 3	0	1.00	0	1.0E+00	1	5.3E-02	2	1.3E-02
Q9NQW7	Xaa-Pro aminopeptidase 1	1	0.00	0	1.0E+00	1	5.0E-02	0	1.0E+00
Q9NR30	Nucleolar RNA helicase 2	20	0.00	14	2.4E-11	13	9.0E-05	28	1.3E-25
Q9NR31	GTP-binding protein SAR1a	0	1.00	0	1.0E+00	5	3.4E-07	0	1.0E+00
Q9NR46	Endophilin-B2	0	1.00	0	1.0E+00	7	1.6E-05	2	1.8E-03
Q9NR56	Muscleblind-like protein 1	0	1.00	0	1.0E+00	14	3.9E-03	4	1.8E-03
Q9NRC6	Spectrin beta chain, brain 4	0	1.00	0	1.0E+00	0	1.0E+00	2	3.6E-03
Q9NRG9	Aladin	0	1.00	0	1.0E+00	42	1.6E-05	1	1.8E-03
Q9NRY5	Protein FAM114A2	0	1.00	0	1.0E+00	2	4.1E-03	0	1.0E+00
Q9NSA2	Potassium voltage-gated channel subfamily D member 1	0	1.00	0	1.0E+00	1	1.9E-02	1	9.0E-02
Q9NSD9	Phenylalanine--tRNA ligase beta subunit	2	0.00	0	1.0E+00	12	3.4E-05	5	3.4E-06
Q9NSE4	Isoleucine--tRNA ligase, mitochondrial	18	0.00	16	3.7E-06	19	1.8E-05	9	3.1E-06
Q9NTI5	Sister chromatid cohesion protein PDS5 homolog B	13	0.00	0	1.0E+00	2	4.6E-03	0	1.0E+00
Q9NTJ3	Structural maintenance of chromosomes protein 4	0	1.00	1	6.5E-02	2	3.9E-03	4	8.6E-06

Q9NTK5	Obg-like ATPase 1	5	0.00	8	1.9E-03	2	3.9E-03	7	7.8E-05
Q9NU22	Midasin	1	0.00	0	1.0E+00	5	2.6E-06	0	1.0E+00
Q9NUU7	ATP-dependent RNA helicase DDX19A	3	1.00	14	1.9E-03	17	1.0E+00	8	2.4E-06
Q9NVI1	Fanconi anemia group I protein	1	0.00	1	1.9E-03	19	3.9E-07	3	2.2E-03
Q9NVI7	ATPase family AAA domain-containing protein 3A	7	0.00	3	2.1E-03	56	4.9E-03	11	1.0E+00
Q9NVN8	Guanine nucleotide-binding protein-like 3-like protein	1	0.03	0	1.0E+00	1	8.0E-02	0	1.0E+00
Q9NVP1	ATP-dependent RNA helicase DDX18	19	0.00	22	1.4E-11	42	5.8E-09	18	9.4E-12
Q9NVP4	Double zinc ribbon and ankyrin repeat-containing protein 1	0	1.00	0	1.0E+00	1	4.0E-02	1	4.7E-02
Q9NXF1	Testis-expressed sequence 10 protein	1	0.02	0	1.0E+00	7	3.9E-03	0	1.0E+00
Q9NY12	H/ACA ribonucleoprotein complex subunit 1	0	1.00	0	1.0E+00	0	1.0E+00	3	2.8E-04
Q9NY93	Probable ATP-dependent RNA helicase DDX56	0	1.00	0	1.0E+00	33	2.5E-16	1	6.4E-02
Q9NYL4	Peptidyl-prolyl cis-trans isomerase FKBP11	12	0.03	5	2.0E-02	0	1.0E+00	4	1.0E+00
Q9NYQ8	Protocadherin Fat 2	0	1.00	1	6.3E-02	1	3.8E-02	0	1.0E+00
Q9NYU1	UDP-glucose:glycoprotein glucosyltransferase 2	0	1.00	1	6.6E-02	0	1.0E+00	2	1.1E-02
Q9NZ01	Trans-2,3-enoyl-CoA reductase	16	0.00	0	1.0E+00	18	4.1E-05	4	8.8E-06
Q9NZL9	Methionine adenosyltransferase 2 subunit beta	0	1.00	0	1.0E+00	0	1.0E+00	11	1.0E-14
Q9NZR2	Low-density lipoprotein receptor-related protein 1B	0	1.00	0	1.0E+00	1	5.6E-02	1	6.9E-02
Q9P0M9	39S ribosomal protein L27, mitochondrial	0	1.00	0	1.0E+00	1	8.5E-02	1	5.7E-02
Q9P1U1	Actin-related protein 3B	6	1.00	7	1.0E+00	36	4.6E-08	15	1.1E-06
Q9P258	Protein RCC2	2	0.00	0	1.0E+00	1	6.0E-03	0	1.0E+00
Q9P2D7	Dynein heavy chain 1, axonemal	1	0.08	0	1.0E+00	2	1.5E-03	0	1.0E+00
Q9P2I0	Cleavage and polyadenylation specificity factor subunit 2	0	1.00	0	1.0E+00	16	3.9E-03	5	3.8E-03
Q9P2N2	Rho GTPase-activating protein 28	1	0.04	0	1.0E+00	0	1.0E+00	1	6.8E-02
Q9P2P1	Protein NYNRIN	0	1.00	0	1.0E+00	7	4.2E-04	0	1.0E+00
Q9UBM7	7-dehydrocholesterol reductase	0	1.00	6	1.9E-03	4	3.9E-03	0	1.0E+00
Q9UBU9	Nuclear RNA export factor 1	0	1.00	0	1.0E+00	14	2.6E-10	0	1.0E+00
Q9UFH2	Dynein heavy chain 17, axonemal	1	0.08	1	8.1E-02	1	5.7E-02	0	1.0E+00
Q9UGL1	Lysine-specific demethylase 5B	1	0.02	0	1.0E+00	1	7.3E-02	0	1.0E+00
Q9UH17	Probable DNA dC->dU-editing enzyme APOBEC-3B	2	0.03	0	1.0E+00	6	3.9E-03	0	1.0E+00
Q9UHA3	Probable ribosome biogenesis protein RLP24	0	1.00	0	1.0E+00	0	1.0E+00	7	3.9E-06
Q9UHB9	Signal recognition particle 68 kDa protein	6	0.00	0	1.0E+00	0	1.0E+00	4	1.8E-03
Q9UHD1	Cysteine and histidine-rich domain-containing protein 1	1	0.00	0	1.0E+00	0	1.0E+00	3	1.8E-03
Q9UHX1	Poly(U)-binding-splicing factor PUF60	2	0.00	4	1.9E-03	0	1.0E+00	6	5.4E-09
Q9UI17	Dimethylglycine dehydrogenase, mitochondrial	1	0.09	0	1.0E+00	1	5.0E-02	0	1.0E+00

Q9UI26	Importin-11	5	0.00	0	1.0E+00	28	1.4E-14	0	1.0E+00
Q9UID3	Protein fat-free homolog	0	1.00	0	1.0E+00	6	3.4E-04	0	1.0E+00
Q9UIG0	Tyrosine-protein kinase BAZ1B	5	0.00	0	1.0E+00	0	1.0E+00	5	3.5E-06
Q9UIQ6	Leucyl-cystinyl aminopeptidase	1	0.00	1	5.4E-03	23	1.6E-05	0	1.0E+00
Q9UIR0	Butyrophilin-like protein 2	0	1.00	0	1.0E+00	2	3.4E-03	0	1.0E+00
Q9UJS0	Calcium-binding mitochondrial carrier protein Aralar2	9	0.05	24	4.6E-11	73	1.8E-20	5	8.5E-03
Q9UJZ1	Stomatin-like protein 2	26	0.00	11	3.7E-06	2	4.0E-03	13	2.0E-13
Q9UK45	U6 snRNA-associated Sm-like protein LSm7	0	1.00	0	1.0E+00	1	2.6E-02	7	1.8E-03
Q9UKD2	mRNA turnover protein 4 homolog	0	1.00	0	1.0E+00	0	1.0E+00	7	4.7E-09
Q9UKM9	RNA-binding protein Raly	13	0.00	0	1.0E+00	72	1.0E-15	5	1.8E-03
Q9UKN7	Unconventional myosin-XV	0	1.00	2	2.1E-03	0	1.0E+00	0	1.0E+00
Q9UKN8	General transcription factor 3C polypeptide 4	12	0.00	0	1.0E+00	41	1.9E-05	0	1.0E+00
Q9UKV3	Apoptotic chromatin condensation inducer in the nucleus	6	0.00	0	1.0E+00	0	1.0E+00	2	1.8E-03
Q9UKY7	Protein CDV3 homolog	0	1.00	0	1.0E+00	0	1.0E+00	21	7.3E-18
Q9UL46	Proteasome activator complex subunit 2	0	1.00	0	1.0E+00	12	8.5E-07	31	2.9E-17
Q9ULJ7	Ankyrin repeat domain-containing protein 50	1	0.03	0	1.0E+00	2	4.3E-04	0	1.0E+00
Q9ULL5	Proline-rich protein 12	2	0.00	0	1.0E+00	0	1.0E+00	0	1.0E+00
Q9ULT8	E3 ubiquitin-protein ligase HECTD1	1	0.09	1	6.2E-02	0	1.0E+00	0	1.0E+00
Q9ULV4	Coronin-1C	0	1.00	0	1.0E+00	0	1.0E+00	2	5.5E-05
Q9UM00	Transmembrane and coiled-coil domain-containing protein 1	17	0.00	6	1.9E-03	0	1.0E+00	0	1.0E+00
Q9UMR2	ATP-dependent RNA helicase DDX19B	3	1.00	13	1.0E+00	17	1.0E+00	7	1.9E-03
Q9UMS4	Pre-mRNA-processing factor 19	6	0.00	1	2.0E-03	21	1.6E-05	16	5.7E-18
Q9UNM6	26S proteasome non-ATPase regulatory subunit 13	3	0.00	0	1.0E+00	12	2.9E-12	13	7.3E-13
Q9UNQ2	Probable dimethyladenosine transferase	1	0.00	0	1.0E+00	17	1.6E-05	13	1.0E-13
Q9UNX4	WD repeat-containing protein 3	0	1.00	0	1.0E+00	2	9.7E-05	0	1.0E+00
Q9UPN3	Microtubule-actin cross-linking factor 1, isoforms 1/2/3/5	0	1.00	0	1.0E+00	3	3.0E-05	1	4.4E-02
Q9UQ35	Serine/arginine repetitive matrix protein 2	1	0.03	0	1.0E+00	0	1.0E+00	5	1.8E-03
Q9UQ80	Proliferation-associated protein 2G4	5	0.00	0	1.0E+00	0	1.0E+00	22	5.8E-18
Q9Y221	60S ribosome subunit biogenesis protein NIP7 homolog	0	1.00	0	1.0E+00	13	3.9E-03	4	1.7E-06
Q9Y230	RuvB-like 2	0	1.00	3	1.9E-03	8	1.0E-04	0	1.0E+00
Q9Y238	Deleted in lung and esophageal cancer protein 1	0	1.00	0	1.0E+00	1	6.2E-02	1	5.6E-02
Q9Y262	Eukaryotic translation initiation factor 3 subunit L	7	0.00	1	3.3E-02	6	6.3E-08	14	5.4E-09
Q9Y263	Phospholipase A-2-activating protein	0	1.00	4	1.9E-03	1	1.2E-02	0	1.0E+00
Q9Y266	Nuclear migration protein nudC	0	1.00	0	1.0E+00	0	1.0E+00	2	3.4E-03
Q9Y277	Voltage-dependent anion-selective channel protein 3	24	0.00	28	1.6E-11	29	3.9E-03	14	6.3E-11

Q9Y285	Phenylalanine--tRNA ligase alpha subunit	0	1.00	8	7.2E-09	17	2.3E-09	9	1.1E-11
Q9Y2Q3	Glutathione S-transferase kappa 1	1	0.00	2	1.9E-03	30	3.3E-12	0	1.0E+00
Q9Y2W1	Thyroid hormone receptor-associated protein 3	7	0.00	0	1.0E+00	5	4.6E-03	3	5.5E-06
Q9Y2X0	Mediator of RNA polymerase II transcription subunit 16	1	0.10	0	1.0E+00	0	1.0E+00	1	9.6E-02
Q9Y2X3	Nucleolar protein 58	69	0.00	5	1.2E-08	4	1.8E-05	47	1.3E-26
Q9Y2X7	ARF GTPase-activating protein GIT1	0	1.00	1	1.9E-03	2	6.4E-02	0	1.0E+00
Q9Y383	Putative RNA-binding protein Luc7-like 2	0	1.00	0	1.0E+00	0	1.0E+00	12	3.0E-04
Q9Y3I0	tRNA-splicing ligase RtcB homolog	0	1.00	0	1.0E+00	28	4.1E-15	10	3.1E-06
Q9Y3R0	Glutamate receptor-interacting protein 1	0	1.00	0	1.0E+00	2	2.7E-03	0	1.0E+00
Q9Y3T9	Nucleolar complex protein 2 homolog	9	0.00	3	1.9E-03	0	1.0E+00	0	1.0E+00
Q9Y3Z3	SAM domain and HD domain-containing protein 1	28	0.00	1	1.9E-03	17	3.9E-03	1	1.8E-03
Q9Y490	Talin-1	23	0.00	123	7.4E-79	41	2.6E-07	14	3.7E-15
Q9Y4A5	Transformation/transcription domain-associated protein	0	1.00	1	2.5E-02	4	1.7E-02	1	3.6E-02
Q9Y4C0	Neurexin-3-alpha	0	1.00	4	5.2E-05	0	1.0E+00	0	1.0E+00
Q9Y4E6	WD repeat-containing protein 7	0	1.00	0	1.0E+00	2	2.1E-03	0	1.0E+00
Q9Y4F9	Protein FAM65B	0	1.00	2	2.0E-02	1	9.6E-02	0	1.0E+00
Q9Y4G8	Rap guanine nucleotide exchange factor 2	0	1.00	0	1.0E+00	1	7.9E-02	1	5.2E-02
Q9Y4I1	Unconventional myosin-Va	11	0.00	10	7.1E-09	5	2.9E-04	1	8.7E-02
Q9Y4R8	Telomere length regulation protein TEL2 homolog	0	1.00	9	3.7E-06	0	1.0E+00	0	1.0E+00
Q9Y512	Sorting and assembly machinery component 50 homolog	1	0.02	5	1.9E-03	2	1.6E-05	1	7.0E-03
Q9Y536	Peptidyl-prolyl cis-trans isomerase A-like 4A/B/C	7	0.00	15	1.1E-02	36	4.8E-02	10	1.0E+00
Q9Y5B9	FACT complex subunit SPT16	26	0.00	0	1.0E+00	6	1.7E-04	24	2.1E-28
Q9Y5G0	Protocadherin gamma-B5	0	1.00	1	6.1E-02	1	1.6E-02	0	1.0E+00
Q9Y5K6	CD2-associated protein	0	1.00	0	1.0E+00	1	9.4E-02	5	1.5E-02
Q9Y5L0	Transportin-3	4	0.00	0	1.0E+00	18	1.1E-04	0	1.0E+00
Q9Y5M8	Signal recognition particle receptor subunit beta	0	1.00	1	1.7E-02	12	4.5E-09	3	1.8E-03
Q9Y5U8	Brain protein 44-like protein	0	1.00	0	1.0E+00	7	3.9E-06	0	1.0E+00
Q9Y5Y2	Cytosolic Fe-S cluster assembly factor NUBP2	5	0.00	9	2.7E-07	0	1.0E+00	0	1.0E+00
Q9Y678	Coatomer subunit gamma	5	0.00	14	3.4E-10	16	1.4E-12	25	1.7E-26
Q9Y6C9	Mitochondrial carrier homolog 2	14	0.00	14	4.4E-08	50	5.2E-16	1	8.6E-03
Q9Y6E2	Basic leucine zipper and W2 domain-containing protein 2	0	1.00	5	1.9E-03	2	3.1E-04	6	3.2E-09
Q9Y6M1	Insulin-like growth factor 2 mRNA-binding protein 2	8	0.00	8	5.7E-06	0	1.0E+00	0	1.0E+00
Q9Y6X6	Unconventional myosin-XVI	0	1.00	0	1.0E+00	2	8.0E-02	1	6.4E-02

Appendix Table 3. List of proteins identified from conventional (CON) and inflammatory (INF) MDSC and their spectral counts. $R_{sc} = \log_2$ ratio of abundance between inflammatory vs. conventional MDSC proteins.

Accession number	Description	# Spectra		Fisher p -value	R_{sc}
		CON	INF		
P11276	Fibronectin	0	53	1.76E-13	5.0
Q8K0E8	Fibrinogen beta chain	0	53	1.76E-13	5.0
Q8BWM3	MCG130173	0	31	3.50E-08	4.3
Q8VCM7	Fibrinogen gamma chain	1	53	4.15E-12	4.2
B2RV77	MCG130182, isoform CRA_a	0	22	5.12E-06	3.8
D3Z3G6	Mitogen-activated protein kinase 3	0	21	8.91E-06	3.7
Q9WVK4	EH domain-containing protein 1	0	18	4.69E-05	3.5
Q8CIZ8	von Willebrand factor	0	17	8.17E-05	3.4
P09411	Phosphoglycerate kinase 1	0	17	8.17E-05	3.4
Q497J0	MCG130175, isoform CRA_b	0	17	8.17E-05	3.4
Q9QZU3	Platelet glycoprotein V (Fragment)	1	28	2.38E-06	3.3
A2AE89	Glutathione S-transferase Mu 1 (Fragment)	0	15	2.47E-04	3.3
Q9R0P5	Destrin	0	11	2.27E-03	2.9
P20152	Vimentin	3	38	6.59E-07	2.8
Q9D023	Mitochondrial pyruvate carrier 2	0	10	3.94E-03	2.7
P17742	Peptidyl-prolyl cis-trans isomerase A	4	44	1.87E-07	2.7
Q61598	Rab GDP dissociation inhibitor beta	0	9	6.86E-03	2.6
P80314	T-complex protein 1 subunit beta	0	9	6.86E-03	2.6
Q61096	Myeloblastin	7	64	1.55E-09	2.6
P47811	Mitogen-activated protein kinase 14	0	8	1.19E-02	2.5
Q09PK2	Retroviral-like aspartic protease 1	0	8	1.19E-02	2.5
D3YXG6	Actin-related protein 2/3 complex subunit 2	2	22	2.87E-04	2.4
Q61210	Rho guanine nucleotide exchange factor 1	3	29	4.64E-05	2.4
Q9QUM0	Integrin alpha-IIb	1	14	2.99E-03	2.3
P17710	Hexokinase-1	1	14	2.99E-03	2.3
O35744	Chitinase-3-like protein 3	0	7	2.08E-02	2.3

Q6PK77	Adenine phosphoribosyltransferase	0	7	2.08E-02	2.3
Q9WU78	Programmed cell death 6-interacting protein	0	7	2.08E-02	2.3
Q9JKR6	Hypoxia up-regulated protein 1	2	20	7.36E-04	2.3
Q9D154	Leukocyte elastase inhibitor A	16	107	1.17E-12	2.2
P24452	Macrophage-capping protein	0	6	3.61E-02	2.1
Q6ZQ38	Cullin-associated NEDD8-dissociated protein 1	0	6	3.61E-02	2.1
Q921T2	Torsin-1A-interacting protein 1	0	6	3.61E-02	2.1
Q9D0I9	Arginine--tRNA ligase, cytoplasmic	0	6	3.61E-02	2.1
Q00612	Glucose-6-phosphate 1-dehydrogenase X	26	147	6.06E-15	2.0
O70145	Neutrophil cytosol factor 2	2	16	4.61E-03	2.0
P59999	Actin-related protein 2/3 complex subunit 4	2	16	4.61E-03	2.0
A6ZI44	Fructose-bisphosphate aldolase	6	36	8.61E-05	1.9
P47753	F-actin-capping protein subunit alpha-1	2	15	7.19E-03	1.9
P49446	Receptor-type tyrosine-protein phosphatase epsilon	0	5	6.28E-02	1.9
P50516	V-type proton ATPase catalytic subunit A	0	5	6.28E-02	1.9
Q80YQ1	Thrombospondin 1	0	5	6.28E-02	1.9
Q99PT1	Rho GDP-dissociation inhibitor 1	0	5	6.28E-02	1.9
P63158	High mobility group protein B1	0	5	6.28E-02	1.9
F6QY34	Beta-adrenergic receptor kinase 1 (Fragment)	0	5	6.28E-02	1.9
P11352	Glutathione peroxidase 1	0	5	6.28E-02	1.9
Q3TBD2	Minor histocompatibility protein HA-1	0	5	6.28E-02	1.9
Q6GT24	Peroxiredoxin 6	0	5	6.28E-02	1.9
Q9D4E6	Protein Pabpc6	0	5	6.28E-02	1.9
Q9DBJ1	Phosphoglycerate mutase 1	9	49	1.03E-05	1.9
P27005	Protein S100-A8	97	469	1.09E-38	1.8
P04919	Band 3 anion transport protein	12	62	1.24E-06	1.8
Q61233	Plastin-2	33	158	7.88E-14	1.8
P26041	Moesin	17	83	4.70E-08	1.8
O70503	Estradiol 17-beta-dehydrogenase 12	1	9	3.31E-02	1.8
P35700	Peroxiredoxin-1	1	9	3.31E-02	1.8

O08808	Protein diaphanous homolog 1	10	47	5.67E-05	1.7
Q61599	Rho GDP-dissociation inhibitor 2	4	21	4.77E-03	1.6
F8WHL2	Coatomer subunit alpha	0	4	1.09E-01	1.6
G3UZD3	Ras-related protein Rab-11B	0	4	1.09E-01	1.6
P35173	Stefin-3	0	4	1.09E-01	1.6
P61089	Ubiquitin-conjugating enzyme E2 N	0	4	1.09E-01	1.6
E9PZF0	Nucleoside diphosphate kinase	1	8	5.25E-02	1.6
Q99PV0	Pre-mRNA-processing-splicing factor 8	2	12	2.63E-02	1.6
Q8K1B8	Fermitin family homolog 3	7	32	1.07E-03	1.6
Q9WV32	Actin-related protein 2/3 complex subunit 1B	4	19	1.04E-02	1.5
P99029	Peroxiredoxin-5, mitochondrial	15	60	3.33E-05	1.5
Q9CXR1	Dehydrogenase/reductase SDR family member 7	2	11	3.99E-02	1.5
Q91V92	ATP-citrate synthase	6	26	4.16E-03	1.5
Q99JY9	Actin-related protein 3	23	89	7.72E-07	1.5
P48025	Tyrosine-protein kinase SYK	1	7	8.25E-02	1.4
Q64324	Syntaxin-binding protein 2	1	7	8.25E-02	1.4
P80316	T-complex protein 1 subunit epsilon	1	7	8.25E-02	1.4
Q80UM7	Mannosyl-oligosaccharide glucosidase	1	7	8.25E-02	1.4
P40124	Adenylyl cyclase-associated protein 1	40	145	1.72E-09	1.4
Q9DBS1	Transmembrane protein 43	5	21	1.14E-02	1.4
P26040	Ezrin	16	59	9.61E-05	1.4
P84078	ADP-ribosylation factor 1	5	20	1.62E-02	1.3
Q99K47	Fibrinogen, alpha polypeptide	0	3	1.90E-01	1.3
D3YTT7	MCG2650	0	3	1.90E-01	1.3
P68037	Ubiquitin-conjugating enzyme E2 L3	0	3	1.90E-01	1.3
Q9WVA4	Transgelin-2	4	16	3.15E-02	1.3
P07901	Heat shock protein HSP 90-alpha	17	58	2.58E-04	1.3
P17182	Alpha-enolase	91	295	3.91E-15	1.3
P52480	Pyruvate kinase isozymes M1/M2	60	196	1.15E-10	1.3
P97369	Neutrophil cytosol factor 4	8	28	9.14E-03	1.2
P17225	Polypyrimidine tract-binding protein 1	8	28	9.14E-03	1.2
P31725	Protein S100-A9	145	447	2.08E-20	1.2
Q7TPR4	Alpha-actinin-1	11	36	5.05E-03	1.2

Q3TRM8	Hexokinase-3	16	51	1.15E-03	1.2
P11499	Heat shock protein HSP 90-beta	22	69	2.03E-04	1.2
P27773	Protein disulfide-isomerase A3	4	14	6.32E-02	1.1
P80315	T-complex protein 1 subunit delta	3	11	8.97E-02	1.1
P56480	ATP synthase subunit beta, mitochondrial	2	8	1.30E-01	1.1
P24527	Leukotriene A-4 hydrolase	2	8	1.30E-01	1.1
P62962	Profilin-1	36	104	2.60E-05	1.1
Q922R8	Protein disulfide-isomerase A6	1	5	1.96E-01	1.0
P49718	DNA replication licensing factor MCM5	1	5	1.96E-01	1.0
Q8BYI6	Lysophosphatidylcholine acyltransferase 2	1	5	1.96E-01	1.0
Q9CWJ9	Bifunctional purine biosynthesis protein PURH	1	5	1.96E-01	1.0
Q64727	Vinculin	14	41	6.58E-03	1.0
Q922Q8	Leucine-rich repeat-containing protein 59	5	16	6.22E-02	1.0
Q9D2V7	Coronin-7	4	13	8.79E-02	1.0
A2ACG7	Dolichyl-diphosphooligosaccharide--protein glycosyltransferase subunit 2	18	50	4.52E-03	1.0
P10126	Elongation factor 1-alpha 1	81	215	4.20E-08	1.0
P16858	Glyceraldehyde-3-phosphate dehydrogenase	106	280	5.17E-10	1.0
Q8C253	Galectin-3	15	41	1.10E-02	0.9
O55222	Integrin-linked protein kinase	0	2	3.31E-01	0.9
P08113	Endoplasmin	0	2	3.31E-01	0.9
E9Q7Q3	Tropomyosin alpha-3 chain	0	2	3.31E-01	0.9
E9PYL9	Uncharacterized protein	0	2	3.31E-01	0.9
E9Q070	Uncharacterized protein	0	2	3.31E-01	0.9
O54950	5'-AMP-activated protein kinase subunit gamma-1	0	2	3.31E-01	0.9
P62751	60S ribosomal protein L23a	0	2	3.31E-01	0.9
Q61362	Chitinase-3-like protein 1	0	2	3.31E-01	0.9
Q8BH59	Calcium-binding mitochondrial carrier protein Aralar1	0	2	3.31E-01	0.9
Q8C166	Copine-1	0	2	3.31E-01	0.9
Q9CQC9	GTP-binding protein SAR1b	0	2	3.31E-01	0.9

Q9Z2W0	Aspartyl aminopeptidase	0	2	3.31E-01	0.9
P06151	L-lactate dehydrogenase A chain	12	33	2.09E-02	0.9
Q9DCD0	6-phosphogluconate dehydrogenase, decarboxylating	61	158	4.76E-06	0.9
P63101	14-3-3 protein zeta/delta	2	7	1.88E-01	0.9
Q6ZWR6	Nesprin-1	2	7	1.88E-01	0.9
P06745	Glucose-6-phosphate isomerase	63	161	5.58E-06	0.9
P00405	Cytochrome c oxidase subunit 2	4	12	1.21E-01	0.9
Q02053	Ubiquitin-like modifier-activating enzyme 1	6	17	8.11E-02	0.9
Q9JHU4	Cytoplasmic dynein 1 heavy chain 1	13	34	2.60E-02	0.9
O54734	Dolichyl-diphosphooligosaccharide--protein glycosyltransferase 48 kDa subunit	11	29	3.70E-02	0.9
Q9QUI0	Transforming protein RhoA	5	14	1.14E-01	0.9
P63260	Actin, cytoplasmic 2	289	692	7.87E-18	0.8
P68134	Actin, alpha skeletal muscle	108	261	8.95E-08	0.8
P16879	Tyrosine-protein kinase Fes/Fps	3	9	1.76E-01	0.8
P27870	Proto-oncogene vav	3	9	1.76E-01	0.8
Q922U2	Keratin, type II cytoskeletal 5	18	44	2.02E-02	0.8
P02088	Hemoglobin subunit beta-1	4	11	1.64E-01	0.8
P43275	Histone H1.1	4	11	1.64E-01	0.8
P40240	CD9 antigen	1	4	2.95E-01	0.8
P54823	Probable ATP-dependent RNA helicase DDX6	1	4	2.95E-01	0.8
Q3TJH8	Corticosteroid 11-beta-dehydrogenase isozyme 1	1	4	2.95E-01	0.8
Q8K1X4	NCK associated protein 1 like	1	4	2.95E-01	0.8
Q3T9X3	Dynamin-2	6	15	1.42E-01	0.7
O55143	Sarcoplasmic/endoplasmic reticulum calcium ATPase 2	2	6	2.65E-01	0.7
P60335	Poly(rC)-binding protein 1	2	6	2.65E-01	0.7
Q8BYK4	Retinol dehydrogenase 12	7	17	1.31E-01	0.7
Q8QZW8	Protein Arhgap9	7	17	1.31E-01	0.7
Q8BMS1	Trifunctional enzyme subunit alpha, mitochondrial	17	39	4.23E-02	0.7
P07356	Annexin A2	13	30	6.84E-02	0.7

Q62422	Osteoclast-stimulating factor 1	3	8	2.40E-01	0.7
Q62261	Spectrin beta chain, non-erythrocytic 1	5	12	2.00E-01	0.6
O08692	Myeloid bactenecin (F1)	34	73	1.48E-02	0.6
Q5SQX6	Cytoplasmic FMR1-interacting protein 2	11	24	1.23E-01	0.6
Q80W54	CAAX prenyl protease 1 homolog	7	15	2.14E-01	0.5
E9PVA8	Protein Gcn111	4	9	2.87E-01	0.5
P80317	T-complex protein 1 subunit zeta	4	9	2.87E-01	0.5
Q3UP87	Neutrophil elastase	24	48	7.13E-02	0.5
Q8K2Z4	Condensin complex subunit 1	3	7	3.22E-01	0.5
Q99P88	Nuclear pore complex protein Nup155	2	5	3.67E-01	0.5
P15864	Histone H1.2	21	41	1.05E-01	0.5
P46467	Vacuolar protein sorting-associated protein 4B	1	3	4.32E-01	0.5
Q9Z0P5	Twinfilin-2	1	3	4.32E-01	0.5
Q9D8N0	Elongation factor 1-gamma	7	14	2.67E-01	0.5
P68368	Tubulin alpha-4A chain	133	246	1.82E-03	0.5
P50637	Translocator protein	20	38	1.34E-01	0.5
Q99JI6	Ras-related protein Rap-1b	13	25	1.93E-01	0.4
Q91YQ5	Dolichyl-diphosphooligosaccharide--protein glycosyltransferase subunit 1	19	36	1.45E-01	0.4
Q61937	Nucleophosmin	12	23	2.09E-01	0.4
E9Q616	Protein Ahnak	6	12	2.95E-01	0.4
P58252	Elongation factor 2	108	197	6.59E-03	0.4
P47757	F-actin-capping protein subunit beta	15	28	1.96E-01	0.4
Q8BJS4	SUN domain-containing protein 2	36	64	1.11E-01	0.4
P61161	Actin-related protein 2	7	13	3.29E-01	0.4
O88342	WD repeat-containing protein 1	3	6	4.21E-01	0.3
Q60597	2-oxoglutarate dehydrogenase, mitochondrial	3	6	4.21E-01	0.3
Q923B6	Metalloreductase STEAP4	13	23	2.74E-01	0.3
Q9D0E1	Heterogeneous nuclear ribonucleoprotein M	16	28	2.52E-01	0.3
O35350	Calpain-1 catalytic subunit	9	16	3.28E-01	0.3
Q8CG29	Myosin IF	26	44	2.16E-01	0.3
P26039	Talin-1	331	545	2.23E-03	0.3
P60766	Cell division control protein 42 homolog	39	65	1.75E-01	0.3

G3UY93	Valine--tRNA ligase (Fragment)	16	27	2.94E-01	0.3
P63325	40S ribosomal protein S10	16	27	2.94E-01	0.3
Q9ET01	Glycogen phosphorylase, liver form	74	121	1.11E-01	0.3
P40142	Transketolase	291	472	7.29E-03	0.3
Q62465	Synaptic vesicle membrane protein VAT-1 homolog	2	4	4.92E-01	0.3
P68369	Tubulin alpha-1A chain	119	188	1.01E-01	0.2
Q6R0H7	Guanine nucleotide-binding protein G(s) subunit alpha isoforms XLas	11	18	3.82E-01	0.2
P63017	Heat shock cognate 71 kDa protein	87	137	1.48E-01	0.2
Q68FD5	Clathrin heavy chain 1	38	60	2.60E-01	0.2
Q9Z1N5	Spliceosome RNA helicase Ddx39b	42	66	2.54E-01	0.2
E9Q6H6	Arachidonate 5-lipoxygenase	6	10	4.45E-01	0.2
P41245	Matrix metalloproteinase-9	17	27	3.60E-01	0.2
O89053	Coronin-1A	147	226	1.22E-01	0.2
P11672	Neutrophil gelatinase-associated lipocalin	25	39	3.35E-01	0.2
Q8C147	Dedicator of cytokinesis protein 8	12	19	4.06E-01	0.2
P70460	Vasodilator-stimulated phosphoprotein	18	28	3.79E-01	0.2
P43274	Histone H1.4	28	43	3.45E-01	0.2
G5E8Y7	MCG1031571	65	98	2.75E-01	0.1
Q9QZQ8	Core histone macro-H2A.1	49	74	3.07E-01	0.1
G3UWA6	4F2 cell-surface antigen heavy chain	5	8	5.00E-01	0.1
P13020	Gelsolin	3	5	5.35E-01	0.1
Q922B2	Aspartate--tRNA ligase, cytoplasmic	3	5	5.35E-01	0.1
Q3U7R1	Extended synaptotagmin-1	92	135	2.96E-01	0.1
Q99K48	Non-POU domain-containing octamer-binding protein	10	15	4.84E-01	0.1
Q9WTR1	Transient receptor potential cation channel subfamily V member 2	1	2	6.12E-01	0.1
O89086	Putative RNA-binding protein 3	1	2	6.12E-01	0.1
Q6P5F9	Exportin-1	1	2	6.12E-01	0.1
Q8K4Z5	Splicing factor 3A subunit 1	1	2	6.12E-01	0.1
Q9DBG7	Signal recognition particle receptor subunit alpha	1	2	6.12E-01	0.1
Q9ERN0	Secretory carrier-associated membrane protein 2	1	2	6.12E-01	0.1

Q9EQ06	Estradiol 17-beta-dehydrogenase 11	31	45	4.28E-01	0.1
Q8BG67	Protein EFR3 homolog A	8	12	5.04E-01	0.1
Q61990	Poly(rC)-binding protein 2	13	19	4.89E-01	0.1
Q9CQQ7	ATP synthase subunit b, mitochondrial	14	20	5.10E-01	0.0
O35841	Apoptosis inhibitor 5	4	6	5.69E-01	0.0
P54071	Isocitrate dehydrogenase [NADP], mitochondrial	7	10	5.58E-01	0.0
Q09014	Neutrophil cytosol factor 1	46	63	5.15E-01	0.0
O70133	ATP-dependent RNA helicase A	25	34	5.47E-01	0.0
P30355	Arachidonate 5-lipoxygenase-activating protein	17	23	5.66E-01	0.0
H3BIY9	AP-2 complex subunit beta	11	15	5.74E-01	0.0
P62702	40S ribosomal protein S4, X isoform	15	20	5.48E-01	0.0
P99024	Tubulin beta-5 chain	194	252	3.52E-01	-0.1
P20029	78 kDa glucose-regulated protein	27	35	4.82E-01	-0.1
P27601	Guanine nucleotide-binding protein subunit alpha-13	13	17	5.33E-01	-0.1
Q99NB9	Splicing factor 3B subunit 1	6	8	5.91E-01	-0.1
Q9R233	Tapasin	10	13	5.42E-01	-0.1
O08917	Flotillin-1	37	47	4.28E-01	-0.1
Q8VDL4	ADP-dependent glucokinase	41	52	4.17E-01	-0.1
A3KGU5	Protein Spna2	3	4	6.33E-01	-0.1
P80318	T-complex protein 1 subunit gamma	3	4	6.33E-01	-0.1
P84096	Rho-related GTP-binding protein RhoG	3	4	6.33E-01	-0.1
Q8VDD5	Myosin-9	347	422	7.40E-02	-0.2
E9QNP0	Protein 2810422J05Rik	65	79	2.88E-01	-0.2
Q8VED5	Keratin, type II cytoskeletal 79	9	11	4.96E-01	-0.2
Q03265	ATP synthase subunit alpha, mitochondrial	36	43	3.29E-01	-0.2
Q9D6F9	Tubulin beta-4A chain	164	193	1.03E-01	-0.2
P60843	Eukaryotic initiation factor 4A-I	76	89	1.98E-01	-0.2
P30681	High mobility group protein B2	11	13	4.47E-01	-0.2
Q8BU31	Ras-related protein Rap-2c	5	6	5.36E-01	-0.2
P35564	Calnexin	18	21	3.80E-01	-0.2
Q64522	Histone H2A type 2-B	1010	1178	1.95E-04	-0.2
F8WGL3	Cofilin-1	25	29	3.33E-01	-0.2

Q64523	Histone H2A type 2-C	1081	1259	1.02E-04	-0.2
P60867	40S ribosomal protein S20	26	30	3.21E-01	-0.2
P63038	60 kDa heat shock protein, mitochondrial	37	42	2.52E-01	-0.3
D3Z5X4	Uncharacterized protein	46	52	2.15E-01	-0.3
P62301	40S ribosomal protein S13	23	26	3.13E-01	-0.3
P97807	Fumarate hydratase, mitochondrial	7	8	4.69E-01	-0.3
P80313	T-complex protein 1 subunit eta	25	28	2.90E-01	-0.3
Q3UW53	Protein Niban	28	31	2.61E-01	-0.3
Q8CGP7	Histone H2A type 1-K	1156	1292	5.63E-07	-0.3
P84228	Histone H3.2	328	362	3.99E-03	-0.3
P01027	Complement C3	21	23	2.90E-01	-0.3
Q91Y57	Sialic acid-binding Ig-like lectin 12	11	12	3.77E-01	-0.3
B1ATS4	ATPase, Ca ⁺⁺ transporting, ubiquitous	13	14	3.42E-01	-0.3
Q91VB8	Alpha globin 1	14	15	3.27E-01	-0.3
Q91V55	40S ribosomal protein S5	15	16	3.13E-01	-0.3
Q3U9G9	Lamin-B receptor	36	38	1.70E-01	-0.4
Q61093	Cytochrome b-245 heavy chain	166	175	1.21E-02	-0.4
P08249	Malate dehydrogenase, mitochondrial	29	30	1.83E-01	-0.4
P97384	Annexin A11	33	34	1.60E-01	-0.4
P10854	Histone H2B type 1-M	603	619	5.43E-07	-0.4
Q9JKF1	Ras GTPase-activating-like protein IQGAP1	80	81	3.90E-02	-0.4
Q3THW5	Histone H2A.V	206	208	1.64E-03	-0.4
P51410	60S ribosomal protein L9	1	1	6.69E-01	-0.4
Q5SX46	Mitochondrial 2-oxoglutarate/malate carrier protein (Fragment)	1	1	6.69E-01	-0.4
Q64511	DNA topoisomerase 2-beta	1	1	6.69E-01	-0.4
Q9EQH3	Vacuolar protein sorting-associated protein 35	1	1	6.69E-01	-0.4
Q61805	Lipopolysaccharide-binding protein	2	2	5.68E-01	-0.4
Q99KI0	Aconitate hydratase, mitochondrial	2	2	5.68E-01	-0.4
Q60930	Voltage-dependent anion-selective channel protein 2	3	3	5.08E-01	-0.4
F8WHR6	Probable ATP-dependent RNA helicase DDX46	6	6	4.03E-01	-0.4
P43276	Histone H1.5	9	9	3.40E-01	-0.4

O35129	Prohibitin-2	10	10	3.23E-01	-0.4
O88569	Heterogeneous nuclear ribonucleoproteins A2/B1	12	12	2.94E-01	-0.4
Q01853	Transitional endoplasmic reticulum ATPase	15	15	2.58E-01	-0.4
A2AQR0	Glycerol phosphate dehydrogenase 2, mitochondrial	16	16	2.47E-01	-0.4
B5THE2	Maltase-glucoamylase	16	16	2.47E-01	-0.4
P86048	60S ribosomal protein L10-like	31	31	1.43E-01	-0.4
F6SVV1	Protein Gm9493	34	34	1.30E-01	-0.4
Q05144	Ras-related C3 botulinum toxin substrate 2	59	59	6.04E-02	-0.4
P10107	Annexin A1	844	845	1.80E-10	-0.5
Q8BTM8	Filamin-A	328	324	3.06E-05	-0.5
P47738	Aldehyde dehydrogenase, mitochondrial	101	98	1.14E-02	-0.5
P11835	Integrin beta-2	209	202	3.69E-04	-0.5
E9Q604	Integrin alpha-M	409	393	5.85E-07	-0.5
Q6NXH9	Keratin, type II cytoskeletal 73	17	16	1.91E-01	-0.5
Q8VEK3	Heterogeneous nuclear ribonucleoprotein U	34	32	8.79E-02	-0.5
Q9Z183	Protein-arginine deiminase type-4	15	14	2.06E-01	-0.5
Q8R2S8	CD177 antigen	124	116	2.55E-03	-0.5
P32037	Solute carrier family 2, facilitated glucose transporter member 3	39	36	6.15E-02	-0.5
Q8BMK4	Cytoskeleton-associated protein 4	12	11	2.32E-01	-0.5
Q5EBP8	Heterogeneous nuclear ribonucleoprotein A1	21	19	1.32E-01	-0.6
Q80VQ0	Aldehyde dehydrogenase family 3 member B1	19	17	1.41E-01	-0.6
P62908	40S ribosomal protein S3	39	35	4.93E-02	-0.6
P08071	Lactotransferrin	53	47	2.20E-02	-0.6
Q8R081	Heterogeneous nuclear ribonucleoprotein L	7	6	2.90E-01	-0.6
P22437	Prostaglandin G/H synthase 1	15	13	1.60E-01	-0.6
P11247	Myeloperoxidase	173	152	5.92E-05	-0.6
P04104	Keratin, type II cytoskeletal 1	30	26	6.24E-02	-0.6
P06800	Receptor-type tyrosine-protein phosphatase C	77	67	5.11E-03	-0.6

O35286	Putative pre-mRNA-splicing factor ATP-dependent RNA helicase DHX15	22	19	9.96E-02	-0.6
P54116	Erythrocyte band 7 integral membrane protein	14	12	1.66E-01	-0.6
A2AL12	Heterogeneous nuclear ribonucleoprotein A3	14	12	1.66E-01	-0.6
P51150	Ras-related protein Rab-7a	6	5	3.05E-01	-0.7
Q9D3G5	Syntaxin-11	6	5	3.05E-01	-0.7
D3Z678	Protein Gm15448	37	31	3.17E-02	-0.7
Q9CPR4	60S ribosomal protein L17	5	4	3.21E-01	-0.7
Q9DBG5	Perilipin-3	11	9	1.83E-01	-0.7
Q3TLP8	RAS-related C3 botulinum substrate 1, isoform CRA_a	35	29	3.31E-02	-0.7
P62320	Small nuclear ribonucleoprotein Sm D3	26	21	5.23E-02	-0.7
O88593	Peptidoglycan recognition protein 1	4	3	3.40E-01	-0.7
Q99020	Heterogeneous nuclear ribonucleoprotein A/B	4	3	3.40E-01	-0.7
H3BKL5	3-ketoacyl-CoA thiolase A, peroxisomal	9	7	1.94E-01	-0.7
Q5SS83	Flotillin 2	38	30	1.79E-02	-0.8
E9Q0F0	Protein Krt78	28	22	3.76E-02	-0.8
P62806	Histone H4	1214	986	0.00E+00	-0.8
P08752	Guanine nucleotide-binding protein G(i) subunit alpha-2	138	108	1.15E-05	-0.8
Q6IFX2	Keratin, type I cytoskeletal 42	17	13	8.38E-02	-0.8
Q62167	ATP-dependent RNA helicase DDX3X	71	55	1.19E-03	-0.8
Q8VIJ6	Splicing factor, proline- and glutamine- rich	21	16	5.69E-02	-0.8
P35343	C-X-C chemokine receptor type 2	3	2	3.62E-01	-0.8
P27659	60S ribosomal protein L3	3	2	3.62E-01	-0.8
Q6ZWN5	40S ribosomal protein S9	7	5	2.06E-01	-0.8
Q6PHN9	Ras-related protein Rab-35	14	10	8.73E-02	-0.9
P62245	40S ribosomal protein S15a	10	7	1.33E-01	-0.9
F6YVP7	Uncharacterized protein	30	21	1.38E-02	-0.9
P25911	Tyrosine-protein kinase Lyn	39	27	4.84E-03	-0.9
Q61735	Leukocyte surface antigen CD47	38	26	4.81E-03	-1.0
O35639	Annexin A3	2	1	3.88E-01	-1.0
P17809	Solute carrier family 2, facilitated	2	1	3.88E-01	-1.0

	glucose transporter member 1				
F6U2H0	Uncharacterized protein (Fragment)	2	1	3.88E-01	-1.0
G3UZI2	Heterogeneous nuclear ribonucleoprotein Q	2	1	3.88E-01	-1.0
Q61881	DNA replication licensing factor MCM7	2	1	3.88E-01	-1.0
Q9CQM8	60S ribosomal protein L21	2	1	3.88E-01	-1.0
Q91V41	Ras-related protein Rab-14	8	5	1.34E-01	-1.0
Q9Z1R9	MCG124046	196	132	2.13E-10	-1.0
A2AQ07	Tubulin beta-1 chain	43	28	1.63E-03	-1.0
P35979	60S ribosomal protein L12	7	4	1.33E-01	-1.1
P68040	Guanine nucleotide-binding protein subunit beta-2-like 1	16	9	2.49E-02	-1.2
P09405	Nucleolin	23	13	7.88E-03	-1.2
Q8C3J5	Dedicator of cytokinesis protein 2	6	3	1.30E-01	-1.2
Q5SUA5	Unconventional myosin-Ig	44	25	2.97E-04	-1.2
P14115	60S ribosomal protein L27a	15	8	2.37E-02	-1.2
Q6ZQM8	UDP-glucuronosyltransferase 1-7C	15	8	2.37E-02	-1.2
P23116	Eukaryotic translation initiation factor 3 subunit A	54	30	4.62E-05	-1.3
P14234	Tyrosine-protein kinase Fgr	37	20	5.33E-04	-1.3
P51437	Cathelin-related antimicrobial peptide	55	30	3.00E-05	-1.3
P62855	40S ribosomal protein S26	12	6	3.38E-02	-1.3
P57787	Monocarboxylate transporter 4	33	17	6.79E-04	-1.3
Q3U435	Matrix metalloproteinase-25	5	2	1.23E-01	-1.4
P62267	40S ribosomal protein S23	5	2	1.23E-01	-1.4
P61021	Ras-related protein Rab-5B	11	5	3.12E-02	-1.4
Q7TPV4	Myb-binding protein 1A	11	5	3.12E-02	-1.4
E9QKR0	Guanine nucleotide-binding protein G(I)/G(S)/G(T) subunit beta-2	15	7	1.35E-02	-1.4
P07724	Serum albumin	15	7	1.35E-02	-1.4
F6Q5Z8	Uncharacterized protein	8	3	4.29E-02	-1.6
Q9QXS1	Plectin	17	7	4.74E-03	-1.6
P62852	40S ribosomal protein S25	6	2	6.72E-02	-1.6
P08103	Tyrosine-protein kinase HCK	24	10	8.67E-04	-1.6
P28293	Cathepsin G	118	51	4.45E-13	-1.6
Q9D1D4	Transmembrane emp24 domain-	4	1	1.08E-01	-1.7

	containing protein 10				
Q3TEA8	Heterochromatin protein 1-binding protein 3	4	1	1.08E-01	-1.7
D3Z627	Integrin alpha-L	35	14	3.94E-05	-1.7
P62843	40S ribosomal protein S15	16	6	4.04E-03	-1.7
P49290	Eosinophil peroxidase	208	87	0.00E+00	-1.7
Q9ERI2	Ras-related protein Rab-27A	7	2	3.58E-02	-1.8
Q61656	Probable ATP-dependent RNA helicase DDX5	25	9	2.44E-04	-1.8
P02535	Keratin, type I cytoskeletal 10	20	7	8.89E-04	-1.8
Q9DB20	ATP synthase subunit O, mitochondrial	2	0	1.81E-01	-1.8
Q8BP67	60S ribosomal protein L24	10	3	1.28E-02	-1.8
Q9JIZ9	Phospholipid scramblase 3	13	4	4.78E-03	-1.9
P51881	ADP/ATP translocase 2	96	32	0.00E+00	-2.0
P14131	40S ribosomal protein S16	21	6	2.08E-04	-2.1
Q61878	Bone marrow proteoglycan	151	48	0.00E+00	-2.1
Q9CPN9	Protein 2210010C04Rik	22	6	1.11E-04	-2.1
Q99N16	Leukotriene-B(4) omega-hydroxylase 2	6	1	2.62E-02	-2.1
P47963	60S ribosomal protein L13	3	0	7.68E-02	-2.2
Q80WS3	rRNA/tRNA 2'-O-methyltransferase fibrillar-like protein 1	3	0	7.68E-02	-2.2
Q80ZX0	Protein Sec24b	3	0	7.68E-02	-2.2
Q9R112	Sulfide:quinone oxidoreductase, mitochondrial	3	0	7.68E-02	-2.2
Q9R190	Metastasis-associated protein MTA2	3	0	7.68E-02	-2.2
G5E902	MCG10343, isoform CRA_b	20	5	1.48E-04	-2.2
Q61462	Cytochrome b-245 light chain	14	3	9.42E-04	-2.3
P62281	40S ribosomal protein S11	4	0	3.26E-02	-2.5
Q9CPQ8	ATP synthase subunit g, mitochondrial	4	0	3.26E-02	-2.5
Q9CQW2	ADP-ribosylation factor-like protein 8B	4	0	3.26E-02	-2.5
Q8VDN2	Sodium/potassium-transporting ATPase subunit alpha-1	56	12	2.36E-11	-2.6
Q62178	Semaphorin-4A	13	2	5.69E-04	-2.6
P01900	H-2 class I histocompatibility antigen, D-D alpha chain	5	0	1.39E-02	-2.8
Q8VEH3	ADP-ribosylation factor-like protein 8A	5	0	1.39E-02	-2.8
Q9D1G1	Ras-related protein Rab-1B	37	6	4.35E-09	-2.8

P62754	40S ribosomal protein S6	10	0	1.92E-04	-3.6
Q5SZV3	40S ribosomal protein S8	20	1	4.60E-07	-3.7
Q8CFQ9	Fusion, derived from t(12;16) malignant liposarcoma (Human)	15	0	2.66E-06	-4.1
Total		13912	18817		

Bibliography

1. Sprenger, R. R.; Jensen, O. N., Proteomics and the dynamic plasma membrane: Quo Vadis? *Proteomics* **2010**, 10, 3997-4011.
2. Josic, D.; Clifton, J. G., Mammalian plasma membrane proteomics. *Proteomics* **2007**, 7, 3010-29.
3. Josic, D.; Clifton, J. G.; Kovac, S.; Hixson, D. C., Membrane proteins as diagnostic biomarkers and targets for new therapies. *Curr Opin Mol Ther* **2008**, 10, 116-23.
4. Overington, J. P.; Al-Lazikani, B.; Hopkins, A. L., How many drug targets are there? *Nat Rev Drug Discov* **2006**, 5, 993-6.
5. Polanski, M.; Anderson, N. L., A list of candidate cancer biomarkers for targeted proteomics. *Biomark Insights* **2007**, 1, 1-48.
6. Stevens, T. J.; Arkin, I. T., Do more complex organisms have a greater proportion of membrane proteins in their genomes? *Proteins* **2000**, 39, 417-20.
7. Choksawangkarn, W.; Edwards, N.; Wang, Y.; Gutierrez, P.; Fenselau, C., Comparative Study of Workflows Optimized for In-gel, In-solution, and On-filter Proteolysis in the Analysis of Plasma Membrane Proteins. *J Proteome Res* **2012**, 11, 3030-4.
8. Choksawangkarn, W.; Kim, S. K.; Cannon, J. R.; Edwards, N. J.; Lee, S. B.; Fenselau, C., Enrichment of Plasma Membrane Proteins Using Nanoparticle Pellicles:

- Comparison between Silica and Higher Density Nanoparticles. *J Proteome Res* **2013**, 12, 1134-41.
9. Kearney, P.; Thibault, P., Bioinformatics meets proteomics--bridging the gap between mass spectrometry data analysis and cell biology. *J Bioinform Comput Biol* **2003**, 1, 183-200.
10. Bretscher, M. S.; Raff, M. C., Mammalian plasma membranes. *Nature* **1975**, 258, 43-9.
11. Cordwell, S. J.; Thingholm, T. E., Technologies for plasma membrane proteomics. *Proteomics* **2010**, 10, 611-27.
12. Zhang, L.; Xie, J.; Wang, X.; Liu, X.; Tang, X.; Cao, R.; Hu, W.; Nie, S.; Fan, C.; Liang, S., Proteomic analysis of mouse liver plasma membrane: use of differential extraction to enrich hydrophobic membrane proteins. *Proteomics* **2005**, 5, 4510-24.
13. Huber, L. A.; Pfaller, K.; Vietor, I., Organelle proteomics: implications for subcellular fractionation in proteomics. *Circ Res* **2003**, 92, 962-8.
14. Spector, D. L. G., R.D.; Leinwand, L.A., Cells: A Laboratory Manual, part II: Culture and Biochemical Analysis of Cells. . *Cold Spring Harbor, NY: Cold Spring Harbor Laboratory Press*. **1998**.
15. Nunomura, K.; Nagano, K.; Itagaki, C.; Taoka, M.; Okamura, N.; Yamauchi, Y.; Sugano, S.; Takahashi, N.; Izumi, T.; Isobe, T., Cell surface labeling and mass spectrometry reveal diversity of cell surface markers and signaling molecules expressed in undifferentiated mouse embryonic stem cells. *Mol Cell Proteomics* **2005**, 4, 1968-76.

16. Elia, G., Biotinylation reagents for the study of cell surface proteins. *Proteomics* **2008**, 8, 4012-24.
17. Gundry, R. L.; Raginski, K.; Tarasova, Y.; Tchernyshyov, I.; Bausch-Fluck, D.; Elliott, S. T.; Boheler, K. R.; Van Eyk, J. E.; Wollscheid, B., The mouse C2C12 myoblast cell surface N-linked glycoproteome: identification, glycosite occupancy, and membrane orientation. *Mol Cell Proteomics* **2009**, 8, 2555-69.
18. Zhang, H.; Li, X. J.; Martin, D. B.; Aebersold, R., Identification and quantification of N-linked glycoproteins using hydrazide chemistry, stable isotope labeling and mass spectrometry. *Nat Biotechnol* **2003**, 21, 660-6.
19. Weekes, M. P.; Antrobus, R.; Talbot, S.; Hor, S.; Simecek, N.; Smith, D. L.; Bloor, S.; Randow, F.; Lehner, P. J., Proteomic plasma membrane profiling reveals an essential role for gp96 in the cell surface expression of LDLR family members, including the LDL receptor and LRP6. *J Proteome Res* **2012**, 11, 1475-84.
20. Cao, R.; Li, X.; Liu, Z.; Peng, X.; Hu, W.; Wang, X.; Chen, P.; Xie, J.; Liang, S., Integration of a two-phase partition method into proteomics research on rat liver plasma membrane proteins. *J Proteome Res* **2006**, 5, 634-42.
21. Everberg, H.; Gustavasson, N.; Tjerner, F., Enrichment of membrane proteins by partitioning in detergent/polymer aqueous two-phase systems. *Methods Mol Biol* **2008**, 424, 403-12.
22. Schindler, J.; Lewandrowski, U.; Sickmann, A.; Friauf, E.; Nothwang, H. G., Proteomic analysis of brain plasma membranes isolated by affinity two-phase partitioning. *Mol Cell Proteomics* **2006**, 5, 390-400.

23. Jacobson, B. S.; Stolz, D. B.; Schnitzer, J. E., Identification of endothelial cell-surface proteins as targets for diagnosis and treatment of disease. *Nat Med* **1996**, 2, 482-4.
24. Chaney, L. K.; Jacobson, B. S., Coating cells with colloidal silica for high yield isolation of plasma membrane sheets and identification of transmembrane proteins. *J Biol Chem* **1983**, 258, 10062-72.
25. Rahbar, A. M.; Fenselau, C., Integration of Jacobson's pellicle method into proteomic strategies for plasma membrane proteins. *J Proteome Res* **2004**, 3, 1267-77.
26. Cox, J.; Mann, M., Quantitative, high-resolution proteomics for data-driven systems biology. *Annu Rev Biochem* **2011**, 80, 273-99.
27. Wilkins, M. R.; Sanchez, J. C.; Gooley, A. A.; Appel, R. D.; Humphery-Smith, I.; Hochstrasser, D. F.; Williams, K. L., Progress with proteome projects: why all proteins expressed by a genome should be identified and how to do it. *Biotechnol Genet Eng Rev* **1996**, 13, 19-50.
28. Patterson, S. D.; Aebersold, R. H., Proteomics: the first decade and beyond. *Nat Genet* **2003**, 33 Suppl, 311-23.
29. Han, X.; Aslanian, A.; Yates, J. R., 3rd, Mass spectrometry for proteomics. *Curr Opin Chem Biol* **2008**, 12, 483-90.
30. Yates, J. R.; Ruse, C. I.; Nakorchevsky, A., Proteomics by mass spectrometry: approaches, advances, and applications. *Annu Rev Biomed Eng* **2009**, 11, 49-79.
31. Cannon, J. R.; Edwards, N. J.; Fenselau, C., Mass-biased partitioning to enhance middle down proteomics analysis. *J Mass Spectrom* **2013**, 48, 340-3.

32. Aebersold, R.; Mann, M., Mass spectrometry-based proteomics. *Nature* **2003**, 422, 198-207.
33. Fenn, J. B.; Mann, M.; Meng, C. K.; Wong, S. F.; Whitehouse, C. M., Electrospray ionization for mass spectrometry of large biomolecules. *Science* **1989**, 246, 64-71.
34. Tanaka, K. W., H.; Ido, Y.; Akita, S.; Yoshida, Y; Yoshida, T.; Matsuo, T., Protein and polymer analyses up to m/z 100 000 by laser ionization time-of-flight mass spectrometry. *Rapid Commun Mass Spectrom* **1988**, 2, 151-153.
35. Banerjee, S.; Mazumdar, S., Electrospray ionization mass spectrometry: a technique to access the information beyond the molecular weight of the analyte. *Int J Anal Chem* **2012**, 282574.
36. Shukla, A. K.; Futrell, J. H., Tandem mass spectrometry: dissociation of ions by collisional activation. *J Mass Spectrom* **2000**, 35, 1069-90.
37. Wells, J. M.; McLuckey, S. A., Collision-induced dissociation (CID) of peptides and proteins. *Methods Enzymol* **2005**, 402, 148-85.
38. Syka, J. E.; Coon, J. J.; Schroeder, M. J.; Shabanowitz, J.; Hunt, D. F., Peptide and protein sequence analysis by electron transfer dissociation mass spectrometry. *Proc Natl Acad Sci U S A* **2004**, 101, 9528-33.
39. Stafford, G. C.; Kelley, P. E.; Syka, J. E. P.; Reynolds, W. E.; Todd, J. F. J., Recent Improvements in and Analytical Applications of Advanced Ion Trap Technology. *International Journal of Mass Spectrometry and Ion Processes* **1984**, 60, 85-98.

40. Makarov, A., Electrostatic axially harmonic orbital trapping: a high-performance technique of mass analysis. *Anal Chem* **2000**, *72*, 1156-62.
41. Perry, R. H.; Cooks, R. G.; Noll, R. J., Orbitrap mass spectrometry: instrumentation, ion motion and applications. *Mass Spectrom Rev* **2008**, *27*, 661-99.
42. Sadygov, R. G.; Cociorva, D.; Yates, J. R., 3rd, Large-scale database searching using tandem mass spectra: looking up the answer in the back of the book. *Nat Methods* **2004**, *1*, 195-202.
43. Perkins, D. N.; Pappin, D. J.; Creasy, D. M.; Cottrell, J. S., Probability-based protein identification by searching sequence databases using mass spectrometry data. *Electrophoresis* **1999**, *20*, 3551-67.
44. Eng, J. K.; McCormack, A. L.; Yates, J. R., An Approach to Correlate Tandem Mass-Spectral Data of Peptides with Amino-Acid-Sequences in a Protein Database. *Journal of the American Society for Mass Spectrometry* **1994**, *5*, 976-989.
45. Yang, P.; Ma, J.; Wang, P.; Zhu, Y.; Zhou, B. B.; Yang, Y. H., Improving X!Tandem on peptide identification from mass spectrometry by self-boosted Percolator. *IEEE/ACM Trans Comput Biol Bioinform* **2012**, *9*, 1273-80.
46. Barsnes, H.; Huber, S.; Sickmann, A.; Eidhammer, I.; Martens, L., OMSSA Parser: an open-source library to parse and extract data from OMSSA MS/MS search results. *Proteomics* **2009**, *9*, 3772-4.
47. Tanner, S.; Shu, H.; Frank, A.; Wang, L. C.; Zandi, E.; Mumby, M.; Pevzner, P. A.; Bafna, V., InsPecT: identification of posttranslationally modified peptides from tandem mass spectra. *Anal Chem* **2005**, *77*, 4626-39.

48. Edwards, N., Wu, X., Tseng, T.W., An unsupervised, model-free, machine-learning combiner for peptide identifications from tandem mass spectra. *Clinical Proteomics* **2009**, 5, 23-36.
49. Choi, H.; Nesvizhskii, A. I., False discovery rates and related statistical concepts in mass spectrometry-based proteomics. *J Proteome Res* **2008**, 7, 47-50.
50. Gabrilovich, D. I.; Nagaraj, S., Myeloid-derived suppressor cells as regulators of the immune system. *Nat Rev Immunol* **2009**, 9, 162-74.
51. Ostrand-Rosenberg, S.; Sinha, P., Myeloid-derived suppressor cells: linking inflammation and cancer. *J Immunol* **2009**, 182, 4499-506.
52. Youn, J. I.; Gabrilovich, D. I., The biology of myeloid-derived suppressor cells: the blessing and the curse of morphological and functional heterogeneity. *Eur J Immunol* **2010**, 40, 2969-75.
53. Bronte, V.; Serafini, P.; Mazzoni, A.; Segal, D. M.; Zanovello, P., L-arginine metabolism in myeloid cells controls T-lymphocyte functions. *Trends Immunol* **2003**, 24, 302-6.
54. Bronte, V.; Zanovello, P., Regulation of immune responses by L-arginine metabolism. *Nat Rev Immunol* **2005**, 5, 641-54.
55. Nagaraj, S.; Gupta, K.; Pisarev, V.; Kinarsky, L.; Sherman, S.; Kang, L.; Herber, D. L.; Schneck, J.; Gabrilovich, D. I., Altered recognition of antigen is a mechanism of CD8⁺ T cell tolerance in cancer. *Nat Med* **2007**, 13, 828-35.
56. Srivastava, M. K.; Sinha, P.; Clements, V. K.; Rodriguez, P.; Ostrand-Rosenberg, S., Myeloid-derived suppressor cells inhibit T-cell activation by depleting cystine and cysteine. *Cancer Res* **2010**, 70, 68-77.

57. Hanson, E. M.; Clements, V. K.; Sinha, P.; Ilkovitch, D.; Ostrand-Rosenberg, S., Myeloid-derived suppressor cells down-regulate L-selectin expression on CD4+ and CD8+ T cells. *J Immunol* **2009**, 183, 937-44.
58. Hopkins, A. L.; Groom, C. R., The druggable genome. *Nat Rev Drug Discov* **2002**, 1, 727-30.
59. Rahbar, A. M.; Fenselau, C., Unbiased examination of changes in plasma membrane proteins in drug resistant cancer cells. *J Proteome Res* **2005**, 4, 2148-53.
60. Li, X.; Jin, Q.; Cao, J.; Xie, C.; Cao, R.; Liu, Z.; Xiong, J.; Li, J.; Yang, X.; Chen, P.; Liang, S., Evaluation of two cell surface modification methods for proteomic analysis of plasma membrane from isolated mouse hepatocytes. *Biochim Biophys Acta* **2009**, 1794, 32-41.
61. Durr, E.; Yu, J.; Krasinska, K. M.; Carver, L. A.; Yates, J. R.; Testa, J. E.; Oh, P.; Schnitzer, J. E., Direct proteomic mapping of the lung microvascular endothelial cell surface in vivo and in cell culture. *Nat Biotechnol* **2004**, 22, 985-92.
62. Graham, J. M., *Biological centrifugation*. Bios Scientific publishers: 2001.
63. Millonig, G., Further observations on a phosphate buffer for Osmium solutions in fixation. *Fifth International Congress for Electron Microscopy* **1962**, 2, P8.
64. <http://www.sigmaaldrich.com/life-science/cell-biology/antibodies/antibodies-application/protocols/western-blotting.html> - procedure.
65. Wessel, D.; Flugge, U. I., A method for the quantitative recovery of protein in dilute solution in the presence of detergents and lipids. *Anal Biochem* **1984**, 138, 141-3.

66. Shevchenko, A.; Tomas, H.; Havlis, J.; Olsen, J. V.; Mann, M., In-gel digestion for mass spectrometric characterization of proteins and proteomes. *Nat Protoc* **2006**, 1, 2856-60.
67. <http://www.matrixscience.com/>
68. Ashburner, M.; Ball, C. A.; Blake, J. A.; Botstein, D.; Butler, H.; Cherry, J. M.; Davis, A. P.; Dolinski, K.; Dwight, S. S.; Eppig, J. T.; Harris, M. A.; Hill, D. P.; Issel-Tarver, L.; Kasarskis, A.; Lewis, S.; Matese, J. C.; Richardson, J. E.; Ringwald, M.; Rubin, G. M.; Sherlock, G., Gene ontology: tool for the unification of biology. The Gene Ontology Consortium. *Nat Genet* **2000**, 25, 25-9.
69. Borregaard, N.; Heiple, J. M.; Simons, E. R.; Clark, R. A., Subcellular localization of the b-cytochrome component of the human neutrophil microbicidal oxidase: translocation during activation. *J Cell Biol* **1983**, 97, 52-61.
70. Speers, A. E.; Wu, C. C., Proteomics of integral membrane proteins--theory and application. *Chem Rev* **2007**, 107, 3687-714.
71. Wisniewski, J. R.; Zougman, A.; Nagaraj, N.; Mann, M., Universal sample preparation method for proteome analysis. *Nat Methods* **2009**, 6, 359-62.
72. Manza, L. L.; Stamer, S. L.; Ham, A. J.; Codreanu, S. G.; Liebler, D. C., Sample preparation and digestion for proteomic analyses using spin filters. *Proteomics* **2005**, 5, 1742-5.
73. Fic, E.; Kedracka-Krok, S.; Jankowska, U.; Pirog, A.; Dziejzicka-Wasylewska, M., Comparison of protein precipitation methods for various rat brain structures prior to proteomic analysis. *Electrophoresis* **2010**, 31, 3573-9.

74. Liebler, D. C.; Ham, A. J., Spin filter-based sample preparation for shotgun proteomics. *Nat Methods* **2009**, *6*, 785; author reply 785-6.
75. Bereman, M. S.; Egertson, J. D.; MacCoss, M. J., Comparison between procedures using SDS for shotgun proteomic analyses of complex samples. *Proteomics* **2011**, *11*, 2931-5.
76. Zhang, N.; Chen, R.; Young, N.; Wishart, D.; Winter, P.; Weiner, J. H.; Li, L., Comparison of SDS- and methanol-assisted protein solubilization and digestion methods for Escherichia coli membrane proteome analysis by 2-D LC-MS/MS. *Proteomics* **2007**, *7*, 484-93.
77. Sun, L.; Tao, D.; Han, B.; Ma, J.; Zhu, G.; Liang, Z.; Shan, Y.; Zhang, L.; Zhang, Y., Ionic liquid 1-butyl-3-methyl imidazolium tetrafluoroborate for shotgun membrane proteomics. *Anal Bioanal Chem* **2011**, *399*, 3387-97.
78. Chen, E. I.; Cociorva, D.; Norris, J. L.; Yates, J. R., 3rd, Optimization of mass spectrometry-compatible surfactants for shotgun proteomics. *J Proteome Res* **2007**, *6*, 2529-38.
79. Blonder, J.; Chan, K. C.; Issaq, H. J.; Veenstra, T. D., Identification of membrane proteins from mammalian cell/tissue using methanol-facilitated solubilization and tryptic digestion coupled with 2D-LC-MS/MS. *Nat Protoc* **2006**, *1*, 2784-90.
80. Yao, X.; Freas, A.; Ramirez, J.; Demirev, P. A.; Fenselau, C., Proteolytic 18O labeling for comparative proteomics: model studies with two serotypes of adenovirus. *Anal Chem* **2001**, *73*, 2836-42.

81. Sun, D.; Wang, N.; Li, L., Integrated SDS removal and peptide separation by strong-cation exchange liquid chromatography for SDS-assisted shotgun proteome analysis. *J Proteome Res* **2012**, 11, 818-28.
82. Liu, H.; Sadygov, R. G.; Yates, J. R., 3rd, A model for random sampling and estimation of relative protein abundance in shotgun proteomics. *Anal Chem* **2004**, 76, 4193-201.
83. Krogh, A.; Larsson, B.; von Heijne, G.; Sonnhammer, E. L., Predicting transmembrane protein topology with a hidden Markov model: application to complete genomes. *J Mol Biol* **2001**, 305, 567-80.
84. Kyte, J.; Doolittle, R. F., A simple method for displaying the hydrophobic character of a protein. *J Mol Biol* **1982**, 157, 105-32.
85. Macher, B. A.; Yen, T. Y., Proteins at membrane surfaces-a review of approaches. *Mol Biosyst* **2007**, 3, 705-13.
86. Strader, M. B.; Tabb, D. L.; Hervey, W. J.; Pan, C.; Hurst, G. B., Efficient and specific trypsin digestion of microgram to nanogram quantities of proteins in organic-aqueous solvent systems. *Anal Chem* **2006**, 78, 125-34.
87. Thingholm, T. E.; Larsen, M. R.; Ingrell, C. R.; Kassem, M.; Jensen, O. N., TiO₂-based phosphoproteomic analysis of the plasma membrane and the effects of phosphatase inhibitor treatment. *J Proteome Res* **2008**, 7, 3304-13.
88. Washburn, M. P.; Wolters, D.; Yates, J. R., 3rd, Large-scale analysis of the yeast proteome by multidimensional protein identification technology. *Nat Biotechnol* **2001**, 19, 242-7.

89. Eichacker, L. A.; Granvogl, B.; Mirus, O.; Muller, B. C.; Miess, C.; Schleiff, E., Hiding behind hydrophobicity. Transmembrane segments in mass spectrometry. *J Biol Chem* **2004**, *279*, 50915-22.
90. Fischer, F.; Poetsch, A., Protein cleavage strategies for an improved analysis of the membrane proteome. *Proteome Sci* **2006**, *4*, 2.
91. Belrhali, H.; Nollert, P.; Royant, A.; Menzel, C.; Rosenbusch, J. P.; Landau, E. M.; Pebay-Peyroula, E., Protein, lipid and water organization in bacteriorhodopsin crystals: a molecular view of the purple membrane at 1.9 Å resolution. *Structure* **1999**, *7*, 909-17.
92. Russell, W. K.; Park, Z. Y.; Russell, D. H., Proteolysis in mixed organic-aqueous solvent systems: applications for peptide mass mapping using mass spectrometry. *Anal Chem* **2001**, *73*, 2682-5.
93. Thingholm, T. E.; Jorgensen, T. J.; Jensen, O. N.; Larsen, M. R., Highly selective enrichment of phosphorylated peptides using titanium dioxide. *Nat Protoc* **2006**, *1*, 1929-35.
94. Zhang, W.; Zhao, C.; Wang, S.; Fang, C.; Xu, Y.; Lu, H.; Yang, P., Coating cells with cationic silica-magnetite nanocomposites for rapid purification of integral plasma membrane proteins. *Proteomics* **2011**, *11*, 3482-90.
95. Shin, B. K.; Wang, H.; Yim, A. M.; Le Naour, F.; Brichory, F.; Jang, J. H.; Zhao, R.; Puravs, E.; Tra, J.; Michael, C. W.; Misek, D. E.; Hanash, S. M., Global profiling of the cell surface proteome of cancer cells uncovers an abundance of proteins with chaperone function. *J Biol Chem* **2003**, *278*, 7607-16.

96. Zhao, Y.; Zhang, W.; Kho, Y., Proteomic analysis of integral plasma membrane proteins. *Anal Chem* **2004**, 76, 1817-23.
97. Stolz, D. B.; Jacobson, B. S., Examination of transcellular membrane protein polarity of bovine aortic endothelial cells in vitro using the cationic colloidal silica microbead membrane-isolation procedure. *J Cell Sci* **1992**, 103, 39-51.
98. Stolz, D. B.; Ross, M. A.; Salem, H. M.; Mars, W. M.; Michalopoulos, G. K.; Enomoto, K., Cationic colloidal silica membrane perturbation as a means of examining changes at the sinusoidal surface during liver regeneration. *Am J Pathol* **1999**, 155, 1487-98.
99. Robinson, J. M.; Ackerman, W. E. t.; Tewari, A. K.; Kniss, D. A.; Vandre, D. D., Isolation of highly enriched apical plasma membranes of the placental syncytiotrophoblast. *Anal Biochem* **2009**, 387, 87-94.
100. Harvey, S.; Zhang, Y.; Landry, F.; Miller, C.; Smith, J. W., Insights into a plasma membrane signature. *Physiological Genomics* **2001**, 5, 129-136.
101. Li, X.; Xie, C.; Cao, J.; He, Q.; Cao, R.; Lin, Y.; Jin, Q.; Chen, P.; Wang, X.; Liang, S., An in vivo membrane density perturbation strategy for identification of liver sinusoidal surface proteome accessible from the vasculature. *J Proteome Res* **2009**, 8, 123-32.
102. Leduc-Nadeau, A.; Lahjouji, K.; Bissonnette, P.; Lapointe, J. Y.; Bichet, D. G., Elaboration of a novel technique for purification of plasma membranes from *Xenopus laevis* oocytes. *Am J Physiol Cell Physiol* **2007**, 292, C1132-6.
103. Li, X.; Jia, X.; Xie, C.; Lin, Y.; Cao, R.; He, Q.; Chen, P.; Wang, X.; Liang, S., Development of cationic colloidal silica-coated magnetic nanospheres for highly

selective and rapid enrichment of plasma membrane fractions for proteomics analysis.

Biotechnol Appl Biochem **2009**, 54, 213-20.

104. Prior, M. J.; Larance, M.; Lawrence, R. T.; Soul, J.; Humphrey, S.; Burchfield, J.; Kistler, C.; Davey, J. R.; La-Borde, P. J.; Buckley, M.; Kanazawa, H.; Parton, R. G.; Guilhaus, M.; James, D. E., Quantitative proteomic analysis of the adipocyte plasma membrane. *J Proteome Res* **2011**, 10, 4970-82.

105. Mathias, R. A.; Chen, Y. S.; Goode, R. J.; Kapp, E. A.; Mathivanan, S.; Moritz, R. L.; Zhu, H. J.; Simpson, R. J., Tandem application of cationic colloidal silica and Triton X-114 for plasma membrane protein isolation and purification: towards developing an MDCK protein database. *Proteomics* **2011**, 11, 1238-53.

106. Vandre, D. D.; Ackerman, W. E. t.; Tewari, A.; Kniss, D. A.; Robinson, J. M., A placental sub-proteome: the apical plasma membrane of the syncytiotrophoblast. *Placenta* **2012**, 33, 207-13.

107. Arjunan, S.; Reinartz, M.; Emde, B.; Zanger, K.; Schrader, J., Limitations of the colloidal silica method in mapping the endothelial plasma membrane proteome of the mouse heart. *Cell Biochem Biophys* **2009**, 53, 135-43.

108. Jang, J. H.; Hanash, S., Profiling of the cell surface proteome. *Proteomics* **2003**, 3, 1947-54.

109. Kessner, D.; Chambers, M.; Burke, R.; Agus, D.; Mallick, P., ProteoWizard: open source software for rapid proteomics tools development. *Bioinformatics* **2008**, 24, 2534-6.

110. Lu, H.; Ouyang, W.; Huang, C., Inflammation, a key event in cancer development. *Mol Cancer Res* **2006**, 4, 221-33.

111. Marx, J., Cancer immunology. Cancer's bulwark against immune attack: MDS cells. *Science* **2008**, 319, 154-6.
112. Gabrilovich, D. I.; Ostrand-Rosenberg, S.; Bronte, V., Coordinated regulation of myeloid cells by tumours. *Nat Rev Immunol* **2012**, 12, 253-68.
113. Sinha, P.; Okoro, C.; Foell, D.; Freeze, H. H.; Ostrand-Rosenberg, S.; Srikrishna, G., Proinflammatory S100 proteins regulate the accumulation of myeloid-derived suppressor cells. *J Immunol* **2008**, 181, 4666-75.
114. Bunt, S. K.; Sinha, P.; Clements, V. K.; Leips, J.; Ostrand-Rosenberg, S., Inflammation induces myeloid-derived suppressor cells that facilitate tumor progression. *J Immunol* **2006**, 176, 284-90.
115. Bunt, S. K.; Yang, L.; Sinha, P.; Clements, V. K.; Leips, J.; Ostrand-Rosenberg, S., Reduced inflammation in the tumor microenvironment delays the accumulation of myeloid-derived suppressor cells and limits tumor progression. *Cancer Res* **2007**, 67, 10019-26.
116. Gabrilovich, D.; Ishida, T.; Oyama, T.; Ran, S.; Kravtsov, V.; Nadaf, S.; Carbone, D. P., Vascular endothelial growth factor inhibits the development of dendritic cells and dramatically affects the differentiation of multiple hematopoietic lineages in vivo. *Blood* **1998**, 92, 4150-66.
117. Serafini, P.; Carbley, R.; Noonan, K. A.; Tan, G.; Bronte, V.; Borrello, I., High-dose granulocyte-macrophage colony-stimulating factor-producing vaccines impair the immune response through the recruitment of myeloid suppressor cells. *Cancer Res* **2004**, 64, 6337-43.

118. Sinha, P.; Clements, V. K.; Fulton, A. M.; Ostrand-Rosenberg, S., Prostaglandin E2 promotes tumor progression by inducing myeloid-derived suppressor cells. *Cancer Res* **2007**, *67*, 4507-13.
119. Markiewski, M. M.; DeAngelis, R. A.; Benencia, F.; Ricklin-Lichtsteiner, S. K.; Koutoulaki, A.; Gerard, C.; Coukos, G.; Lambris, J. D., Modulation of the antitumor immune response by complement. *Nat Immunol* **2008**, *9*, 1225-35.
120. Chornoguz, O.; Grmai, L.; Sinha, P.; Artemenko, K. A.; Zubarev, R. A.; Ostrand-Rosenberg, S., Proteomic pathway analysis reveals inflammation increases myeloid-derived suppressor cell resistance to apoptosis. *Mol Cell Proteomics* **2011**, *10*, M110 002980.
121. Bronte, V.; Serafini, P.; De Santo, C.; Marigo, I.; Tosello, V.; Mazzoni, A.; Segal, D. M.; Staib, C.; Lowel, M.; Sutter, G.; Colombo, M. P.; Zanovello, P., IL-4-induced arginase 1 suppresses alloreactive T cells in tumor-bearing mice. *J Immunol* **2003**, *170*, 270-8.
122. Aslakson, C. J.; Miller, F. R., Selective events in the metastatic process defined by analysis of the sequential dissemination of subpopulations of a mouse mammary tumor. *Cancer Res* **1992**, *52*, 1399-405.
123. Pulaski, B. A.; Ostrand-Rosenberg, S., Reduction of established spontaneous mammary carcinoma metastases following immunotherapy with major histocompatibility complex class II and B7.1 cell-based tumor vaccines. *Cancer Res* **1998**, *58*, 1486-93.

124. Huang da, W.; Sherman, B. T.; Lempicki, R. A., Systematic and integrative analysis of large gene lists using DAVID bioinformatics resources. *Nat Protoc* **2009**, 4, 44-57.
125. Szklarczyk, D.; Franceschini, A.; Kuhn, M.; Simonovic, M.; Roth, A.; Minguéz, P.; Doerks, T.; Stark, M.; Müller, J.; Bork, P.; Jensen, L. J.; von Mering, C., The STRING database in 2011: functional interaction networks of proteins, globally integrated and scored. *Nucleic Acids Res* **2011**, 39, D561-8.
126. Brohee, S.; van Helden, J., Evaluation of clustering algorithms for protein-protein interaction networks. *BMC Bioinformatics* **2006**, 7, 488.
127. Beissbarth, T.; Hyde, L.; Smyth, G. K.; Job, C.; Boon, W. M.; Tan, S. S.; Scott, H. S.; Speed, T. P., Statistical modeling of sequencing errors in SAGE libraries. *Bioinformatics* **2004**, 20, i31-9.
128. Old, W. M.; Meyer-Arendt, K.; Aveline-Wolf, L.; Pierce, K. G.; Mendoza, A.; Sevinsky, J. R.; Resing, K. A.; Ahn, N. G., Comparison of label-free methods for quantifying human proteins by shotgun proteomics. *Mol Cell Proteomics* **2005**, 4, 1487-502.
129. Kanehisa, M.; Goto, S.; Sato, Y.; Furumichi, M.; Tanabe, M., KEGG for integration and interpretation of large-scale molecular data sets. *Nucleic Acids Res* **2012**, 40, D109-14.
130. Benjamini, Y. H., Y., Controlling the false discovery rate: a practical and powerful approach to multiple testing. *Journal of the Royal Statistical Society. Serie B (Methodological)* **1995**, 57, 289-300.

131. Cheng, P.; Corzo, C. A.; Luetkeke, N.; Yu, B.; Nagaraj, S.; Bui, M. M.; Ortiz, M.; Nacken, W.; Sorg, C.; Vogl, T.; Roth, J.; Gaborilovich, D. I., Inhibition of dendritic cell differentiation and accumulation of myeloid-derived suppressor cells in cancer is regulated by S100A9 protein. *J Exp Med* **2008**, 205, 2235-49.
132. Ridley, A. J.; Schwartz, M. A.; Burridge, K.; Firtel, R. A.; Ginsberg, M. H.; Borisy, G.; Parsons, J. T.; Horwitz, A. R., Cell migration: integrating signals from front to back. *Science* **2003**, 302, 1704-9.
133. Kareva, I.; Hahnfeldt, P., The emerging "hallmarks" of metabolic reprogramming and immune evasion: distinct or linked? *Cancer Res* **2013**, 73, 2737-42.
134. Ong, S. E.; Blagoev, B.; Kratchmarova, I.; Kristensen, D. B.; Steen, H.; Pandey, A.; Mann, M., Stable isotope labeling by amino acids in cell culture, SILAC, as a simple and accurate approach to expression proteomics. *Mol Cell Proteomics* **2002**, 1, 376-86.
135. Wiese, S.; Reidegeld, K. A.; Meyer, H. E.; Warscheid, B., Protein labeling by iTRAQ: a new tool for quantitative mass spectrometry in proteome research. *Proteomics* **2007**, 7, 340-50.
136. Carvalho, P. C.; Hewel, J.; Barbosa, V. C.; Yates, J. R., 3rd, Identifying differences in protein expression levels by spectral counting and feature selection. *Genet Mol Res* **2008**, 7, 342-56.
137. Chelius, D.; Bondarenko, P. V., Quantitative profiling of proteins in complex mixtures using liquid chromatography and mass spectrometry. *J Proteome Res* **2002**, 1, 317-23.